

July 2020

A Health Evaluation of Gulf of Mexico Golden Tilefish (*Lopholatilus chamaeleonticeps*) and Red Snapper (*Lutjanus campechanus*) Following the Deepwater Horizon Oil Spill

Kristina Leigh Deak
University of South Florida

Follow this and additional works at: <https://digitalcommons.usf.edu/etd>



Part of the [Biology Commons](#), [Molecular Biology Commons](#), and the [Toxicology Commons](#)

Scholar Commons Citation

Deak, Kristina Leigh, "A Health Evaluation of Gulf of Mexico Golden Tilefish (*Lopholatilus chamaeleonticeps*) and Red Snapper (*Lutjanus campechanus*) Following the Deepwater Horizon Oil Spill" (2020). *USF Tampa Graduate Theses and Dissertations*.
<https://digitalcommons.usf.edu/etd/9022>

This Dissertation is brought to you for free and open access by the USF Graduate Theses and Dissertations at Digital Commons @ University of South Florida. It has been accepted for inclusion in USF Tampa Graduate Theses and Dissertations by an authorized administrator of Digital Commons @ University of South Florida. For more information, please contact digitalcommons@usf.edu.

A Health Evaluation of Gulf of Mexico Golden Tilefish (*Lopholatilus chamaeleonticeps*) and
Red Snapper (*Lutjanus campechanus*) Following the *Deepwater Horizon* Oil Spill

by

Kristina Leigh Deak

A dissertation submitted in partial fulfillment
of the requirements for the degree of
Doctor of Philosophy in Marine Science
with a concentration in Biological Oceanography
College of Marine Science
University of South Florida

Major Professor: Steven A. Murawski, Ph.D.
Mya Breitbart, Ph.D.
Larry Dishaw, Ph.D.
David Portnoy, Ph.D.
Cathy Walsh, Ph.D.

Date of Approval
March 27, 2020

Keywords: biomarkers, oxidative stress, transcriptomics, toxicology, teleost

Copyright © 2020, Kristina Leigh Deak

DEDICATION

To my parents, for laying the foundation that made this work possible.

To my husband, for his loving support throughout this journey.

To our son, for supplying the incentive to finish this dissertation before his birth!

ACKNOWLEDGEMENTS

I would like to extend my most sincere gratitude to my advisor, Dr. Steven Murawski, for his assistance throughout this dissertation. It has been a privilege to work with such an accomplished mentor with a truly inspiring drive both on land and at sea. I have thoroughly enjoyed our years of fishing and researching together and will look back fondly on the time spent wrestling *Ophichthus rex*, feisty gulpers, and pesky data.

Thank you to my committee, Dr. Larry Dishaw, Dr. Mya Breitbart, Dr. Cathy Walsh, and Dr. David Portnoy, for their thorough, thoughtful review of this work. A special thanks to Dr. Larry Dishaw for the use of his laboratory for much of the molecular studies conducted within this dissertation. I greatly appreciate all of your support, encouragement, and thought-provoking questions throughout this journey.

During the last two years of my PhD I rejoined the professional world, first as a Research Associate with Fish Health at the Fish and Wildlife Research Institute in St Petersburg, before transitioning to an appointment as a Staff Environmental Scientist with the Environmental Flows and Assessments team at the Southwest Florida Water Management District. I thank both agencies, the University of South Florida, and my colleagues among all groups, for helping me to balance all of these commitments and to deepen my educational and professional experience.

I am indebted to my family, friends, and farm critters for adding levity and love to this process. The adventures at sea, laughs in the lab, and countless Wine Wednesdays, made the long nights and sacrificed weekends far more palatable. My husband, Trent, deserves a world of

praise for keeping me sane and moderately balanced, especially during these last few months while I juggled writing my dissertation, a new career, and preparing for the birth of our son.

This research was made possible by generous financial support provided by the William and Elsie Knight Endowed Fellowship Fund for Marine Science, the Gulf Oceanographic Charitable Trust Endowed Fellowship, and the Gulf of Mexico Research Initiative/C-IMAGE II and III (SA 12-10, SA 18-16).

TABLE OF CONTENTS

List of Tables	iv
List of Figures	vi
Abstract	xii
Chapter 1. Introduction	1
1.1 <i>Deepwater Horizon</i> and the Gulf of Mexico	1
1.2 Xenobiotic metabolism and the acute stress response in fish	4
1.3 The chronic stress response in fish	7
1.4 Resilience to xenobiotic exposure	8
1.5 Study rationale	10
1.6 Study species	11
1.7 Biomarker selection	12
1.8 RNA sequencing	14
1.9 Objectives	15
Chapter 2. The establishment of reference intervals for oxidative stress and immune response biomarkers in Golden Tilefish (<i>Lopholatilus chamaeleonticeps</i>) and Red Snapper (<i>Lutjanus campechanus</i>), caught throughout the Gulf of Mexico in 2015-2017	17
2.1 Abstract	17
2.2 Introduction	18
2.3 Methods	21
2.3.1 Sampling	21
2.3.2 Superoxide dismutase	22
2.3.3 Malondialdehyde	22
2.3.4 Sorbitol dehydrogenase	22
2.3.5 Micronuclei and nuclear abnormalities	23
2.3.6 Hematocrit and leukocrit	23
2.3.7 Differential white blood cell counts	24
2.3.8 Lysozyme	24
2.3.9 Data analysis	25
2.3.10 Geozone definitions	26
2.4 Results	26
2.5 Discussion	28
2.6 Conclusions	32
2.7 Tables	33
2.8 Figures	36

Chapter 3. Relationships between polycyclic aromatic hydrocarbon exposure and biomarker response in Gukf of Mexico Golden Tilefish (<i>Lopholatilus chamaeleonticeps</i>) caught 2015-2017	45
3.1 Abstract	45
3.2 Introduction	46
3.3 Methods	51
3.3.1 Sampling	51
3.3.2 Oxidative stress biomarkers	52
3.3.3 Immune response biomarkers	52
3.3.4 Polycyclic aromatic hydrocarbon metabolites	53
3.3.5 Liver lipid fraction	53
3.3.6 Data analysis	54
3.4 Results	55
3.4.1 Comparison of biomarker expression throughout the Gulf of Mexico	55
3.4.2 Geozone-specific variability	58
3.4.2.1 North central 2015	58
3.4.2.2 North central 2017	59
3.4.2.3 Northwest	61
3.4.2.4 Southwest	62
3.4.2.5 Campeche Bay	63
3.4.2.6 Yucatan Peninsula	64
3.4.3 Comparisons between fish from the north central Gulf of Mexico	66
3.4.3.1 Stations grouped regardless of year	66
3.4.3.2 Comparison of stations by year	67
3.5 Discussion	68
3.6 Conclusions	73
3.7 Figures	75
Chapter 4. Relationships between polycyclic aromatic hydrocarbon exposure and biomarker response in Red Snapper (<i>Lutjanus campechanus</i>) caught throughout the northern Gulf of Mexico in 2015-2017	108
4.1 Abstract	108
4.2 Introduction	109
4.3 Methods	111
4.3.1 Sampling	111
4.3.2 Oxidative stress biomarkers	111
4.3.3 Immune response biomarkers	111
4.3.4 Polycyclic aromatic hydrocarbon metabolites	112
4.3.5 Liver lipid fraction	112
4.3.6 Data analysis	112
4.4 Results	112
4.4.1 Biomarker variability across the northern Gulf of Mexico	112
4.4.2 Biomarker variability by sampling group	115
4.4.2.1 North central 2015	115
4.4.2.2 North central 2017	116
4.4.2.3 Northwest	118

4.4.3 Biomarker variability among fish from north central stations	120
4.4.3.1 By sampling year	120
4.4.3.2 By sex and sampling year	121
4.4.3.3 At station 10-40	123
4.4.3.4 At station 12-40	123
4.5 Discussion	124
4.6 Conclusions	127
4.7 Figures	128
Chapter 5. <i>De novo</i> Golden Tilefish (<i>Lopholatilus chamaeleonticeps</i>) transcriptome assembly and differential gene expression in fish caught from the De Soto Canyon, Campeche Bay, and Yucatan Peninsula, in the Gulf of Mexico	165
5.1 Abstract	165
5.2 Introduction	166
5.3 Methods	168
5.3.1 Sampling	168
5.3.2 RNA sequencing	169
5.3.3 <i>De novo</i> Golden Tilefish transcriptome assembly	169
5.3.4 Annotation and gene ontology	170
5.3.5 Biomarkers and liver lipid fraction	171
5.3.6 Polycyclic aromatic hydrocarbon metabolites	171
5.3.7 Biometrics, biomarker, liver lipid fraction and polycyclic aromatic hydrocarbon metabolite data analysis	171
5.4 Results	172
5.4.1 <i>De novo</i> assembly of the Golden Tilefish transcriptome	170
5.4.2 Differential gene expression	172
5.4.3 Annotation and gene ontology	173
5.4.4 Biomarker response and liver lipid fraction	173
5.4.5 Polycyclic aromatic hydrocarbon metabolites	173
5.5 Discussion	174
5.6 Conclusions	181
5.7 Tables	183
5.8 Figures	203
Chapter 6. Conclusions	209
6.1 Summary of dissertation	209
6.2 Implications for future field studies	213
Chapter 7. References	216
Appendix A. Station and catch data	237
Appendix B. Biometrics data for fish utilized in the creation of reference intervals	239

LIST OF TABLES

Table 2.1	Golden Tilefish reference interval statistics.	33
Table 2.2	Red Snapper reference interval statistics.	34
Table 2.3	Statistically significant differences ($p < 0.05$) in mean values for biomarkers by macroscopically identified sex.	35
Table 5.1	Sampling station data.	183
Table 5.2	Raw sequence data.	184
Table 5.3	Results of the trimming method used in Trimmomatic that resulted in acceptable FastQC metrics for each sequence.	185
Table 5.4	Statistics for Trinity assemblies and Bowtie2 alignments.	187
Table 5.5	Annotation statistics for differentially expressed (DE) genes between stations.	188
Table 5.6	The ten most frequent gene ontology biological function terms associated with annotated differentially expressed (DE) genes ($FDR < 0.05$), between stations.	189
Table 5.7	The ten most frequent gene ontology molecular function terms associated with annotated differentially expressed (DE) genes ($FDR < 0.05$), between stations.	190
Table 5.8	The ten most frequent gene ontology cellular component terms associated with annotated differentially expressed (DE) genes ($FDR < 0.05$), between stations.	191
Table 5.9	Relative up-regulation (red) and down-regulation (green) of differentially expressed genes ($FDR < 0.05$) associated with xenobiotic metabolism, between stations.	192
Table 5.10	Relative up-regulation (red) and down-regulation (green) of differentially expressed genes ($FDR < 0.05$) associated with lipid metabolism, between stations.	193
Table 5.11	Relative up-regulation (red) and down-regulation (green) of differentially expressed genes ($FDR < 0.05$) associated with glucose metabolism and release, between stations.	194

Table 5.12 Relative up-regulation (red) and down-regulation (green) of differentially expressed genes (FDR < 0.05) associated with cholesterol biosynthesis, between stations.	195
Table 5.13 Relative up-regulation (red) and down-regulation (green) of differentially expressed genes (FDR < 0.05) associated with reproduction, between stations.	196
Table 5.14 Relative up-regulation (red) and down-regulation (green) of differentially expressed genes (FDR < 0.05) associated with immune response, between stations.	197
Table 5.15 Relative up-regulation (red) and down-regulation (green) of differentially expressed genes (FDR < 0.05) associated with oxidative stress and debris clearance, between stations.	199
Table 5.16 Relative up-regulation (red) and down-regulation (green) of differentially expressed genes (FDR < 0.05) associated with circadian rhythm, between stations.	201
Table 5.17 Relative up-regulation (red) and down-regulation (green) of differentially expressed genes (FDR < 0.05) associated with transcription factors and solute carriers, between stations.	202

LIST OF FIGURES

Figure 2.1	All demersal longline stations included in this study, fished in the months of July-August in 2015-2017, color-coded by species.	36
Figure 2.2	Biomarkers for which Golden Tilefish reference intervals were significantly higher than Red Snapper intervals.	37
Figure 2.3	Biomarkers for which Red Snapper reference intervals were significantly higher than Golden Tilefish intervals.	38
Figure 2.4	Comparisons in mean biomarker expression in superoxide dismutase (SOD) for Golden Tilefish by total weight (TW) quartile, after outlier removal.	39
Figure 2.5	Comparisons in mean biomarker expression in sorbitol dehydrogenase (SDH) for Golden Tilefish by total weight (TW) quartile, after outlier removal.	40
Figure 2.6	Comparisons in mean neutrophil count in Red Snapper by total weight (TW) quartile, after outlier removal.	41
Figure 2.7	Differences in expression of sorbitol dehydrogenase (SDH) in Golden Tilefish by geozone, after outlier removal.	42
Figure 2.8	Differences in sum nuclear abnormalities (SumNA) in Red Snapper by geozone, after outlier removal.	43
Figure 2.9	Differences in neutrophil count in Red Snapper by geozone, after outlier removal.	44
Figure 3.1	Distribution of sampling stations among geographic zones.	75
Figure 3.2	Oxidative stress biomarkers for which NC fish varied significantly from those in other regions sampled.	76
Figure 3.3	Immune system biomarkers for which NC fish varied significantly from those in other regions sampled.	77
Figure 3.4	Polycyclic aromatic hydrocarbon levels for which NC fish varied significantly from those in other regions sampled.	78

Figure 3.5 Body condition variables for which NC fish varied significantly from those in other regions sampled.	79
Figure 3.6 A) NMDS and B) PCA for GoM-wide explanatory variables and oxidative stress biomarkers.	80
Figure 3.7 A) NMDS and B) PCA for GoM-wide explanatory variables and oxidative stress biomarkers upon removal of biliary PAH data.	81
Figure 3.8 A) NMDS and B) PCA for GoM-wide explanatory variables and oxidative Stress biomarkers upon removal of PAH data.	82
Figure 3.9 A) NMDS and B) PCA for GoM-wide explanatory variables and oxidative stress biomarkers upon removal of PAH and liver lipid fraction data.	83
Figure 3.10 A) NMDS, B) PCA, and C) RDA for GoM-wide explanatory variables and immune system biomarkers.	84
Figure 3.11 Station locations in zone NC, sampled in both 2015 (purple) and 2017 (pink).	85
Figure 3.12 A) NMDS, B) PCA, and C) RDA for explanatory variables and oxidative stress biomarkers in NC2015 specimens.	86
Figure 3.13 A) NMDS, B) PCA, and C) RDA for explanatory variables and immune system biomarkers in NC2015 specimens.	87
Figure 3.14 A) NMDS, B) PCA, and C) RDA for explanatory variables and oxidative stress biomarkers in NC2017 specimens.	88
Figure 3.15 A) NMDS, B) PCA, and C) RDA for explanatory variables and immune system biomarkers In NC2017 specimens.	89
Figure 3.16 Station locations in NW zone.	90
Figure 3.17 A) NMDS, B) PCA, and C) RDA for explanatory variables and oxidative stress biomarkers in NW specimens.	91
Figure 3.18 A) NMDS, B) PCA, and C) RDA for explanatory variables and immune system biomarkers in NW specimens.	92
Figure 3.19 Station locations in SW zone.	93
Figure 3.20 A) NMDS, B) PCA, and C) RDA for explanatory variables and oxidative stress biomarkers in SW specimens.	94

Figure 3.21 A) NMDS, B) PCA, and C) RDA for explanatory variables and immune system biomarkers in SW specimens.	95
Figure 3.22 Station locations in CB zone.	96
Figure 3.23 A) NMDS, B) PCA, and C) RDA for explanatory variables and oxidative stress biomarkers in CB specimens.	97
Figure 3.24 A) NMDS, B) PCA, and C) RDA for explanatory variables and immune system biomarkers in CB specimens.	98
Figure 3.25 Station locations in YP zone.	99
Figure 3.26 A) NMDS, B) PCA, and C) RDA for explanatory variables and oxidative stress biomarkers in YP specimens.	100
Figure 3.27 A) NMDS, B) PCA, and C) RDA for explanatory variables and immune system biomarkers in YP specimens.	101
Figure 3.28 A) NMDS, B) PCA, and C) RDA for explanatory variables and oxidative stress biomarkers in specimens from NC stations, grouped regardless of sampling year.	102
Figure 3.29 A) NMDS and B) PCA for explanatory variables and oxidative stress biomarkers in specimens from NC stations, grouped regardless of sampling year, upon removal of PAH data.	103
Figure 3.30 A) NMDS, B) PCA, and C) RDA for explanatory variables and immune system biomarkers in specimens from NC stations, grouped regardless of sampling year.	104
Figure 3.31 A) NMDS and B) PCA of oxidative stress and explanatory variable data in specimens from NC2015 and NC2017 upon removal of PAH data.	105
Figure 3.32 A) NMDS and B) PCA of immune system biomarker and explanatory variable data in specimens from NC2015 and NC2017 upon removal of PAH data.	106
Figure 3.33 RDA for A) oxidative stress and B) immune system biomarkers and explanatory variables for specimens from NC2015 and NC2017.	107
Figure 4.1 Map of the sampling groups at which Red Snapper collection occurred in 2015-2017.	128
Figure 4.2 A) NMDS, B) PCA, and C) RDA for explanatory variables and oxidative stress biomarkers in NC2015, NC2017 and NW specimens.	129

Figure 4.3 A) NMDS, B) PCA, and C) RDA for explanatory variables and immune system biomarkers in NC2015, NC2017 and NW specimens.	130
Figure 4.4 A) NMDS and B) RDA for explanatory variables and oxidative stress biomarkers in NC2015, NC2017, and NW specimens, grouped by sex.	131
Figure 4.5 A) NMDS and B) RDA for explanatory variables and immune system biomarkers in NC2015, NC2017, and NW specimens, grouped by sex.	132
Figure 4.6 Station locations within the NC2015 sampling group.	133
Figure 4.7 A) NMDS, B) PCA, and C) RDA for explanatory variables and oxidative stress biomarkers in the NC2015 sampling group.	134
Figure 4.8 A) NMDS, B) PCA, and C) RDA for explanatory variables and immune system biomarkers in the NC2015 sampling group.	135
Figure 4.9 A) NMDS and B) RDA for explanatory variables and oxidative stress biomarkers in the NC2015 sampling group, by sex.	136
Figure 4.10 A) NMDS and B) RDA for explanatory variables and oxidative stress biomarkers in the NC2015 sampling group, by sex.	137
Figure 4.11 Map of station locations within sampling group NC2017.	138
Figure 4.12 A) NMDS, B) PCA, and C) RDA for explanatory variables and oxidative stress biomarkers in NC2017 specimens.	139
Figure 4.13 A) NMDS, B) PCA, and C) RDA for explanatory variables and immune system biomarkers in NC2017 specimens.	140
Figure 4.14 A) NMDS and B) RDA for explanatory variables and oxidative stress biomarkers in the NC2017 sampling group, by sex.	141
Figure 4.15 A) NMDS and B) RDA for explanatory variables and immune system biomarkers in the NC2017 sampling group, by sex.	142
Figure 4.16 Station locations within the NW sampling group.	143
Figure 4.17 A) NMDS, B) PCA, and C) RDA for explanatory variables and oxidative stress biomarkers in NW specimens.	144
Figure 4.18 A) NMDS, B) PCA, and C) RDA for explanatory variables and immune system biomarkers in NW specimens.	145

Figure 4.19 A) NMDS and B) PCA for explanatory variables and immune system biomarkers in NW specimens upon removal of PAH data.	146
Figure 4.20 A) NMDS and B) RDA for oxidative stress and explanatory variables in NW specimens, by sex.	147
Figure 4.21 NMDS of immune system biomarkers and explanatory variables upon removal of PAH data.	148
Figure 4.22 RDA of immune system biomarkers and explanatory variables for NW specimens, by sex.	149
Figure 4.23 Map of NC stations sampled in 2015 and 2017.	150
Figure 4.24 A) NMDS, B) PCA, and C) RDA of oxidative stress biomarkers and explanatory variables for specimens from NC, by sampling year.	151
Figure 4.25 A) NMDS and B) PCA of oxidative stress biomarkers and explanatory variables for specimens from NC, by sampling year, upon removal of biliary PAH data.	152
Figure 4.26 A) NMDS, B) PCA, and C) RDA of immune response biomarkers and explanatory variables for specimens from NC, by sampling year.	153
Figure 4.27 A) NMDS, B) PCA, and C) RDA for oxidative stress biomarkers and explanatory variables for females from NC stations sampled in 2015 and 2017.	154
Figure 4.28 A) NMDS and B) PCA for oxidative stress biomarkers and explanatory variables for females from NC stations sampled in 2015 and 2017, upon removal of biliary PAH data.	155
Figure 4.29 A) NMDS, B) PCA, and C) RDA for immune system biomarkers and explanatory variables for females from NC stations sampled in 2015 and 2017.	156
Figure 4.30 A) NMDS and B) PCA for oxidative stress biomarkers and explanatory variables in males caught within NC in 2015 and 2017.	157
Figure 4.31 A) NMDS and B) PCA for immune system biomarkers and explanatory variables in males caught within NC in 2015 and 2017.	158
Figure 4.32 A) NMDS, B) PCA, and C) RDA for oxidative stress biomarkers and explanatory variables from specimens caught at stations 10-40, compared by sampling year.	159

Figure 4.33 A) NMDS and B) PCA for oxidative stress biomarkers and explanatory variables from specimens caught at stations 10-40, compared by sampling year, upon removal of biliary PAH data.	160
Figure 4.34 A) NMDS, B) PCA, and C) RDA for immune system biomarkers and explanatory variables from specimens caught at stations 10-40, compared by sampling year.	161
Figure 4.35 A) NMDS, B) PCA, and C) RDA for oxidative stress biomarkers and explanatory variables from specimens caught at stations 12-40, compared by sampling year.	162
Figure 4.36 A) NMDS and B) PCA for oxidative stress biomarkers and explanatory variables from specimens caught at stations 12-40, compared by sampling year, upon removal of PAH data.	163
Figure 4.37 A) NMDS, B) PCA, and C) RDA for immune system biomarkers and explanatory variables from specimens caught at stations 12-40, compared by sampling year.	164
Figure 5.1 Map of sampling locations.	203
Figure 5.2 Heat map of differentially expressed genes ($p < 0.001$) in individuals From various sampling stations (Fig. 5.1) based upon TMM-normalized transcripts, after outlier removal.	204
Figure 5.3 Cluster analysis of differentially expressed genes ($p < 0.001$) in individuals From various stations (Fig. 5.1) based upon TMM-normalized transcripts, after outlier removal.	205
Figure 5.4 Volcano plots displaying the significance (false discover rate; FDR) versus magnitude (fold change; FC) of differential gene expression (FDR < 0.05) between stations: A) 8-100 versus 31-150, B) 8-100 versus 36-150, and C) 31-150 vs 36-150.	206
Figure 5.5 Immune system biomarkers that varied significantly between stations, following outlier removal.	207
Figure 5.6 Biliary PAH values that varied significantly between stations, following outlier removal.	208

ABSTRACT

A lack of baseline health indices for offshore Gulf of Mexico (GoM) teleosts complicated impact assessments of the *Deepwater Horizon* (DWH) oil spill. While measurement of contaminant levels in fish after a pollution event can document exposure, such data fail to provide meaningful information about how this contact affects an animal's physiology. Controlled exposure studies have highlighted the utility of biomarkers that may indicate deleterious, long-lasting effects of pollutant exposure on various life stages of fish, however, their extrapolation to wild-caught, non-model species is challenging. In an increasingly chemically-saturated environment, it can also be difficult to separate the influence of chronic background contamination from that of a significant acute event, like an oil spill. This dissertation assessed the health of Golden Tilefish (*Lopholatilus chamaeleonticeps*) and Red Snapper (*Lutjanus campechanus*) caught throughout the GoM in 2015-2017, using both biomarkers of oxidative stress and immune response, and transcriptomics. Samples were collected several years after the DWH event, therefore, this study investigated putative lasting effects of exposure on benthic and reef-associated fishes.

In Chapter II, the first known reference intervals for oxidative stress and immune system biomarkers were created for Golden Tilefish (n = 255) and Red Snapper (n = 125) from the GoM, consistent with guidelines of the American Society for Veterinary Clinical Pathology. This included intervals for: malondialdehyde, sorbitol dehydrogenase, sum erythrocyte nuclear abnormalities, superoxide dismutase, hematocrit, leukocrit, lysozyme, and differential white

blood cell counts. Species differences were observed, indicating higher levels of genotoxicity and antioxidant response in Golden Tilefish than in Red Snapper, throughout the GoM.

Chapters III and IV compared the relationships between biomarker response and polycyclic aromatic hydrocarbon (PAH) exposure in Golden Tilefish and Red Snapper, respectively. Fish included in this study were selected only when a sufficient number of specimens ($n \geq 3$) were caught at each sampling station, and sampling stations were grouped into defined geographic zones. Temporal variation in biomarker response at north central GoM stations (where the DWH event occurred) sampled in both 2015 and 2017 was also evaluated. Results reported in chapter III indicated differential biomarker patterns in Golden Tilefish collected from the north central GoM compared to those from other regions and evidence was observed for a possible compensatory metabolic shift due to chronic PAH contamination. Chapter IV revealed limited negative health effects from background PAH exposure on Red Snapper in the northern GoM, however, possible maternal offloading of PAHs was noted in fish from the north central GoM, which may have influenced observed biomarker response.

In chapter V, next generation RNA sequencing was utilized to determine whether geographically grouped populations of Golden Tilefish ($n = 15$) had signatures of differential gene expression, and if these differences may be attributed to PAH exposure. The first *de novo* assembly of the Golden Tilefish transcriptome was performed, and differential gene expression was compared in female fish caught from the De Soto Canyon, Campeche Bay, and the Yucatan Peninsula. Patterns of differential expression were observed between groups. Fish collected within the De Soto Canyon, likely exposed to DWH oil, displayed an altered metabolic response, activated pathways of cellular debris clearance, and down-regulation of reproductive genes compared to the other regions. These results support the compensatory metabolic shift

hypothesis in fish with ongoing exposure to PAHs in the region. Golden Tilefish sampled from the oil fields of Campeche Bay, Mexico, displayed possible immunosuppression and reduced protective mechanisms, despite evidence of oxidative-stress-induced damage, which may indicate an acute response to contaminant exposure. Fish collected offshore the Yucatan Peninsula had more similar patterns of gene expression to fish from the De Soto Canyon than those from Campeche Bay, possibly as a result of significant variation in Campeche Bay specimens. The transcriptome suggest further exploration of pathways involved with lipid and carbohydrate metabolism, oxidative stress and clearance of cellular damage, and reproduction may be useful for PAH-related work in wild-caught teleosts. Furthermore, this study demonstrated the utility of pooling individuals from field sites to yield targets for data exploration.

This work adds significantly to an understanding of the health of non-model, offshore teleosts in the GoM. While variation in biomarker response was observed throughout dispersed regions of the GoM, likely in relation to the varying stressors and contaminants dominating each system, both Red Snapper and Golden Tilefish appear resilient. Despite possible acclimation to adverse conditions, the *Deepwater Horizon* oil spill continued to impart sublethal effects on Golden Tilefish through 2017. The long-term effects of putative reproductive suppression and metabolic shifts in these organisms warrant further monitoring and analysis.

CHAPTER ONE:

INTRODUCTION

1.1 *Deepwater Horizon* and the Gulf of Mexico

Beginning with an explosion at Macondo Prospect 252 on April 20, 2010, the *Deepwater Horizon* (DWH) accident released approximately 4 million barrels of oil into the northern Gulf of Mexico (GoM) over 87 days, causing ecosystem-level impacts (Beyer et al., 2016; US District Court 2015). A unique challenge to capping the well, aiding recovery, and assessing injury, was the depth at which the accident occurred, 1,552 meters below sea surface in the eastern Mississippi Canyon (Beyer et al., 2016). Approximately 30-50% of hydrocarbons were retained in the deep ocean in subsurface plumes at depths of 900 to 1500 m, partially aided by the application of nearly 700,000 gallons of chemical dispersant at the wellhead (Babcock-Adams et al., 2017; McNutt et al., 2012; Valentine et al., 2012). Marine oil snow and flocculent accumulation (MOSSFA) events during and after the spill were significant in distributing oil to the deep sea as well, accounting for 14% of the oil released and resulting in a three-fold increase in polycyclic aromatic hydrocarbon (PAH) deposition to sediments (Daly et al., 2016; Romero et al., 2015). Spill-associated hydrocarbons may have continued their descent to the benthos through 2013 (Yan et al., 2016). The spatial footprint of the spill to the deep sea (>200 m) includes an area of approximately 110,000 km² and a distance of approximately 180 km from the wellhead, with contamination primarily occurring in the Mississippi and De Soto Canyons

(Romero et al., 2017). Approximately 4% of the oil from surface slicks released reached shorelines, affecting approximately 2100 km of northern GoM coastline (Beyer et al., 2016).

Notable impacts of sediment PAH deposition were observed in benthic communities of microbes, foraminifera, seaweeds, and corals (Felder et al., 2014; Joye et al., 2014; Schwing et al., 2015). An immediate and robust shift in microbial communities that occurred during the spill aided the degradation of low molecular weight hydrocarbons (Joye et al., 2014). A decline of 80-93% in benthic foraminifera was observed at sites within 120 km northeast of the DWH wellhead in 2010-2011, with recovery in subsequent years (Schwing et al., 2015, 2018).

Seaweed die-offs were observed through 2013, resulting in an 83% reduction in species diversity along the Ewing Bank, west of the wellhead, with corresponding decline in decapod abundance (Felder et al., 2014). Coral loss of up to 90% was observed at a site within 6 km of the wellhead (White et al., 2012).

Studies of the effects of the oil spill on offshore teleost communities have been limited to analysis of contaminant body burdens, lesion prevalence, larval abundance, otolith analysis, and hepatic biomarkers (Granneman et al., 2017; Herdter et al., 2017; Murawski et al., 2014; Pulster et al., 2020; Rooker et al., 2013; Smeltz et al., 2017; Snyder et al., 2015; Struch et al., 2019).

Time-series biliary and hepatic PAH data from Golden Tilefish (*Lopholatilus chamaeleonticeps*), Red Snapper (*Lutjanus campechanus*), hakes (*Urophycis* spp.) and a variety of grouper species (genera *Epinephelus*, *Hyprothodus* and *Mycteroperca*) indicated spikes in contamination following the spill (Pulster et al., 2020; Snyder et al., 2015, 2020; Struch et al., 2019). Dermal lesion prevalence was higher in 2011 than in 2012 for fish caught from repeat sampling efforts in the northern GoM, particularly in Golden Tilefish, Southern Hake (*Urophycis floridana*), and large pelagic specimens (Murawski et al., 2014). Otolith microchemistry of lesioned fishes

indicated a correlation with life-time exposure to metals, indicating the existence of a pre-spill stressor in these organisms (Granneman et al., 2017). The larval abundance of several pelagic fish species, including Blackfin Tuna (*Thunnus atlanticus*), Blue Marlin (*Makaira nigricans*), and Dolphinfish (*Corphaena hypirrus*) declined immediately following the spill (Rooker et al., 2013). Analysis of otoliths from wild fish indicated that growth of Red Snapper (*Lutjanus campechanus*) may have been suppressed following the spill (Herdter et al., 2017), but this was not observed in Golden Tilefish (HelmueLLer, 2019). Limited biomarker data are available for offshore fish species, however one study noted a spike and subsequent decline in glutathione transferase and glutathione peroxidase in Red Snapper caught in the northern GoM between 2011 and 2014, suggesting a temporary induction of oxidative stress (Smeltz et al., 2017).

Analysis of the health of offshore teleosts following the DWH event is complicated by both the lack of pre-spill baseline data on these species and the need to separate the effects of the spill from that of background chronic contamination. The GoM is a hydrocarbon-rich region, with over 22,000 natural seeps that release up 95% of the total oil input to the waterbody (Joye et al., 2014, Coleman et al., 2003). This includes approximately 350 constant seeps, which contribute to the formation of perennial oil slicks throughout the GoM (Macdonald, 1993). Oil extraction activity is prevalent throughout the northern, northwestern, and southwestern GoM, with over 4,000 active wells accounting for approximately 27% of United States oil production (U.S. Bureau of Ocean Energy Management 2012). The Campeche Bay region offshore Mexico is another prolific oil source, from which Mexico extracts more than 2 million barrels of crude oil each day (Scholz-Böttcher et al., 2008). This area was also the site of the 1979 *Ixtoc I* spill, which released 476,000 tons of oil to the GoM over a nine-month period, with a surface slick extending towards the Texas Coast (Coleman et al., 2003). Discharges from extraction activity,

particularly from produced water discharges and contaminated drilling muds, can also affect local benthic offshore communities (Kennicutt, 2017, Coleman et al., 2003). In addition to known PAH contamination, various pesticides, metals, and legacy contaminants such as polychlorinated biphenyls (PCBs) have been documented in sediments and organisms throughout coastal and continental shelf communities in the GoM, likely from significant contributions of major runoff from the Mississippi and Coatazacoalcos Rivers and atmospheric deposition (Harris, et al., 2012; Kennicutt, 2017). Researchers were therefore challenged with separating the effects of acute versus chronic pollutant exposure following the DWH spill.

1.2 Xenobiotic metabolism and the acute stress response in fish

Bioavailable components of xenobiotics enter the body of a fish through a number of pathways. Principal among them are: inhalation during respiration, bioaccumulation through ingested prey items (and the accompanying substrate), and to a lesser extent, through dermal contact (Meador 1995). In immediate proximity to water-borne PAHs, gills are an important site for toxicant interaction with the organism due to the high volumes of water passing over the dense lamellae, accompanied by rich blood flow through the tissue, and the short distance across which xenobiotics pass to enter the blood stream via counter current exchange (Cappello et al., 2016). Depending on the hydrophobicity and ionic characteristics of the molecule in question, toxicants can cross epithelial barriers through disruption of lipid membranes, passing through ion channels, or by passive diffusion (Cappello et al., 2016; Meador et al., 1995). The ingestion of xenobiotics can also induce toxicity, given high levels of vascularization throughout the gastrointestinal tract, increased surface area of mucosal epithelia in the intestines, and the enhanced degradative capacity of resident gut microbiota, the latter of which can induce the formation of toxic metabolites (Claus et al., 2016). In addition, whereas the volume of water

passing over the gills is high, but the contact time is short, xenobiotic materials that enter the gastrointestinal tract tend to remain with the animal for a longer period of time and therefore react with additional enzymes during digestion.

Xenobiotics can be biotransformed via Phase I and Phase II enzymatic systems, in order to make compounds water soluble and thereby more easily excreted (Hao & Whitelaw, 2013; Omiecinski et al., 2011). This process can result in the formation of reactive metabolites that can manifest a number of deleterious physiological outcomes. Essentially, Phase I processes either oxidize, reduce, or hydrolyze compounds, in order to enhance exposure of polar atoms (Omiecinski et al., 2011; Santana et al., 2018). One of the most effective groups of Phase I oxidizers for xenobiotics are enzymes in the Cytochrome P450 family (CYPs), in which a variety of isoforms have evolved for processing an expanded range of compounds across taxa (Burkina et al., 2017). Phase II enzymatic processes include conjugation activities that can further enhance hydrophilicity in compounds through sulfation, acetylation, or glucuronidation (Omiecinski et al., 2011; Santana et al., 2018). Some of the most potent enzymes in this class, with regards to xenobiotic metabolism, are glutathione-S-transferases and UDP-glucuronosyl transferases (Franco & Lavado, 2019). Higher molecular weight molecules tend to be excreted into the bile for elimination, whereas lower molecular weight compounds can enter an enterohepatic circulation cycle, through which sequential de-conjugation and reduction by gut microbiota can aid in their eventual elimination (Claus et al., 2016; Meador et al., 1995). A caveat to this is the ability for higher molecular weight molecules to be sequestered into lipid-rich tissues, including eggs in gonads, where subsequent availability for metabolic transformation or mobilization is reduced (González-Doncel et al., 2017; Sammarco et al., 2013).

In order for enzymatic activation to occur, the xenobiotic ligand must first bind an adequate receptor, which may then induce pathways leading to excretion. For example, planar, hydrophobic, dioxin-like compounds, including PAHs, must bind to the PasB region of the cytosolic aryl hydrocarbon receptor (AhR; Hao & Whitelaw, 2013). The complex will then undergo conformational change, shedding scaffold proteins to expose a nuclear translocation site, and binding to a dimerization partner, the aryl hydrocarbon nuclear translocator (Stevens et al., 2009). Through subsequent attachment to the xenobiotic response element of DNA, the transcription of the AhR gene battery can commence, including upregulation of CYP1A isoforms, UDP-glucuronosyl-transferases, and glutathione-S-transferases (Hao & Whitelaw, 2013). For teleosts, activation of AHR2 leads to CYP1A induction, catalyzing Phase I metabolism of PAHs (Oziolor et al., 2014). Other toxicants may impact other receptors with differential transcription factor stimulation. For example, endocrine disruptors may bind to glucocorticoid receptors, insecticides may interact with acetylcholinesterase and metals may interfere with metal-responsive transcription factors, leading to production of metallothionein for sequestration and elimination (Bantz et al., 2018; Beg et al., 2015; Lauretta et al., 2019).

If xenobiotics and their metabolites are not rapidly cleared from an organism, or if they are produced in large quantities, these compounds can create a physiological legacy of disruption that can lead to oxidative stress, the formation of DNA adducts, immunomodulation, neuroendocrine challenge, altered metabolism, and reproductive failure (Balk et al., 2011; Hao & Whitelaw, 2013; Rahal et al., 2014). Toxic PAH metabolites can induce the production of reactive oxygen species, which at high levels can overwhelm antioxidant capacities leading to the peroxidation of lipid membranes, carbonylation of proteins, and clastogenic damage to DNA or induction of aneuploidy (Hook et al., 2014; Rahal et al., 2014). The stimulation of pro-

inflammatory immune molecules and alteration of T and B cell populations may occur throughout the acute stress response (Hao & Whitelaw, 2013; Reynaud & Deschaux, 2006; Stevens et al., 2009).

1.3 The chronic stress response in fish

When stress persists in an organism, resistance or compensation mechanisms can be engaged, through the induction of cellular defense systems and subsequent alterations to basal metabolism (Gandar et al., 2017; Petitjean et al., 2019). This can result in tradeoffs with growth and reproduction, leading to adverse outcomes on the overall success and fitness of an organism (Gandar et al., 2017). Under excessive stress, lipid stores may be mobilized to aid gluconeogenesis and protein synthesis, and to continue the production of protective molecules like antioxidants (Gandar et al., 2017; Petitjean et al., 2019).

Chronic stress can interfere with the capacity of the immune response to function normally (Padgett & Glaser, 2003). Many immune cell types, including lymphocytes, macrophages, and granulocytes, feature glucocorticoid cell surface receptors. These can bind the circulating cortisol or catecholamines during chronic stress, leading to interference with NF- κ B signaling pathways and affecting cytokine secretion, cell proliferation, and cellular trafficking, ultimately resulting in either compromised immunomodulation or immunosuppression (Padgett & Glaser, 2003; Tort, 2011). Chronic stress appears to suppress complement and lysozyme activity, reduce circulating B lymphocyte numbers and decreases the capacity to launch antibody responses (Tort, 2011).

Immunosuppression caused by PAH exposures may be due to their induction of AhR during metabolic transformation (Hao & Whitelaw, 2013). In recent years, the role of AhR as an important secondary messenger for a number of systems involved with maintaining homeostatic

and developmental processes has been discovered (Hao & Whitelaw, 2013; Stevens et al., 2009). It has also been implicated in regulation of the immune response (Esser et al., 2009). In particular, the xenobiotic-mediated activation of AhR can influence critical lymphocyte balances, resulting in shifts among T helper and T regulatory cell subsets, and leading to an overall suppression of the capacity for organisms to defend themselves from extracellular pathogens (Esser et al., 2009; Hao & Whitelaw, 2013). Stimulation of T helper 17 cells, coupled with alteration of T regulatory cells, can enhance the autoimmune response (Khan & Wang, 2018). This can have further deleterious effects on the ability of the immune system to function in external defense. In addition, B cell maturation can be adversely impacted, suppressing humoral immunity and antibody production (Hao & Whitelaw, 2013; Stevens et al., 2009).

One dramatic endpoint from chronic contaminant stress in fishes is the formation of dermal ulcerations (Murawski et al., 2014; Noga, n.d.; Vethaak et al., 2011). This is likely the result of secondary, opportunistic infections by environmentally available microbial pathogens following the immunosuppressive effects of chronic oil exposure. In a compelling experiment by Bayha et al., (2017) oil-exposed Southern Flounder were significantly more susceptible to *Vibrio* infection and mortality than non-exposed animals. They observed the now-classical signature of PAH's effects on the immune system, including IgM reduction and lower expression of genes involved with the regulation of immune cells and B cell differentiation. They hypothesized this immunosuppression was a result of the high allostatic load associated with simultaneously fighting infection while metabolizing toxic compounds (Bayha et al., 2017).

1.4 Resilience to xenobiotic exposure

Anthropogenic evolutionary change occurs when organisms adapt to synthetically derived toxicants. Examples of this includes the relatively rapid adaptation of pests to

insecticides or herbicides and antibiotic resistance in pathogens (Bantz et al., 2018; Ben et al., 2019; Heap, 2014). The accelerated rate at which these organisms acquire resistance is possible, because insecticides, pesticides, herbicides, and antibiotics are specifically designed to interact with highly specific biochemical pathways within their targeted organism. Adaptation to complex industrial pollutants, like PCBs and PAHs is more challenging, as these compounds can exert their toxic effects on multiple of physiological systems. They are not designed with an acute toxicity goal, rather an engineered purpose in manufacturing or energy production, and they typically enter the environments in complex mixtures, with potentially additive or synergistic effects (Crain et al., 2008; Martins et al., 2015; Whitehead et al., 2017). Given the intricacy of molecular pathways involved and the vast disparity in the impacts various compounds can have on physiological systems, it is not surprising that adaptation to polluted systems requires longer timescales.

In teleosts, numerous studies describe the adaptation of wild-caught fishes to chronic PCB and PAH exposure, including populations of Atlantic Killifish (*Fundulus heteroclitus*), Gulf Killifish (*Fundulus grandis*), Atlantic Tomcod (*Microgadus tomcod*), and European Flounder (*Platichthys flesus*; Aluru et al., 2015; Clark & Di Giulio, 2012; Marchand et al., 2004; Munns et al., 1997; Oziolor et al., 2014; Whitehead et al., 2017; Wirgin et al., 2011). Multiple genetic and transcriptomic evaluations of these species have linked tolerance to pollutants with desensitization of aryl hydrocarbon receptor (AhR) signaling pathways and subsequent depression of cytochrome P450 (Aluru et al., 2015; Clark & Di Giulio, 2012; Osterberg et al., 2018; Oziolor et al., 2014; Whitehead et al., 2017). However, tolerance does not appear to be exclusively correlated with AHR modification, but also with a number of genes associated along

its pathway, including those involved in cardiac development, ion channels, and oxidoreductase activity (Incardona et al., 2013; Nacci et al., 2016; Whitehead et al., 2017).

Enhanced levels of antioxidant defenses have been associated with resistant fish and insect populations (Gandar et al., 2017; Oliver & Brooke, 2018; Osterberg et al., 2018). This is not surprising, given the various ways in which oxidative stress can be induced in a stressed fish, including through production of reactive oxygen intermediaries during xenobiotic metabolism. Molecules elevated to combat oxidative stress in fish include superoxide dismutase, catalase, ascorbic acid, and glutathione, among others. Alterations in DNA repair pathways have also been observed, which could be a protective mechanism against intense oxidative stress causing lesions or breakages in DNA (Holth et al., 2008; Martins et al., 2015). The elevation of Phase II enzymes and transport proteins in resilient fish populations may underscore the importance of enhanced biotransformation pathways to facilitate rapid xenobiotic clearance (Bacanskas et al., 2004; Bard, 2000; Lohitnavy et al., 2008). Often, changes in resilient populations appear to be compensatory alterations in gene expression, rather than modifications to genes at the genetic level, however, they can incur physiological costs in terms of reduced growth rates, condition factor, and fecundity (Marchand et al., 2004).

1.5 Study Rationale

While a substantial body of work has evaluated acute and chronic effects of contaminant exposure in teleosts, much of this research has been limited to laboratory studies, primarily focused on short-term dosages of single contaminant exposures at unrealistically elevated levels, and have been performed on immature life-stages of model species. While useful in identifying potential pathways for research, these studies may have limited applications in understanding the effects of pollution exposure on wild-caught, sexually mature species, already exposed to much more dilute

levels of contaminants over their lifetimes. Furthermore, baseline health information is lacking in many offshore GoM fish species, which complicates analysis of pulse event impacts. Therefore, the goal of this study was to provide health data for wild-caught, mature, non-model fish species sampled in the GoM, using a comparative approach between individuals likely exposed to DWH crude and those from other geographic regions of the GoM where exposure was less likely.

1.6 Study Species

Two species were evaluated in this study, Golden Tilefish (*Lopholatilus chamaeleonticeps*) and Red Snapper (*Lutjanus campechanus*). Given differences in life history and documented levels of PAH exposure (Snyder et al., 2015, Pulster et al., 2020), it was anticipated that distinct patterns of basal biomarker expression would be observed between these species throughout the GoM. These difference may potentially allow an analysis of differential response between acute and chronic PAH exposure in wild-caught fish.

Golden Tilefish are a relatively long-lived, demersal, burrow-forming fish commonly found in silt-clay sediments at 200-500 m depths (Able et al., 1982; Farmer et al., 2016; Lombardi-Carlson & Andrews, 2015). Their high site fidelity and intimate association with sediments allows them to accumulate localized metals and lipophilic contaminants at comparatively higher rates than other marine species (Hall et al., 1978; Harris et al., 2012; Steimle et al., 1990). Male Golden Tilefish grow more rapidly and to larger sizes than females, and there is evidence of both gonochoristic and protogynous hermaphroditic reproductive strategies in the literature (de Mitcheson & Liu, 2008; Grimes et al., 1988; Lombardi-Carlson & Andrews, 2015; McBride et al., 2013). Northern GoM populations have a spawning period from January through June, while their Atlantic counterparts appear to spawn year-round, with peaks in the spring and summer (Lombardi et al., 2010; Palmer et al., 2004). Data regarding

reproduction strategies in the southern GoM are absent. Following the DWH spill, elevated levels of biliary and hepatic PAH levels were observed in Golden Tilefish from the northern GoM, with possible correlations to declines in condition factor and liver lipid levels (Snyder et al., 2019).

Red Snapper are an iconic, reef-associated, omnivorous fish with significant recreational and commercial importance throughout the GoM. They occupy waters 25-200 m deep and are found in association with oil rigs and pipelines (Doerpinghaus et al., 2014; Farmer et al., 2016; Gallaway et al., 2009; Williams-Grove & Szedlmayer, 2017). Red Snapper are gonochoristic broadcast spawners with peak spawning from May through August in the GoM, although reproductive biology and demographics can vary by location and associated habitat (Glenn et al., 2017; Porch et al., 2015). The species has a documented temporal decline in progression to sexual maturity over time in response to fishing pressure (Brulé et al., 2010; Kulaw et al., 2017). Following the DWH spill, a decline in condition of larval Red Snapper was observed offshore Alabama, a decline in growth in maturing fish was observed in the northern GoM (Herdter et al., 2017), along with temporal declines in hepatic EROD levels and expression of biotransformation enzymes were observed (Smeltz et al., 2017). Laboratory dosing studies of Macondo crude on juvenile Red Snapper indicated suppressive effects on immune response biomarkers and reduced growth in oil and pathogen stressed fish (Rodgers et al., 2018).

1.7 Biomarker Selection

Biomarkers are molecular indicators of biological effect or exposure and can be expressed upon pollutant contact or during a stress response (Van der Oost et al., 2003). Biomarker selection for this study was based upon several limiting factors. Given the large number of samples necessary to generate meaningful reference intervals, total analytical costs

were considered in terms of time and materials. Furthermore, as both Red Snapper and Golden Tilefish are a non-model species, biomarkers requiring species-specific antibodies or the generation of sequence information for qPCR were not evaluated. Consideration of limited sampling time in the field was critical in terms of minimizing additional organism stress associated with capture and handling, and facilitating the processing of multiple animals in a short time-frame. Sample storage while working offshore and in international waters was a fundamental consideration, particularly in limiting the ability to flash freeze tissues and to rapidly transfer fresh samples to the land-based laboratory. Finally, biomarkers were only included if they had documented utility in fish health assessments.

Biomarkers of oxidative stress were evaluated in this work. In order to adequately measure this complex system, the analysis of both antioxidants and indicators of downstream, oxidative-stress induced damage were proposed. Superoxide dismutase is a potent antioxidant and primary scavenger of superoxide radicals that aids the conversion of radicals into molecular oxygen and hydrogen peroxide for secretion (Nahrgang et al., 2009). While hydrogen peroxide is damaging due to its lack of charge and ability to diffuse readily across biological membrane, it is rapidly reduced to water and molecular oxygen by either catalase or peroxidases (Schieber & Chandel, 2014a). Damage indicators include thiobarbituric acid reactive substances (TBARS), sorbitol dehydrogenase and nuclear abnormalities. Measurement of TBARS serves as a proxy for malondialdehyde, a product released following polyunsaturated fatty acid peroxidation. While measurement of TBARS does not perfectly correspond to the extent of membrane damage, due to their ability to react with other aldehydes and carbohydrates, a body of literature has documented their utility in aquatic animal studies, and they can be measured through commercially available kits (Hook et al., 2014; Lushchak, 2011). Elevated levels of sorbitol

dehydrogenase can indicate acute hepatotoxicity and has been utilized for the detection of sublethal polycyclic aromatic hydrocarbon exposure in fish species (Dixon et al., 1987; Shailaja & D'Silva, 2003; Webb & Gagnon, 2007). Genotoxicity can be rapidly and economically assessed by quantifying micronuclei and nuclear abnormalities in erythrocytes. Although the exact etiology of different abnormality types remains to be explored, their prevalence has been linked to xenobiotic exposure in several species (Baršiene et al., 2006a; Çakal Arslan et al., 2015; Cavas et al., 2005; Hussain et al., 2018). Current hypotheses suggest their formation due to aneuploidy, chromosomal degradation, or amplification via the breakage-fusion-bridge cycle, eventually accumulating along and distorting the nuclear membrane (Weldetinsae et al., 2017).

Biomarkers of the non-specific immune response were also evaluated. Measures of hematocrit, leukocrit, and differential white blood cell counts can be indicators of fish health in peripheral blood samples and document potential immune system activation (Harr et al., 2018; Hogan et al., 2010; Kennedy & Farrell, 2008; Wedemeyer et al., 1983). Additionally, lysozyme is an important non-specific factor of immunity that confers natural resistance to bacterial infection (Ellis, 1999; Subbotkina & Subbotkin, 2003). Lysozyme levels have generally been observed to decrease with exposure to hydrocarbons and other pollutants, which can indicate immunosuppression (Bado-Nilles et al., 2009; Balfry & Iwama, 2004; Kennedy & Farrell, 2008). This can in turn cause the fish to become more susceptible to infection, leading to the development of additional pathologies (Bayha et al., 2017; Reynaud & Deschaux, 2006).

1.8 RNA sequencing

Next generation sequencing (NGS) methods have revolutionized the ability to study non-model species (Qian et al., 2014). RNA sequencing (RNA-seq) allows for the examination of the entire transcriptome of a cell, tissue, or organism under a given exposure regime or

developmental stage, including both protein-coding and non-coding RNA. This can be utilized for differential expression analysis, transcriptome mapping, single nucleotide polymorphism discovery, novel transcript discovery, and investigations of RNA splicing and post-translational modifications (Qian et al., 2014; Wang et al., 2009). Critically important for investigations in non-model species, there is no need to have a genome sequence for an organism prior to running an RNA-seq experiment (Oshlack et al., 2010; Wang et al., 2009). In addition, RNA-seq can detect a wide range of expression levels with relatively low background noise while requiring only a small amount of RNA from the original sample. The resulting data from these studies may reveal novel response pathways or individual genetic targets for further research. In the wake of the DWH event, RNA-seq has been used to evaluate alterations in PAH-exposed wild-caught killifish (*Fundulus grandis*), and laboratory exposed Red Drum (*Sciaenops ocellatus*), Southern Flounder (*Paralichthys lethostigma*) and Mahi-mahi (*Coryphaena hippurus*; Bayha et al., 2017; Whitehead et al., 2012; Xu, Khursigara, et al., 2017; Xu, Mager, et al., 2017)

1.9 Objectives

This dissertation had multiple objectives. The first objective was to establish biomarker indices for Golden Tilefish and Red Snapper in the GoM. Second, the GoM-wide variability of biomarker expression was determined in these fish, with analysis of possible correlations with PAH body burdens. In so doing, it was possible to determine whether fish caught in the vicinity of the *Deepwater Horizon* (DWH) spill exhibited an altered biomarker response in comparison to fish from other parts of the GoM. Third, a Golden Tilefish transcriptome was developed through RNA-seq and resulting differential patterns of gene expression were compared between different geographic zones of the GoM, with unique relationships to known oil extraction activities and oil spill histories.

These objectives are described in the four research chapters of this dissertation. In Chapter II, the first GoM-wide reference intervals were established for sexually mature Golden Tilefish and Red Snapper for biomarkers of oxidative stress (malondialdehyde, sorbitol dehydrogenase, sum erythrocyte nuclear abnormalities, and superoxide dismutase) and non-specific indicators of immune response (hematocrit, leukocrit, lysozyme, and differential white blood cell counts). In Chapters III and IV, putative relationships between biomarker response and polycyclic aromatic hydrocarbon (PAH) exposure in Golden Tilefish and Red Snapper were explored, respectively, along with spatial and temporal analysis of variation in biomarker response. In Chapter V, the first *de novo* assembly of the Golden Tilefish transcriptome was performed, and differential gene expression was compared in female fish caught from the De Soto Canyon, Campeche Bay, and offshore the Yucatan Peninsula. The ultimate goal of these studies was to better understand the health of fish in the GoM and to elucidate molecular targets for future health assessments of wild-caught fishes exposed to PAHs.

CHAPTER TWO:

THE ESTABLISHMENT OF REFERENCE INTERVALS FOR OXIDATIVE STRESS AND IMMUNE RESPONSE BIOMARKERS IN GOLDEN TILEFISH (*LOPHOLATILUS CAMAELEONTICEPS*) AND RED SNAPPER (*LUTJANUS CAMPECHANUS*), CAUGHT THROUGHOUT THE GULF OF MEXICO IN 2015-2017

2.1 Abstract

A lack of pre-spill baseline health indices for non-model, Gulf of Mexico (GoM) fishes complicated both immediate contaminant event response and subsequent effect evaluations. From 2015-2017, Golden Tilefish (*Lopholatilus chamaeleonticeps*, n = 255) and Red Snapper (*Lutjanus campechanus*, n = 125) were caught throughout the GoM continental shelf via demersal longline, and were evaluated for a number of health biomarkers. Following outlier removal (as determined by physical abnormalities and statistical identification), reference intervals were created for oxidative stress, genotoxicity, and immune response variables, according to the American Society for Veterinary Clinical Pathology guidelines. Species differences were evident, with Golden Tilefish having elevated baseline levels of antioxidant activity (by superoxide dismutase levels) and genotoxicity (by sum erythrocyte nuclear abnormalities) as compared to Red Snapper. Subtle sex, size, and geozone differences were apparent in mean biomarker levels for each species, although the level of statistical significance between groups did not warrant interval partitioning. The reference intervals developed here will assist future

studies of teleost health, particularly within the sampled regions, and in the event of future large-scale oil spills.

2.2 Introduction

The GoM is a large (1.6 million km²; Zaldívar-Jiménez et al., 2017) biologically diverse (more than 1,770 fish species; Álvarez Torres et al., 2017), economically important water body, under increasing insult from both anthropogenic and natural stressors (Laurent et al., 2018; Murawski et al., 2018; Rebich et al., 2011). In the United States, GoM fisheries account for 41% of marine recreational catch, over 16% of commercial fish landings, and the addition of \$7.9 billion annually to the gross domestic product (Harris, et al., 2012; Miller et al., 2018). Additionally, 27% of United States domestic oil production is derived from the GoM, while Mexico extracts significant petroleum resources from the southern basin, including more than 2 million barrels of crude oil produced from the Campeche region each day (García-Cruz et al., 2018; Sammarco et al., 2013; Scholz-Böttcher et al., 2008).

There is continual deposition of organic and inorganic pollutants into the GoM from a variety of sources. The 47 estuaries bordering the GoM deposit wastes from the industrial, agricultural, and urban activities prevalent in the drainage basin, and significant pollutants are released through major rivers including the Mississippi and Coatzacoalcos (García-Cruz et al., 2018; Harris et al., 2012; Perry et al., 2015; Ponce-Vélez et al., 2006). Hydrocarbons are released into the waters by over 22,000 natural seeps and from shipping and oil and gas extraction activities (Daneshgar et al., 2016; Joye et al., 2014; Macdonald, 1993). Mercury and other contaminants are continually carried into and dispersed throughout the GoM by the Loop Current, and atmospheric deposition of mercury is higher in this region than in other parts of the world (Harris et al., 2012). Chronic exposure to these pollutants can be detrimental to the

valuable and diverse organisms living in these waters, as reflected in the expression of health markers (Aluru et al., 2011; Daneshgar et al., 2016; Miller et al., 2018; Serra-Sogas et al., 2008; Whitehead et al., 2017; Wirgin et al., 2011). In the wake of large pulse events, like the 2010 *Deepwater Horizon* oil spill, it has become evident that a lack of baseline health data for species living in the GoM can complicate restoration efforts and the analysis of event driven impact studies (Granneman et al., 2017; Lubchenco et al., 2012; Smeltz et al., 2017).

Biomarkers are molecular indicators of biological effect or exposure and can be elevated or depressed expressed upon pollutant contact or during a stress response (Livingstone, 2007; Van der Oost et al., 2003). Biomarkers of oxidative stress, genotoxicity, and immune status are commonly evaluated to determine impacts of hydrocarbon, metals, and wastewater exposure on fishes (Ameur et al., 2015; Benedetti et al., 2015; Javed et al., 2017). For example, increased levels of malondialdehyde (MDA; a marker of lipid peroxidation) and superoxide dismutase (SOD; an antioxidant) in tissue homogenate or plasma, can demonstrate a response to the proliferation of reactive oxygen species commonly observed after exposure to toxicants in fishes (Crowe et al., 2014; Martins et al., 2015; Nahrgang et al., 2009). The elevation of sorbitol dehydrogenase (SDH) can indicate acute hepatotoxicity and has been utilized for the detection of sublethal polycyclic aromatic hydrocarbon (PAH) exposure in fish species (Dixon et al., 1987; Shailaja & D'Silva, 2003; Webb & Gagnon, 2007). Chronic oxidative stress and exposure to genotoxic pollutants can lead to a failure of chromosome separation during mitosis, and the subsequent formation of micronuclei (MN) or other nuclear abnormalities (NA) in teleost erythrocytes (Baršiene et al., 2006a; Çakal Arslan et al., 2015; Cavas et al., 2005; Hussain et al., 2018). The prevalence of these abnormal chromatin bodies in the cell cytoplasm can activate the innate immune response (Gekara, 2017; MacKenzie et al., 2017).

Measures of hematocrit (HCT), leukocrit (LCT), and differential white blood cell (DWBC) counts can be used as both general indicators of fish health in peripheral blood samples and to document potential immune system activation (Harr et al., 2018; Hogan et al., 2010; Kennedy & Farrell, 2008; Wedemeyer et al., 1983). In addition, lysozyme (LYS) is an important non-specific factor of immunity that confers natural resistance to bacterial infection (Ellis, 1999; Subbotkina & Subbotkin, 2003). Lysozyme levels have generally been observed to decrease with exposure to hydrocarbons and other pollutants, which can indicate immunosuppression (Bado-Nilles et al., 2009; Balfry & Iwama, 2004; Kennedy & Farrell, 2008). This can in turn cause the fish to become more susceptible to infection, leading to the development of additional pathologies (Bayha et al., 2017; Reynaud & Deschaux, 2006).

While the targets described above have documented utility in pollution studies, many biomarkers have variable responses depending upon the species, biometrics, and sex of the organism studied, and upon the environmental conditions in which the fish are found (Balfry & Iwama, 2004; Fonseca et al., 2011; Rehberger et al., 2017; Wunderlich et al., 2015). Reference intervals are utilized to describe likely response values in a biomarker for 95% of the healthy population (Geffré et al., 2009). The identification of outliers in a monitoring study can then indicate compromised individuals (Harr et al., 2018). Therefore, completion of baseline health evaluations of non-model species in order to generate reference intervals for biomarkers of interest can significantly assist in the interpretation of subsequent data (Friedrichs et al., 2012; Matsche et al., 2014).

In this study, reference intervals were established for biomarkers of oxidative stress and immune response in Golden Tilefish (*Lopholatilus chamaeleonticeps*) and Red Snapper (*Lutjanus campechanus*), caught throughout the continental shelf of the GoM in 2015-2017.

Golden Tilefish are demersal, benthic-feeding, long-lived, burrow-forming fish with high site fidelity, commonly found in silt-clay sediments at depths of 200-500 meters (Able et al., 1982; Farmer et al., 2016; Lombardi-Carlson & Andrews, 2015; Steimle et al., 1990). Given their close association with the sediment, Golden Tilefish are known to bioaccumulate metals and other pollutants at a higher rate than other marine fishes (Hall et al., 1978; Harris et al., 2012; Snyder et al., 2015). Red Snapper are an iconic, reef-associated, omnivorous fish with significant recreational and commercial importance throughout the GoM. They occupy waters of 25-100 meters and can frequently be found around structured habitat, including oil rigs and pipelines (Doerpinghaus et al., 2014; Farmer et al., 2016; Gallaway et al., 2009; Williams-Grove & Szedlmayer, 2017). The generation of reference intervals for these non-model species will assist interpretation of future biomarker measurement in these animals from the GoM and elsewhere and provides baseline data for comparison in the event of another pulse stress event.

2.3 Methods

2.3.1 Sampling

Fishes were obtained from the GoM (Fig. 2.1) via demersal longline, aboard the *R/V Weatherbird II* from July-August 2015-2017, in accordance with state and federal permitting (Murawski et al., 2018). Immediately upon landing on deck, animals were sacrificed by pithing, each fish was weighed, and standard, fork, and total length measurements were taken. Within 15 minutes of landing on deck, 2-4 mL of whole blood was collected from each specimen into 4mL lithium heparin tubes (BD Vacutainer, Franklin Lakes, NJ) via caudal dissection and placed on ice. Plasma was separated from the whole blood within one hour of collection, by centrifuging the tubes at 1600 x g for 15 minutes, and the supernatant was stored at -20°C, prior to long-term storage at -80 °C. Fish were sexed macroscopically and internal and external evaluations were

performed to document any abnormalities. All station and catch data are available in Appendix A.

2.3.2 Superoxide dismutase

Levels of plasma SOD were determined in the laboratory using commercial kits according to manufacturers' protocols (Cayman Chemicals, Ann Arbor, MI, SOD Assay Kit #706002).

2.3.3 Malondialdehyde

Levels of plasma MDA (via measurement of thiobarbituric acid reactive substances) were determined in the laboratory using commercial kits according to manufacturers' protocols (Cayman Chemicals, Ann Arbor, MI, TCA Assay Kit #700870).

2.3.4 Sorbitol dehydrogenase

Plasma SDH was measured in the laboratory according to methods developed by Dixon (1987) and modified by others (Dixon et al., 1987; Pandelides et al., 2014; Shailaja & D'Silva, 2003; Webb & Gagnon, 2007). Briefly, 20 μL of each sample was added to a 96-well plate well, in triplicate, followed by the addition of 180 μL of 1.28 μM NADH (Sigma) in 0.1 M Tris buffer (Fisher Scientific, Norcross, GA) at pH 7.5. The plate was protected from light exposure and incubated at room temperature for 10 minutes. The reaction was initiated by adding 40 μL of 4 M D-fructose (Fisher) to each well, and the absorbance was read initially and after 120 seconds at 340 nm in an ELISA plate reader. Total milli-international units (mIU) were calculated as: [(change in absorbance over 1 minute) x (reaction volume) / (micromolar extinction coefficient of NADH x sample volume)].

2.3.5 Micronuclei and nuclear abnormalities

Within two hours of collection, well-mixed whole blood was collected into a microhematocrit capillary tube. Duplicate blood smears were prepared via standard methods. Slides were air dried for 24 hours and subsequently fixed in 95% methanol (Sigma-Aldrich, St. Louis, MO) for 10 minutes, with long-term storage at room temperature.

Slides were stained with 10% Giemsa solution (Sigma-Aldrich) for 20 minutes, rinsed briefly with deionized water, and air dried. Using oil immersion microscopy, one thousand erythrocytes were evaluated per fish, in duplicate, for the presence of micronuclei and nuclear abnormalities, classified as: binucleation, nuclear blebs, nuclear buds, and notched nuclei. Micronuclei were non-refractive, separated from the nucleus with the same staining coloration, and had a diameter of approximately 1/3 - 1/20 the nuclear diameter (Baršiene et al., 2006b; Carrasco et al., 1990; Furnus et al., 2014). Binucleated cells had two nuclei of approximately the same size and staining shade. Nuclear buds were small, nearly circular masses still attached to the nucleus, and nuclear blebs were irregularly shaped protrusions from the nucleus (Baršiene et al., 2006b; Bolognesi et al., 2006; Fenech, 2000). Notched nuclei featured invaginations into the nucleus, which lacked nuclear material (Ayllon & Garcia-Vazquez, 2000; Bolognesi et al., 2006). For the purpose of reference interval generation, the sum of all micronuclei and nuclear abnormalities ($\sum(\text{NA})$) in each sample was calculated and averaged across duplicates.

2.3.6. Hematocrit and leukocrit

As described above, whole blood was collected into lithium heparin tubes, the sample was well-mixed by inversion, and within two hours of collection it was distributed into duplicate glass microhematocrit capillary tubes. The capillary tubes were spun at 2300 x g for one minute

(HemataStat II Hematocrit Analyzer, San Antonio, TX, EKF Diagnostics) and HCT and LCT values were evaluated using a manual hematocrit reader card.

2.3.7 Differential white blood cell counts

Two additional blood smears were prepared, per fish, as described above. Prior to visual scoring, slides were stained with May-Grunwald-Giemsa solution (Sigma-Aldrich) for five minutes, followed by a 90-second incubation in phosphate buffer solution (pH 7.5), and a 20 minute stain in 5% Giemsa solution (Sigma-Aldrich). After a brief rinse with deionized water, slides were allowed to air dry for thirty minutes. One hundred white blood cells (lymphocytes, thrombocytes, monocytes, basophils, eosinophils, and neutrophils) were classified per animal, in duplicate, using oil immersion microscopy. White blood cell morphology for both species was similar to that described in other teleosts (Ellis, 1977; Tavares-Dias & Moraes, 2007). Due to very low prevalence, basophils and eosinophils were later excluded from the generation of reference intervals.

2.3.8 Lysozyme

Plasma LYS was determined in the laboratory using a turbidimetric assay developed by Parry (1965) and modified for a 96-well microplate (Bado-Nilles et al., 2009; Grinde et al., 1988; Parry et al., 1965; Perrault et al., 2017). A suspension of 0.2 mg mL⁻¹ *Micrococcus lysodeikticus* (Sigma-Aldrich) was prepared in sodium phosphate buffer (10 mM, pH 6.4). Twenty microliters of plasma was placed into each well of a 96-well plate, with each sample run in triplicate, followed by the addition of 20 µL sodium phosphate buffer and 180 µL of the bacterial suspension. Absorbance was monitored over 10 minutes at 520 nm using an ELISA microplate reader. The unit of enzyme activity was defined as the amount of the enzyme that caused a

decrease in the absorbance at a rate of $0.001 \text{ minute}^{-1}$. Values were converted to mg mL^{-1} using a linear reference curve established by a hen egg white lysozyme standard (Sigma-Aldrich).

2.3.9 Data analysis

Reference intervals were calculated using Reference Value Advisor (<http://www.biostat.envt.fr/reference-value-advisor/>) in accordance with the American Society for Veterinary Clinical Pathology (ASVCP) guidelines. Any fish with documented physical abnormalities or dermal lesions at the time of collection was excluded from further analysis. Datasets were tested for normality by the Anderson-Darling method and outliers were removed from each variable, as determined by Tukey and Dixon-Reed tests. Samples were removed from further analysis if they were identified as an outlier for any biomarker during initial analysis, as this may be indicative of aberrant health status.

Reference intervals were calculated using pooled samples from all stations and nonparametric methods when sample size was ≥ 120 fish after outlier removal, or using robust methods when sample size was ≥ 40 fish and < 120 fish. The 90% confidence intervals were calculated for upper and lower estimates of each variable, along with the minimum, maximum, mean, median, and standard deviation. The Shapiro-Wilk test was then used to screen for normality and, depending on the results, either Kruskal-Wallis (for nonparametric data) or one-way ANOVA tests with Tukey HSD post-hoc analysis (for normal data), were conducted to determine if species, sex, total length, standard weight, depth, temperature, or geographic zone (geozone) of collection predicted variable response. If significant differences were detected in the datasets based upon the above classifiers ($p < 0.05$), the need for partitioning data into subsets was evaluated, conservatively, by calculating whether the difference between subclass means was greater than 25% of the 95% confidence interval for the entire dataset (Walton,

2001). All data are available at <https://data.gulfresearchinitiative.org/pelagos-symphony/data/R6.x805.000:0083> and <https://data.gulfresearchinitiative.org/pelagos-symphony/data/R6.x805.000:0078>.

2.3.10 Geozone definitions

Four geozones were defined for Golden Tilefish and three for Red Snapper. These included NC (north central), NW (northwest), SW (southwest) and YP (Yucatan Peninsula; Fig. 2.1). Due to low sample size off the West Florida Shelf for both species, and low sample size off YP for Red Snapper, fish from these regions were excluded from geozone analysis. All regions sampled were populated with man-made structures, including significant oil and gas pipelines and platforms, especially in the NC, NW, and SW geozones (Murawski et al., 2018).

2.4 Results

A total of 255 Golden Tilefish were analyzed in this study, including 157 females, 55 males, and 43 fish for which sex could not be determined by macroscopic evaluation. These specimens had an average total weight (TW) of 3.477 ± 2.517 kg and an average standard length (SL) of 54 ± 12 cm (biometrics data available in Appendix B). Golden Tilefish were caught at an average depth of 288.5 ± 60.2 m and temperature of $12.7 \pm 1.8^\circ\text{C}$. A total of 125 Red Snapper were analyzed (65 female, 58 male, two undetermined sex), with an average total weight of 4.529 ± 2.037 kg and an average standard length of 54 ± 9 cm (biometrics data available in Appendix B). Red Snapper were caught at an average depth of 71.6 ± 22.5 m and temperature of $21.4 \pm 1.6^\circ\text{C}$. Neither temperature nor depth had a significant impact on biomarker expression in either species.

Variability in blood yields by fish and occasional blood coagulation or hemolysis of samples led to inconsistent numbers of specimens measured for each biomarker for both Golden

Tilefish (Table 2.1) and Red Snapper (Table 2.2). Thirty-six Golden Tilefish and four Red Snapper samples were identified as statistical outliers in at least one biomarker for each species and were excluded from all datasets as potentially unhealthy or non-representative animals (Friedrichs 2012). When comparing species, statistically significant differences were observed in reference value means, with Golden Tilefish having higher levels (Fig. 2.2) of SOD ($p < 0.001$), $\Sigma(\text{NA}; p < 0.001)$, HCT ($p < 0.001$), thrombocyte count ($p = 0.003$), and LYS ($p < 0.001$). Red Snapper demonstrated higher values (Fig. 2.3) for SDH ($p = 0.008$) and monocyte count ($p < 0.001$).

Within species, sex differences were statistically significant in reference interval means for Golden Tilefish: SOD (females higher, $p = 0.002$), lymphocytes (females higher, $p = 0.002$), thrombocytes (males higher, $p = 0.002$), and LYS (males higher, $p = 0.005$, Table 2.3). Sex-specific statistical differences were observed in Red Snapper MDA (males higher, $p < 0.001$), LCT (females higher, $p = 0.006$), and LYS (males higher, $p = 0.005$; Table 2.3). Standard length and total weight quartiles were also calculated and compared for each variable, by species. Golden Tilefish in the upper quartiles of length ($SL > 64$ cm) and weight ($TW > 4.543$ kg) had lower mean levels of SOD (Fig. 2.4) and SDH (Fig. 2.5). Red Snapper in the upper quartiles of length ($SL > 60$ cm) and weight ($TW > 5.412$ kg) had higher mean neutrophil counts (Fig. 2.6).

Subtle geozone differences in biomarker mean expression values were evident for both species. Golden Tilefish caught in SW had elevated mean values of SDH compared to those from NC ($p < 0.001$), NW ($p = 0.031$), and YP ($p < 0.001$; Fig. 2.7). In addition, mean LYS was elevated in animals from the NW region, compared to the NC ($p = 0.02$) and SW ($p < 0.001$), while LCT was lower in the NW compared to NC ($p < 0.001$), SW ($p < 0.001$), and YP ($p = 0.016$). Red Snapper from the NC geozone had elevated levels of SOD ($p = 0.017$), $\Sigma(\text{NA}; p =$

0.004, Fig. 2.8), HCT ($p = 0.027$), LCT ($p < 0.001$) and lymphocyte count ($p < 0.001$) than Red Snapper from the NW region, and lower thrombocyte ($p < 0.001$) and neutrophil counts ($p < 0.001$, Fig. 2.9) than fish from NW. In addition, Red Snapper from the SW geozone had elevated levels of LCT ($p < 0.001$) and lymphocyte count ($p < 0.001$), as opposed to fish from NW.

2.5 Discussion

The appropriate statistical methods for partitioning of reference interval data into subclasses has been discussed in human and model organism clinical chemistry, where molecular function is understood and sample sizes are large (Ceriotti et al., 2009; E. K. Harris & Boyd, 1990; Lahti et al., 2002, 2004). However, quantifying the clinical significance of these separations is challenging in non-model organisms where physiology is not well understood, samples are both expensive and difficult to obtain, and dividing the dataset further may result in subsets too small to deliver biologically significant results (Ceriotti et al., 2009; Walton, 2001). Therefore, in organisms with limited samples are available, emphasis is placed on the conservative removal of outliers and on retaining as much of the original, high quality data as possible (Walton, 2001).

In this study, each variable was evaluated for variation based upon a suite of conditions (species, sex, standard length, total weight, and geozone), by either ANOVA and Tukey HSD post-hoc analysis or Kruskal-Wallis testing, depending upon the normality of the data set by Shapiro-Wilks testing. The p-value was reported for statistically significant differences in means, however, partitioning of reference intervals was not justified, as the difference between subclass means was not greater than 25% of the 95% confidence interval of the dataset under any condition (Walton, 2001). Furthermore, in a field study on wild organisms, equal sample

selection by sex at each location is impossible. Therefore, different numbers of fish of each sex, standard length, or total weight were caught at various stations throughout the GoM. While this is valuable in terms of amassing a larger reference interval, subtle differences among groups may be difficult to characterize due to these sampling limitations.

Species differences in biomarker reference intervals were expected, given the different life histories, habitats, metabolism, pollutant body burdens, and prey items of Golden Tilefish and Red Snapper in the GoM. Reference intervals for SOD, Σ NA, HCT, monocyte count, and LYS, were statistically different between species. The elevated reference intervals for the sum of erythrocyte nuclear abnormalities, indicative of genotoxicity, in Golden Tilefish (0.5-47.9/1000 erythrocytes) as compared to Red Snapper (0-3.08/1000 erythrocytes) is compelling, given the known link between DNA and chromosomal damage and exposure to metals and petrochemicals (Fig. 2.2; Baršiene et al., 2006b; Çakal Arslan et al., 2015). This increased prevalence of nuclear abnormalities in this species, therefore, may correlate with previous studies citing elevated toxicants, and especially PAH levels, observed in Golden Tilefish (Hall et al., 1978; R. Harris et al., 2012; Sinkus et al., 2017; Snyder et al., 2015). The elevation of SOD in Golden Tilefish as compared to Red Snapper may also be indicative of their increased exposure to toxic elements, leading to subsequent enhancement of protective mechanisms against incurred oxidative stress (Fig. 2.2; Whitehead et al., 2017).

Within Golden Tilefish, females had higher levels of SOD and males had slightly higher mean levels of LYS, along with differences in DWBC proportions (Table 2.3). It should be noted, however, that the sampling size for females (n = 157) was greater than males (n = 55), which could have introduced greater variability in the results. In addition, determining the sex and reproductive status of tilefish based upon gross morphology has been historically

complicated. It has been established that male tilefish grow more rapidly and to a larger size than females, however, there is evidence of both gonochoristic and protogynous hermaphroditic reproductive strategies in the literature (de Mitcheson & Liu, 2008; Lombardi-Carlson & Andrews, 2015; McBride et al., 2013). For female tilefish from the GoM, size and age at 50% maturity is 34.4 cm total length and 2 years, with a spawning period from January-June, while males show seasonal synchrony (Lombardi et al., 2010). Other studies in the Atlantic have demonstrated year-round spawning with a peak period in the spring and summer (Lombardi et al., 2010; Palmer et al., 2004). In this study, Golden Tilefish were caught at the end of the predicted spawning season, and the majority showed visible displays of sexual maturation. It is possible that energy displacement during spawning could have led to altered expression of the enzymes in fish. It is not unusual for LYS to fluctuate with the reproductive cycle of females in other fish species (Balfry & Iwama, 2004; Fletcher et al., 1977; Ghafoori et al., 2014). In addition, previous studies have documented sex-based alterations in the expression of xenobiotic metabolizing genes, suggesting that oxidative stress management may be related to sex as well (Vega-López et al., 2007; Winzer et al., 2001).

Red Snapper are gonochoristic broadcast spawners that reach peak spawning potential from May to August in the GoM, although reproductive biology and demographics can vary by location and associated habitat (Glenn et al., 2017; Porch et al., 2015). Females become sexually mature at two years of age, with 50% maturity at a total length of 31.5 cm. The species has a shown a slowing progression to sexual maturity in response to fishing pressure (Brulé et al., 2010; Kulaw et al., 2017). Given the size of fish collected and time of year they were sampled, it is possible that hormone fluctuation during reproductive cycles drove the discrepancies in MDA, LCT, and LYS response in male versus female fishes in this study (Table 2.3).

Both Golden Tilefish and Red Snapper have well-defined age-length relationships, with larger fish generally having increased pollutant body burdens (Kulaw et al., 2017; Lombardi-Carlson & Andrews, 2015). Golden Tilefish in the upper quartiles of standard length and total weight had lower levels of SOD (Fig. 2.4) and SDH (Fig. 2.5) compared to smaller fish. Suppression of SOD has been linked to prolonged exposure to contaminants and the overexpression of reactive oxygen species in tissues (Karadag et al., 2014; López-López et al., 2011; Ozmen et al., 2004). Therefore, it is possible that the larger, older fish, are displaying biochemical signatures of long-term exposure to the low levels of contaminants documented in the vicinity of their burrows (Botello et al., 2015; Celis-Hernandez et al., 2017; Sammarco et al., 2013). Larger Red Snapper displayed lower LCT but an elevated proportion of neutrophils (Fig. 2.6), suggesting a slightly altered immune response in these animals.

Slight geozone discrepancies were expected, given the variety of toxicant exposure regimes at each station. This includes influence of the Mississippi River in the NC region, and by the Coatzacoalcos, Jamapa, and Pánuco rivers in the SW (Celis-Hernandez et al., 2017; García-Cruz et al., 2018; Perry et al., 2015; Wise et al., 2014). There are also several industrialized cities bordering the GoM with historically elevated pollutant loads (Miller et al., 2018; Ponce-Vélez et al., 2006). While currents have been demonstrated to distribute anthropogenic pollutants throughout the GoM, localized impacts are possible (Botello et al., 2015; Sammarco et al., 2013). After outlier removal, the majority of biomarkers did not vary in expression between geozones, suggesting that fish caught within all regions are experiencing similar types of stress. A notable exception to this is the elevation of SDH in Golden Tilefish caught in the SW geozone, as compared to those from the remainder of the GoM, indicating increased liver damage in these animals (Fig. 2.7). Among Red Snapper, an increase in the prevalence of nuclear abnormalities

was observed in the NC geozone (Fig. 2.8), indicative of exposure to genotoxicants, and neutrophil count was elevated in the NW (Fig. 2.9), suggesting an activated immune response to a localized challenge.

2.6 Conclusions

This study provides the first reference interval data for select oxidative stress, genotoxicity, and immune response biomarkers in Golden Tilefish and Red Snapper caught within the GoM. The biomarkers evaluated in this study are economical and practical indicators that can be characterized in field-caught fish when immediate bleeding is possible and samples can be stored at -20°C prior to returning to the laboratory. Each fish and geographic location is subject to its own unique milieu of pollutants, natural stressors, and physiologic differences. This may have been reflected in statistically significant differences in means among certain variables by sex, size, or sampling location, although these discrepancies were not severe enough to warrant partitioning of intervals after adoption of conservative methods. Improvements to the intervals are possible by additional sampling, however, by excluding outliers, these data provide a preliminary baseline for future, targeted evaluations of health in these species in the GoM.

2.7 Tables

Table 2.1 Golden Tilefish reference interval statistics. Data includes malondialdehyde (MDA), superoxide dismutase (SOD), sorbitol dehydrogenase (SDH), sum micronuclei and nuclear abnormalities (Σ NA), hematocrit (HCT), leukocrit (LCT), lymphocytes (Lymph), thrombocytes (Thromb), monocytes (Mon), neutrophils (Neut), and lysozyme (LYS). The method used to generate the reference interval was dependent upon the number of fish included in the calculation after outliers were removed, as outlined in the ASVCP guidelines, and was classified as either nonparametric (N) or robust (R).

Biomarker	Units	Total (n)	Excluding outliers (n)	Mean	SD	Median	Min	Max	Reference Interval	Lower Limit 90% CI	Upper Limit 90% CI	Method
MDA	μ M	245	210	23.84	11.96	20.7	7.05	69.43	8.71 - 58.51	7.76 - 10.24	47.61 - 67.71	N
SOD	U/ mL	245	210	0.241	0.09	0.241	0.039	0.474	0.082 - 0.431	0.041 - 0.087	0.410 - 0.445	N
SDH	mIU	231	195	1.879	1.717	1.29	0	7.742	0 - 5.806	0	5.806 - 7.097	N
Σ NA	‰	245	211	13.37	11.69	9.5	0	52.5	0.5 - 47.9	0 - 1	40.5 - 52.5	N
HCT	%	255	224	40.02	6.94	40	18.5	60	23.94 - 53.00	20.00 - 27.50	50.50 - 57.50	N
LCT	%	255	221	0.42	0.37	0.5	0	1.5	0 - 1.25	0	1.00 - 1.50	N
Lymph	%	243	211	74	10.9	76	41	92.5	49.8 - 90.2	41.0 - 52.5	89.0 - 92.5	N
Thromb	%	243	211	18.2	10.3	16	0.5	52.5	4.00 - 41.25	2.5 - 5.0	38.5 - 51.0	N
Mon	%	243	212	6.1	3.3	5.5	0	18	1.5 - 14.5	0 - 1.5	13.5 - 16.5	N
Neut	%	243	212	1.7	1.9	1	0	8.5	0 - 7.34	0	6.00 - 8.50	N
LYS	mg/ mL	244	209	58	23.79	54.91	15.36	143.32	21.28 - 115.6	17.49 - 23.11	104.06 - -136.22	N

Table 2.2 Red Snapper reference interval statistics. Data includes malondialdehyde (MDA), superoxide dismutase (SOD), sorbitol dehydrogenase (SDH), sum micronuclei and nuclear abnormalities (Σ NA), hematocrit (HCT), leukocrit (LCT), lymphocytes (Lymph), thrombocytes (Thromb), monocytes (Mon), neutrophils (Neut), and lysozyme (LYS). The method used to generate the reference interval was dependent upon the number of fish included in the calculation after outliers were removed, as outlined in the ASVCP guidelines, and was classified as either nonparametric (N) or robust (R).

Biomarker	Units	Total (n)	Excluding outliers (n)	Mean	SD	Median	Min	Max	Reference Interval	Lower Limit 90% CI	Upper Limit 90% CI	Method
MDA	μ M	108	105	27.86	21.71	19.05	7.1	120.18	6.94 - 80.53	0 - 7.15	66.47 - 94.25	R
SOD	U/mL	107	104	0.133	0.073	0.123		0.374	0.025 - 0.309	0.170 - 0.034	0.276 - 0.345	R
SDH	mIU	107	104	2.351	1.75	1.935	0	9.677	0 - 6.895	0	5.766 - 9.677	R
Σ NA	%	116	113	0.65	0.86	0.5	0	4	0 - 3.08	0	2.5 - 4.0	R
HCT	%	125	125	34.59	9.55	36.5	2.5	59	11.05 - 51.75	2.5 - 18.0	48.5 - 59.0	N
LCT	%	125	123	0.47	0.47	0.5	0	2	0 - 1.5	0	1.25 - 2.00	N
Lymph	%	112	110	76.44	8.9	77.75	54.5	91	55.27 - 91.13	51.79 - 57.81	89.61 - 91.98	R
Thromb	%	112	110	14.44	8.42	13.5	1	37.5	1.61 - 35.23	1.01 - 2.64	32.34 - 39.15	R
Mon	%	112	110	7.8	3.39	7.5	0.5	18.5	1.95 - 15.26	1.40 - 2.57	13.95 - 16.61	R
Neut	%	112	110	1.36	1.65	0.5	0	7.5	0 - 6.61	0	5.1 - 7.5	R
LYS	mg/mL	117	114	44.41	21.2	39.06	0.33	108.39	12.58 - 97.54	0.33 - 17.93	85.89 - 108.39	R

Table 2.3 Statistically significant differences ($p < 0.05$) in mean values for biomarkers by macroscopically identified sex. Determined by Kruskal-Wallis testing after confirming lack of normality by Shapiro-Wilks.

Biomarker	Units	Species	Mean (\pm Standard Deviation)	
			Females	Males
SOD	U/mL	Golden Tilefish	0.250 \pm 0.097	0.201 \pm 0.071
Lymph	%	Golden Tilefish	75.205 \pm 10.262	69.149 \pm 12.280
LYS	mg/mL	Golden Tilefish	56.760 \pm 20.792	66.992 \pm 29.332
MDA	μ M	Red Snapper	20.188 \pm 15.061	37.017 \pm 24.945
LCT	%	Red Snapper	0.589 \pm 0.485	0.344 \pm 0.420
Thromb	%	Golden Tilefish	16.943 \pm 9.582	22.862 \pm 11.910
LYS	mg/mL	Red Snapper	38.356 \pm 20.438	51.098 \pm 20.406

2.8 Figures

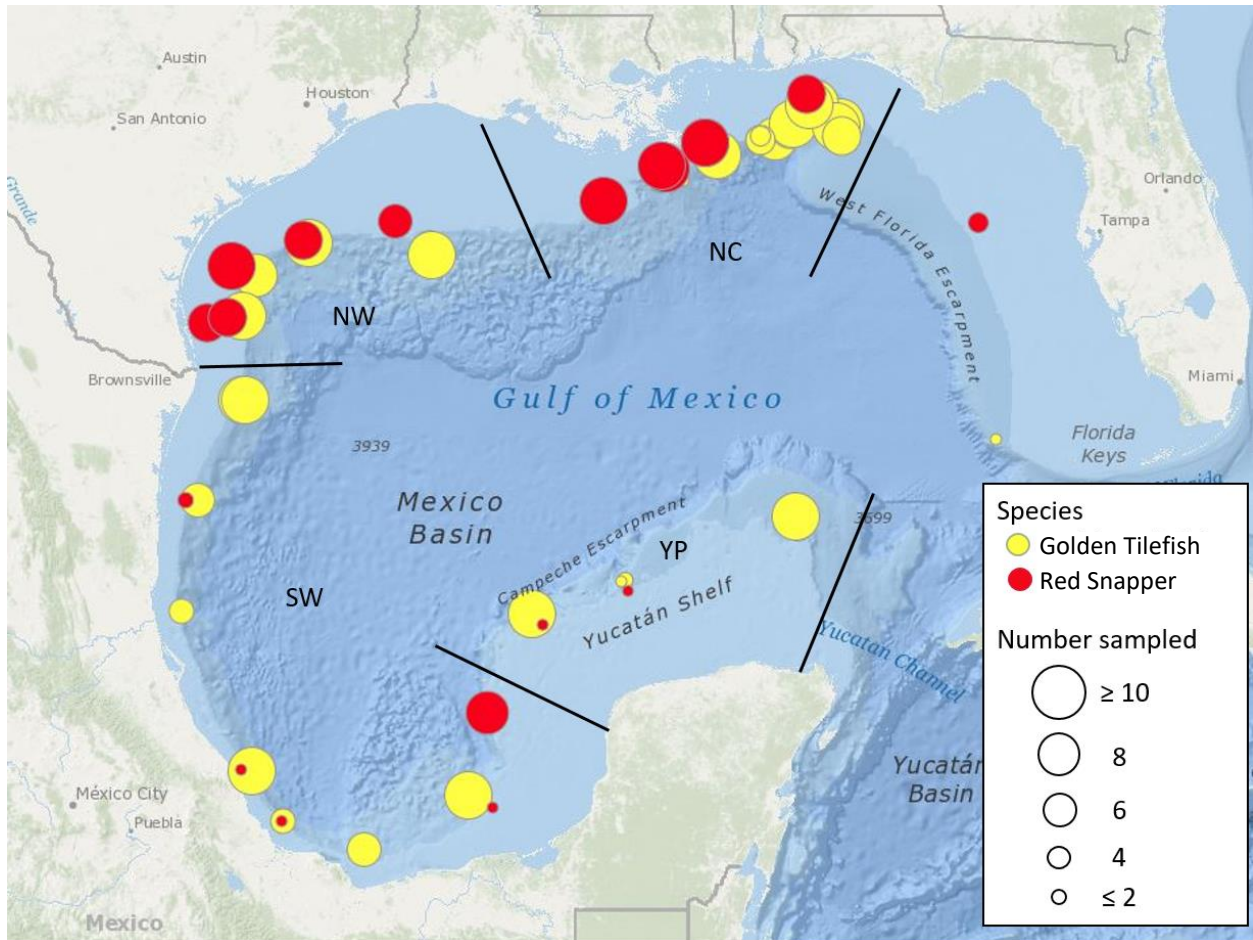


Figure 2.1: All demersal longline stations included in this study, fished in the months of July-August in 2015-2017, color-coded by species. The diameter of the station marker is linearly scaled with the number of fish caught at that location, with the smallest circle indicating $n \leq 2$ and the largest $n \geq 10$. Coordinates, station identifiers, average depth, average temperature, year sampled, and number of fish caught at each station can be found in Appendix A. Geozones are specified as north central (NC), northwest (NW), southwest (SW), and Yucatan Peninsula (YP).

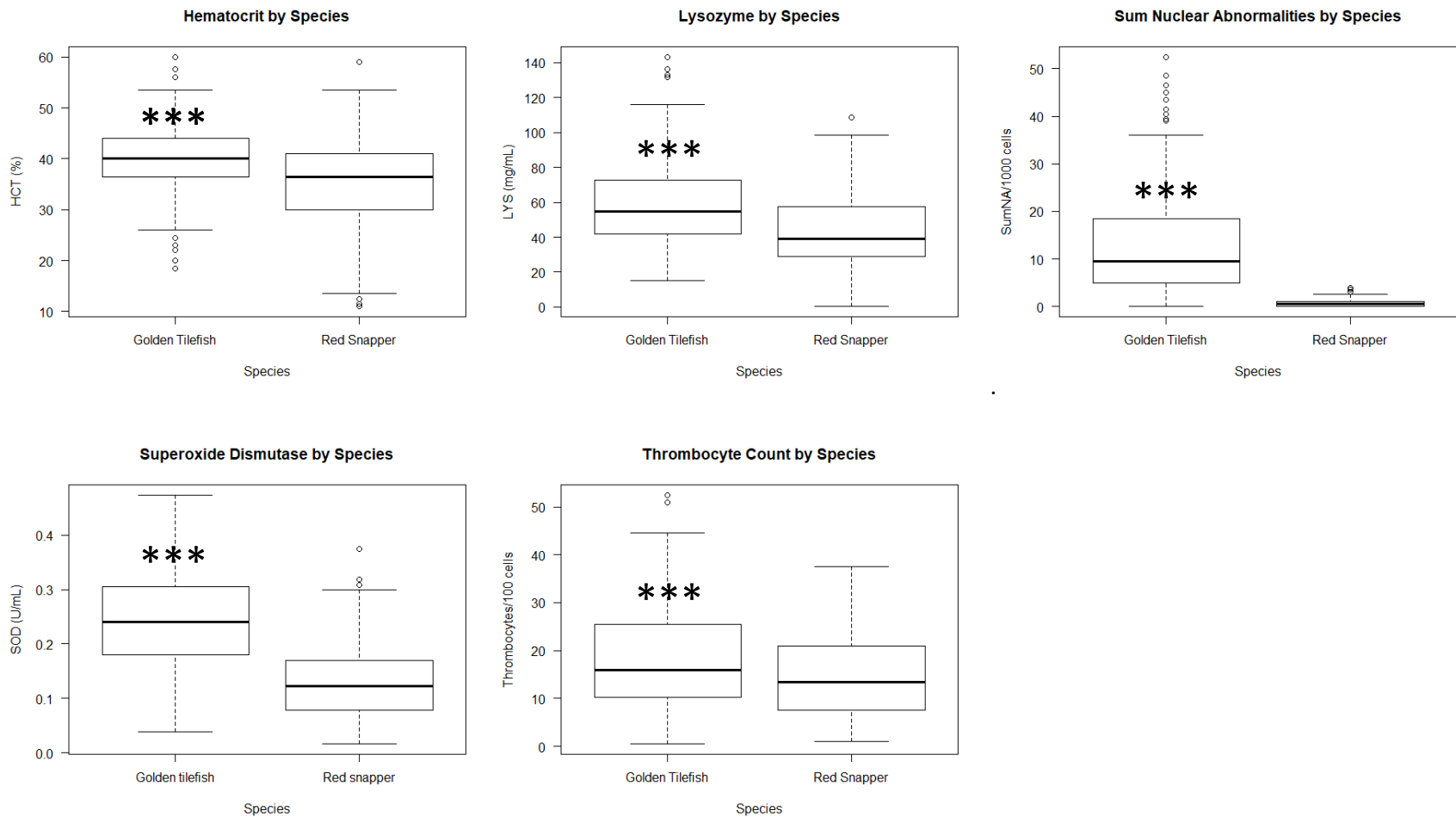


Figure 2.2: Biomarkers for which Golden Tilefish reference intervals were significantly higher than Red Snapper intervals. Statistically significant differences ($p < 0.05$) are marked with asterisks (***) as determined by Kruskal-Wallis analysis after testing for normality by Shapiro-Wilks.

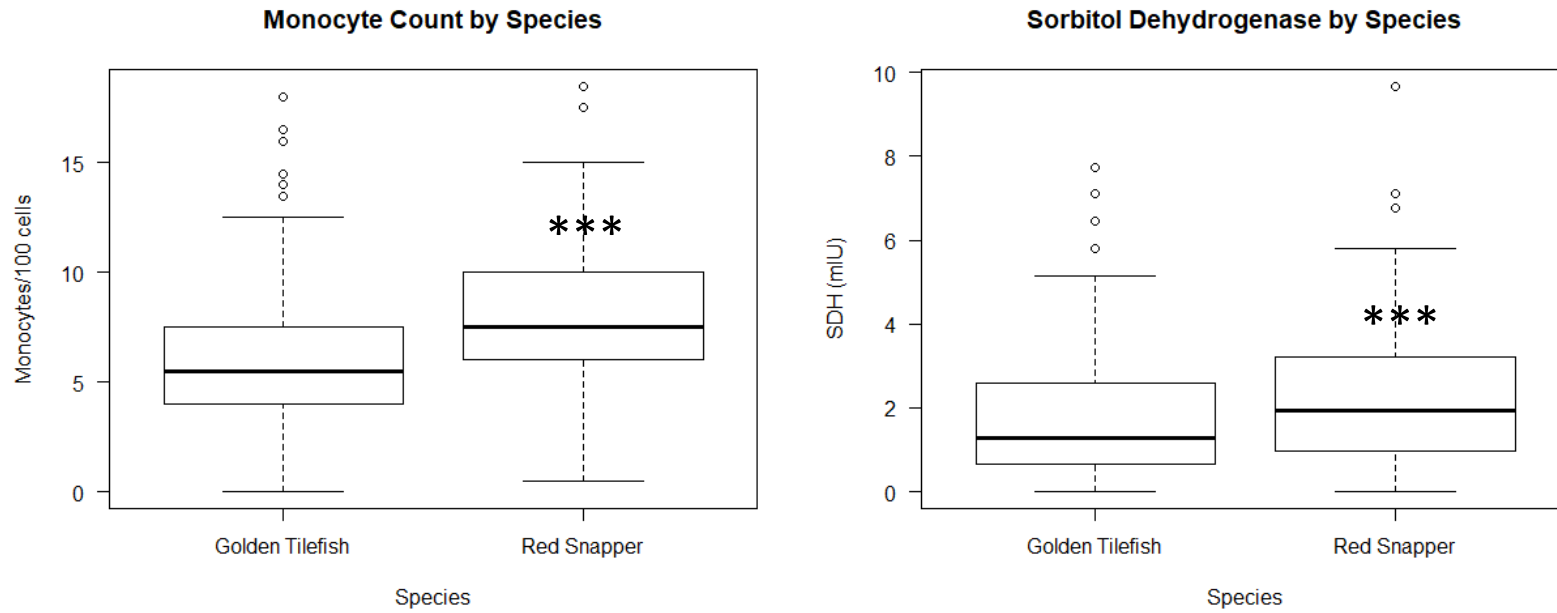


Figure 2.3: Biomarkers for which Red Snapper reference intervals were significantly higher than Golden Tilefish intervals. Statistically significant differences ($p < 0.05$) are marked with asterisks (***) as determined by Kruskal-Wallis analysis after testing for normality by Shapiro-Wi

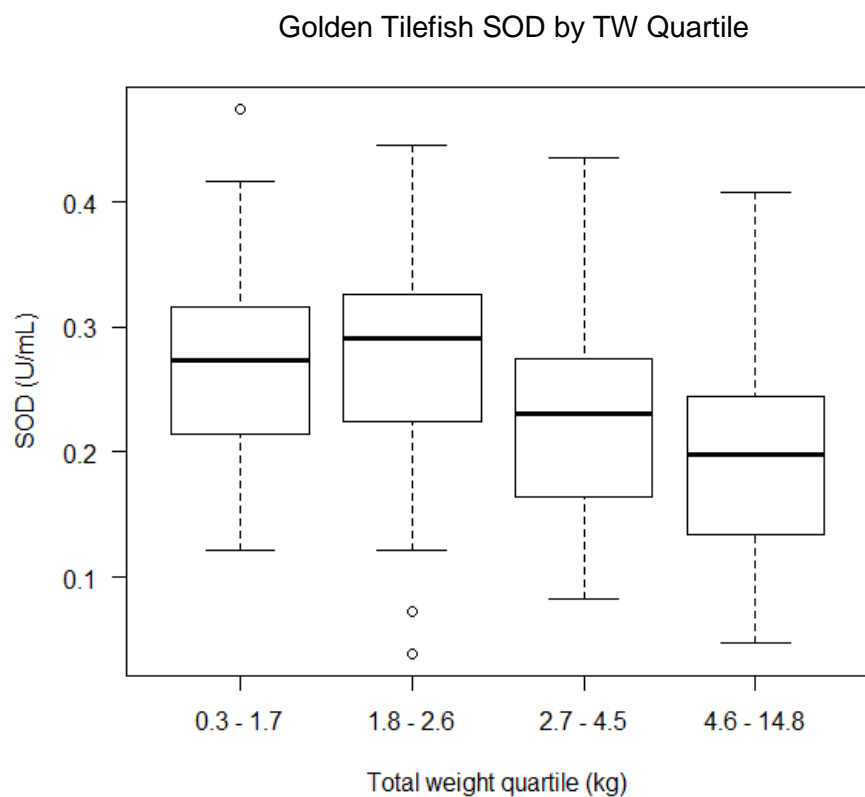


Figure 2.4: Comparisons in mean biomarker expression in superoxide dismutase (SOD) for Golden Tilefish by total weight (TW) quartile, after outlier removal.

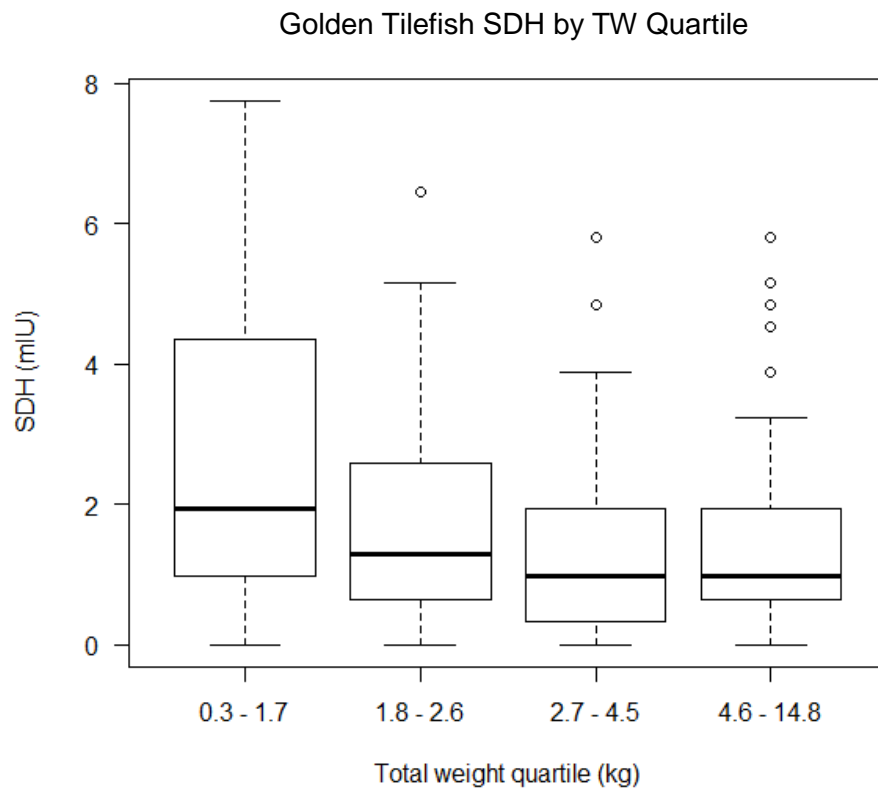


Figure 2.5: Comparisons in mean biomarker expression in sorbitol dehydrogenase (SDH) for Golden Tilefish by total weight (TW) quartile, after outlier removal.

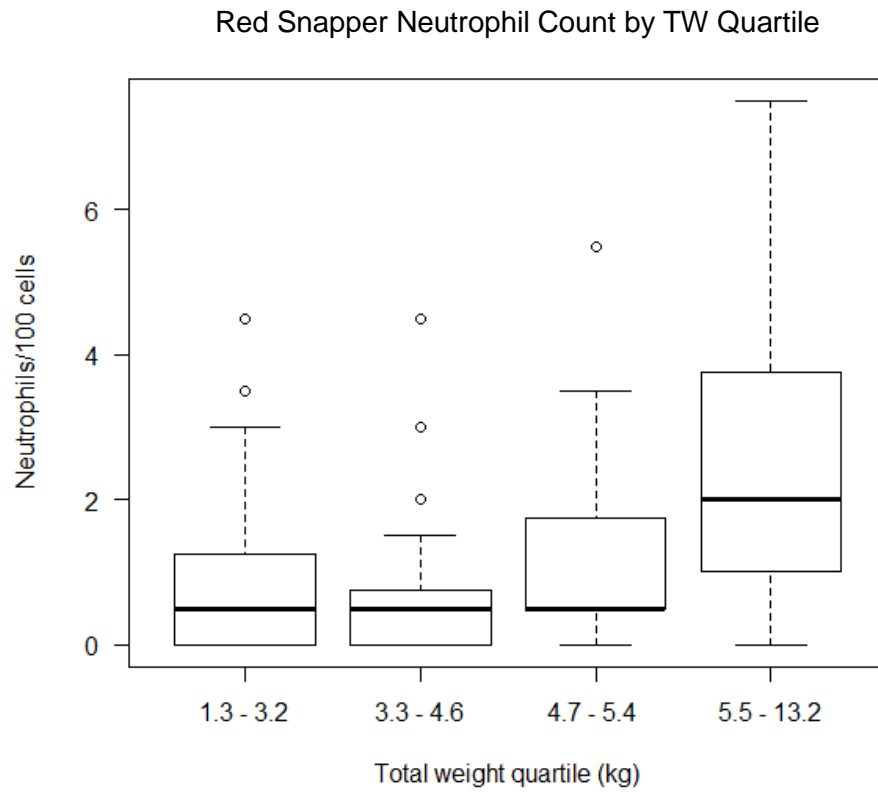


Figure 2.6: Comparisons in mean neutrophil count in Red Snapper by total weight (TW) quartile, after outlier removal.

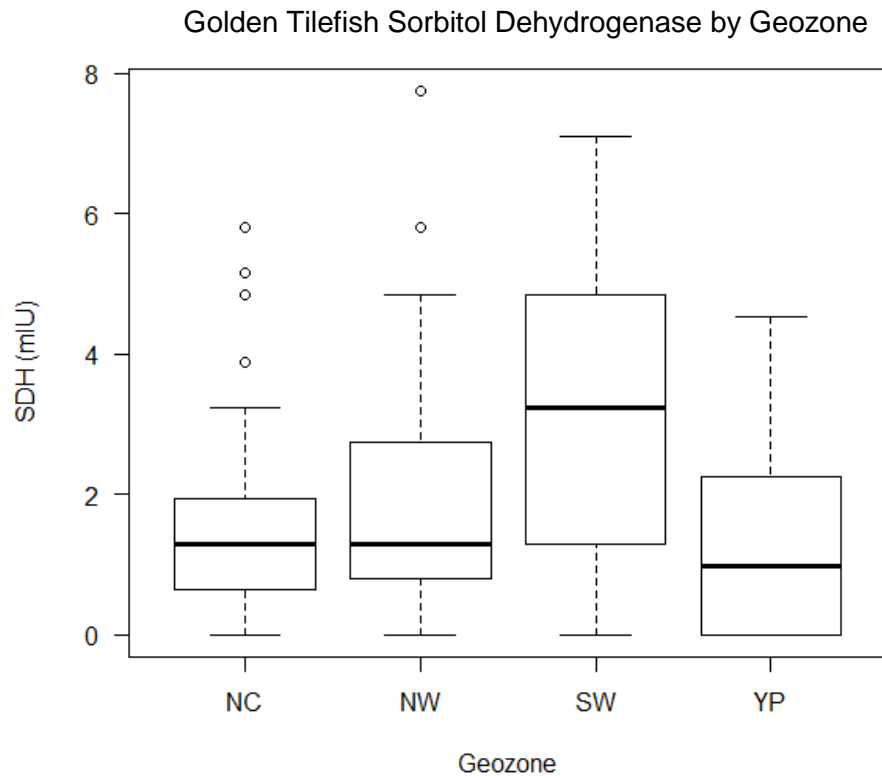


Figure 2.7: Differences in expression of sorbitol dehydrogenase (SDH) in Golden Tilefish by geozone, after outlier removal.

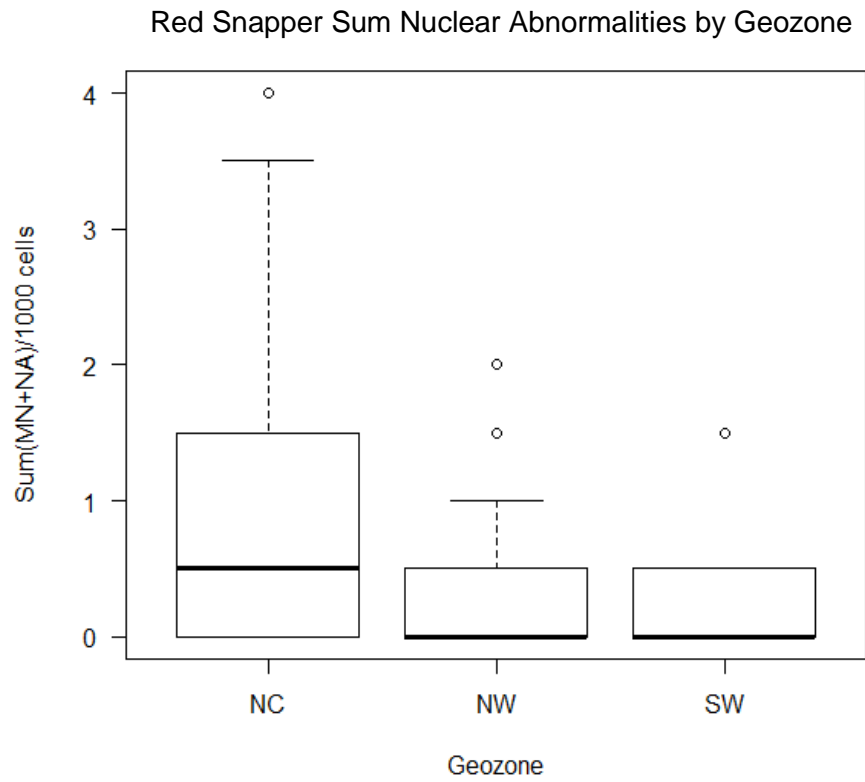


Figure 2.8: Differences in sum nuclear abnormalities (SumNA) in Red Snapper by geozone, after outlier removal.

Red Snapper Sum Neutrophil Count by Geozone

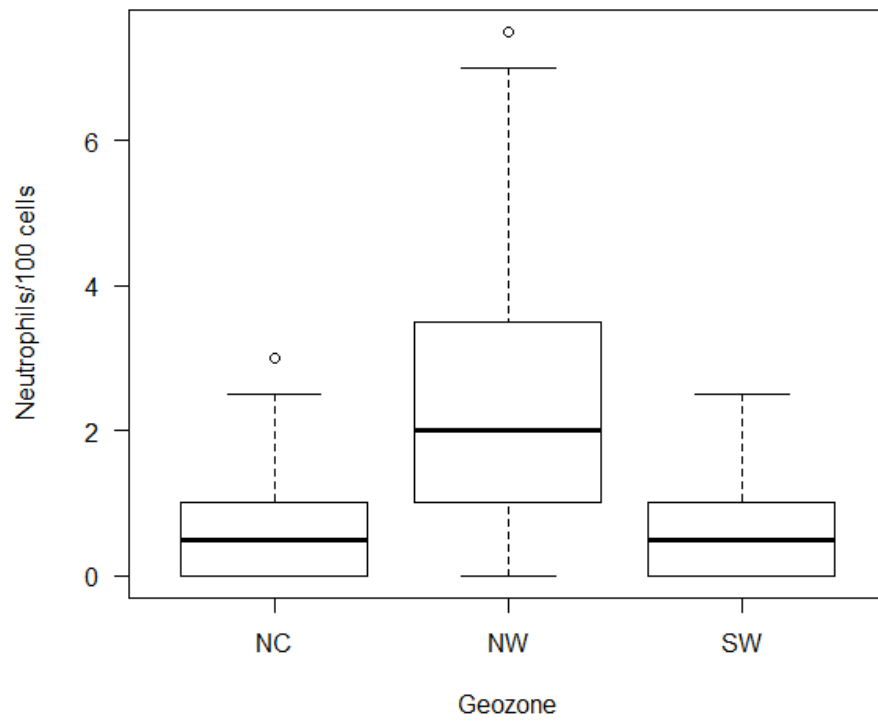


Figure 2.9: Differences in neutrophil count in Red Snapper by geozone, after outlier removal.

CHAPTER THREE:
RELATIONSHIPS BETWEEN POLYCYCLIC AROMATIC HYDROCARBON
EXPOSURE AND BIOMARKER RESPONSE IN GULF OF MEXICO GOLDEN
TILEFISH (*LOPHOLATILUS CHAMAELEONTICEPS*) CAUGHT 2015-2017

3.1 Abstract

Golden Tilefish (*Lopholatilus chamaeleonticeps*) are long-lived, demersal, burrow-forming, omnivorous fish with high site fidelity, which have been historically exposed to mercury and polycyclic aromatic hydrocarbon (PAH) contamination in the Gulf of Mexico (GoM). As such, they provide an important species for the analysis of putative effects of chronic contamination on a benthic organism. Oxidative stress and non-specific immune system biomarkers were quantified in 224 Golden Tilefish caught in diverse communities throughout the GoM between 2015 and 2017. While it is difficult to compare specimens caught across such a large geographic expanse, that were exposed to unknown, but likely different, lifetime contaminant regimes, the 2010 *Deepwater Horizon* (DWH) event may have provided a chronological marker with which to compare specimens from other regions in the GoM. To evaluate possible influence of recent PAH exposure, relating to the DWH spill, biomarker response was correlated with the sum liver and biliary PAH levels in these fish. Fish caught in geographic proximity to the spill in 2015 and 2017 had elevated biliary PAH levels compared to those from other regions of the GoM, however, their oxidative stress biomarkers did not respond as expected upon contaminant exposure. Their liver lipid fraction was lower than in other

regions, and declined between sampling years, suggesting chronic contamination has resulted in a possible shift towards a compensatory metabolic mechanism, whereby energy is mobilized from lipid stores to aid in cellular repair. No consistent trends were observed between non-specific immune response biomarkers and PAH body burden. Aberrant oxidative stress or immune system biomarker expression were observed in isolated instances throughout the GoM, although their etiology remains uncertain.

3.2 Introduction

Contaminants enter the Gulf of Mexico (GoM) through atmospheric deposition, river runoff, oil and gas extraction, and shipping traffic. These contaminants are subsequently dispersed throughout GoM waters by the Loop Current and spin-off eddies (Duteil et al., 2019). Lead, mercury, polychlorinated biphenyls (PCBs), and polycyclic aromatic hydrocarbons (PAHs) have been documented in sediments and organisms from coastal and continental shelf communities throughout the GoM, indicating widespread pollution across the system (Harris et al., 2012; Horta-Puga & Carriquiry, 2014; Perrot et al., 2019). In addition to these relatively well-studied pollutants, over 60,000 synthetic chemicals are discharged into the sea in wastewater from industrial, agriculture, and domestic activities (Hamilton et al., 2016). Pulse events, like the 1979 *Ixtoc I* and 2010 *Deepwater Horizon* oil spills, add additional stress to an already burdened ecosystem, and may provide a chronological marker by which to examine physiological responses of organisms to these additional contaminant loads. Such events may apply selective pressure on population, inherently leading to selective sampling of better adapted individuals in subsequent years.

Acute contaminant exposure can result in an alteration of the endocrine system and stimulation of glucocorticoid hormones to combat the stressor while maintaining homeostatic

balance (Gandar et al., 2017; Marentette et al., 2013). Antioxidant levels may increase to ameliorate the potentially deleterious effects of reactive oxygen species (ROS) produced by the metabolism of contaminants such as PAHs and PCBs (Bacanskas et al., 2004; Sokolova, 2018). Additionally, components of the innate immune system, including lysozyme, acute phase proteins, and leukocytes, may be triggered in response to a transient antagonist, including exposure to xenobiotics (Tort, 2011).

Under chronic contaminant exposure, the organisms' response can become maladaptive. The bioenergetic costs of cellular repair, production of stress proteins, and maintenance of basal processes can result in the accelerated metabolism of internal glycogen and lipid stores, with negative implications for continued growth and reproduction (Marchand et al., 2004; Sokolova, 2018). Prolonged oxidative stress can result in lipid peroxidation, DNA damage, and protein carbonylation (Liguori et al., 2018). Extensive release of glucocorticoids can result in immunomodulation by their aberrant binding to cell receptors on circulating immune cells (Padgett & Glaser, 2003). Chronic toxicant exposure can cause immunosuppression, with documented reductions of lysozyme, complement, and B lymphocyte responses, leaving the host more susceptible to opportunistic pathogen infection (Tort, 2011; Vogelbein et al., 2001). Chronic activation of the hypothalamic-pituitary-interrenal axis can eventually lead to reduced cortisol response, leaving organisms more susceptible to future challenges (Marentette et al., 2013).

Local adaptations and resiliency to chronic pollution have been documented in several fish species, including Killifish (*Fundulus heteroclitus* and *Fundulus grandis*), Atlantic Tomcod (*Microgus tomcod*) and Yellow Perch (*Perca flavescens*; Bélanger-Deschênes et al., 2013; Di Giulio & Clark, 2015; Oziolor et al., 2014; Wirgin et al., 2011). Such resistance in some

populations has been coupled with bioenergetic consequences and reduced fitness, with uncertainty as to whether these fish may then be better or more poorly adapted to defense against future insults (Marchand et al., 2004). A well-documented change in fish exposed to PCBs and PAHs is alteration of the aryl hydrocarbon receptor (AHR) pathway, which is involved in xenobiotic metabolism (Aluru et al., 2015; Whitehead et al., 2017). While adaptation may prevent excess deleterious effects from contaminant exposure, downstream impacts on immune, reproductive, neurological, and cardiovascular systems can occur, due to the importance of AHR in a multitude of non-toxicological signaling pathways (Shinde & McGaha, 2018; Whitehead et al., 2017).

Golden Tilefish (*Lopholatilus chamaeleonticeps*) can serve as a non-model organism for the evaluation of physiological impacts of chronic contamination in the GoM given their life history, prevalence, and past evidence of PAH, mercury, and metal exposures (Granneman et al., 2017; Murawski et al., 2014; Perrot et al., 2019; Snyder et al., 2015, 2019). Golden Tilefish are omnivorous, long-lived (26-40 years), demersal, burrow-forming teleosts, occurring with high site fidelity in muddy continental shelves, GoM-wide (Able et al., 1982; Lombardi-Carlson & Andrews, 2015; Murawski et al., 2018; Palmer et al., 2004; Steimle et al., 1999). Compared to those caught within the Atlantic Ocean, GoM Golden Tilefish have elevated tissue mercury levels and are frequently ranked among the most polluted fish species in the GoM (Harris, Pollman, Hutchinson, et al., 2012; Levenson & Axelrad, 2006). Following the DWH spill in 2010, Golden Tilefish caught at repeat sampling sites in the northern GoM displayed a 178% increase in biliary PAH levels, indicating ongoing exposure in these fish (Snyder et al., 2019).

In this study, a GoM-wide survey of Golden Tilefish was conducted in 2015-2017 to measure oxidative stress and immune system biomarker levels in wild populations. While

different regions of the GoM may be impacted by varying contaminants and stressors, fish collected from the northern GoM were most likely to have sustained physiological impacts from exposure to the *Deepwater Horizon* oil spill. Therefore, biomarker levels were compared to sum liver and biliary PAH levels within each fish. Since PAHs are rapidly metabolized in teleosts, it is difficult to relate their measured levels to more sustained health effects, however, biliary PAH metabolites provide a quantifiable record of recent exposure (Hamilton et al., 2016). The measurement of biomarkers levels are more biologically meaningful than determination of chemical residue concentrations in the body, despite the difficulty in biomarker interpretation in wild populations (Martínez-Gómez & Vethaak, 2019). All biomarkers chosen in this study had previously documented fluctuations with PAH exposure in teleosts, were measurable in whole blood or plasma, and were adaptable to non-model species.

Oxidative stress is an unavoidable byproduct of aerobic life. The ROS produced during respiration function as critical secondary messengers for many important signaling transcription factors and aid in routine immune response to pathogens (Rahal et al., 2014; Schieber & Chandel, 2014a). Given the significance of these physiological roles, antioxidant systems have evolved to maintain intracellular levels of ROS. However, xenobiotics can induce the aberrant proliferation of ROS through impairment of mitochondrial electron transfer chains, interference with enzymatic reactions, or inhibition of antioxidants, resulting in oxidative stress and subsequent cellular damage (Abele et al., 2012).

In this study, superoxide dismutase (SOD), malondialdehyde (MDA), sorbitol dehydrogenase (SDH), and sum erythrocyte nuclear abnormalities (SumNA) were used to quantify oxidative stress and its resultant putative impacts on Golden Tilefish. Superoxide dismutase is a potent antioxidant and primary scavenger of superoxide radicals, aiding in their

conversion to molecular oxygen and hydrogen peroxide, thereby facilitating subsequent conversion to water by catalase (Santana et al., 2018). Lipid peroxidation can be assessed through the measure of thiobarbituric acid reactive substances (TBARS), as a proxy for malondialdehyde, one of the endpoints of the phenomenon (Lushchak, 2011). While measuring TBARs is not a perfect analogy to membrane damage, due to their reaction with other compounds including aldehydes and carbohydrates, a body of literature has documented their utility in aquatic animal studies (Hook et al., 2014; Lushchak, 2011). Elevated SDH levels can be indicative of hepatotoxicity, as a potential impact of circulating ROS (Dixon et al., 1987; Webb & Gagnon, 2007). Erythrocyte nuclear abnormalities have been observed after abnormal chromosomal separation during mitosis due to lesions or adducts in the DNA caused by ROS proliferation and genotoxicant exposure (Baršienė et al., 2006b; Pastore et al., 2014).

The teleost immune system is complex, with evidence of immunomodulation concurrent with extensive toxicant exposure. The non-specific immune response was characterized using lysozyme (LYS), differential white blood cell (DWBC) counts, hematocrit (HCT), and leukocrit (LCT) measurements as proxies. Lysozyme is a significant enzyme of the innate immune system that combats bacterial infection by breaking down peptidoglycan in bacterial cell walls. It has been shown to decline upon exposure to hydrocarbons and other pollutants (Bado-Nilles et al., 2009; Balfry & Iwama, 2004; Ellis, 1999; Kennedy & Farrell, 2008). Differential white blood cell counts provide an economical means for assessing immune system activation (K. B. Tierney et al., 2004). For example, elevation of monocytes may indicate infection and an enhanced neutrophil-to-lymphocyte ratio may suggest an inflammatory response (Faria et al., 2016; Karlmark et al., 2012). Hematocrit counts may be used to assess anemia, a pathological outcome

of oil exposure (Harr et al., 2018). Changes in leukocrit can indicate acute stress in some fish species (McLeay & Gordon, 1977; Wedemeyer et al., 1983).

3.3 Methods

3.3.1 Sampling

Specimens were collected via demersal longline aboard the *R/V Weatherbird II* from July-August 2015-2017, in accordance with state and federal permitting (Murawski et al., 2018). Location, depth, and temperature information were recorded by data loggers (Star:Oddi CDST Centi-TD), attached to the 544-kg-test monofilament at both ends of each 5 mile long set, each of which contained an average of 460 Atlantic Mackerel (*Scomber scombus*) or squid (primarily Humboldt, *Doidicus gigas*) baited size 13/0 circle hooks and an average soak time of two hours. All station and catch data are provided in Appendix A. Neither the depth nor the temperature at which Golden Tilefish were fished had a statistically significant effect on biomarker expression, and therefore these data were eliminated from further analysis.

Within fifteen minutes of landing on deck, fish were weighed, lengths (total, standard, and fork) were measured, and 2-4 mL of whole blood was collected into 4 mL lithium heparin tubes (BD vacutainer, Franklin Lakes, NJ) via caudal dissection. Whole blood was stored on ice prior to separation via centrifugation at 1600 x g for 15 minutes, followed by temporary storage of plasma at -20°C and long-term storage at -80°C. Fish were sexed macroscopically and both internal and external evaluations were performed to screen for gross abnormalities. Although organ weights were taken for liver, spleen, and gonad, they were not included in this analysis due to weather-dependent fluctuations in scale sensitivity while at sea. Sagittal otoliths were taken from each specimen and aged as described by Helmueller (2019). Due to limited staged otolith numbers from the Golden Tilefish utilized in this study and the relationship between age and

fork length, the latter was used for a proxy of age for these specimens (Lombardi-Carlson & Andrews, 2015). Liver and bile samples were taken for PAH analysis and determination of liver lipid fraction (LLF) by collaborators at the University of South Florida, College of Marine Science (Snyder, 2020).

3.3.2 Oxidative stress biomarkers

To characterize oxidative stress, plasma levels of SOD, MDA, and SDH were measured, and erythrocyte nuclear abnormalities were quantified as described in Chapter II. Briefly, SOD and MDA were assessed using commercial kits, according to manufacturer's instructions (Cayman Chemicals, Ann Arbor, MI, SOD Assay Kit #706002, TCA Assay Kit #700870). Plasma SDH was quantified by a modified microplate assay (Dixon et al., 1987; Pandelides et al., 2014; Shailaja & D'Silva, 2003; Webb & Gagnon, 2007). Erythrocyte nuclear abnormalities were classified visually by oil immersion microscopy of blood smears stained with 10% Giemsa solution. Nuclei were documented as either normal, micronuclei, binucleated, notched, blebbed, or budded, as described in Chapter II. Since the exact etiology of each subclass of abnormality has yet to be defined, the sum of nuclear abnormalities (SumNA) per 1000 erythrocytes was calculated for each fish and averaged across sample duplicates.

3.3.3 Immune response biomarkers

Measures of HCT, LCT, LYS, and DWBC were performed to characterize non-specific immune system responses, as described in Chapter II. Both HCT and LCT were measured within two hours of sample collection by transferring whole blood to a microhematocrit capillary tube, centrifuging at 1800 x g for one minute (HemataStat II Hematocrit Analyze, San Antonio, TX, EKF Diagnostics), and quantifying HCT and LCT levels by manual comparison to a hematocrit reader card. Plasma LYS was measured using a modified microplate assay (Bado-

Nilles et al., 2009; Grinde et al., 1988; Parry et al., 1965; Perrault et al., 2017). Briefly, the change in absorbance of plasma was observed over 10 minutes at 520 nm, upon reaction with a freshly prepared *Micrococcus lysodeikticus* suspension (Sigma-Aldrich). Differential white blood cell counts were performed on duplicate blood smears per specimen, stained with May-Grunwald and Giemsa solutions (Sigma-Aldrich). One hundred leukocytes were classified as either: lymphocytes, thrombocytes, monocytes, basophils, eosinophils, or neutrophils based upon comparison to common cell morphologies described in other teleosts (Bado-Nilles et al., 2009; Grinde et al., 1988; Perrault et al., 2017). Due to low prevalence, basophils and eosinophils were excluded from further analysis. The neutrophil to lymphocyte ratio (N/L) and monocyte counts (MON) were considered primary indicators for the non-specific immune system response.

3.3.4 Polycyclic aromatic hydrocarbon metabolites

Liver and biliary PAH metabolites were assessed according to previously described methods (Pulster et al., 2020; Snyder et al., 2019). Briefly, liver tissue was extracted using a modified QuEChERS method and resulting spiked extracts were analyzed by GC-MS/MS for PAHs and alkylated homologs (Lucas & Zhao, 2015). Bile samples were assessed by high performance liquid chromatography and fluorescence detection, using a method developed by the Northwest Fisheries Science Center (Krahn et al., 1984).

3.3.5 Liver lipid fraction

Total liver lipid fraction was determined using a modified Folch method (Matyash et al., 2008; Snyder et al., 2019). Briefly, this involved a two stage extraction, followed by drying via evaporation and gravimetric determination of the liver lipid fraction.

3.3.6 Data analysis

Statistical analysis was performed using the R Project for Statistical Computing version 3.4.1 using the *vegan*, *pastecs*, and *ggplot2* packages and their dependencies. All significant differences were calculated by either ANOVA or Kruskal-Wallis, followed by *post hoc* pairwise comparisons by Tukey HSD, after screening for normality using the Shapiro-Wilk test criterion. Condition factor (K) was calculated as: $K = 100 * W/L^3$, where W was total weight (kg), and L was fork length (cm; Froese 2006). Principal component analysis, non-metric multidimensional scaling, and redundancy analysis were performed in R.

Data were grouped into geographic sampling zones (geozones), based upon geography, oil field boundaries, and national boundaries in order to potentially control for factors influencing pollutant concentration and tilefish population-level stressors. These groups included north central (NC; with duplicate sampling in 2015 and 2017), northwest (NW), southwest (SW), Campeche Bay (CB), and Yucatan Peninsula (YP; Fig. 3.1). Mapping was performed using the Leaflet package in R.

Variables were divided into three classes: oxidative stress biomarkers (SOD, MDA, SDH, SumNA), immune system biomarkers (HCT, LCT, LYS, N/L, MON), and explanatory variables (Sum liver PAH, sum biliary PAH, biliary benzo(a)pyrene (B(a)P), LLF, and condition factor (K)). Biliary B(a)P was considered in addition to sum biliary PAH due to the documented cytotoxicity and mutagenicity of the former compound and its lack of correlation with sum biliary PAH in these data (World Health Organization. et al., 2012). Liver B(a)P levels were low and therefore not distinguished from sum liver PAH. All biomarker data are available at <https://data.gulfresearchinitiative.org/pelagos-symfony/data/R6.x805.000:0078>. All PAH data

are available at Liver and biliary PAH data are available at:

<https://data.gulfresearchinitiative.org/pelagos-symfony/data/etc.4583>.

3.4. Results

3.4.1 Comparison of biomarker expression throughout the Gulf of Mexico

Two hundred and twenty-four Golden Tilefish were included in GoM-wide comparisons, from stations where $n \geq 2$ for the majority of oxidative stress and immune system biomarkers, and explanatory variables (Figure 3.1). By macroscopic identification of gonad tissue, 62% of specimens were female, 22% were male, and 16% could not be identified. There was a significant difference between total length ($p < 0.001$) and weight ($p < 0.001$) by sex; however, there was no difference in K. Females had an average total length of 60 ± 12 cm and an average total weight of 2.693 ± 1.896 kg, while males were generally larger and older than females, with an average total length of 79 ± 11 cm, an average total weight of 5.908 ± 2.595 kg. Fish whose sex could not be identified were likely either immature or spent females, with an average total length of 57 ± 11 cm, an average total weight of 2.133 ± 1.300 kg. It is possible that sex was misclassified for some of these individuals, due to the lack of histological confirmation and the possibility of hermaphroditic specimens in the GoM (Lombardi-Carlson, 2012; Lyon 2010). Given the skewed sex ratio in these data, and due to fork length, total weight, and age differences by sex, these variables were omitted from the analysis, instead using K as a derived biometric.

Statistically significant differences were observed in SumNA, SDH, MON, HCT, LYS, sum biliary PAH, LLF, and K between NC years (2015 and 2017) and the remainder of the GoM sampling groups. Sum erythrocyte abnormalities were lower in NC2015 than SW ($p < 0.001$, Fig. 3.2) and SDH was lower at NC2015 than CB ($p = 0.039$; Fig. 3.2). Monocyte count was elevated in NC2017 compared to SW ($p = 0.035$; Fig. 3.3) and HCT was lower at NC2015

compared to SW ($p = 0.019$; Fig. 3.3). Lysozyme was lower at NC2017 than CB ($p = 0.004$), NW ($p < 0.001$), SW ($p < 0.001$) and YP ($p = 0.031$; Fig. 3.3). Sum biliary PAH was higher in both NC2015 and NC2017 than in CB, NW, SW, and YP ($p < 0.001$ for all; Fig. 3.4). Liver lipid fraction was lower in NC2015 than NW ($p < 0.001$), SW ($p = 0.003$), and YP ($p < 0.001$) and lower at NC2017 than NC2015, CB, NW, SW, and YP ($p < 0.001$ for all; Fig. 3.5). Condition factor was lower at NC2017 than YP ($p = 0.003$; Fig. 3.5).

When compared to GoM-wide biomarker reference intervals for Golden Tilefish (described in Chapter II), an average of $27.29 \pm 7.89\%$ of the data within each sampling zone were considered oxidative stress outliers. A notable exception to this is NC2015, where only 4.76% of the data were considered oxidative stress outliers. Outlier prevalence was more uniform among immune system biomarkers, with each group having an average of $20.45 \pm 5.84\%$ of their data classified as outliers. Among individual biomarkers, the dispersion of outliers among groups was generally varied. However, NC2017 constituted 87.5% of the SOD outliers (both above and below the reference interval), which comprised 12.97% of NC2017 samples. Groups CB, NW, and SW dominated the high SDH outliers, wherein outliers accounted for $12.12 \pm 0.007\%$ of their individual group data.

Non-metric multidimensional scaling (nMDS) of oxidative stress biomarkers, LLF, PAH levels, and K, demonstrated a statistically significant ($p = 0.003$) difference in the clustering of statistically homogenous groups (Fig. 3.6). Group NC2017 was differentiated from the remaining groups, having the most overlap with NC2015 specimens (Fig. 3.6). The SW sampling zone was the most distant from both years of NC collections (Fig. 3.6). Principal component analysis (PCA) of these data indicated the variability among these groups was mostly driven by sum biliary PAH, LLF, and K, although the first two principal components described

33.6% of the total dataset variability (Fig. 3.6). Weak negative correlations were observed between sum liver PAH and SumNA ($R = -0.15$, $p = 0.022$), SDH ($R = -0.15$, $p = 0.035$), and SOD ($R = -0.16$, $p = 0.018$). A weak, but statistically significant, negative correlation was observed between sum biliary PAH and SOD ($R = -0.15$, $p = 0.04$). Redundancy analysis (RDA) of these data indicated PAH levels, LLF, and K described 5% of the variance, and trends among sampling zones were not apparent along explanatory variable vectors.

When biliary PAH data were removed from the analysis, NC2017 remained differentiated by NMDS, with more overlap between NC2015 and the remaining groups (Fig. 3.7). Principal component analysis indicated a greater descriptive role of SumNA for these data (Fig. 3.7). These trends persisted when all PAH data were removed, with SumNA, MDA, and K contributing to the description of the variability (Fig. 3.8). When lipid data were removed, groups had less distinction between them, although there was still a significant difference ($p = 0.002$) between NC2015 and SW (Fig. 3.9). The description of variability was dominated by MDA and SumNA by PCA (Fig. 3.9).

Non-metric multidimensional scaling of immune system biomarkers, LLF, PAH levels, and condition factor demonstrated a statistically significant ($p = 0.001$) difference in the clustering of homogenous groups (Fig. 3.10). Again, NC2017 was the most differentiated sampling zone, but overlapped with both NC2015 and NW. Principal component analysis of these data indicated that sum biliary PAH, N/L, LLF, and MON described most of the variability among these data, with the first two principal components accounting for 30.2% of total variation (Fig. 3.10). A positive correlation was observed between MON and N/L ($R = 0.41$, $p < 0.001$). A weakly, but statistically significant, positive correlation was noted between sum biliary PAH and Mon ($R = 0.16$, $p = 0.031$) and negative correlations were observed between sum liver PAH

and both HCT ($R = -0.20$, $p = 0.004$) and LCT ($r = -0.15$, $p = 0.027$). Redundancy analysis demonstrated that 3.73% of the variation among the data could be explained by PAH levels, LLF, and K (Fig. 3.10). Despite the low predictive power of the model, the variability in immune markers for NC2015 fish can be described primarily by sum liver and biliary PAH and LLF, while variability in SW specimens is described by K and LLF (Fig. 3.10). Trends were not apparent for the remaining groups.

When biliary PAH data were removed from the analyses, the separation between statistically homogenous groups became less pronounced, although still statistically significant ($p = 0.005$), with overlap between NC2017 and NW, in a slightly offset cluster from the remaining groups, driven by the prevalence of zero LCT values and comparable LYS response within these two stations. When analyzed by principal component analysis, MON, LYS, and N/L contributed significantly to the description of variability among the data. When all PAH values were removed, similar patterns were evident in both NMDS and PCA plots, underscoring the lack of correlation between liver PAH values and immune system biomarkers in these data. The same is true upon removal of LLF data.

3.4.2 Geozone-specific variability

3.4.2.1 North central 2015

Forty-two Golden Tilefish were included in the NC2015 sampling zone, caught from stations 11-150 ($n = 4$), 14-60 ($n = 7$), 7-150 ($n = 12$), 8-100 ($n = 10$), 9-150 ($n = 6$), and MC04 ($n = 3$; Fig. 3.11), with an average fork length of 69 ± 14 cm and average total weight of 3.807 ± 2.491 kg. Sex distribution was skewed, as 74.81% of specimens caught were classified as female by macroscopic evaluation. Males accounted for 14.28% of the specimens and the remaining 10.91% were unidentified.

Statistically significant differences in biomarker response between stations were observed for MDA, LYS, and N/L. Lipid peroxidation (MDA) was significantly elevated at station 11-150 compared to 14-60 ($p = 0.002$), 7-150 ($p = 0.008$), 8-100 ($p < 0.001$), and 9-150 ($p < 0.001$). The lowest MDA levels were observed at 8-100, which were also significantly lower than MDA at 7-150 and MC04. A weakly positive, but statistically significant, correlation was observed between MDA and condition factor ($R = 0.24$, $p = 0.03$). Lysozyme was significantly higher at 14-60 than at 7-150 ($p = 0.023$) and at 8-100 ($p = 0.044$). The N/L ratio was significantly different between 9-150 and 11-150 ($p = 0.039$) and there was a statistically significant positive correlation between N/L and MON ($R = 0.52$, $p < 0.001$).

Non-metric multidimensional scaling of oxidative stress biomarkers and explanatory variables indicated a statistically significant ($p = 0.001$) differential clustering between 11-150 and the remainder of the homogeneously dispersed stations (Fig. 3.12). By principal component analysis, MDA, SOD, biliary PAHs, and K described the majority of the variability among stations (Fig. 3.12). Redundancy analysis showed the explanatory variables described 15.35% of the variation among oxidative stress response by station, with possible influence of sum liver PAH on expression at stations 8-100 and 9-150 (Fig. 3.12).

Non-metric multidimensional scaling of the immune system biomarkers and explanatory variables also indicated a statistically significant ($p = 0.034$) difference among statistically homogenous stations, with the most separation between 8-100 and the remainder of the fairly dispersed stations (Fig. 3.13). By principal component analysis, MON, K, N/L, and sum biliary PAH described the majority of the variability in these data (Fig. 3.13). Redundancy analysis indicated explanatory variables described 10.24% of the variability among the data, with biliary B(a)P describing slightly more variability at 14-60 (Fig. 3.13).

3.4.2.2 North central 2017

The NC2017 group was comprised of 54 Golden Tilefish from stations 11-150 (n = 10), 14-60 (n = 10), 7-150 (n = 10), 8-100 (n = 10), 9-150 (n = 6), and MC04 (n = 8; Fig. 3.11), with an average fork length of 59 ± 12 cm and an average total weight of 2.703 ± 2.053 kg. Females accounted for 81.48% of the specimens by macroscopic identification, 5.56% were male, and 12.96% were unidentified.

Statistically significant differences in variable response between stations were observed for LYS, HCT, and K. Significantly lower values of LYS were observed at 11-150 and 14-60 compared to 7-150 ($p = 0.002$), 8-100 ($p = 0.002$), 9-150 ($p < 0.001$) and MC04 ($p < 0.001$). Station 8-100 had significantly lower HCT than 11-150 ($p = 0.020$) and MC04 ($p = 0.002$). Condition factor was higher at 11-150 than at 14-60 ($p < 0.001$), 7-150 ($p = 0.003$), 8-100 ($p < 0.001$) and MC04 ($p < 0.001$). A weak negative correlation was observed between sum liver PAH and SOD ($R = -0.33$, $p = 0.015$).

Non-metric multidimensional scaling of oxidative stress biomarkers and explanatory variables indicated no significant difference ($p = 0.293$) among statistically homogenous groups, with liver PAH, SOD, MDA, and biliary B(a)P explaining the majority of variability among sampling stations (Fig. 3.14). Explanatory variables described 6.76% of the variability among oxidative stress expression by station, although no trends among sampling stations were evident (Fig. 3.14).

Significant differences ($p = 0.022$) were observed between statistically homogenous groups by NMDS of immune system biomarkers and explanatory variables. The variability among groups was primarily driven by K, LLF, N/L, and LYS, with 8-100, 14-60, and MC04 clustering together (Fig. 3.15). With removal of PAH data, clustering among stations shifted to a

significant ($p = 0.001$) separation of MC04, with K, LLF, and N/L contributing to the description of variability among groups. Redundancy analysis resulted in explanatory variables describing 13.87% of the total variability among immune system biomarkers by station, with sum biliary PAH and K explaining more of the variability in 14-60 and 11-150 and biliary B(a)P and LLF contributing to the explanation of variability at 11-150 (Fig. 3.15).

3.4.2.3 Northwest

Forty-four Golden Tilefish were included in the NW group from stations 20-100 ($n = 5$), 20-150 ($n = 10$), 21-100 ($n = 10$), 22-150 ($n = 9$), and 23-150 ($n = 10$) with an average fork length of 66 ± 16 cm and an average total weight of 3.535 ± 2.620 kg (Fig. 3.16). The proportion of female and male fish caught was nearly equivalent (40.91% and 43.18%, respectively), with the remaining 15.91% of specimens unidentified by macroscopic evaluation.

Statistically significant differences were observed between stations in LYS, LCT, K, and sum liver PAH values. Lysozyme was significantly lower at 20-100 than in 21-100 ($p < 0.001$), 22-150 ($p = 0.006$), and 23-150 ($p < 0.001$), and a weak positive correlation was observed between K and LYS ($R = 0.37$, $p = 0.013$). Condition factor was significantly lower at 20-100 ($p = 0.002$) and 20-150 ($p < 0.001$) compared to 21-100. Leukocrit was significantly higher at 20-150 than at 21-100 ($p = 0.010$) and 22-150 ($p = 0.013$) and was positively correlated with biliary B(a)P ($R = 0.88$, $p < 0.001$). Liver PAH was significantly higher at station 20-150 than 23-150 ($p = 0.023$). Weak positive correlations were observed between biliary B(a)P and SDH ($R = 0.44$, $p = 0.015$), and between N/L and MON ($R = 0.6$, $p < 0.001$).

Non-metric multidimensional scaling of oxidative stress biomarkers and explanatory variables failed to reveal significant differences among stations (Fig. 3.17). Principal component analysis of these data indicated that K, biliary B(a)P, SDH, SOD, and biliary sum PAH played a

significant role in the description of variability among stations (Fig. 3.17). Explanatory variables accounted for 19.99% of the variation among these data by RDA, with LLF and K describing much of the oxidative stress expression at station 23-150, and PAH levels describing expression at 20-150 (Fig. 3.17).

Statistically significant ($p = 0.006$) separation was observed between statistically heterogeneous stations, with 20-150 more distant from the remaining cluster of stations (Fig. 3.18). Liver PAH, K, HCT, and biliary B(a)P dominated the description of the variability among these data by PCA (Fig. 3.18). Redundancy analysis showed explanatory variables explained 14.88% of the variation among immune biomarkers with a notable influence of sum liver and biliary PAH on specimens at station 20-100 (Fig. 3.18).

3.4.2.4 Southwest

The SW group was comprised of 22 specimens from 24-150 ($n = 10$), 25-150 ($n = 7$), and 26-150 ($n = 5$) with an average fork length of 62 ± 12 cm and an average total weight of 2.578 ± 1.524 kg (Fig. 3.19). Of the specimens collected, 45.46% were macroscopically identified as female, and 27.27% were identified as either male or were unidentified.

Statistically significant differences in variables were observed between stations for the N/L ratio, LYS, and HCT. The N/L ratio was significantly lower at 25-150 than at 26-150 ($p = 0.020$). Lysozyme was significantly higher at 24-150 than the remaining two stations ($p < 0.001$) and HCT was lower at 24-150 than at 25-150 ($p = 0.024$). A weakly negative correlation was observed between LLF and MON ($R = -0.46$, $p = 0.032$).

Non-metric multidimensional scaling of oxidative stress biomarkers and explanatory variables failed to reveal significant differences among stations ($p = 0.551$), with K and PAH levels having the greatest contributions to explanations of the variability among stations (Fig.

3.20). Redundancy analysis indicated that explanatory variables can account for 18.83% of the variability among oxidative stress biomarkers in the stations, although no trends among sampling stations were evident (Fig. 3.20).

No significant difference among stations was observed by NMDS of immune system biomarkers and explanatory variables, with sum liver and biliary PAH levels, LLF, and N/L having the largest contributions to describing the variability among stations by PCA (Fig. 3.21). The explanatory variables could account for 20.16% of the variation among immune biomarker expression in the stations, with a separation evident between 24-150 and the remaining groups (Fig. 3.21). Biliary B(a)P and K played a larger role in the explanation of variability within 24-150, while sum liver and biliary PAH and LLF contributed more to the explanation of variability for 25-150 and 26-150 (Fig. 3.21).

3.4.2.5 Campeche Bay

Thirty-four Golden Tilefish were included in CB from stations 27-150 (n = 10), 28-150 (n = 5), 30-100 (n = 2), 30-150 (n = 7), and 31-150 (n = 10) with an average fork length 61.44 ± 14.31 cm and an average total weight of 3.20 ± 2.73 kg (Fig. 3.22). The majority (58.82%) of the specimens were female, 20.59% were male, and 20.59% were unidentified by macroscopic evaluation.

Statistically significant differences in biomarker expression between stations were observed for SumNA, LCT, N/L, and LYS. The sum of erythrocyte nuclear abnormalities was elevated at 28-150 in comparison with 30-100 ($p = 0.0358$), 30-150 ($p = 0.003$), and 31-150 ($p = 0.016$). Station 27-150 had elevated LCT compared to 28-150 ($p = 0.004$), 30-100 ($p = 0.017$), and 30-150 ($p < 0.001$). The N/L ratio was higher at 30-100 than at 27-150 ($p = 0.027$), 28-150 ($p = 0.018$), 30-150 ($p = 0.002$), and 31-150 ($p = 0.020$). Lysozyme was significantly lower at

28-150 than at 30-100 ($p = 0.025$), 30-150 ($p = 0.003$), and 31-150 ($p = 0.003$), and the latter station had significantly higher LYS levels than 27-150 ($p = 0.005$). A weakly negative correlation was observed between HCT and MON ($R = -0.45$, $p = 0.008$).

Non-metric multidimensional scaling of oxidative stress biomarkers and explanatory variables failed to reveal significant differences ($p = 0.229$) among homogenous stations, with sum liver and biliary PAH, K, and LLF contributing the most to the explanation of variability among stations by PCA (Fig. 3.23). By RDA, 14.06% of the variability in oxidative stress biomarker expression among stations could be accounted for by explanatory variables, with responses at stations 30-100 and 30-150 most explained by K and sum liver PAH and 31-150 variability best described by K, sum liver PAH, and biliary B(a)P (Fig. 3.23).

No significant difference among homogenous stations was observed by NMDS on immune system biomarkers and explanatory variables, with HCT, MN, LYS, and sum liver and biliary PAH most contributing to the explanation of variability among stations by PCA (Fig. 3.24). Redundancy analysis indicated that explanatory variables may account for 29.36% of the variation among immune system biomarker expression by station, with LLF, K, and biliary B(a)P most explaining variability in 31-150 (Fig. 3.24).

3.4.2.6 Yucatan Peninsula

Group YP consisted of 28 Golden Tilefish from stations 33-150 ($n = 10$), 34-100 ($n = 3$), 36-100 ($n = 5$), and 36-150 ($n = 10$), with an average total length of 68 ± 12 cm and an average total weight of 4.057 ± 2.607 kg (Fig. 3.25). Females accounted for 57.14% of the specimens by macroscopic identification, 28.57% were male, and 14.26% were unidentified.

Statistically significant differences in biomarker expression between stations were evident for SDH, HCT, and LYS. Station 36-100 had significantly elevated SDH compared to

33-150 ($p = 0.002$), 34-100 ($p = 0.025$), and 36-150 ($p < 0.001$). A positive correlation was observed between SDH and biliary B(a)P ($R = 0.85$, $p < 0.001$). Hematocrit was significantly lower at 36-150 than at 33-150 ($p = 0.028$) and LYS was significantly higher at 33-150 than at 36-100 ($p = 0.015$) and 36-150 ($p = 0.015$). A positive correlation was observed between K and LYS ($R = 0.61$, $p < 0.001$). Positive correlations were also observed between SumNA and MDA ($R = 0.6$, $p = 0.001$), between SOD and biliary B(a)P ($R = 0.4$, $p = 0.047$), and between LCT and MON ($R = 0.47$, $p = 0.014$).

A significant difference ($p = 0.007$) among stations was observed by NMDS of oxidative stress biomarkers and explanatory variables, with 36-100 differentiated from the remaining heterogeneous stations (Fig. 3.26). Principal component analysis indicated that MDA, SumNA, SOD, SDH, and biliary B(a)P had the largest contributions to the description of the variability among stations (Fig. 3.26). Explanatory variables accounted for 15.97% of the variation among stations by RDA, with biliary PAHs explaining more of the oxidative stress expression in 36-100 and 36-150, and liver PAH and K explaining more of the variation in 33-150 (Fig. 3.26).

Non-metric multidimensional scaling of immune system biomarkers and explanatory variables also produced a significant difference ($p = 0.042$) among homogenous stations, with a greater dispersion of stations 36-150 and 36-100 compared to the remaining groups (Fig. 3.27). The variability among these stations was primarily explained by HCT, K, MON, LYS, and LCT, according to PCA (Fig. 3.27). Explanatory variables could account for 69.16% of the variation among immune response in this group, with K and biliary B(a)P explaining much of the variation in 33-150, and sum liver and biliary PAH explaining more variation in 36-100 and 36-150 (Fig. 3.27). The variation in 34-100 may have been explained by sum biliary PAH levels (Fig. 3.27).

3.4.3 Comparisons between fish from the north central Gulf of Mexico

3.4.3.1 Stations grouped regardless of year

A total of 96 Golden Tilefish were collected from six NC stations sampled in both 2015 and 2017: 11-150, 14-60, 7-150, 8-100, 9-150, and MC04. When fish were grouped by station, irrespective of the sampling year, statistically significant differences were observed between stations for MDA, LYS, HCT, and K. Station 9-150 had significantly lower MDA than MC04 ($p = 0.034$). Station MC04 had significantly higher LYS than 14-60 ($p = 0.010$) and 11-150 ($p = 0.005$). Station 8-100 had significantly lower HCT than MC04 ($p < 0.001$), 7-150 ($p = 0.037$), and 11-150 ($p = 0.003$). Condition factor was significantly lower in 9-150 ($p = 0.037$) and MC04 ($p = 0.042$) than in 11-150. A weak negative correlation was observed between SOD and LLF ($R = -0.25$, $p = 0.013$) and a weakly positive correlation was noted between SOD and SumNA ($R = 0.25$, $p = 0.014$).

Non-metric multidimensional scaling of oxidative stress and explanatory variables in NC stations, grouped regardless of sampling year, revealed a significant ($p = 0.029$) difference among homogenous groups (Fig. 3.28). Three clusters were evident, one with 7-150, 8-100, and 14-60, another with 9-150 and 11-150, while MC04 was slightly separated, overlapping both clusters (Fig. 25a). Principal component analysis indicated MDA, SOD, and biliary PAHs had the greatest contributions to the description of variability among stations (Fig. 3.28). By redundancy analysis, only 7.46% of the variation among stations could be accounted for by explanatory variables, with no clear trends in station delineations (Fig. 3.28). Upon removal of PAH data from NMDS, a significant ($p = 0.040$) difference among homogenous groups still occurred, however all stations except MC04 clustered with one another (Fig. 3.29). The main contributors to the variability among stations were SDH, SOD, and SumNA (Fig. 3.29).

Non-metric multidimensional scaling of immune biomarkers and explanatory variables showed a significant difference ($p = 0.002$) among homogenous groups, with a cluster of 7-150, 14-60, and 8-100, and slight separation among the remaining stations (Fig. 3.30). Liver lipid fraction, LYS, HCT, N/L, and MON had the greatest contributions to the description of variability among stations, with little input from PAH values (Fig. 3.30). While 17.31% of the variation is accounted for by explanatory variables by RDA, LLF and K appeared to play the greatest role in this description and there were no consistent trends between stations (Fig. 3.30).

3.4.3.2 Comparison of stations by year

When variables were compared between NC2015 and NC2017, statistically significant variation was observed in SOD, SumNA, LYS, LCT, HCT, N/L, LLF, and K. Some of these variables appeared to be influenced by the contributions of statistically significant differences in individual stations between sampling years, while others reflected overall trends in the data. Superoxide dismutase and SumNA were significantly higher in 2017 than 2015 ($p = 0.006$ and $p = 0.001$, respectively), with no differences among individual stations between years. Lysozyme was significantly elevated in 2017 ($p < 0.001$), with statistically significant elevated levels in 7-150, 8-100, and 9-150 ($p < 0.001$ for all) in 2015 compared to 2017. Hematocrit was higher in 2017 than 2015 ($p = 0.007$) with no significant differences between individual stations. In 2017, LCT was significantly lower ($p < 0.001$), and LCT at station 9-150 was significantly lower in 2017 than 2015 ($p = 0.019$). The N/L ratio was also lower in 2017 ($p < 0.001$), and N/L was significantly lower at station 14-60 in 2017 than in 2015 ($p = 0.010$). Liver lipid fraction and K were lower in 2017 ($p < 0.001$ and $p = 0.049$ respectively). Stations 14-60 and 7-150 had significantly lower liver lipid fractions in 2017 than in 2015 ($p < 0.001$ and $p = 0.004$, respectively).

Non-metric multidimensional scaling of oxidative stress biomarkers and explanatory variables failed to reveal significant differences between 2015 and 2017 ($p = 0.631$), however, upon removal of PAH data, there were statistically significant differences ($p = 0.001$) among the heterogeneous groups (Fig. 3.31), primarily driven by SDH, SOD, and SumNA (Fig. 3.31). The same trend was observed between immune biomarkers and explanatory variables, with significant ($p = 0.001$) variability between heterogeneous stations driven by MON and N/L upon removal of PAH data (Fig. 3.32). Redundancy analysis showed that explanatory variables only described 7.46% of the variation among oxidative stress biomarkers between years, although there is differential grouping by year, with PAH variables better describing 2015 specimens (Fig. 3.33). Explanatory variables better described immune system biomarker response by redundancy analysis (17.31% of variation), although groupings among variables were less distinct (Fig. 3.33).

3.5 Discussion

Due to sampling limitations, biliary PAH measurements were not obtained from every specimen evaluated for biomarkers in this research. Therefore, when biliary PAH data were removed from sequential NMDS and PCA analysis, the size of the resulting dataset always increased. Regardless of this impact, potentially biologically relevant trends were observed upon sequential removal of explanatory variables.

The lack of overall change in NMDS structure after the sequential removal of both sum liver and biliary PAH levels suggests these variables did not uniformly affect oxidative stress biomarker expression, GoM-wide. This is further supported by the low success of the RDA model of explanatory variables' ability to describe variance in oxidative stress response, indicating PAH levels alone cannot adequately model immune and oxidative stress response in

these fish. While stations within individual regions did not separate well by nMDS, the predictive power of PAHs increased, suggesting Golden Tilefish in different regions are experiencing unique responses to PAH exposure.

Weak, but statistically significant, negative correlations were consistently observed in the GoM-wide dataset between sum liver PAH and oxidative stress biomarkers SOD, SDH, and SumNA, and between sum biliary PAH and SOD. These trends are contrary to literature-substantiated hypotheses in which oxidative stress damage indicators are typically elevated with exposure to PAHs. The measurable biliary PAH levels observed in nearly all Golden Tilefish in this study indicate recent exposure. Measurable liver PAH levels in these specimens are also notable, as tissue accumulation of PAH metabolites can occur when the organisms' capacity to metabolize the toxic compounds is overwhelmed, leaving behind a record of putative chronic exposure. With such long-term exposure, it is possible that resiliency or compensation mechanisms develop, reducing the oxidative stress response, which will have deleterious consequences on lipids, proteins, and DNA when perpetually engaged.

The majority (43%) of these GoM-wide data are comprised of specimens from the vicinity of the DWH spill (from NC2015 and NC2017). These fish have significantly elevated biliary PAH levels compared to the other sampling zones and have had records of chronically elevated PAH body burdens since the DWH spill (Murawski et al., 2014; Snyder et al., 2015, 2019). Despite their higher contaminant levels, the oxidative stress biomarkers for NC fish do not correspond as traditionally hypothesized with short-term PAH exposure, but may be exhibiting a metabolic conservation strategy with elevated chronic exposure (Petitjean et al., 2019). Fish from NC2015 have the lowest percentage of oxidative stress biomarkers classified as outliers relative to the remainder of the GoM. However, there is no true baseline in the GoM

for an unpolluted site, and it is likely that other toxicants or stressors impact oxidative stress expression in other regions of the GoM, so direct comparisons in biomarker fluctuation between geographic zones is incomplete without further contaminant analysis. For example, SW displays elevated levels of SumNA and SDH compared to NC groups, despite having lower levels of PAH exposure. Therefore, it is likely that some other unquantified stressor is inducing DNA and liver damage in this region.

The collapse of sampling zone separation by NMDS of GoM-wide explanatory variable and oxidative stress data upon the removal of LLF suggests that this indicator, while significant in describing overall variability among these data, does not significantly affect oxidative stress response and may be correlated with some other stressor or physiological mechanism. The weakly negative, but statistically significant, correlation between LLF and sum biliary PAH, and significantly lower levels of LLF in chronically exposed NC2015 and especially NC2017 Golden Tilefish, may indicate a shift in metabolic response in these specimens to facilitate sublethal stress from increased contaminants (Petitjean et al., 2019). It's also possible that benthic prey availability has shifted for these specimens, following the DWH event (McClain et al., 2019; Montagna et al., 2013).

Sum liver PAH also had weakly negative, but statistically significant, correlations with HCT ($R = -0.2$, $p = 0.004$) and LCT ($R = -0.15$, $p = 0.027$) in the GoM-wide dataset, which supports both mild anemia and immunosuppression upon chronic PAH exposure. Upon evaluation of the NMDS of explanatory variables and immune biomarkers, however, sum liver PAH could only minimally describe the potential health impacts of PAH exposure in the GoM-wide data, although inclusion of sum biliary PAH was able to distinguish NC2017 from NW zones. Removal of biliary PAH data, results in NW and NC2017 being grouped closer together,

driven by low LCT values and similar LYS expression at both stations. Overall, liver PAH did not contribute significantly to the description of variability among these data, suggesting the immune system endpoints utilized in this work may be affected by other variables or chemical exposures.

Despite similar levels of sum liver and biliary PAH in both years, specimens caught in the NC zone in 2015 could be described as having lower oxidative stress levels (SOD and SumNA), possible immunosuppression (lower LYS), and slight anemia (lower HCT) relative to those in 2017. Specimens caught in 2017, however, had lower condition factor and liver lipid fraction, which may support a compensation strategy to managing sublethal effects of chronic contamination from grounded DWH oil.

Variability among station response was observed within each sampling zone, with PAH levels having differing levels of impact on either oxidative stress or immune system outcomes. In the NW zone, elevated sum liver PAH and biliary B(a)P levels were observed at station 20-150, the eastern-most station in the zone, found within a dense aggregate of active oil platforms. Redundancy analysis suggested that elevated PAH levels described a proportion of oxidative stress and immune biomarker expression at 20-150. Specimens there had reduced K compared to other stations within the zone and an altered immune response (elevated LCT), however, no significant fluctuation in oxidative stress biomarkers among stations was observed. Due to their location within an area of active oil extraction and transport, it's possible these fish are chronically exposed to contaminants, which may play a role in their lower K and lack of significantly altered oxidative stress response, if they are undergoing a putative compensatory metabolic shift.

The SW zone contained geographically dispersed stations, however, RDA of immune biomarkers and explanatory variables in the SW stations indicated biliary B(a)P could describe some immune system response variability at 24-150 compared to the remaining stations. Despite this, no significant oxidative stress outcomes were observed. This station has the closest proximity to US gas and oil extraction activity, and it is possible PAH contamination could be transported to the site through currents.

Within CB, station 28-150 had elevated SumNA levels, as well as suppressed LYS and N/L compared to the remaining stations. By PCA and RDA, no correlation was observed between these fluctuations and PAH levels. This station is southeast of Veracruz, a port with documented multi-source pollutant impacts (Celis-Hernandez et al., 2017; Horta-Puga & Carriquiry, 2014). Station 30-100, offshore of the relatively polluted Coatzacoalcos river and Puerto Mexico, (Ruiz-Fernández et al., 2016; Scholz-Böttcher et al., 2008) had the highest levels of sum liver and biliary PAH in the zone, suggesting both recent and chronic contaminant exposure, however, specimens here also had the highest K on average, a counter trend to observations of chronically PAH exposed specimens in the NC and NW regions. Condition factor can vary with sex, spawning cycle, nutrition, and environmental conditions, and with limited study on Golden Tilefish in the southern GoM, it is difficult to interpret what factors may play a role in this index. Given histological evaluation of Golden Tilefish from the northern GoM, however, these fish should have been nearly recovered from their spawning cycle at the time of capture (Lombardi-Carlson, 2012). Their oxidative stress biomarkers were comparatively low, supporting a compensation mechanism. Redundancy analysis suggested that sum liver PAH and K could explain the variability in oxidative stress biomarker response at

station 30-100. This station appeared to have a slightly activated immune response with significantly elevated LYS and N/L compared to other stations.

In the YP sampling zone, station 34-100 had elevated SumNA that did not appear to be correlated with PAH values. Station 36-100 had significantly elevated SDH and elevated biliary B(a)P, but no statistically significant difference in sum biliary PAH levels compared to the other stations. Explanatory variables accounted for 69.16% of the variation among immune system biomarkers, however, this was primarily driven by K, which was highly variable at station 33-150. Liver and biliary sum PAH described more of the variability in 36-100 and 36-150, stations likely with the closest proximity to the loop current and active shipping channels, and therefore possible transient PAH exposure.

3.6 Conclusions

Differences in the patterns of both oxidative stress and immune system biomarker response were observed in the NC region, near the DWH oil spill, with indicators of resiliency or acclimation in these chronically contaminated tilefish. Relatively high levels of biliary PAH in both NC2015 and NC2017 specimens indicated continual exposure in the region. However, the lack of significantly elevated liver PAH levels in these fish, compared to other specimens from the GoM, suggested that NC Golden Tilefish could still adequately metabolize the oil they encounter. Notably, the increase in SumNA, SOD in NC2017 fish compared to NC2015 specimens, accompanied by lower LLF in NC2017 animals, suggests a putative metabolic compensation strategy, requiring more basal energy input to repair damaged cellular components, fueled by the metabolism of lipid stores. While this does not appear to have had a significant effect on condition factor on the subset of fish evaluated here, a trend towards

decreasing condition factor in Golden Tilefish from the NC region of the GoM was observed by Snyder *et al.*, (2019).

Interpretation of these data was complicated by the sampling limitations inherent to such a geographically diverse study, with stations in the NW, SW, CB, and YP regions sampled one time only. In addition, as these organisms live in contact with sediments that have absorbed contaminants from both natural and anthropogenic influences, diverse inputs apart from measured PAH levels may describe the biomarker fluctuations observed. Notably, no true control exists in the GoM for Golden Tilefish, as all specimens had documented PAH levels in their bile and tissue. At select regions and stations throughout the GoM, biliary and liver PAH appear to influence biomarker response. For example, sum liver PAH had weak, but statistically significant correlations, with SDH, SumNA, and SOD, suggesting possible effects of chronic exposure. Both K and LLF had weak correlations with SOD. Overall, responses are variable and correlations are weak, suggesting multiple influences to any biomarker outcome, as one would expect in natural ecosystems.

Additional monitoring of Golden Tilefish from the region of the GoM impacted by the DWH spill would be necessary to determine whether fish are recovering from continued exposure. While demersal sampling is cost prohibitive, currently no literature describes timescales of long-term recovery in Golden Tilefish or a comparable species following a pollution event. Thorough evaluation of fish from the NC region every five years may provide an indication as to whether resilience or health declines persist in this population.

3.7 Figures

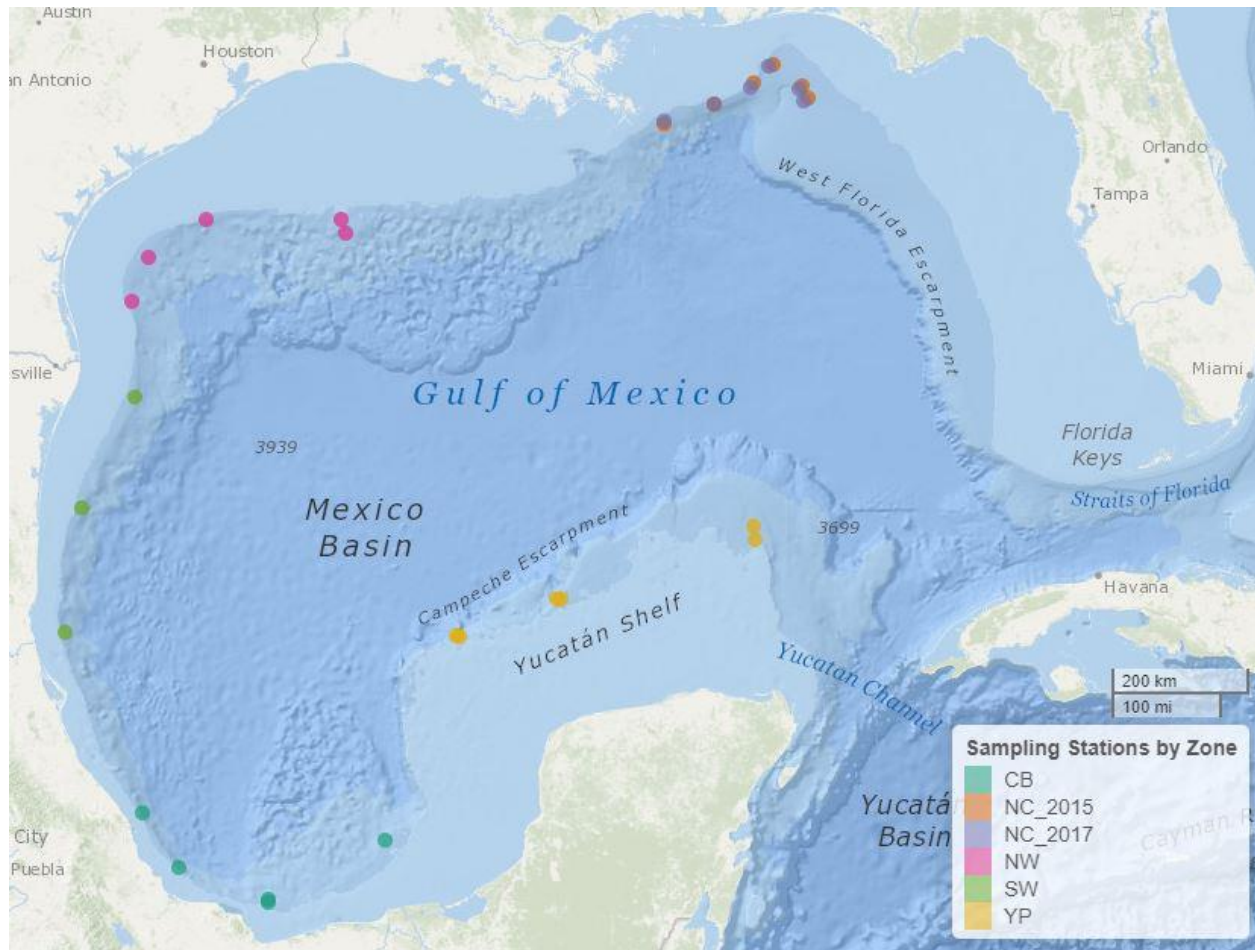


Figure 3.1: Distribution of sampling stations among geographic zones.

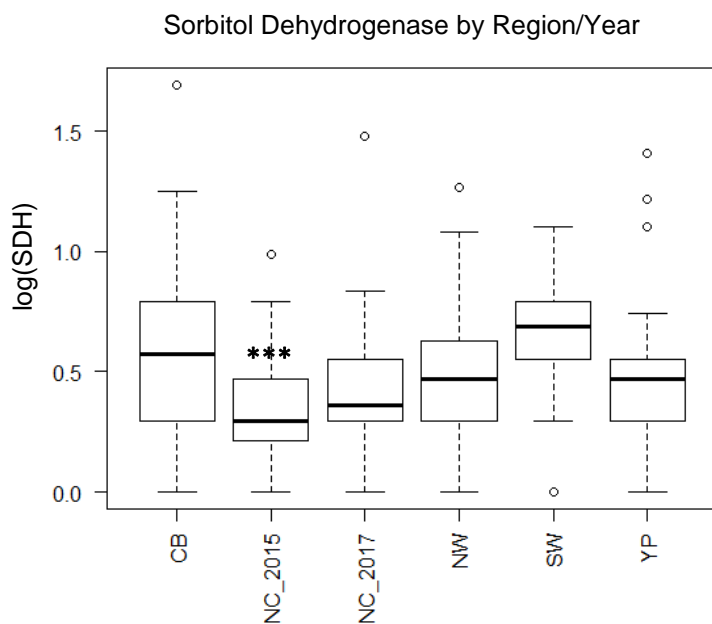
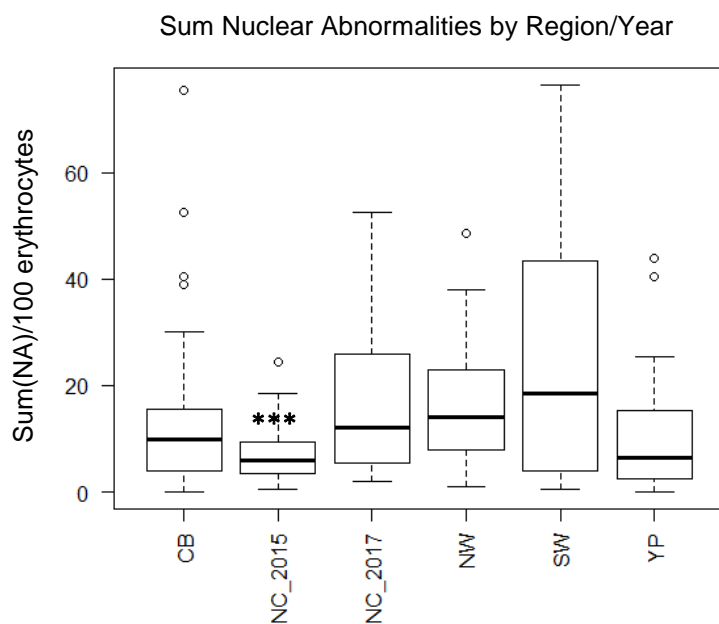


Figure 3.2: Oxidative stress biomarkers for which NC fish varied significantly from those in other regions sampled. The NC sampling group that significantly varied ($p < 0.05$) from another marked with asterisks (***) as determined by Kruskal-Wallis analysis after testing for normality by Shapiro-Wilks.

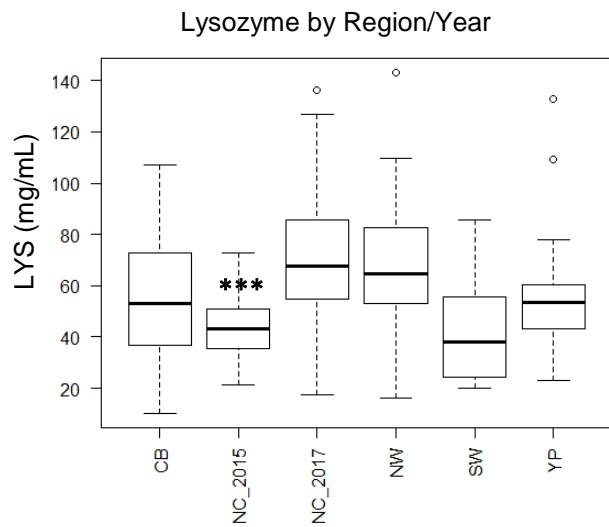
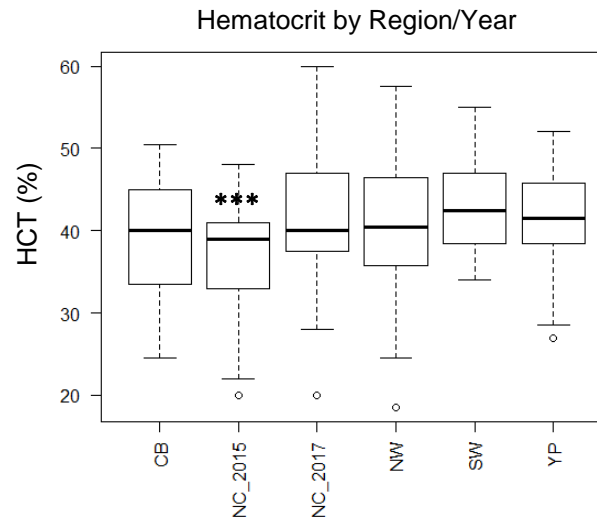
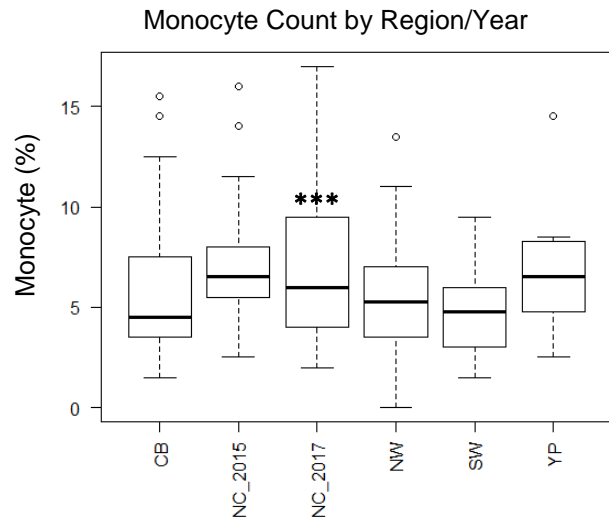


Figure 3.3: Immune system biomarkers for which NC fish varied significantly from those in other regions sampled. The NC sampling group that significantly varied ($p < 0.05$) from another is marked with asterisks (***) as determined by Kruskal-Wallis analysis after testing for normality by Shapiro-Wilks.

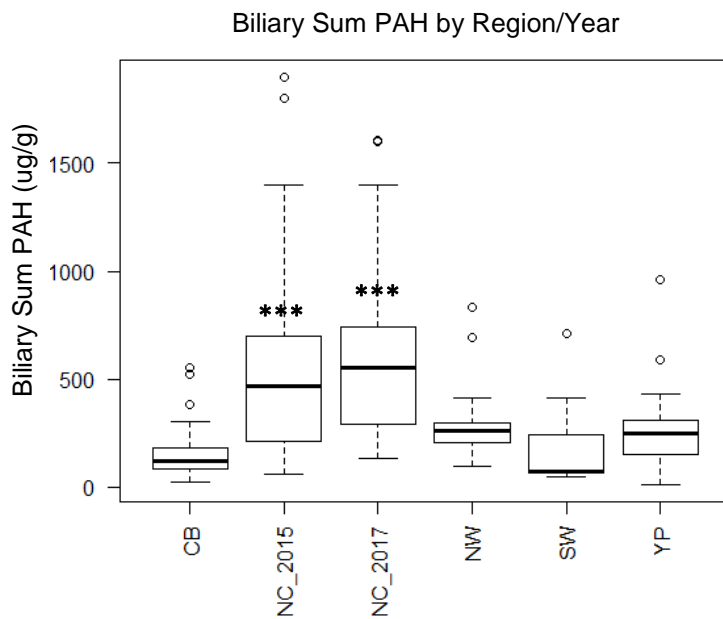


Figure 3.4: Polycyclic aromatic hydrocarbon levels for which NC fish varied significantly from those in other regions sampled. The NC sampling group that significantly varied ($p < 0.05$) from another is marked with asterisks (***) as determined by Kruskal-Wallis analysis after testing for normality by Shapiro-Wilks.

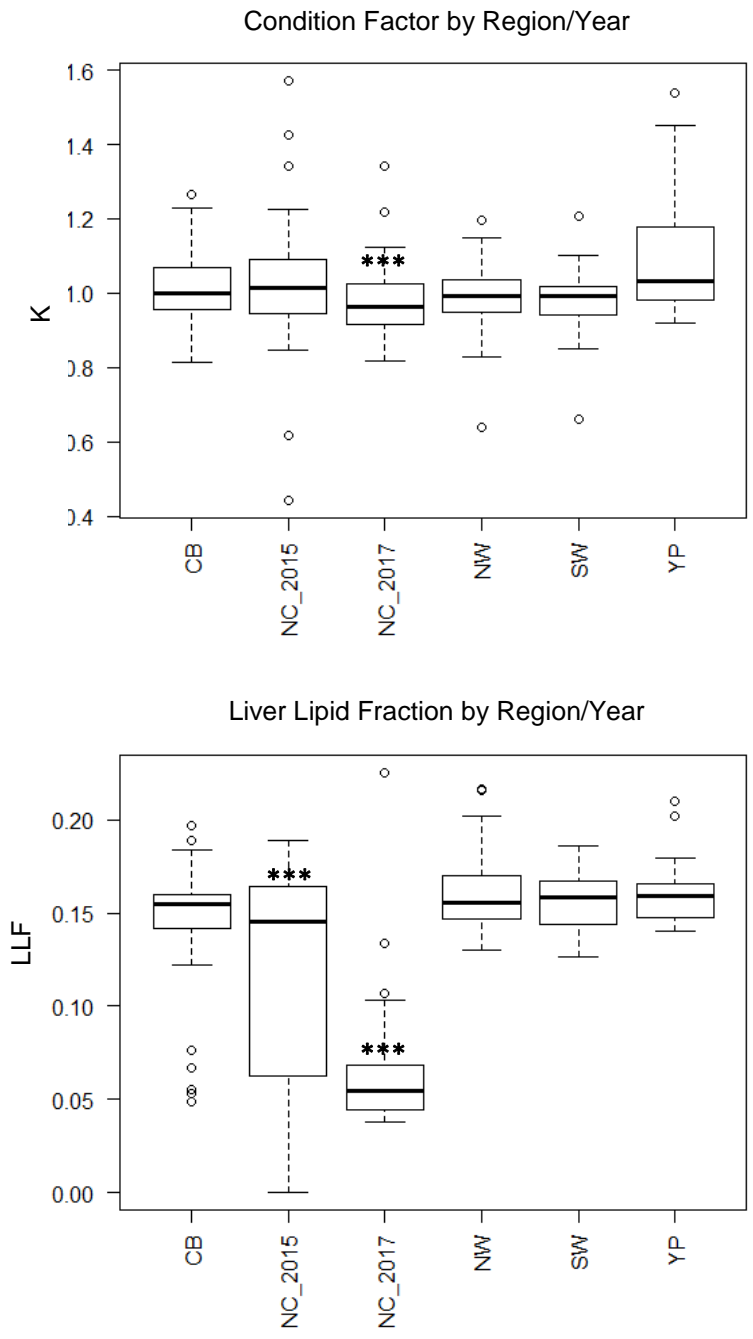


Figure 3.5: Body condition variables for which NC fish varied significantly from those in other regions sampled. The NC sampling group that significantly varied ($p < 0.05$) from another is marked with asterisks (***) as determined by Kruskal-Wallis analysis after testing for normality by Shapiro-Wilks.

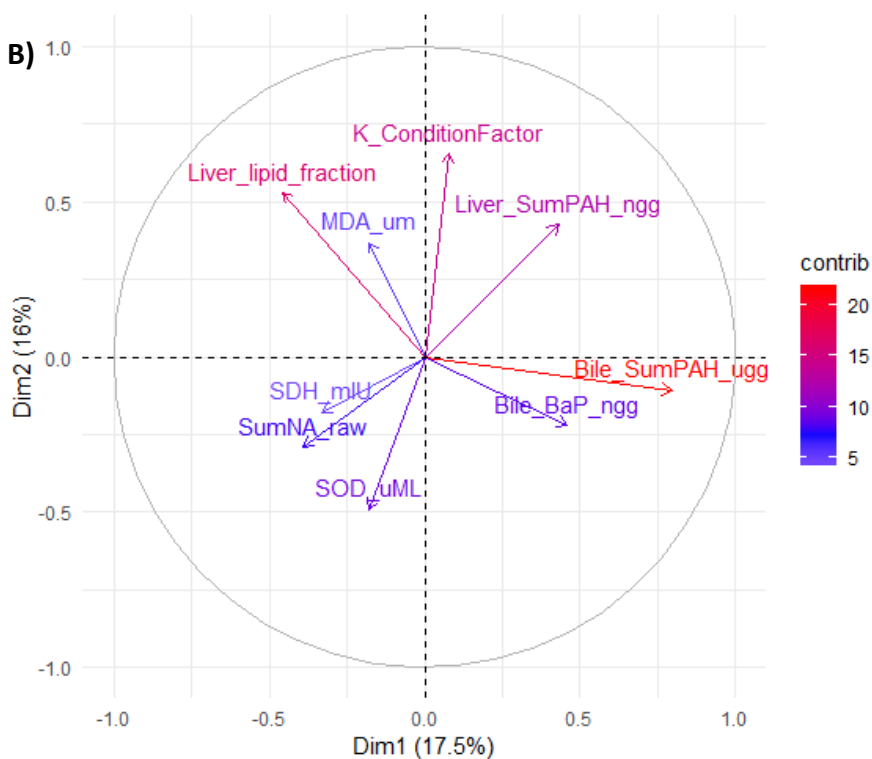
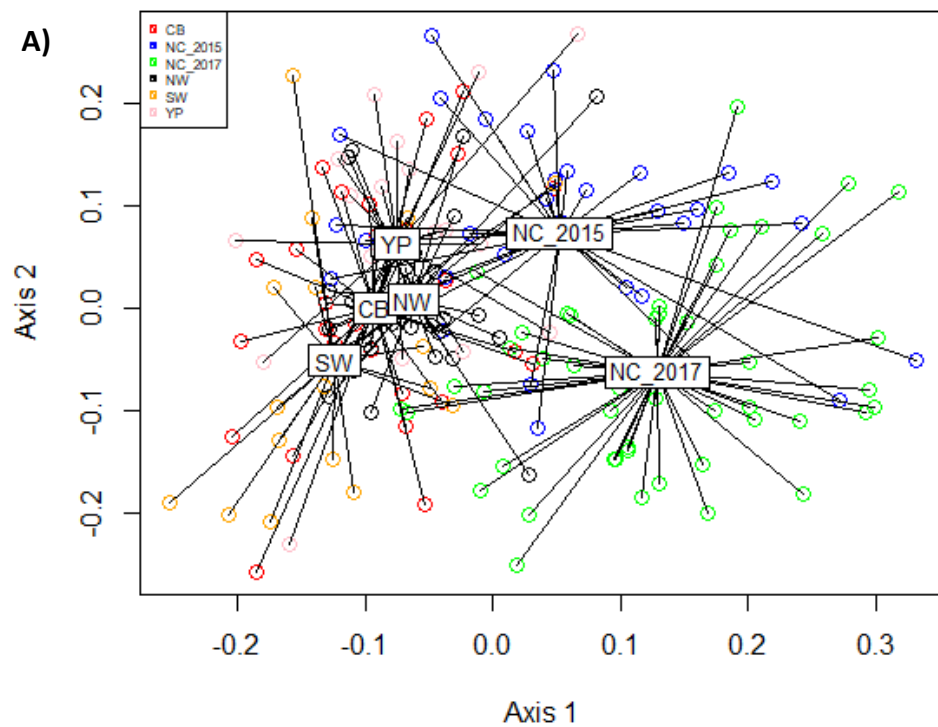


Figure 3.6: A) NMSD and B) PCA for GoM-wide explanatory variables and oxidative stress biomarkers.

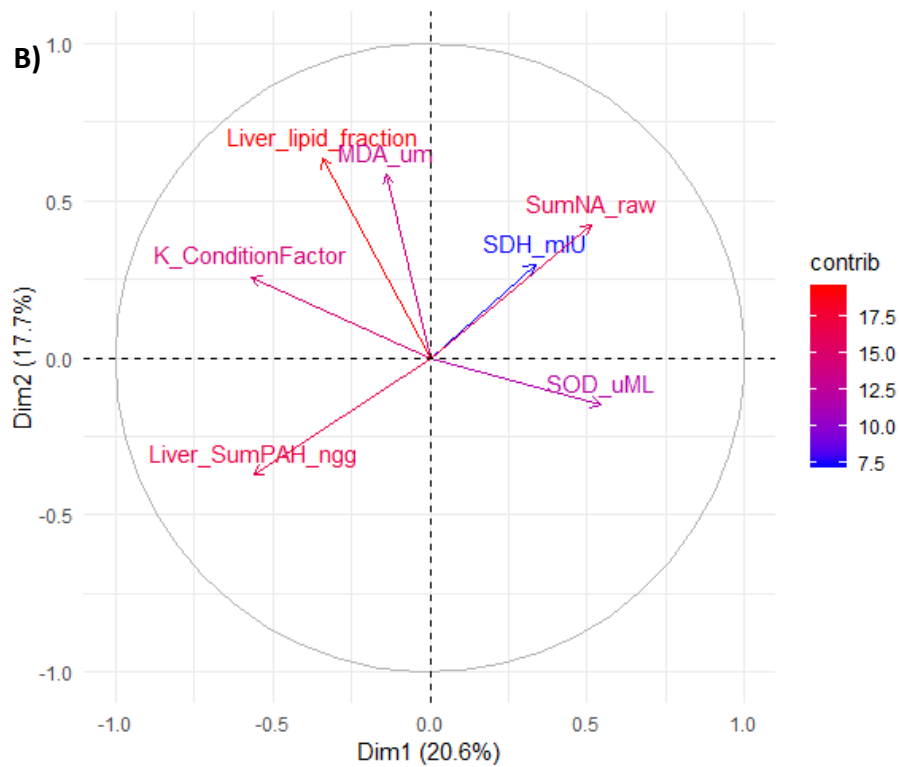
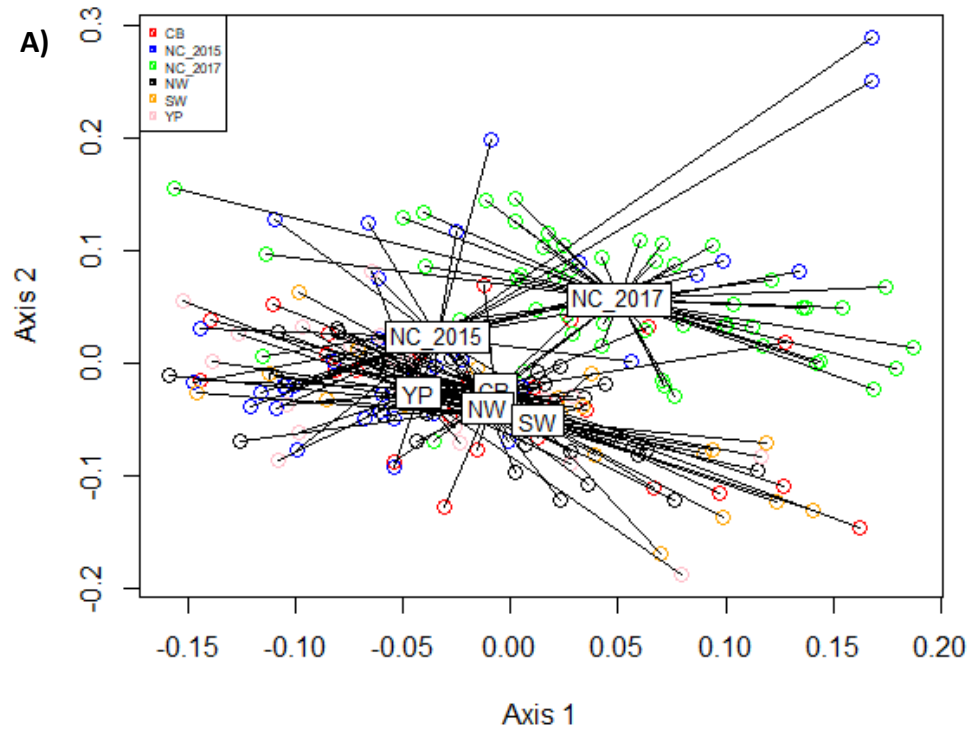


Figure 3.7: A) NMDS and B) PCA for GoM-wide explanatory variables and oxidative stress biomarkers upon removal of biliary PAH data.

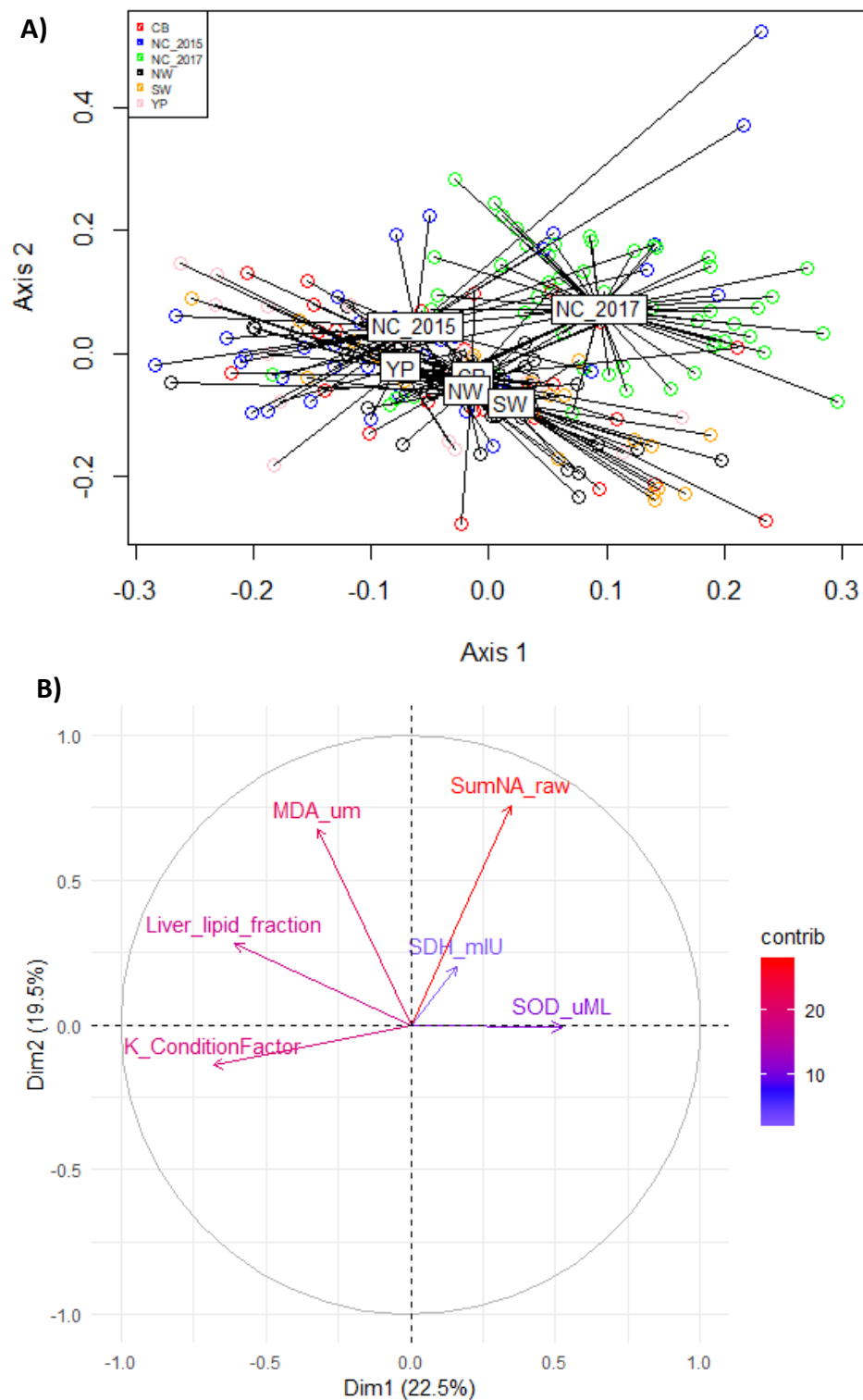


Figure 3.8: A) NMDS and B)PCA for GoM-wide explanatory variables and oxidative stress biomarkers upon removal of PAH data.

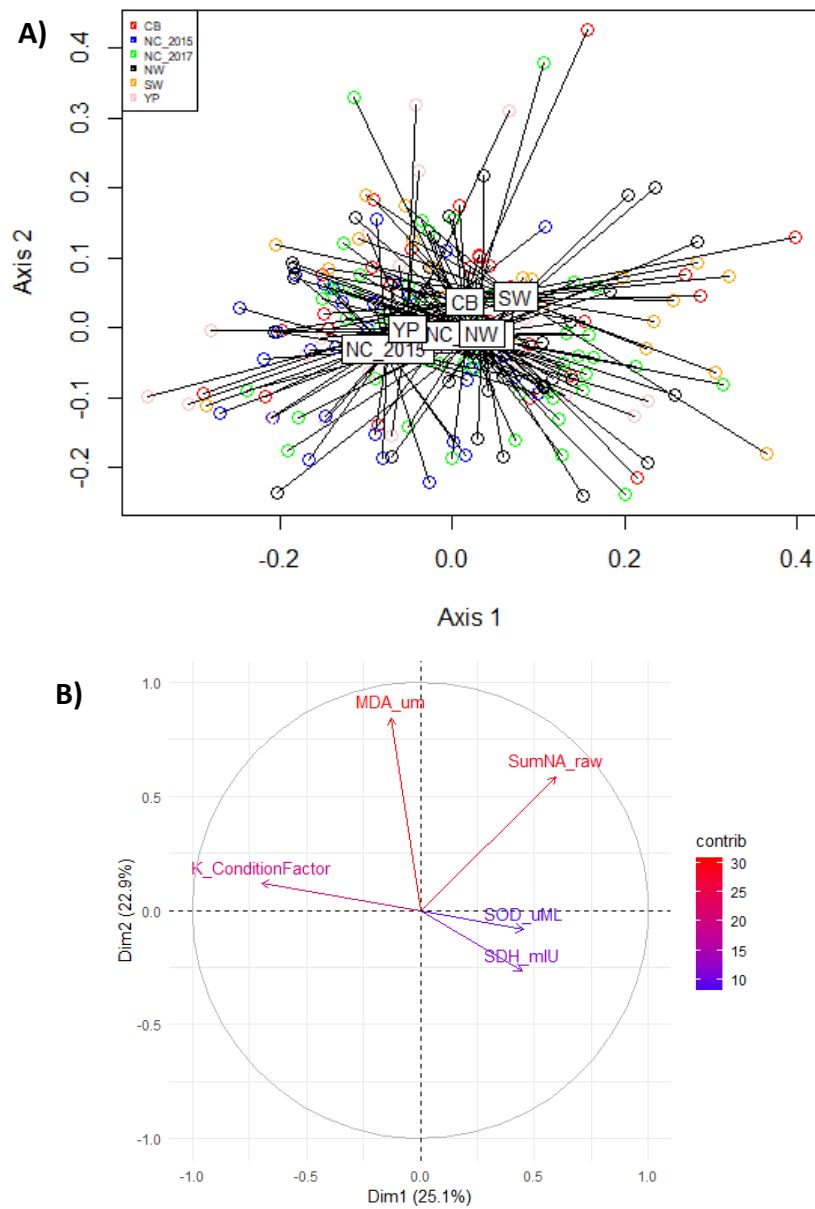


Figure 3.9: A) NMDS and B) PCA for GoM-wide explanatory variables and oxidative stress biomarkers upon removal of PAH and liver lipid fraction a.

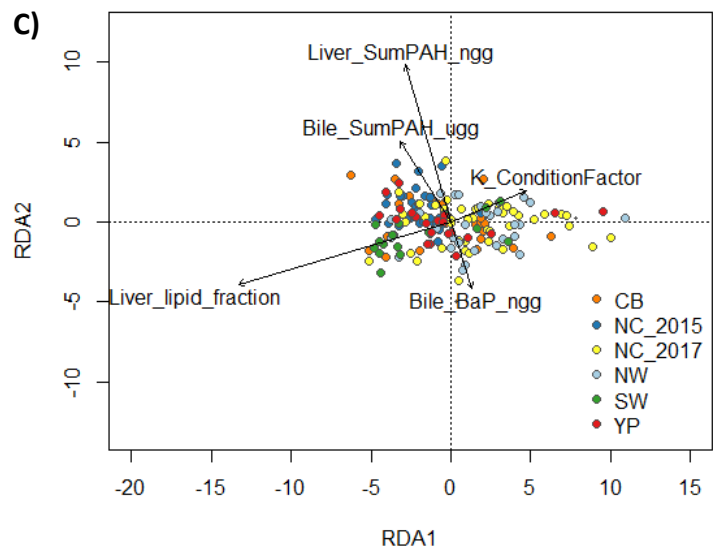
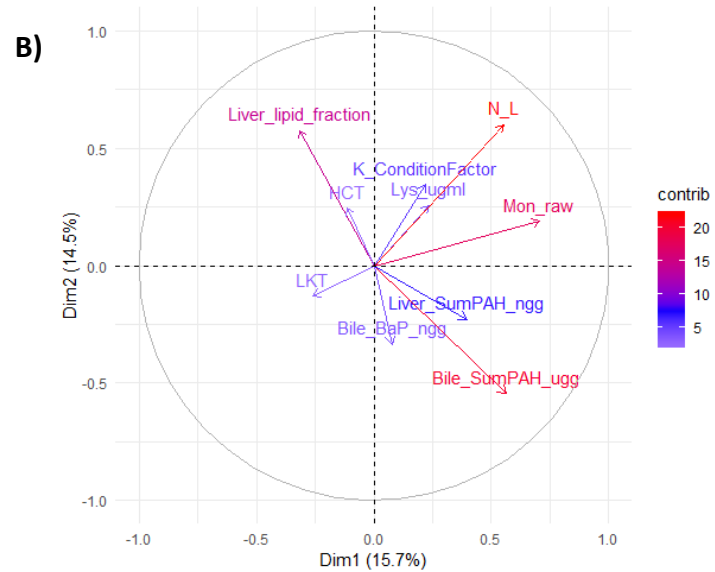
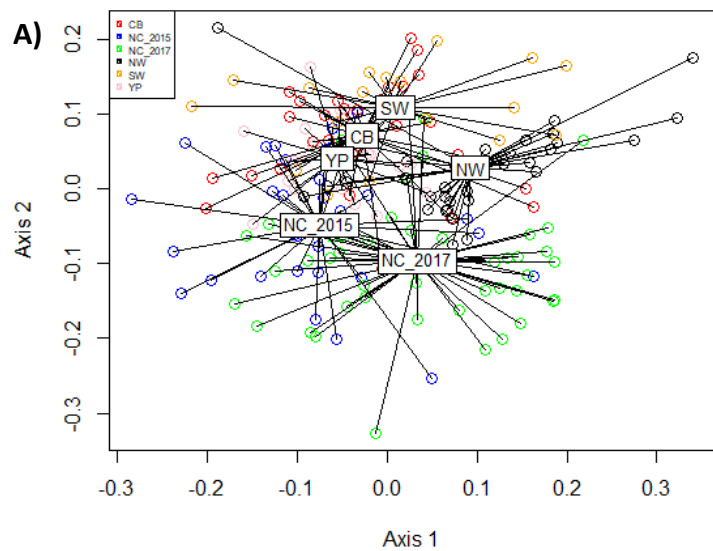


Figure 3.10: A) NMDS, B) PCA, and C) RDA for GoM-wide explanatory variables and immune system biomarkers.

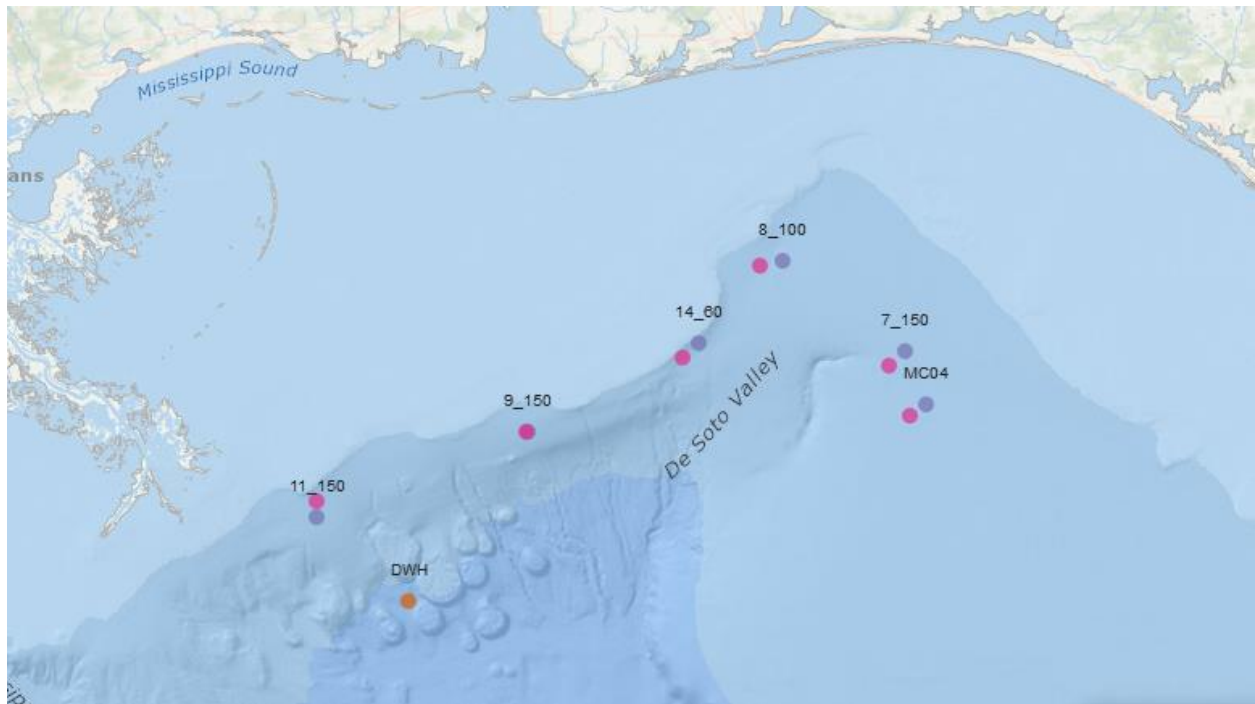


Figure 3.11: Station locations in zone NC, sampled in both 2015 (purple) and 2017 (pink). The DWH wellhead is shown in orange.

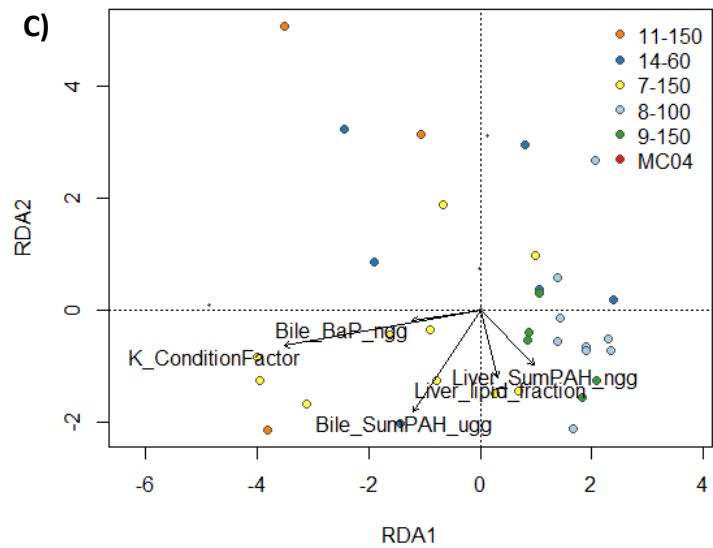
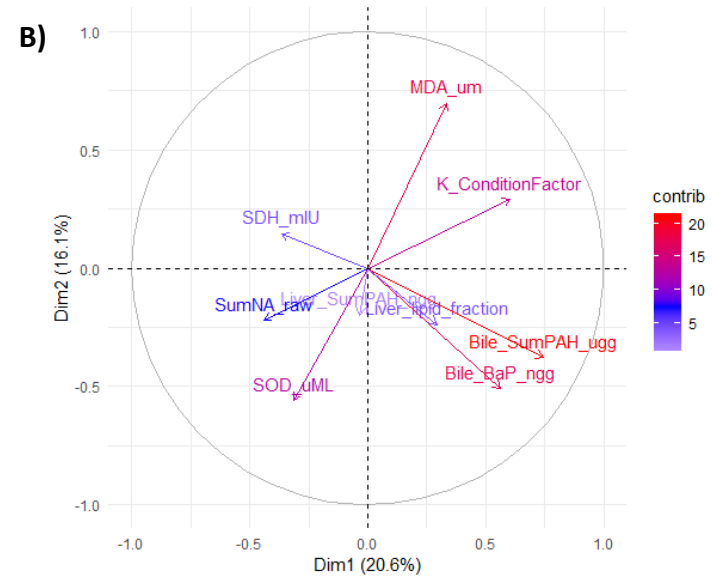
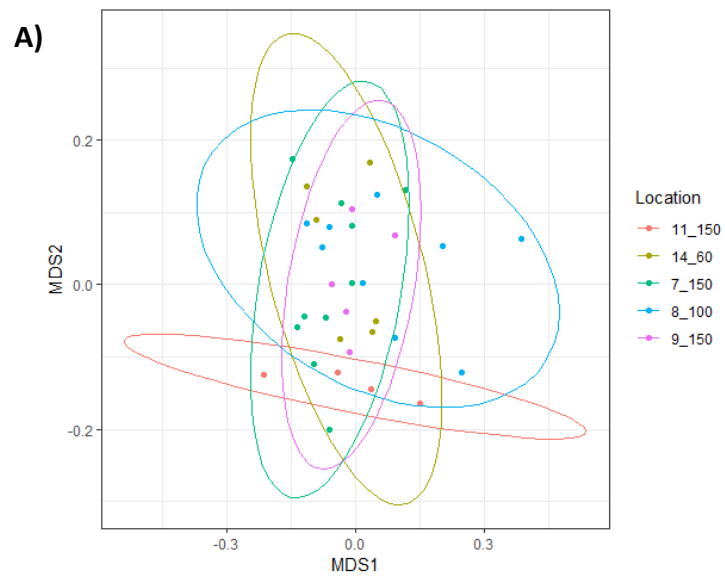


Figure 3.12: A) NMDS, B) PCA, and C) RDA for explanatory variables and oxidative stress biomarkers in NC2015 specimens

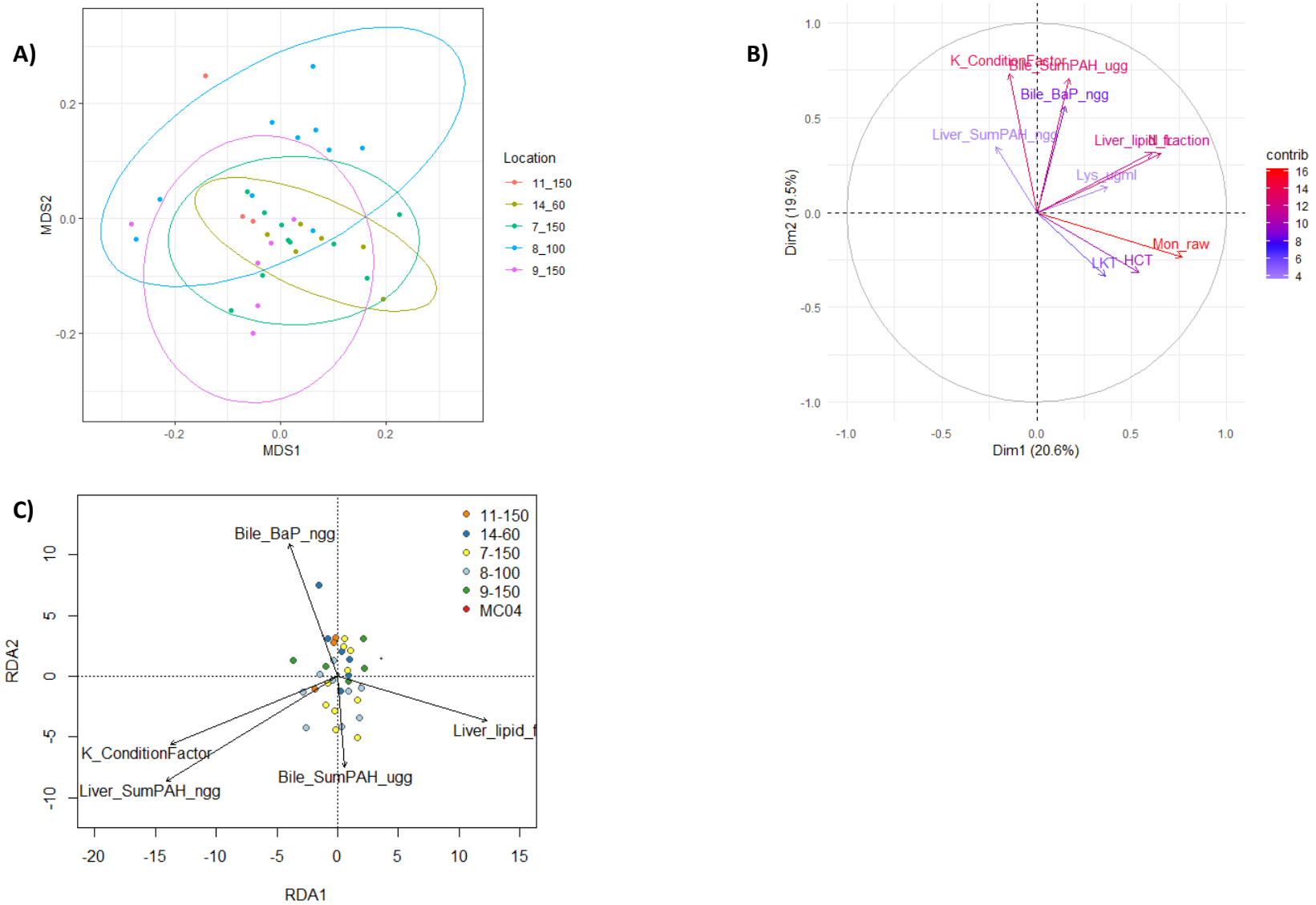


Figure 3.13: A) NMDS, B) PCA, and C) RDA for explanatory variables and immune system biomarkers in NC2015 specimens

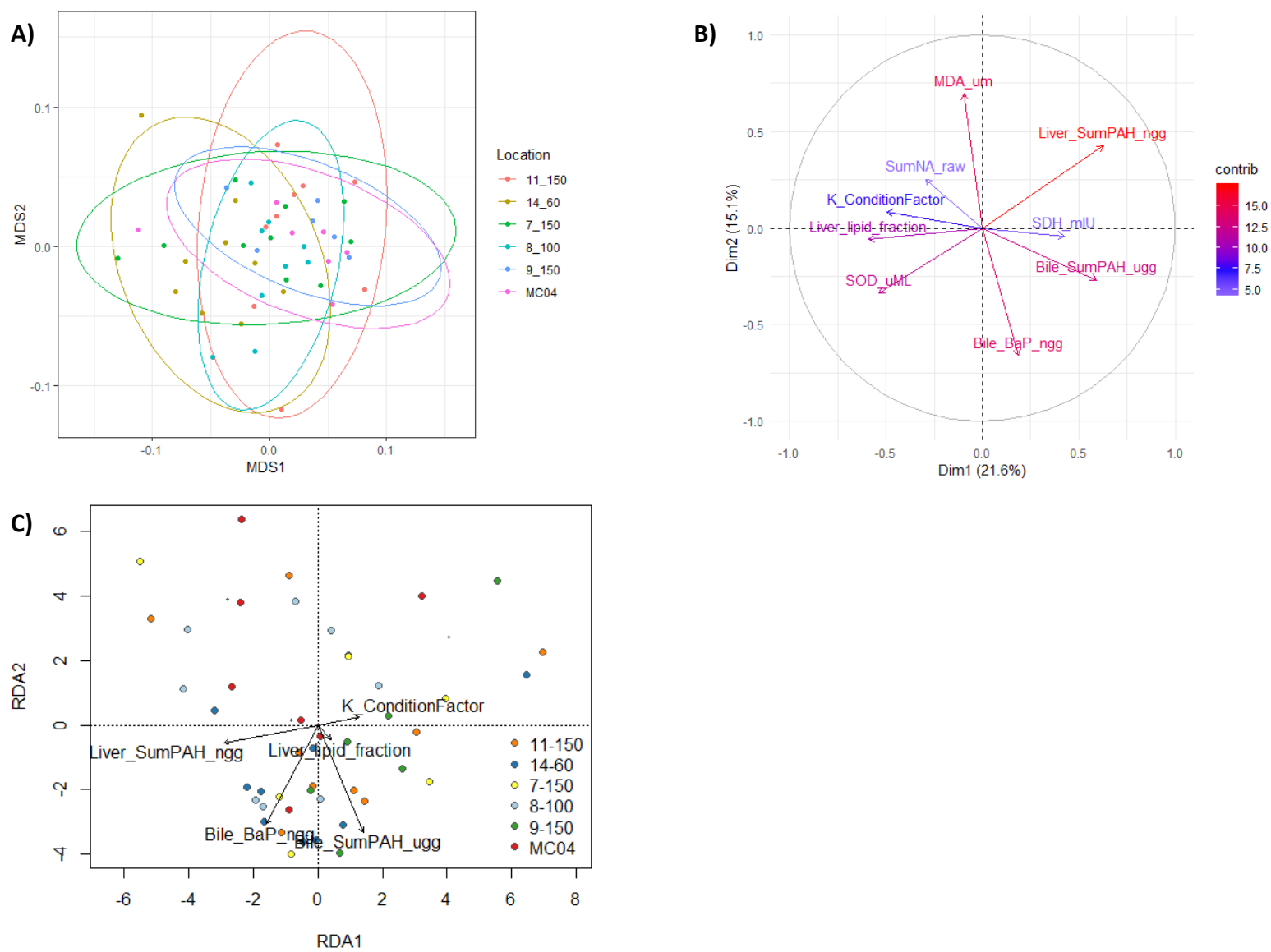


Figure 3.14: A) NMDS, B) PCA, and C) RDA for explanatory variables and oxidative stress biomarkers in NC2017 specimens.

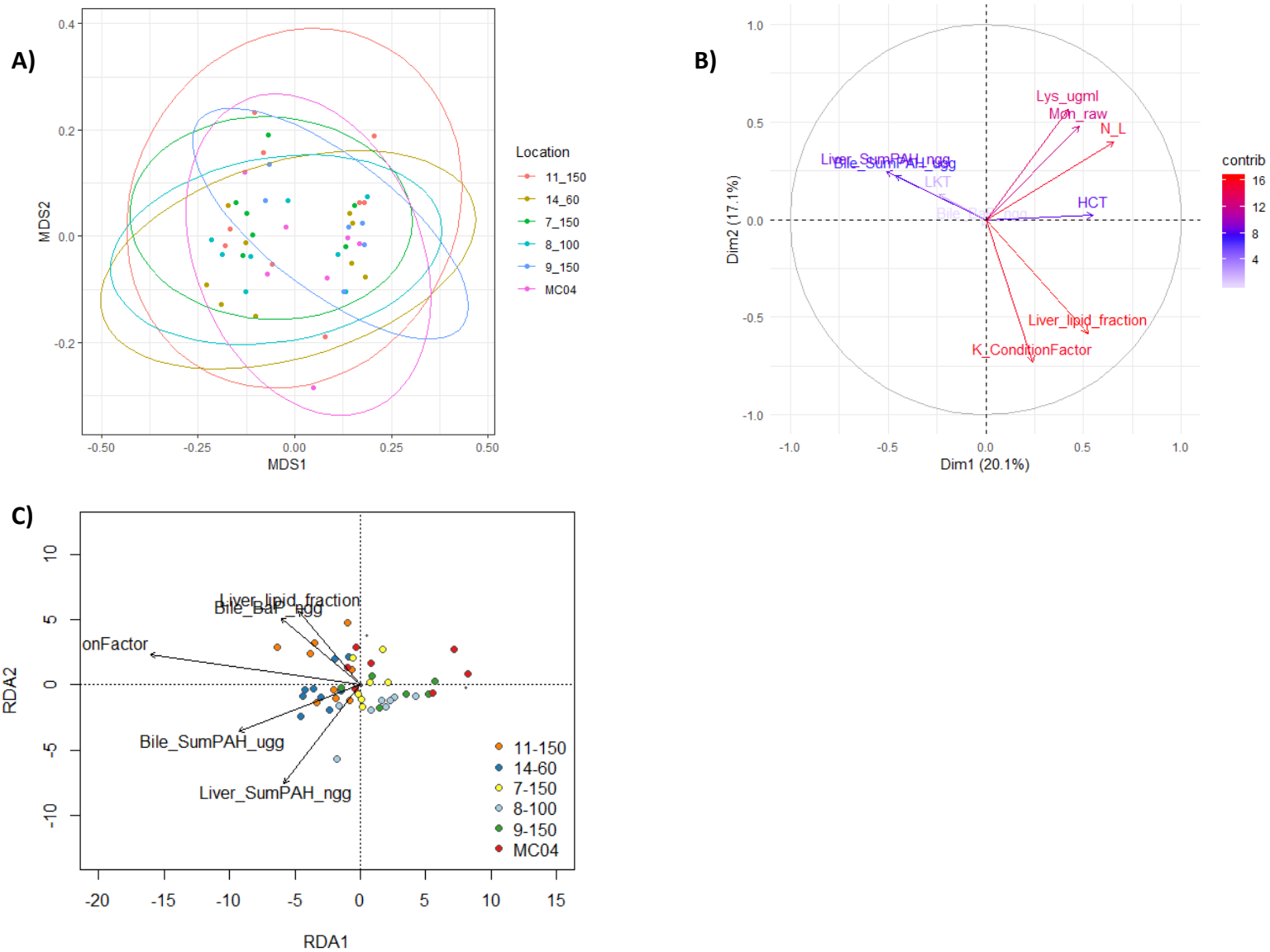


Figure 3.15: A) NMDS, B) PCA, and C) RDA for explanatory variables and immune system biomarkers In NC2017 specimens.

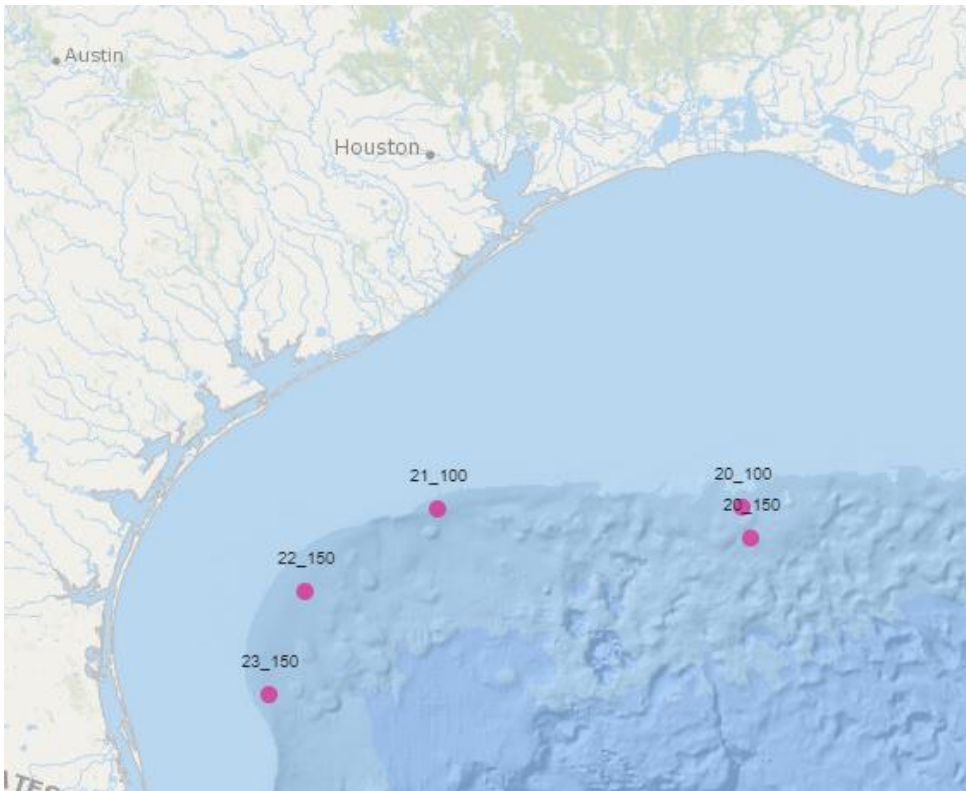


Figure 3.16: Station locations in NW zone.

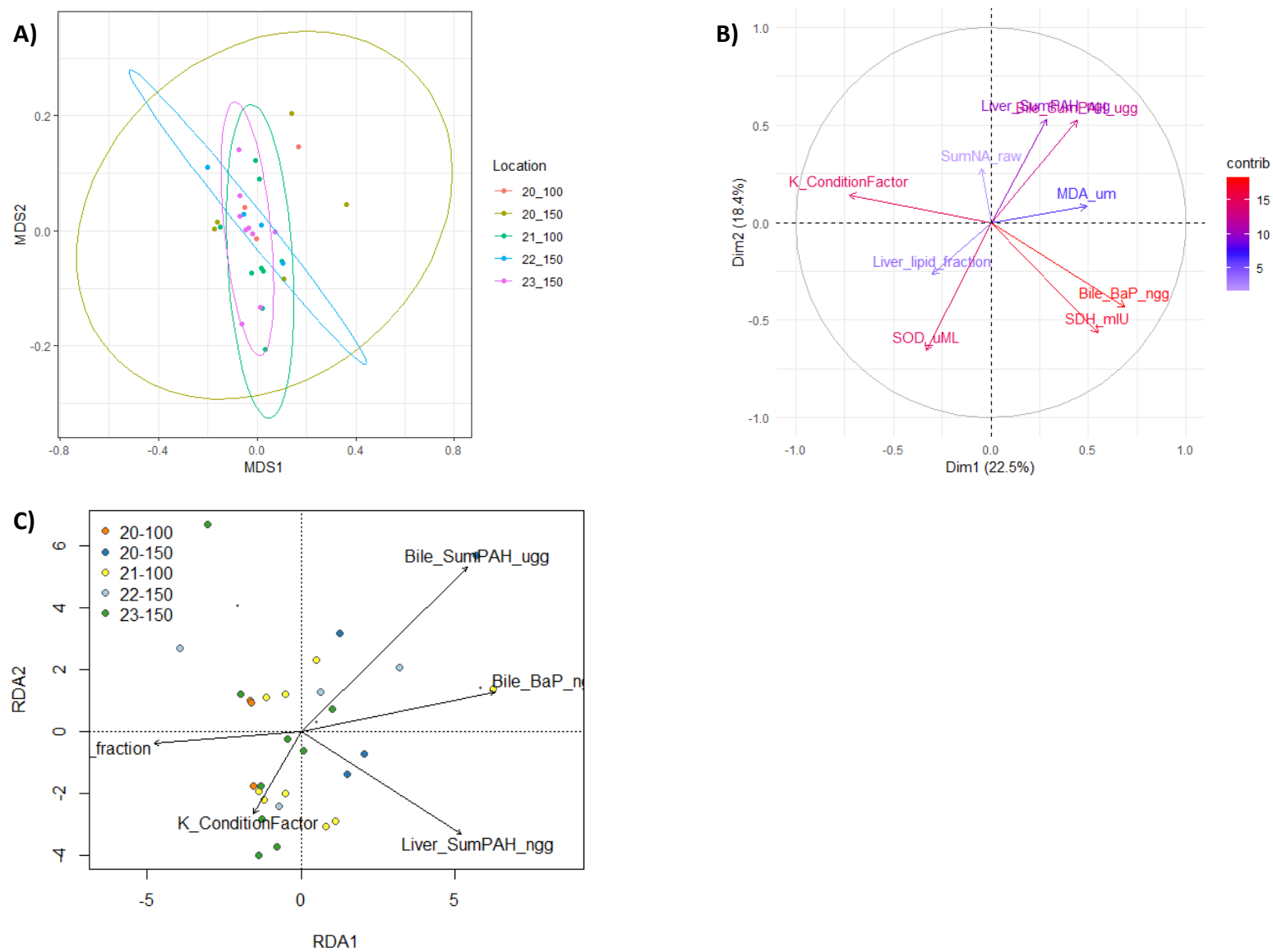


Figure 3.17: A) NMDS, B) PCA, and C) RDA for explanatory variables and oxidative stress biomarkers in NW specimens.

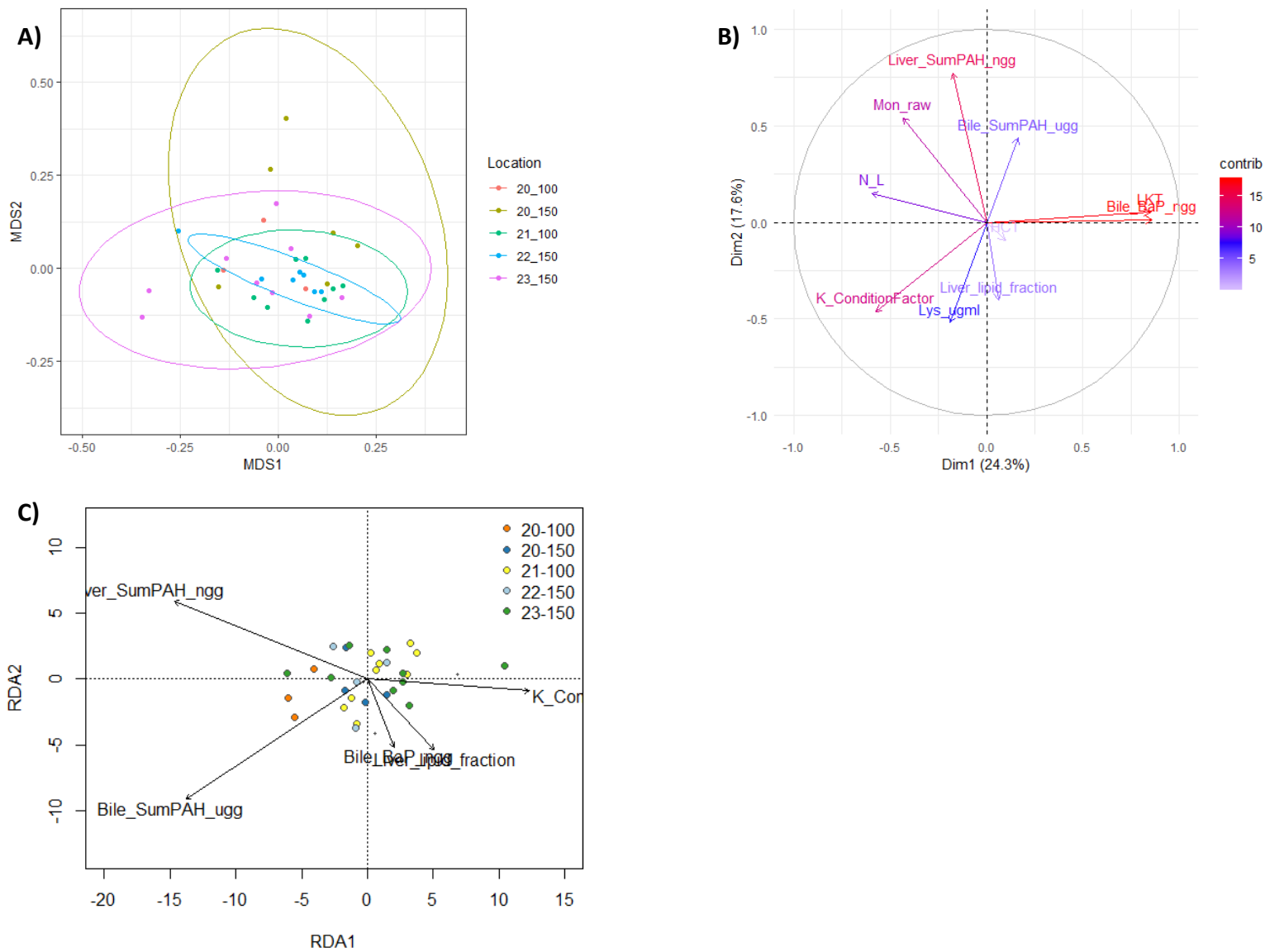


Figure 3.18: A) NMDS, B) PCA, and C) RDA for explanatory variables and immune system biomarkers in NW specimens.



Figure 3.19: Station locations in SW zone.

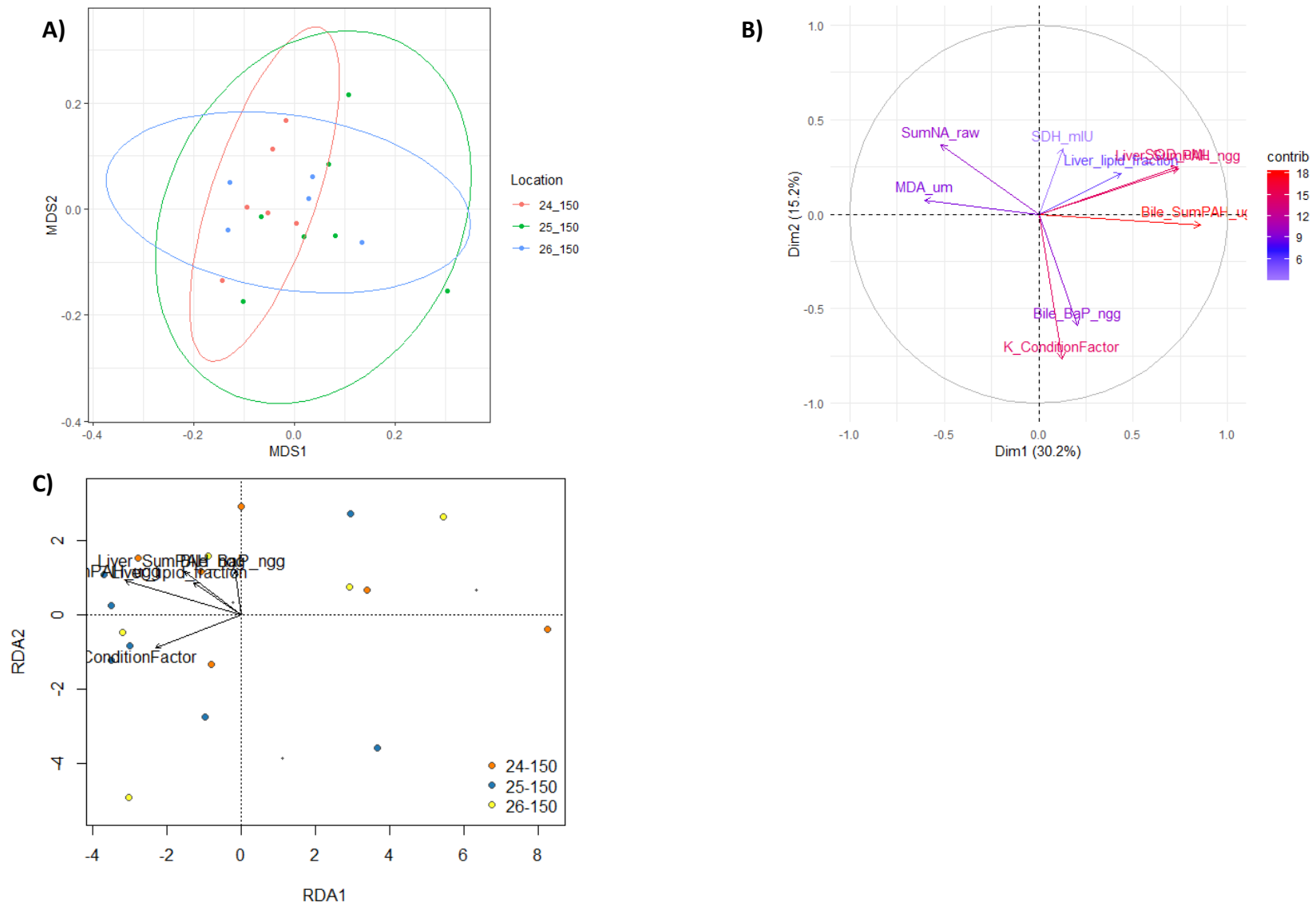


Figure 3.20: A) NMDS, B) PCA, and C) RDA for explanatory variables and oxidative stress biomarkers in SW specimens.

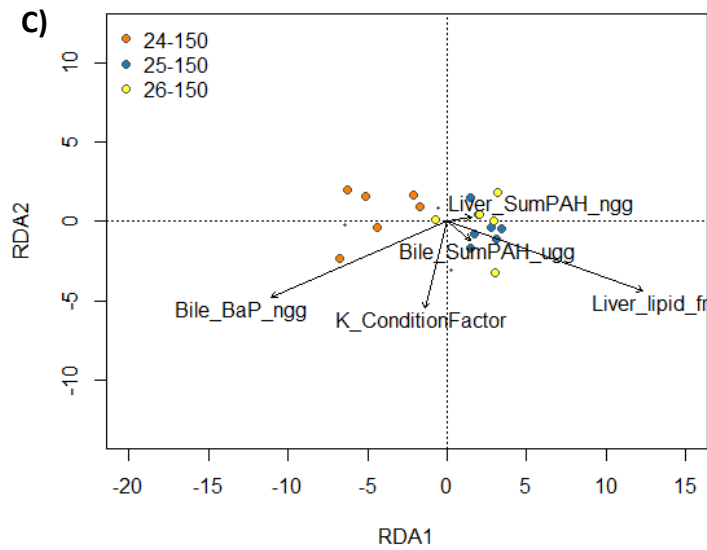
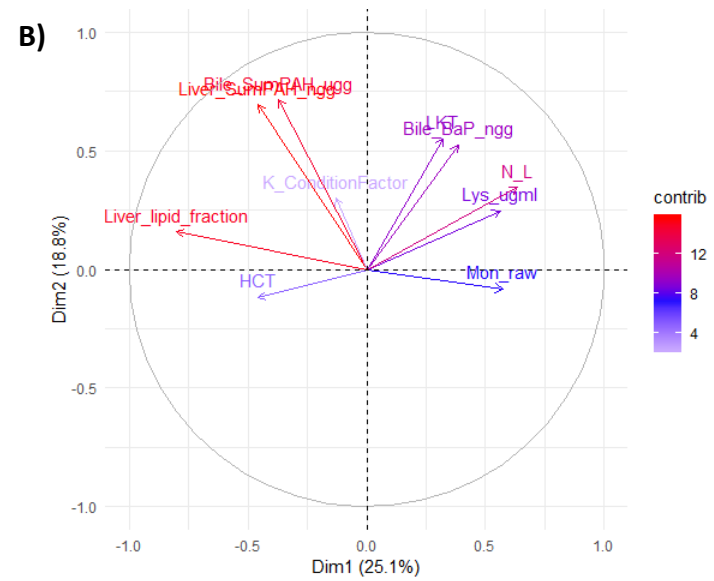
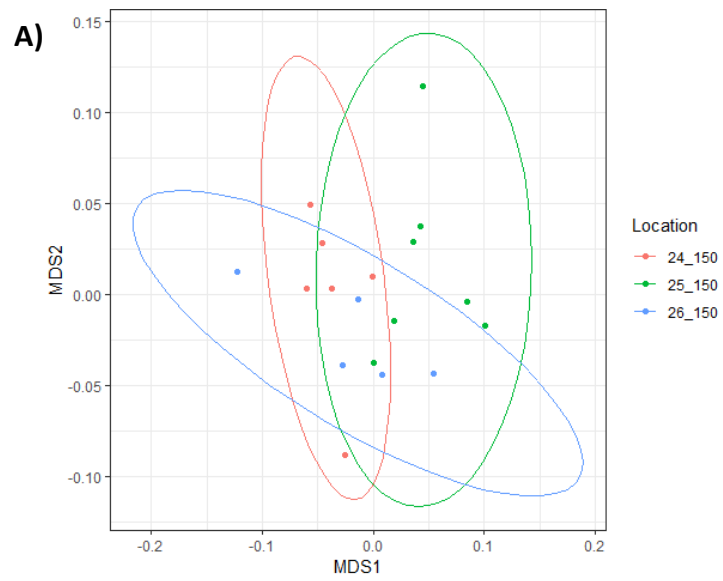


Figure 3.21: A) NMDS, B) PCA, and C) RDA for explanatory variables and immune system biomarkers in SW specimens.

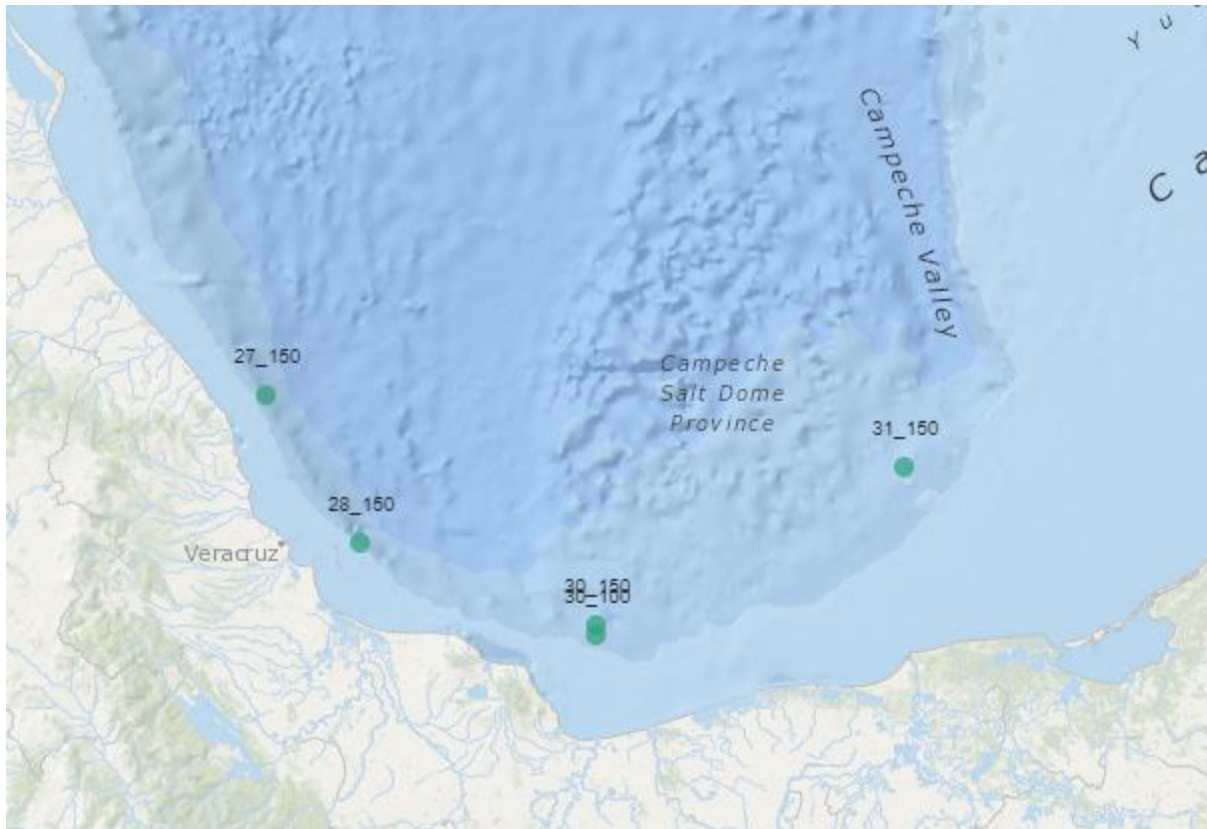


Figure 3.22: Station locations in CB zone.

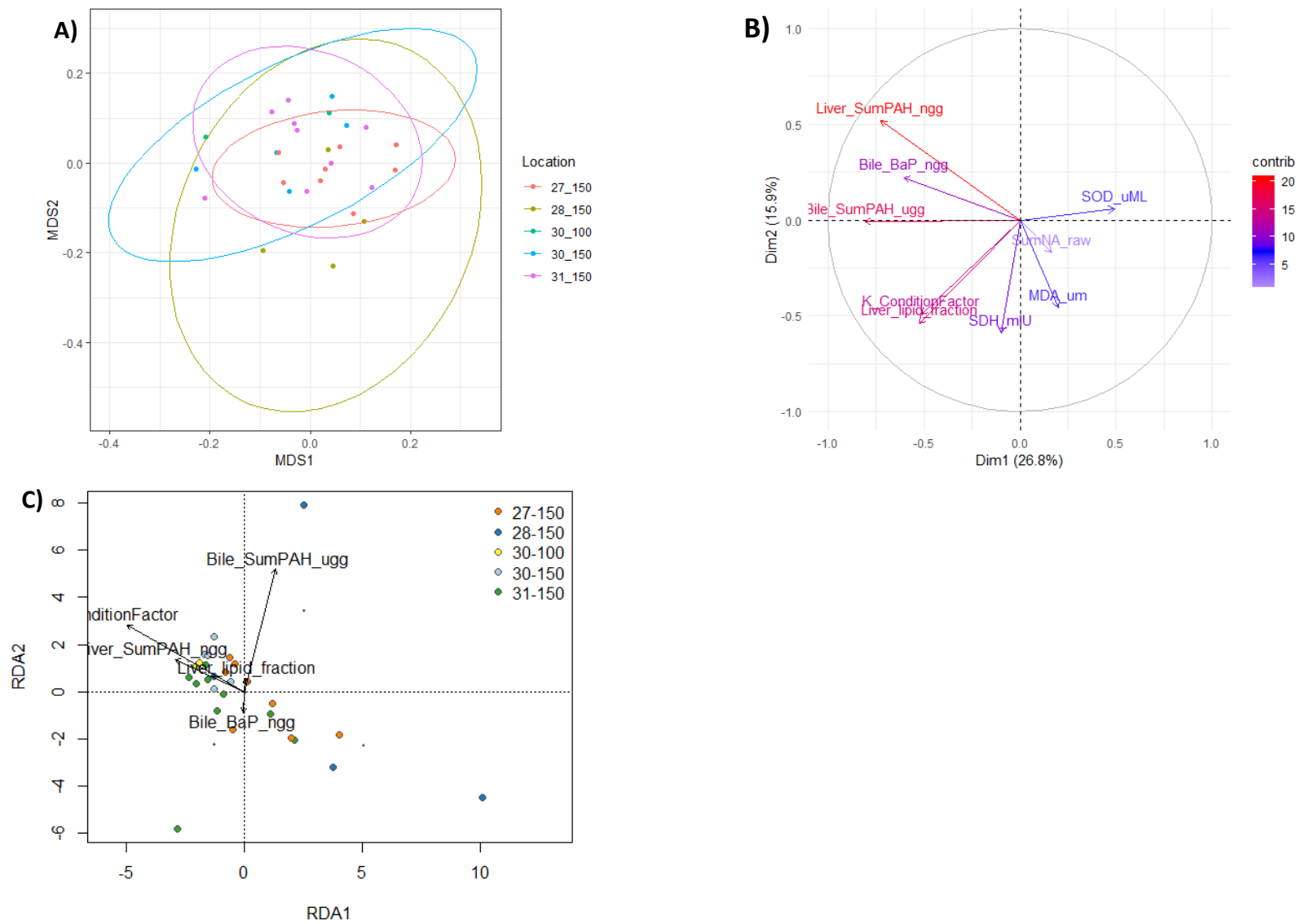


Figure 3.23: A) NMDS, B) PCA, and C) RDA for explanatory variables and oxidative stress biomarkers in CB specimens.

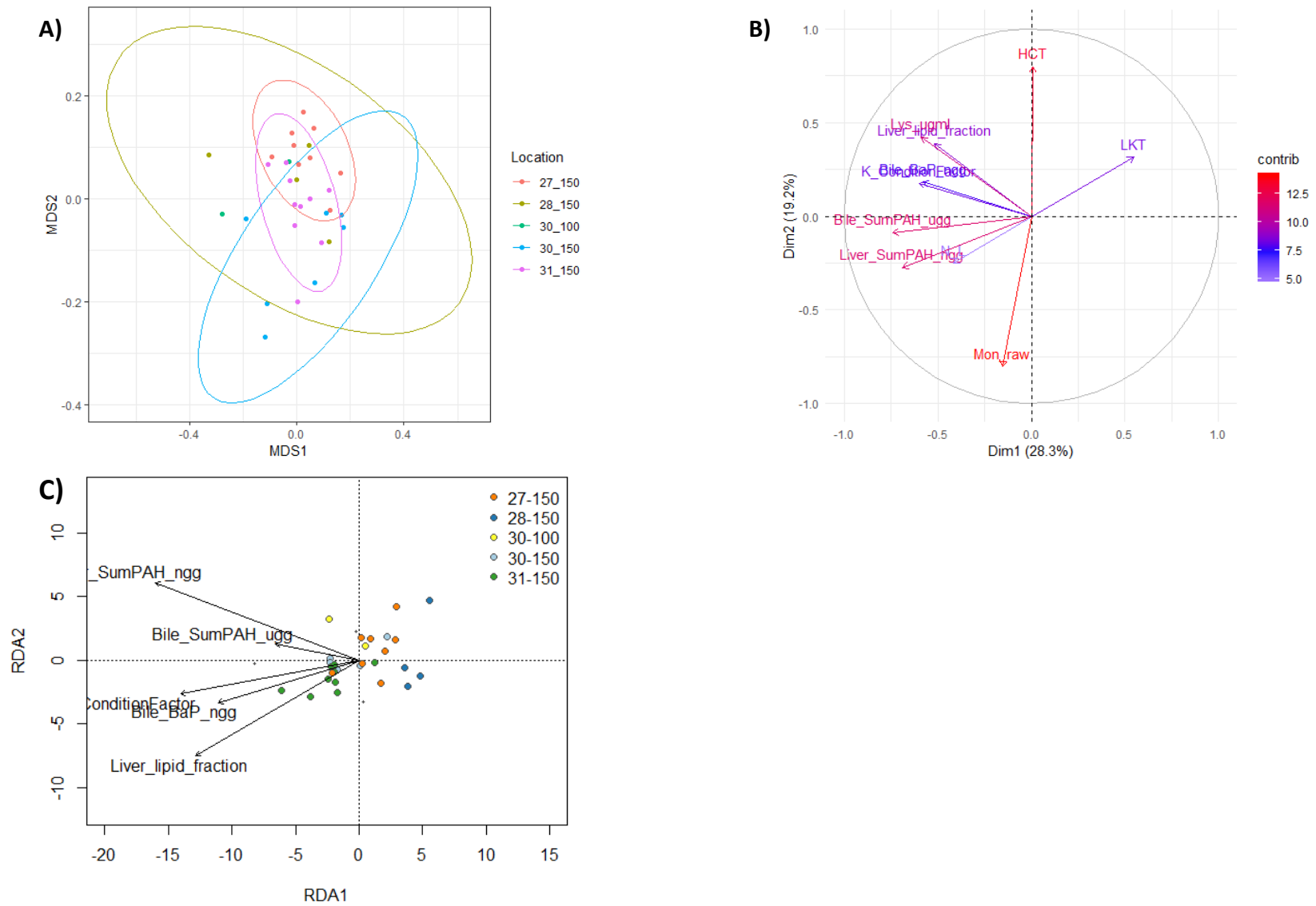


Figure 3.24: A) NMDS, B) PCA, and C) RDA for explanatory variables and immune system biomarkers in CB specimens.

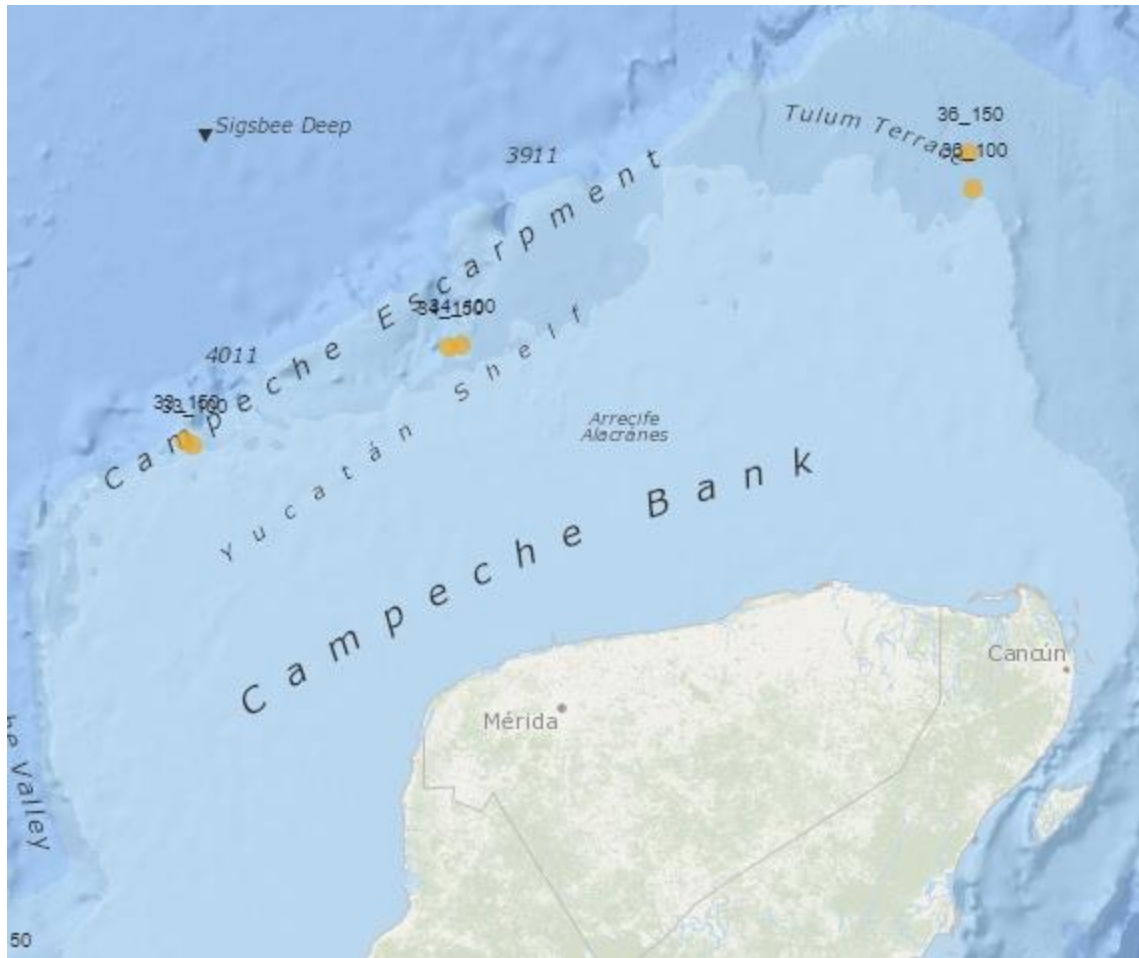


Figure 3.25: Station locations in YP zone.

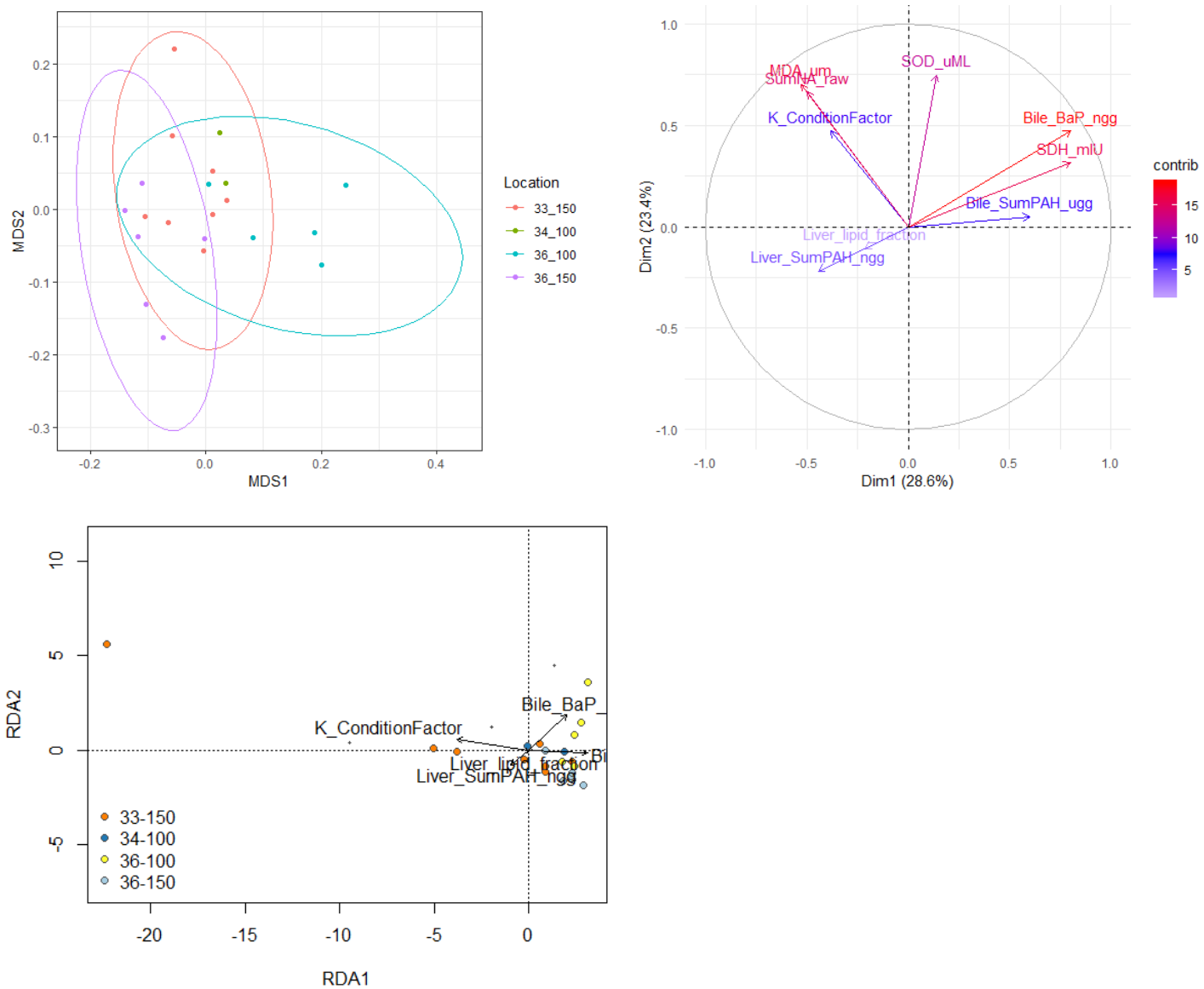


Figure 3.26: A) NMDS, B) PCA, and C) RDA for explanatory variables and oxidative stress biomarkers in YP specimens.

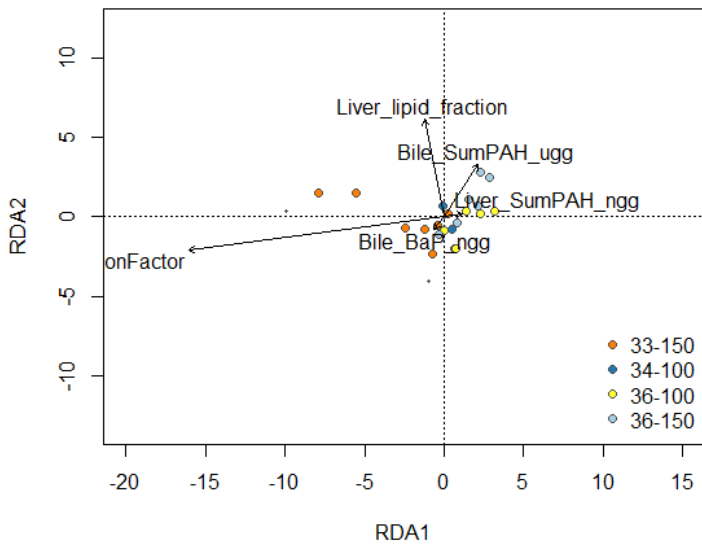
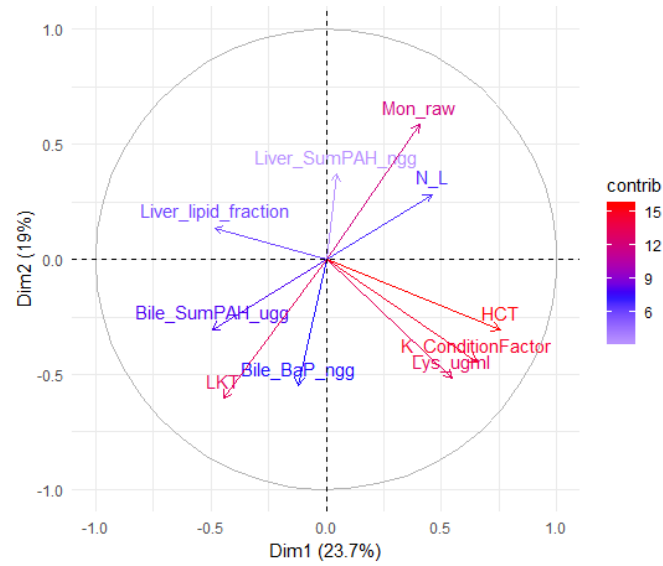
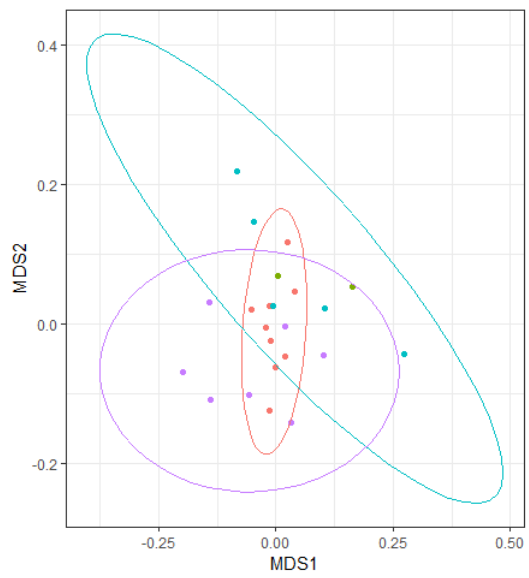


Figure 3.27: A) NMDS, B) PCA, and C) RDA for explanatory variables and immune system biomarkers in YP specimens.

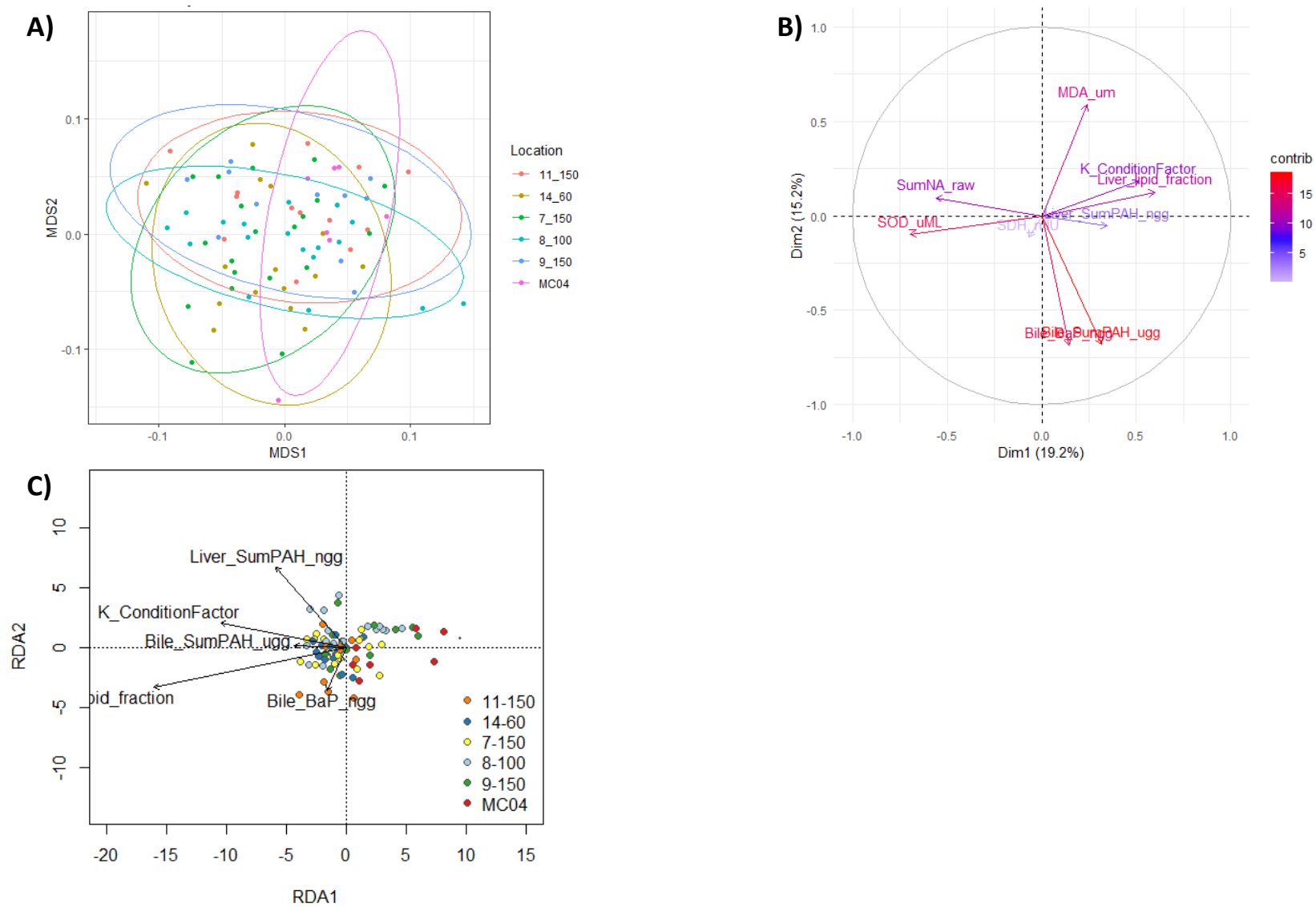


Figure 3.28: A) NMDS, B) PCA, and C) RDA for explanatory variables and oxidative stress biomarkers in specimens from NC stations, grouped regardless of sampling year.

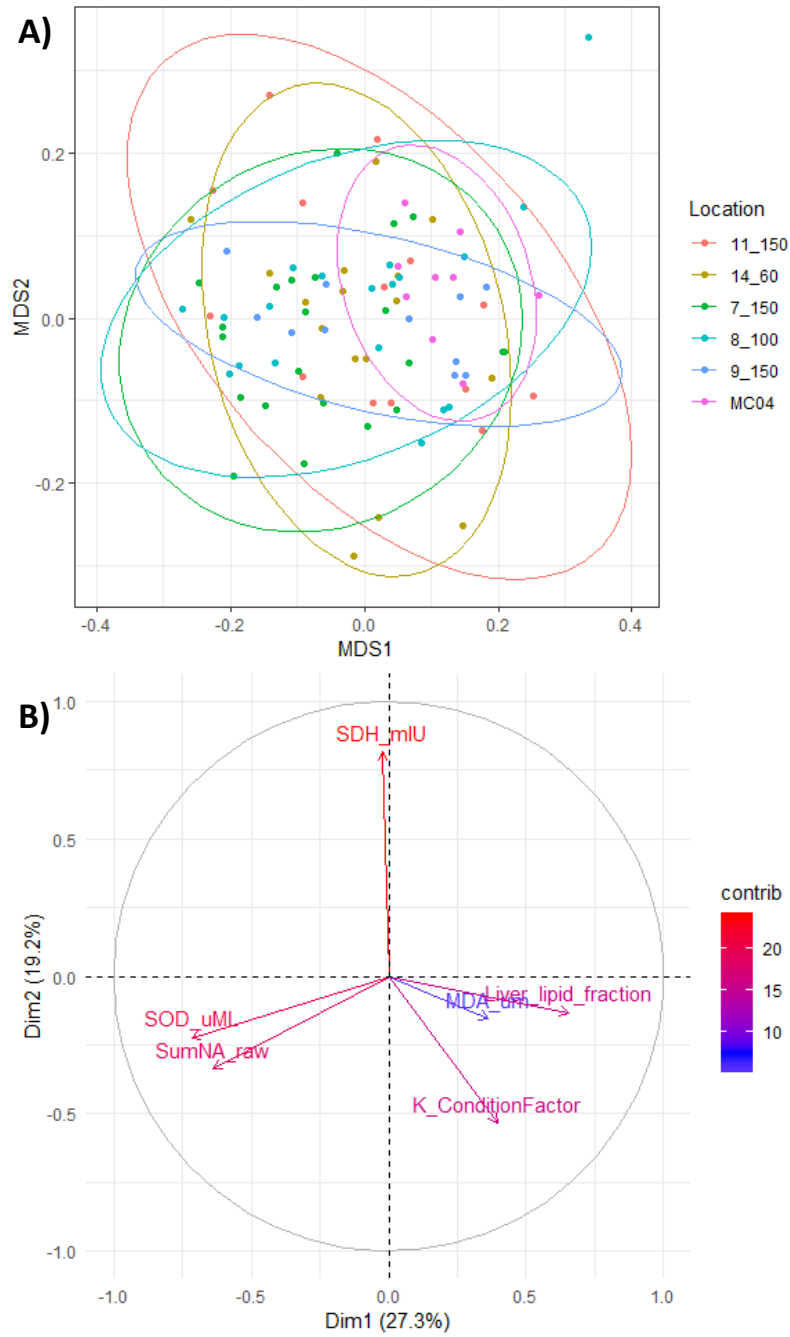


Figure 3.29: A) NMDS and B) PCA for explanatory variables and oxidative stress biomarkers in specimens from NC stations, grouped regardless of sampling year, upon removal of PAH data.

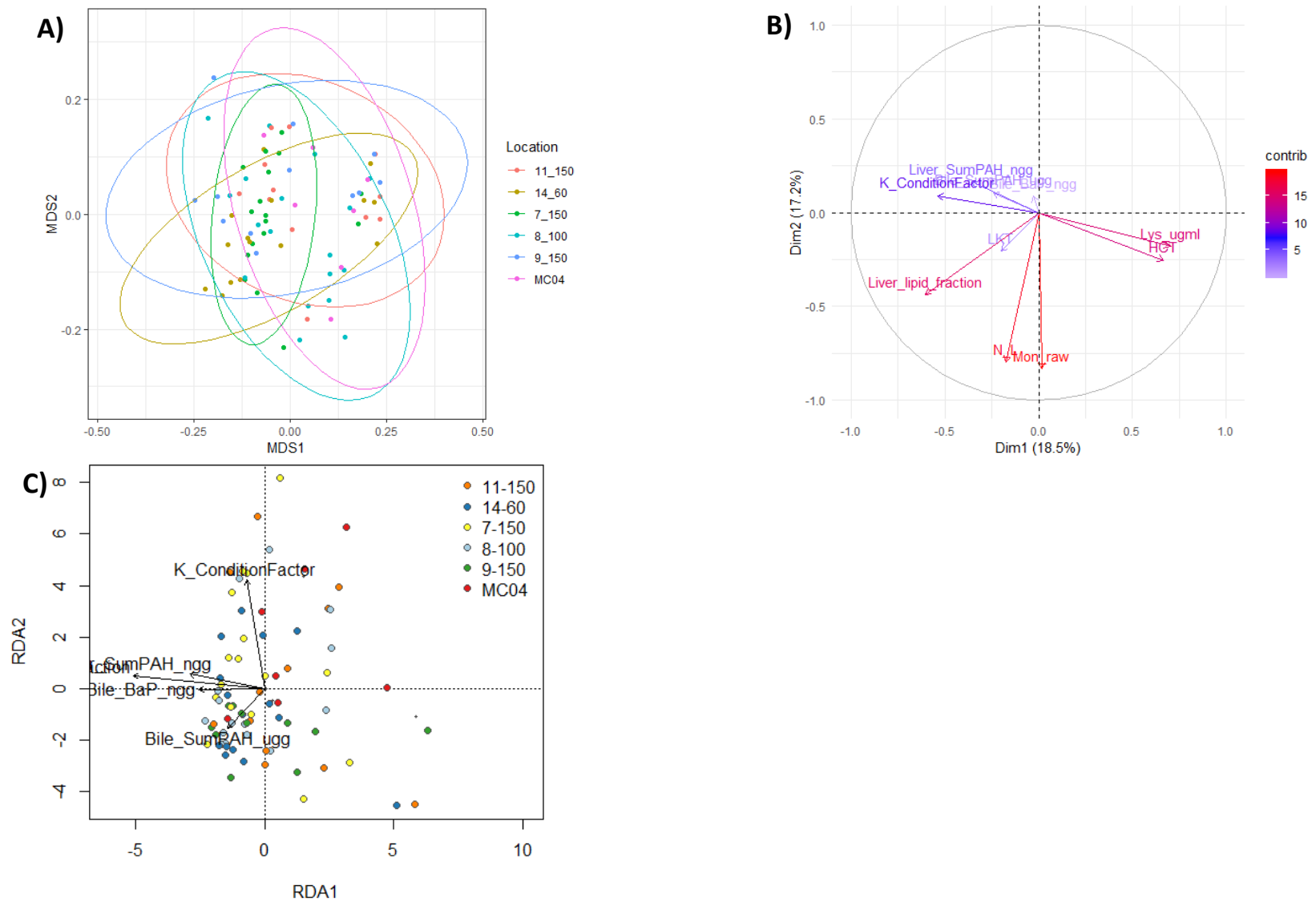


Figure 3.30: A) NMDS, B) PCA, and C) RDA for explanatory variables and immune system biomarkers in specimens from NC stations, grouped regardless of sampling year.

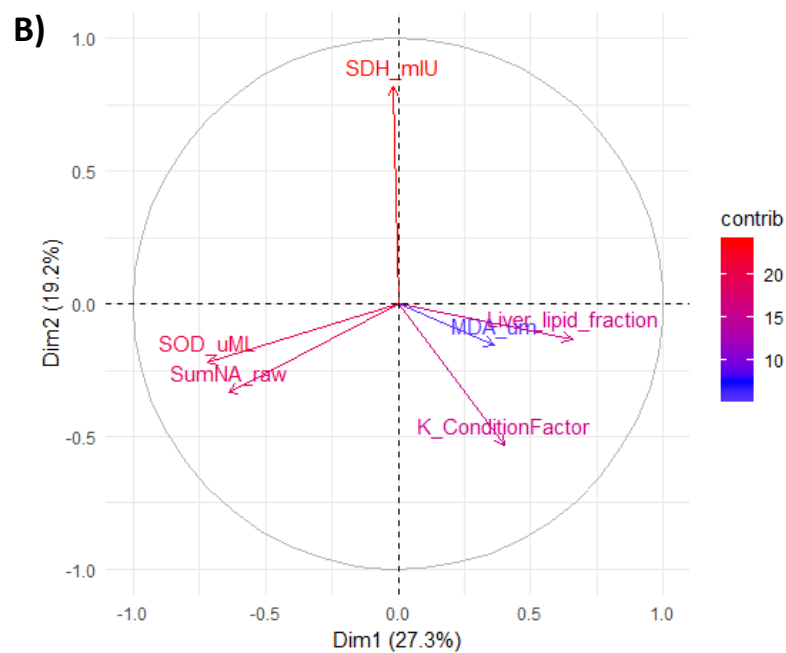
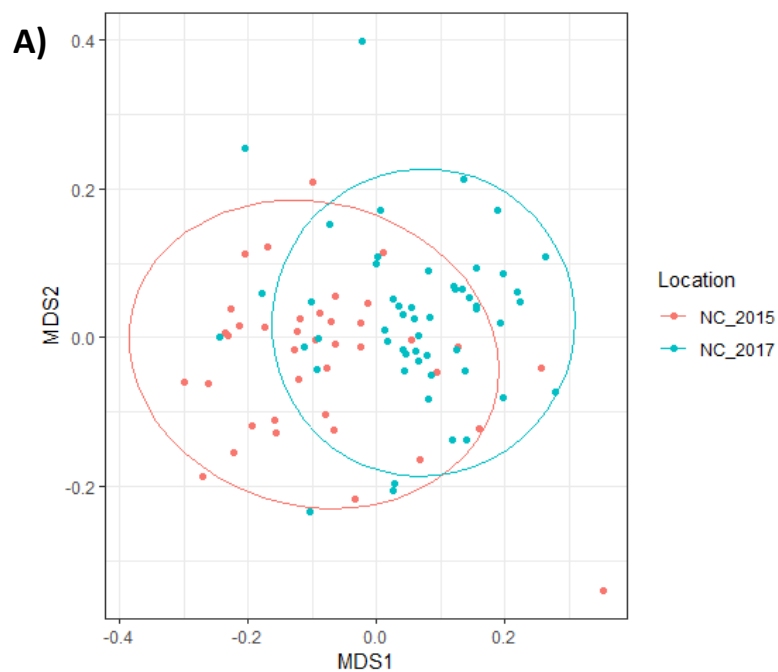


Figure 3.31: A) NMDS and B) PCA of oxidative stress and explanatory variable data in specimens from NC2015 and NC2017 upon removal of PAH data.

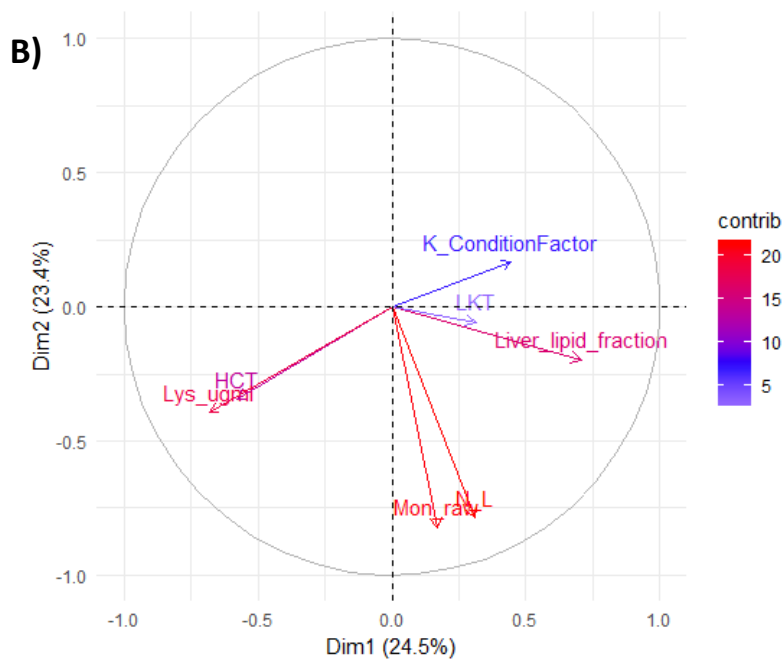
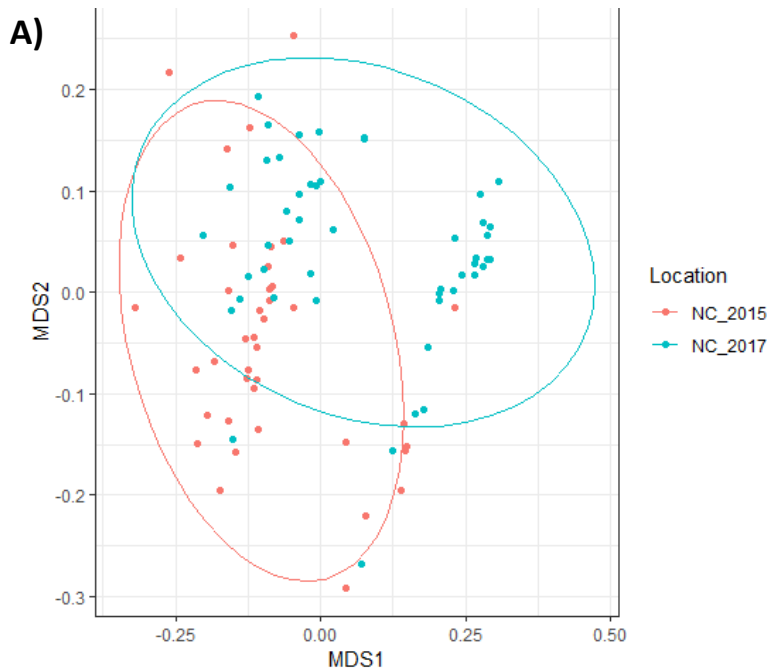


Figure 3.32: A) NMDS and B) PCA of immune system biomarker and explanatory variable data in specimens from NC2015 and NC2017, upon removal of PAH data.

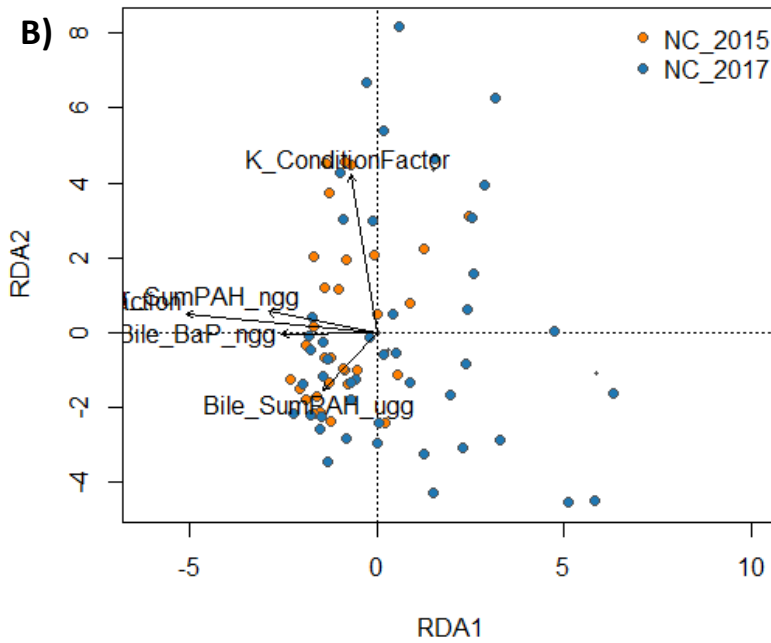
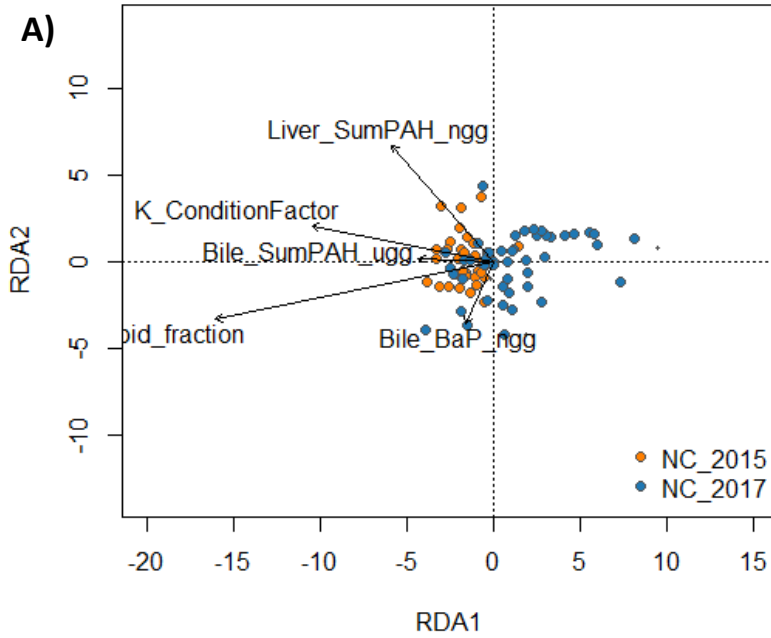


Figure 3.33: RDA for A) oxidative stress and B) immune system biomarkers and explanatory variables for specimens from NC2015 and NC2017.

CHAPTER FOUR:
RELATIONSHIPS BETWEEN POLYCYCLIC AROMATIC HYDROCARBON
EXPOSURE AND BIOMARKER RESPONSE IN RED SNAPPER (*LUTJANUS*
***CAMPECHANUS*) CAUGHT THROUGHOUT THE NORTHERN GULF OF MEXICO**
IN 2015-2017

4.1 Abstract

Red Snapper (*Lutjanus campechanus*) are an economically important fish in the Gulf of Mexico (GoM), typically found in association with natural reefs and artificial structures including oil and gas infrastructure. Prior studies provide evidence of increases in polycyclic aromatic hydrocarbon (PAH) exposure and related metabolism in Red Snapper (*Lutjanus campechanus*) caught in the northern GoM immediately following the 2010 *Deepwater Horizon* (DWH) oil spill, with declines in exposure levels in subsequent years. Possible growth declines, dermal lesions, and trophic level shifts were also documented in exposed populations. In this study, seventy-three Red Snapper caught from the north central and northwestern GoM in 2015-2017 were examined for oxidative stress and non-specific immune system biomarkers. While low levels of PAH contamination were observed in all specimens evaluated in this study, no statistically significant differences in biomarker response were observed between specimens caught within the immediate footprint of the DWH oil spill of 2010 and those from the northwestern GoM. This indicates a continued capacity for Red Snapper to rapidly metabolize and clear PAHs from their bodies prior to the accumulation of deleterious health impacts. In

addition, possible maternal offloading of PAH's to the gonads may assist in contaminant clearance from sexually mature female specimens.

4.2 Introduction

Red snapper (*Lutjanus campechanus*) are an iconic, long-lived, economically valuable, structure-associated reef fish in the Gulf of Mexico (GoM) of both commercial and recreational importance (Cowan et al., 2011; Wilson & Neiland, 2001). Intensive fishing pressure on the species led to historic lows of the stock in 1990 and has resulted in shifts in life history characteristics among northern GoM populations, including a slower progression to sexual maturity and a reduction in overall egg production (Brown-Peterson et al., 2018; Kulaw et al., 2017). Management and conservation strategies have been implemented to increase stocks, with current projections indicating an increase in spawning biomass (SEDAR 52, 2018).

With such interest in the rebuilding of Red Snapper populations in the GoM, it is no surprise the species was studied by multiple research groups in the wake of the *Deepwater Horizon* (DWH) oil spill. An episodic increase in biliary polycyclic aromatic hydrocarbon (PAH) values in Red Snapper from the region of the DWH indicated peak exposure following the spill in 2010, with subsequent declines through at least 2013 (Murawski et al., 2014; Snyder et al., 2015). Hepatic ethoxyresorufin-O-deethylase, glutathione transferase and glutathione peroxidase activity also declined in Red Snapper from the northern GoM in the years following the spill, supporting a brief period of contaminant exposure in the northern GoM and a subsequent return to putative baseline levels (Smeltz et al., 2017). Despite PAH exposure, juvenile recruitment to artificial reefs did not appear to be affected by the DWH spill, nor was a year-class failure observed immediately following DWH in the northeast GoM (Szedlmayer & Mudrak, 2014). Although population collapse was avoided, age-specific growth rate of Red

Snapper caught within the northern GoM declined significantly in 2011-2013, which may indicate adverse health outcomes in exposed fish (Herdter et al., 2017). Dietary shifts and subtle changes in trophic position were also observed, indicating a possible shift in prey abundance following the spill (Tarnecki & Patterson, 2015).

Red Snapper are frequently observed in close association with oil platforms and pipelines (Dance & Rooker, 2019). Such proximity may result in chronic, low-level exposure to PAHs and other contaminants, in addition to their exposure to pollutants from the DWH spill. In fact, studies have demonstrated aberrant metal signatures in otolith microchemistry of Red Snapper found in association with oil platforms as opposed to those using artificial reefs as their dominant habitat (Granneman et al., 2017; Nowling, 2011). Thus, chronic levels of contamination occur in these species. If an aberrant health signature was registered in fish upon exposure to the DWH spill, it is possible their biological response to any additional challenge by chronic contamination would be different from those fish not directly located within the affected geographic region of the DWH.

Oxidative stress and non-specific immune system biomarkers provide practical, economical tools for the analysis of health parameters in non-model teleosts. Oxidative stress is inherently coupled with aerobic respiration, however, the overproduction of radical oxygen species upon exposure to contaminants or physiological stress may lead to lipid, protein, or DNA damage in an organism (Schieber & Chandel, 2014b). Chronic toxicant exposure can also result in immunosuppression, which increases host-pathogen susceptibility (Tort, 2011; Vogelbein et al., 2001). By comparing biomarker response, health indices, and PAH levels in Red Snapper caught within the vicinity of the DWH spill to those caught within oil fields in the northwestern GoM, relative health effects of DWH exposure may be revealed.

4.3 Methods

4.3.1 Sampling

As described in Chapter III, specimens were collected by demersal longlining aboard the *R/V Weatherbird II* from July through September, 2015-2017. All station and catch data are provided in Appendix A. While depth and temperature were recorded by data loggers at each station, these data had no statistically significant effect on biomarker response in Red Snapper and were therefore eliminated from further analysis. The methods for biometrics collection, plasma isolation, bile extraction, and tissue collection were identical to those previously described in Chapter III. Determinations of both liver lipid fraction (LLF) and PAH concentrations was performed by collaborators at the University of South Florida College of Marine Science (Pulster et al., 2020).

4.3.2 Oxidative stress biomarkers

The biomarkers used to characterize oxidative stress in Red Snapper were plasma levels of superoxide dismutase (SOD), malondialdehyde (MDA), and sorbitol dehydrogenase (SDH), along with counts of the sum of erythrocyte nuclear abnormalities (SumNA). All methods utilized for measuring these biomarkers were previously described in Chapter III.

4.3.3 Immune system biomarkers

The non-specific immune response was determined in Red Snapper by utilizing measures of hematocrit (HCT), leukocrit (LCT), plasma lysozyme (LYS), and both monocyte counts (MON) and the neutrophil to lymphocyte ratio (N/L) derived from differential white blood cell counts. All methods utilized for the measuring of these biomarkers were previously described in Chapter III.

4.3.4 Polycyclic aromatic hydrocarbon metabolites

As described in Chapter III, liver PAH concentrations and biliary PAH metabolites were assessed by gas chromatography tandem mass spectrometry and high-performance liquid chromatography, respectively.

4.3.5 Liver lipid fraction

As described in Chapter III, LLF was determined using a modified Folch method.

4.3.6 Data analysis

All data were analyzed in accordance with methods outlined in Chapter III. Data were differentiated into sampling groups, described by geographic region and sampling year (Fig. 4.1). Three groups were considered, the north central GoM sampled in 2015 (NC2015), the north central GoM sampled in 2017 (NC2017), and the northwestern Gulf (NW) sampled in 2016. All data are available at <https://data.gulfresearchinitiative.org/pelagos-symphony/data/R6.x805.000:0083>. Liver and biliary PAH data are available at: <https://data.gulfresearchinitiative.org/pelagos-symphony/data/RX6DR04N> and <https://data.gulfresearchinitiative.org/pelagos-symphony/data/N7X34W1J>.

4.4 Results

4.4.1 Biomarker variability across the northern Gulf of Mexico

Seventy-three Red Snapper were collected from the northern GoM from 2015 through 2017 from three sampling efforts, described by region and year (Fig. 4.1). Twenty specimens were collected from repeat stations in the north central (NC) GoM in 2015 and 2017, and 33 specimens were collected from the northwestern (NW) GoM in 2016. By macroscopic

identification of the gonad tissue, 47.94% of the specimens were female, 49.32% were male, and 2.74% were unidentifiable. There were no significant differences in fork length or total weight by sex. Females had an average total length of 68 ± 9 cm and an average total weight of 4.442 ± 1.435 kg. Males had an average total length of 66 ± 7 cm and an average total weight of 4.050 ± 1.350 kg. Fish of unidentifiable sex had an average total length of 69 cm and an average total weight of 4.134 ± 0.421 kg.

Significant differences in explanatory variable and biomarker expression were observed between sampling groups (NC2015, NC2017 and NW). Sum liver PAH was higher in NW than in NC2015 ($p = 0.033$) and NC2017 ($p < 0.001$), while sum biliary PAH was lower in NW than in NC2017 ($p = 0.011$). Biliary B(a)P was significantly higher in NC2015 than in NC2017 ($p = 0.034$) and NW ($p < 0.001$). The SumNA was lower in NC2015 than in NW ($p = 0.039$) and SOD was higher in NC2017 than in NW ($p = 0.002$). The N/L ratio was elevated in NW compared to NC2015 ($p < 0.001$) and NC2017 ($p = 0.003$) and LCT was lower in NW than in NC2015 ($p = 0.021$) and NC2017 ($p < 0.001$). Hematocrit was lower in NW than in NC2017 ($p = 0.015$) and LYS was lower in NC2015 than in NC2017 ($p = 0.021$). When compared to GoM-wide biomarker reference intervals for Red Snapper (described in Chapter II), 10% of the data from NC2015 and 19.5% of the data from NW were considered high outliers for oxidative stress biomarkers. No outliers were observed for immune system biomarkers when compared to Red Snapper reference intervals.

Non-metric multidimensional scaling (NMDS) of oxidative stress biomarkers and explanatory variables failed to reveal significant differences between heterogeneous sampling groups, with SOD and MDA describing more of the variability among the data than PAH levels by principal component analysis (PCA; Fig 4.2). Redundancy analysis (RDA) indicated PAH

levels, LLF, and K only described 10.45% of the variation in oxidative stress biomarker expression, with sum liver PAH describing more of the variation within the NW group (Fig. 4.2).

No significant difference among statistically homogenous sampling groups was observed by NMDS of immune system biomarkers and explanatory variables, however, there was a significant ($p = 0.014$) separation of NW from a cluster of NC2015 and NC2017 upon removal of biliary PAH data (Fig. 4.3). This separation appears to be driven primarily by low levels of LCT and HCT in NW specimens (Fig. 4.3). Explanatory variables described 25.73% of the variability among immune biomarker expression by RDA, with biliary B(a)P describing slightly more variability at station NC2015 and sum liver and biliary PAH describing slightly more variability in NW data (Fig. 4.3).

Significant differences were observed between males and females in MDA, LCT, HCT, and LYS. Females had lower levels of MDA ($p = 0.004$), HCT ($p = 0.012$), and LYS ($p = 0.003$) and higher levels of LCT ($p = 0.005$) than males. Despite these differences, there was no significant separation among homogenous sex groups by NMDS for oxidative stress (Fig. 4.4) or immune system (Fig. 4.5) biomarkers coupled with explanatory variables. Redundancy analysis indicated subtle differences among the ability of explanatory variables to explain variation in either oxidative stress (Fig. 4.4) or immune system (Fig. 4.5) biomarkers by sex, although results were generally inconclusive. Both LLF and biliary B(a)P may better explain immune system biomarker variability in males than in females (Fig. 4.5).

4.4.2. Biomarker variability by sampling group

4.4.2.1 North central 2015

Twenty Red Snapper were caught at two stations, 10-40 (n = 10) and 12-40 (n = 10) in 2015, with five males and five females caught at each station (Fig. 4.6). Females in the NC2015 sampling group had an average total length of 69 ± 5 cm and a total weight of 4.544 ± 1.106 kg, while males had an average total length of 69 ± 5 cm and an average total weight of 4.329 ± 0.998 kg.

Between sampling stations in this group, there were no significant differences in K, LLF, or PAH levels. Superoxide dismutase levels were significantly higher at 12-40 than at 10-40 ($p = 0.024$) and monocyte count was significantly lower at 12-40 ($p = 0.040$). When variable response was evaluated by sex, HCT and LYS were significantly elevated in males ($p = 0.012$ and $p = 0.034$, respectively). A positive correlation was observed between sum liver PAH and MON ($R = 0.58$, $p = 0.024$) and a negative correlation was noted between sum liver PAH and LLF ($R = -0.52$, $p = 0.027$). A negative correlation was also observed between SOD and MON ($R = -0.54$, $p = 0.038$) although no corresponding relationship was noted between SOD and sum liver PAH.

Non-metric multidimensional scaling of oxidative stress biomarkers and explanatory variables failed to yield significant separation between homogenous sampling station data (Fig. 4.7). By PCA, the majority of the variability among these data appears to be described by biliary PAH levels, K, and LLF, with nearly equivalent contributions by each oxidative stress indicator (Fig. 4.7). Explanatory variables could explain 43.8% of the variation in oxidative stress data by RDA, with biliary PAH levels having a slightly higher contribution at station 10-40 (Fig. 4.7).

A significant difference ($p = 0.032$) was demonstrated between homogenous stations by NMDS of immune system biomarkers and explanatory variables (Fig. 4.8). As suggested by PCA (Fig. 4.8), this separation appears to have been driven primarily by differences in biliary PAH levels, as it is no longer significant ($p = 0.449$) upon removal of these data. Explanatory variables explained 67.52% of the variation in immune response by RDA, however, trends by station were inconclusive (Fig. 4.8).

When sex data were considered, explanatory variables and oxidative stress failed to yield significant separation between sex by NMDS (Fig. 4.9), although a significant separation ($p = 0.031$) was observed between homogenous groups for immune system biomarkers and explanatory variables (Fig. 4.10). Redundancy analysis indicated a slight tendency for biliary PAH values to explain more of the variability in oxidative stress (Fig. 4.9) and immune system (Fig. 4.10) response in females than in males, although this may be biased by the elimination of more males than females from the analysis due to missing values contributing to the model as a result of sampling limitations.

4.4.2.2 North central 2017

Twenty Red Snapper were caught at two stations, 10-40 ($n = 10$) and 12-40 ($n = 10$) in 2017 (Fig. 4.11). Females accounted for 60% of the specimens caught, with seven collected at station 10-40 and five caught at 12-40. Three males were caught at station 10-40 and five males were collected at 12-40. Females had an average total length of 65 ± 10 cm and an average total weight of 4.062 ± 1.695 kg. Males had an average total length of 64 ± 8 cm and an average total weight of 3.893 ± 1.242 kg.

No significant differences in K, LLF, or PAH levels were observed between stations, however, SDH and HCT were significantly higher ($p = 0.009$ and $p = 0.026$, respectively) at station 12-40 than at 10-40, and N/L was significantly lower ($p = 0.019$) at 12-40. When specimens were considered by sex, males had significantly higher levels of LLF ($p = 0.045$), sum biliary PAH ($p = 0.003$), biliary B(a)P ($p = 0.005$), sum liver PAH ($p = 0.017$), and HCT ($p = 0.002$) than females, and significantly lower LCT ($p = 0.018$) and N/L ($p = 0.045$) than females. Positive correlations were observed between biliary B(a)P and both LLF ($R = 0.56$, $p = 0.012$) and HCT ($R = 0.49$, $p = 0.045$). A positive correlation was also observed between sum liver PAH and HCT ($R = 0.49$, $p = 0.038$).

No significant separation was observed between homogenous stations upon NMDS of oxidative stress biomarkers and explanatory variables (Fig. 4.12), with K, LLF, and PAH levels contributing more to the description of the variability among the data by PCA (Fig. 4.12). By RDA, 29.7% of the variation in oxidative stress biomarker response could be described by explanatory variables (Fig. 4.12). A NMDS of immune system biomarkers and explanatory variables also failed to yield separation between sampling groups, with HCT and MON describing much of the variation among the data by PCA (Fig. 4.13). Redundancy analysis indicated the ability of explanatory variables to describe 49.58% of the variation among immune response biomarkers, with a slightly greater influence of biliary PAH values on expression at 12-40 (Fig. 4.13).

Non-metric multidimensional scaling of oxidative stress biomarkers and explanatory variables by sex indicated a significant difference ($p = 0.001$) between homogenous groups (Fig. 4.14). Biliary B(a)P was the largest contributor to the description of this variation by PCA (Fig. 4.14), with the significant difference between sexes disappearing upon the removal of biliary

PAH data from the NMDS. By redundancy analysis, biliary B(a)P may contribute more to variability in female oxidative stress biomarkers than in males (Fig. 4.14).

A significant difference ($p = 0.004$) was observed between homogenous sex groups by NMDS of immune system biomarkers and explanatory variables (Fig. 4.15). This significant trend held through sequential removal of PAH levels, which agrees with the larger contributions played by HCT and MON in describing the variability among these data, according to the PCA (Fig. 4.15). Redundancy analysis shows differential grouping by sex, with explanatory variables being more descriptive of the variability among immune system biomarkers in males (Fig. 4.15).

4.4.2.3 Northwest

Thirty-three Red Snapper were caught at four stations in 2016, 20-40 ($n = 7$), 21-60 ($n = 9$), 22-40 ($n = 9$) and 23-40 ($n = 8$; Fig. 4.16). The majority (54.55%) of specimens were male, 39.39% were female, and 6.06% were unidentified, with both males and females were caught at each station. Females had an average total length of 71 ± 10 cm and an average total weight of 4.738 ± 1.430 kg. Males had an average total length of 66 ± 8 cm and an average total weight of 3.981 ± 1.576 kg. Fish of unidentifiable sex had an average total length of 69 cm and an average total weight of 4.134 ± 0.421 kg.

No statistically significant differences were observed in K, LLF, PAH levels, or oxidative stress biomarkers between stations, however, there were significant differences between stations in LCT, LYS, and MON. Leukocrit was significantly lower at station 21-60 than at 20-40 ($p = 0.025$) and 23-40 ($p = 0.022$). Lysozyme was significantly higher at 23-40 than at 20-40 ($p = 0.003$) and 22-40 ($p = 0.003$). Monocyte count was significantly higher ($p = 0.027$) at station 21-60 than at 23-40. When the sex of specimens was considered, regardless of station, males had

significantly lower ($p = 0.022$) sum biliary PAH than fish with unidentified sex, though this was driven by the aberrantly high levels of PAH in one fish from station 22-40. Males had significantly higher ($p = 0.011$) LYS than females. Correlations were observed between sum biliary PAH and HCT ($R = -0.43$, $p = 0.029$). A positive correlation was noted between sum liver PAH and FL ($R = 0.51$, $p = 0.003$).

No significant separation was observed between homogenous stations upon NMDS of oxidative stress biomarkers and explanatory variables (Fig. 4.17), with SOD, K, SDH, and MDA contributing more to the description of the variability among the data by PCA (Fig. 4.17). By RDA, 13.93% of the variation in oxidative stress biomarker response could be described by explanatory variables (Fig. 4.17). Generally, K better described oxidative stress variation at 20-40 and sum biliary PAH and LLF better described variation at 23-40, although individual data points were fairly dispersed throughout the RDA plot for each station.

No significant difference between stations was observed by NMDS of immune system biomarkers and explanatory variables when all inputs were considered (Fig. 4.18), however, a significant difference ($p = 0.005$) was detected between heterogeneous stations upon removal of PAH data. Stations 23-40 and 20-40 occupied a separate cluster than stations 21-60 and 22-40 (Fig. 4.19). This statistically significant separation and clustering pattern remained between homogenous stations upon sequential removal of LLF and K. When all variables were included, several appeared to contribute significantly to the description of the variability among the data by PCA, with the lowest contributions by K, N/L, and sum liver PAH (Fig. 4.18). Upon removal of PAH data, MON, LYS, HCT, and LLF contributed the most to the description of variability by PCA (Fig. 4.19). According to RDA, explanatory variables could explain 41.30% of the variation among immune response biomarkers, with sum liver PAH describing more of the

variability in response at station 20-40 and biliary PAH and LLF describing more of the variability at 23-40 (Fig. 4.18).

No significant separation between homogenous sex groups was observed by NMDS of oxidative stress biomarkers and explanatory variables (Fig. 4.20) and RDA of the data was inconclusive (Fig. 4.20). As with station data, a significant difference between males and females was observed by NMDS of immune system and explanatory variables upon removal of biliary PAH data (Fig. 4.21). The RDA of these data indicated a slightly greater contribution of sum liver and biliary PAH at describing the variability in immune system biomarker response in females than for males (Fig. 4.22).

4.4.3 Biomarker variability among fish from North central stations

4.4.3.1 By sampling year

Two stations (10-40 and 12-40) were sampled in both 2015 and 2017, with ten specimens collected at each station in each sampling year (Fig. 4.23). When comparing all data by sampling year, both sum liver PAH and biliary B(a)P were higher in 2015 than in 2017 ($p = 0.002$ and $p = 0.045$, respectively), although sum biliary PAH was significantly lower ($p = 0.024$) in 2015. There were no significant differences in oxidative stress biomarker response, however, both N/L and LYS were significantly lower ($p = 0.003$ and $p = 0.006$, respectively) in 2015 than in 2017. When individual stations were compared between 2015 and 2017, both sum liver PAH and biliary B(a)P were significantly higher ($p = 0.013$ for both) in 2015 than in 2017 at station 10-40, and N/L was significantly lower in 2015 at the same station. Trends between years at 10-40 were likely influenced by the significant difference in levels in females within this sampling group, as females at 10-40 in 2015 had significantly higher sum liver PAH ($p = 0.025$)

and biliary B(a)P ($p = 0.011$) than females collected from 10-40 in 2017. Positive correlations were observed between both liver sum PAH ($R = 0.52$, $p = 0.001$) and biliary B(a)P ($R = 0.4$, $p = 0.022$) to MON, although this may be conflated by the positive correlation between biliary B(a)P and sum liver PAH ($R = 0.39$, $p = 0.019$).

A significant difference ($p = 0.001$) between heterogeneous sampling years was observed by NMDS of oxidative stress biomarkers and explanatory variables, however, this appears to be significantly driven by biliary B(a)P values (Fig. 4.24). The separation loses statistical significance upon removal of biliary PAH data (Fig. 4.25) and main contributors to the description of the data include K, MDA, and SumNA (Fig. 4.25). Redundancy analysis was not able to further distinguish contributions of explanatory variables to the description of the oxidative stress response between years (Fig. 4.24).

Non-metric multidimensional scaling of immune system biomarkers and explanatory variables indicated a significant difference ($p = 0.002$) between homogenous sampling years, primarily driven by biliary B(a)P, sum liver PAH, MON, and LLF by PCA (Fig. 4.26). This significant separation between sampling years was apparent upon sequential removal of PAH, LLF, and K, with increasing importance of MON, LYS, and HCT in the description of variability among the data. By RDA, sum biliary PAH and LLF better described the immune response in 2017 and sum liver PAH and biliary B(a)P somewhat better described the immune response in 2015 (Fig. 4.26).

4.4.3.2 By sex and sampling year

A significant difference ($p = 0.001$) was observed between females caught from the NC stations in 2015 and 2017, by NMDS of oxidative stress biomarker and explanatory variable data

(Fig. 4.27). Primary contributors to the explanation of the variability of these data included biliary B(a)P and SumNA, by PCA (Fig. 4.27). With RDA, 29.44% of the variability in oxidative biomarker response in females from NC can be described by explanatory variables, with biliary PAH values contributing to both years of sampling data (Fig. 4.27). Notably, the statistical significance of the separation between sampling years in females by NMDS of oxidative stress biomarker and explanatory variables is eliminated upon removal of biliary PAH data, with SumNA and MDA most contributing to the description of variability among data (Fig. 4.28).

Non-metric multidimensional scaling of immune system biomarkers and explanatory variables indicated a significant difference ($p = 0.002$) between females caught at NC stations in 2015 versus 2017 (Fig. 4.29). Sum liver PAH, HCT, and MON were the primary contributors to the description of the data variability by PCA, with explanatory variables better describing the immune response in females caught in 2014, although the model only explained 24.46% of the immune biomarker variation (Fig. 4.29).

No significant difference was observed between sampling years for NC males by NMDS of oxidative stress (Fig. 4.30) or immune system (Fig. 4.31) biomarkers. Liver sum PAH, K, and SOD had the greatest contributions to the description of variability among the oxidative stress data subset by PCA (Fig. 30b), while LLF and LCT contributed to immune data subset by PCA (Fig. 31b). Due to elimination of missing data points from sampling limitations, redundancy analysis was not useful for male data from these stations.

4.4.3.3 At station 10-40

A significant difference ($p = 0.002$) was observed between homogenous sampling years at station 10-40 by NMDS of oxidative stress biomarkers and explanatory variables (Fig. 4.32). Biliary PAH, SumNA, and SOD were significant contributors to the description of the variability among these data by PCA (Fig. 4.32). The statistical significance of the separation between sampling years is eliminated upon removal of biliary PAH data, with SumNA and SOD contributing more to the description of variability in the resulting data subset (Fig. 4.33). By RDA, 38.86% of the variation among oxidative stress biomarker data in males from station 10-40 may be described by explanatory variables, with a contribution by biliary B(a)P levels in the description of data from both sampling years (Fig 4.32).

A significant difference ($p = 0.001$) was also observed between homogenous sampling years at 10-40 by NMDS of immune system biomarkers and oxidative stress variables (Fig. 4.34). According to PCA, sum liver PAH, LLF, and MON had the greatest contributions to the description of variability among these data (Fig. 4.34). By RDA, 66.29% of variability among immune system biomarkers at station 10-40 could be described by explanatory variables, with LLF contributing primarily to the description of 2017 data (Fig. 4.34).

4.4.3.4 At station 12-40

Non-dimensional multidimensional scaling of oxidative stress biomarkers and explanatory variables indicated a significant difference ($p = 0.009$) between sampling years at station 12-40, with greater dispersal of data in 2015 (Fig. 4.35). Superoxide dismutase, biliary B(a)P, and sum liver PAH contribute the most to the description of the variability among data by PCA (Fig. 35b). Upon removal of PAH data, the statistical significance of the separation

between sampling years is eliminated, with stronger contributions by MDA and SDH in describing the data by PCA (Fig. 4.36). By RDA, 67.32% of the variability among oxidative stress data at 12-40 may be described by explanatory variables, with a strong contribution by sum liver PAH data in 2015 specimens (Fig. 4.35). It should be noted that a significant amount of data was removed from the RDA of 2015 specimens from 12-40 due to missing values, so this analysis is biased towards those remaining samples.

No significant difference was observed between sampling years at 12-40 by NMDS of immune system biomarkers and explanatory variables (Fig. 4.37). Both LCT and LLF were primary contributors to the description of the variability among the data by PCA (Fig. 4.37). According to RDA, 34.54% of the variability among immune system biomarker response at 12-40 could be described by explanatory variables, with stronger contributions of biliary PAH and K in 2017 specimens (Fig. 4.37). However, as mentioned above, several individuals from the 2015 sampling year were removed from the RDA due to missing data points, so this analysis is inconclusive.

4.5 Discussion

Some level of PAH exposure was observed in all Red Snapper evaluated in this study, however, PAH levels did not appear to have a significant effect on biomarker expression. Background PAH levels were expected in these fish, as both NC and NW specimens were caught within zones of high oil extraction and transport activity in the coastal United States, and therefore, likely experience similar levels of chronic PAH exposure. The highest concentrations of sum liver PAH were observed in the NW region, however, the elevated average within this sampling group was driven by a large range in sum liver PAH values for fish collected from station 20-40, located within a dense aggregation of offshore oil platforms. The accumulation of

PAH metabolites in the liver tissue of these fish indicates some chronic contamination at station 20-40 above the level of metabolic clearance, although this contamination did not appear to have a statistically significant impact on biomarker expression in these fish. While a greater percentage of NW fish had oxidative stress biomarkers above the calculated reference interval for GoM Red Snapper than NC fish, and SumNA were significantly higher in NW fish than NC specimens, these outcomes could not be directly linked to PAH body burdens.

The highest concentrations of biliary PAH were observed in NC2017, indicating a recent metabolism of compounds by fish in this region, possibly due to resuspension of DWH crude with normal biological and oceanographic processes. When the entire dataset was considered, no significant differences among sampling groups or by sex were observed by NMDS and RDA had low success at describing biomarker response with the explanatory values provided. Upon removal of biliary PAH data, NMDS of immune system biomarkers revealed significant differences between sampling groups, primarily driven by LCT values, suggesting the biomarker response was not related to PAH levels. It's possible that proximity to outflow from the Mississippi River at both stations 10-40 and 12-40 affected biomarker expression in the fish collected from the NC region.

Within the NC2015 sampling group, a negative correlation was observed between sum liver PAH and LLF. This was due to low levels of LLF in females at station 10-40, in individuals who also had elevated levels of sum liver PAH. No other apparent biomarker responses were linked to this group of fish, and it is possible the lower lipid levels within these fish were a result of spawning cycle recovery. Red Snapper from the northern GoM reach a peak in their spawning activity from May to August (Kulaw et al., 2017). Female gamete production is energetically costly and can lead to a subsequent decline in biomass in post-spawning

individuals (Hayward & Gillooly, 2011). As fish from NC2015 were caught at the end of August, it's likely they were still recovering from spawning. While specimen age was not confirmed by otolith analysis, the average fork length of specimens observed corresponded with mature Red Snapper above 2 years of age, therefore it is highly likely they were spawning capable (Kulaw et al., 2017).

Differences in biomarker response between male and female fish were observed within the NC2017 sampling group, where female specimens had significantly lower LLF, PAH levels, and HCT as compared to males. Sampling occurred one month earlier in 2017 than it had in 2015, within peak Red Snapper spawning months. Lower levels of PAH in female Red Snapper during this sampling cycle may be due to maternal offloading of contaminants to eggs, as observed with other lipophilic compounds, however, this warrants further study (González-Doncel et al., 2017). Despite having significantly higher PAH body burdens than females, male Red Snapper in the NC2017 failed to show statistically significant differences in oxidative stress biomarker expression. Fluctuations in the immune response led to significant differences between sexes in NC2017 data upon removal of PAH data, indicating that something else may have been influencing this complex system.

The most significant differences between repeat stations sampled in 2015 and 2017 were the elevated levels of sum liver PAH and biliary B(a)P in 2015, however, these trends were primarily due to significantly higher PAH concentrations in females from station 10-40 in this sampling year. Corresponding effects of these differences in contamination on oxidative stress and immune system biomarker response were not apparent. While significant differences were observed between sampling years by NMDS of oxidative stress biomarkers and explanatory variables, this appears to have been primarily due to variation among biliary B(a)P

concentrations in this subset of data rather than the oxidative stress indicators, as the separation loses significance upon removal of this variable. Increased sampling numbers may have improved statistical interpretation of data in this study. In addition, robust sampling of stations at a greater distance from the Mississippi River may have increased confidence in the origin of the contaminant load in north central specimens.

4.6 Conclusions

The immune system biomarkers were more variable in response for nearly all data subsets of Red Snapper than oxidative stress indicators were, although they did not appear to be significantly or equivalently influenced by PAH levels across the entire dataset. The interpretation of non-specific immune system biomarkers is highly complex and could be related to a variety of physiological and environmental influences, however, the lack of a coherent response among the dataset precludes a significant impact of PAH exposure on immune response in these fish. Furthermore, the lack of significant change in oxidative stress biomarkers suggests Red Snapper caught five to seven years after the DWH oil spill may not be experiencing significantly deleterious physiological effects from background PAH exposure in the northern GoM. This corresponds with work indicating a decline in Red Snapper PAH levels and dermal lesion prevalence in the years following the spill. No significant differences in biomarker response or condition were observed in specimens caught within the immediate footprint of the Deepwater Horizon oil spill of 2010 and those from the northwestern GoM.

4.7 Figures

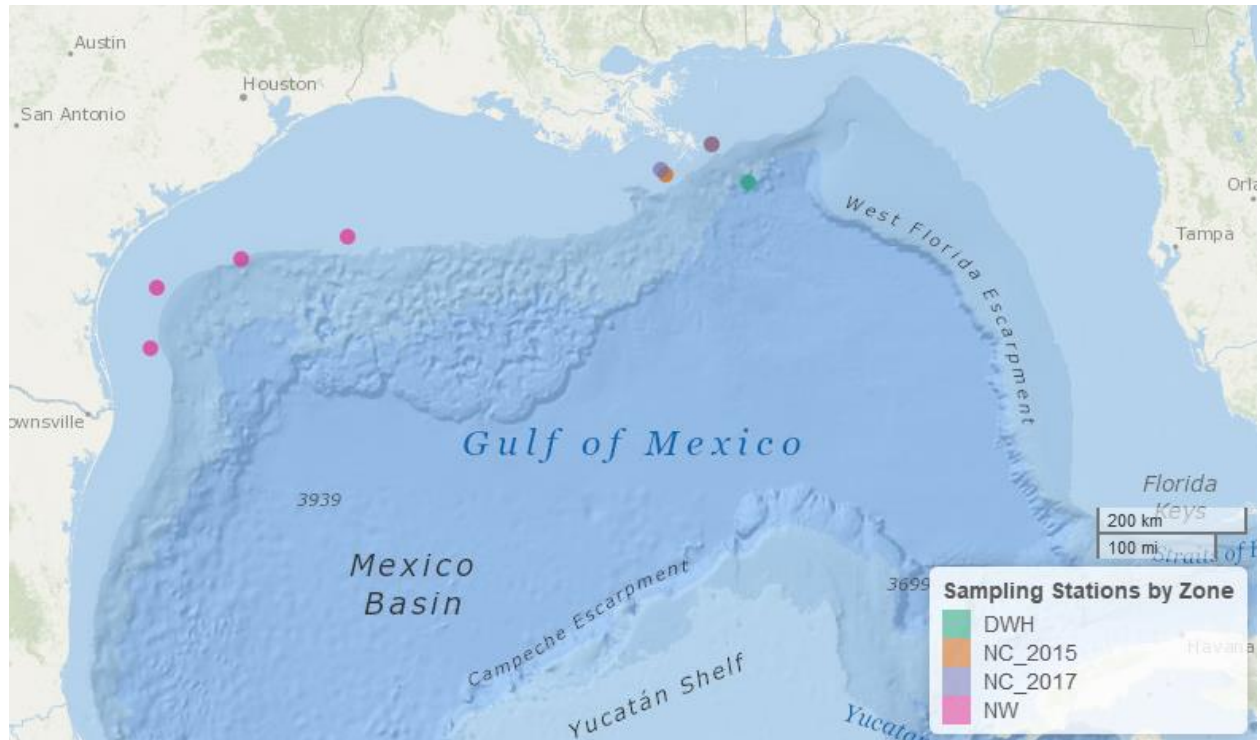


Figure 4.1: Map of the sampling groups at which Red Snapper collection occurred in 2015-2017.

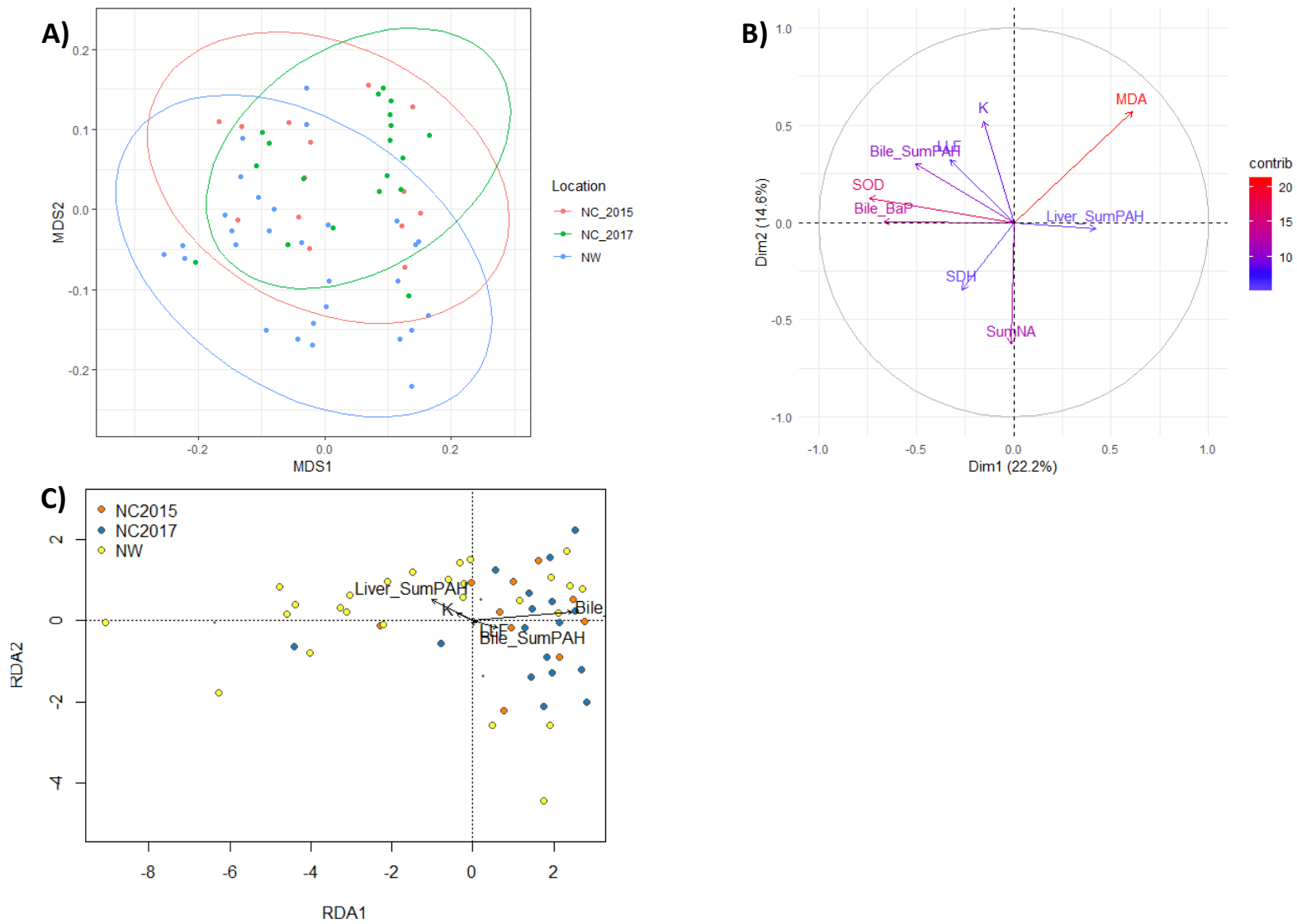


Figure 4.2: A) NMDS, B) PCA, and C) RDA for explanatory variables and oxidative stress biomarkers in NC2015, NC2017 and NW specimens.

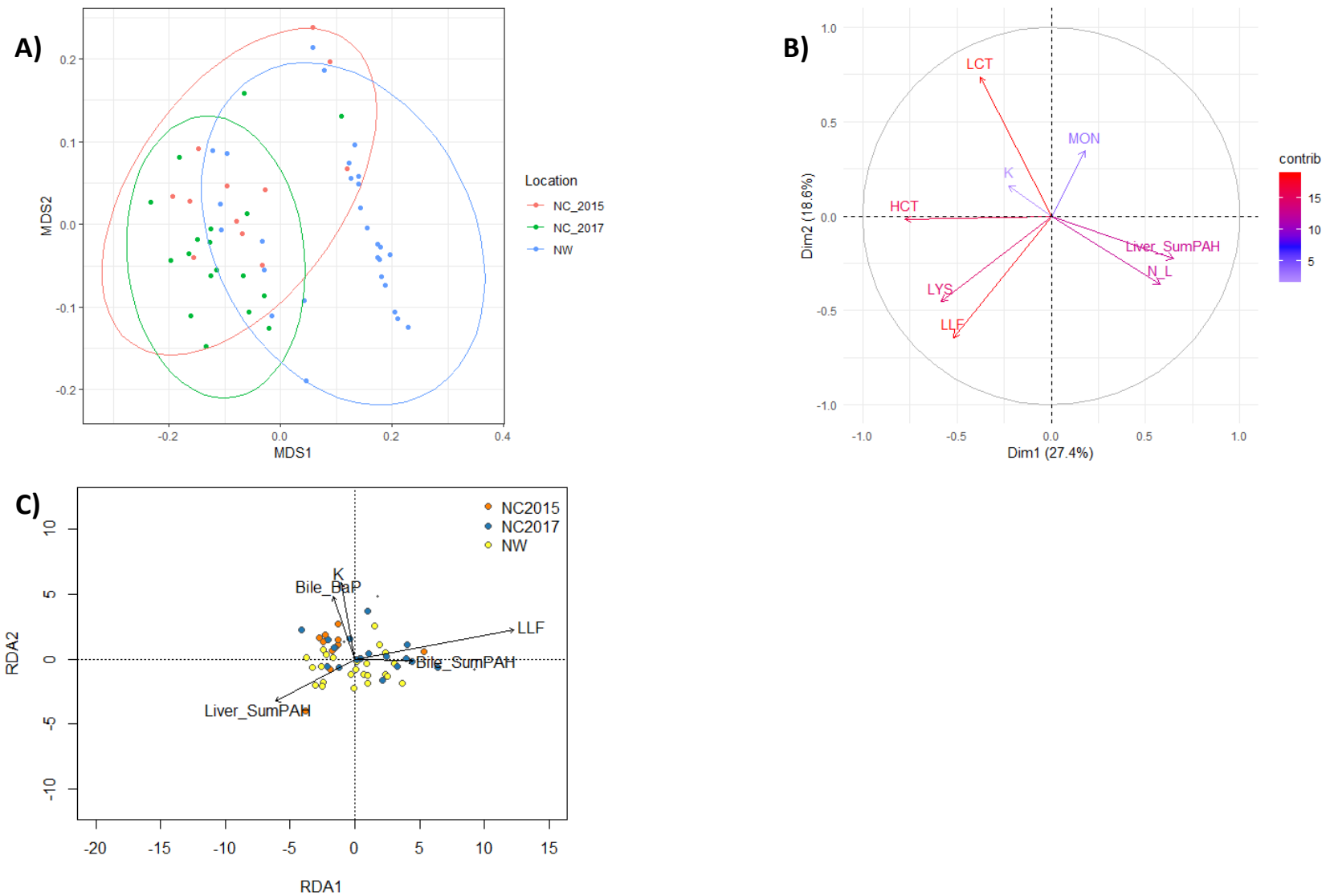


Figure 4.3: A) NMDS, B) PCA, and C) RDA for explanatory variables and immune system biomarkers in NC2015, NC2017 and NW specimens. A and B were constructed upon removal of biliary PAH data.

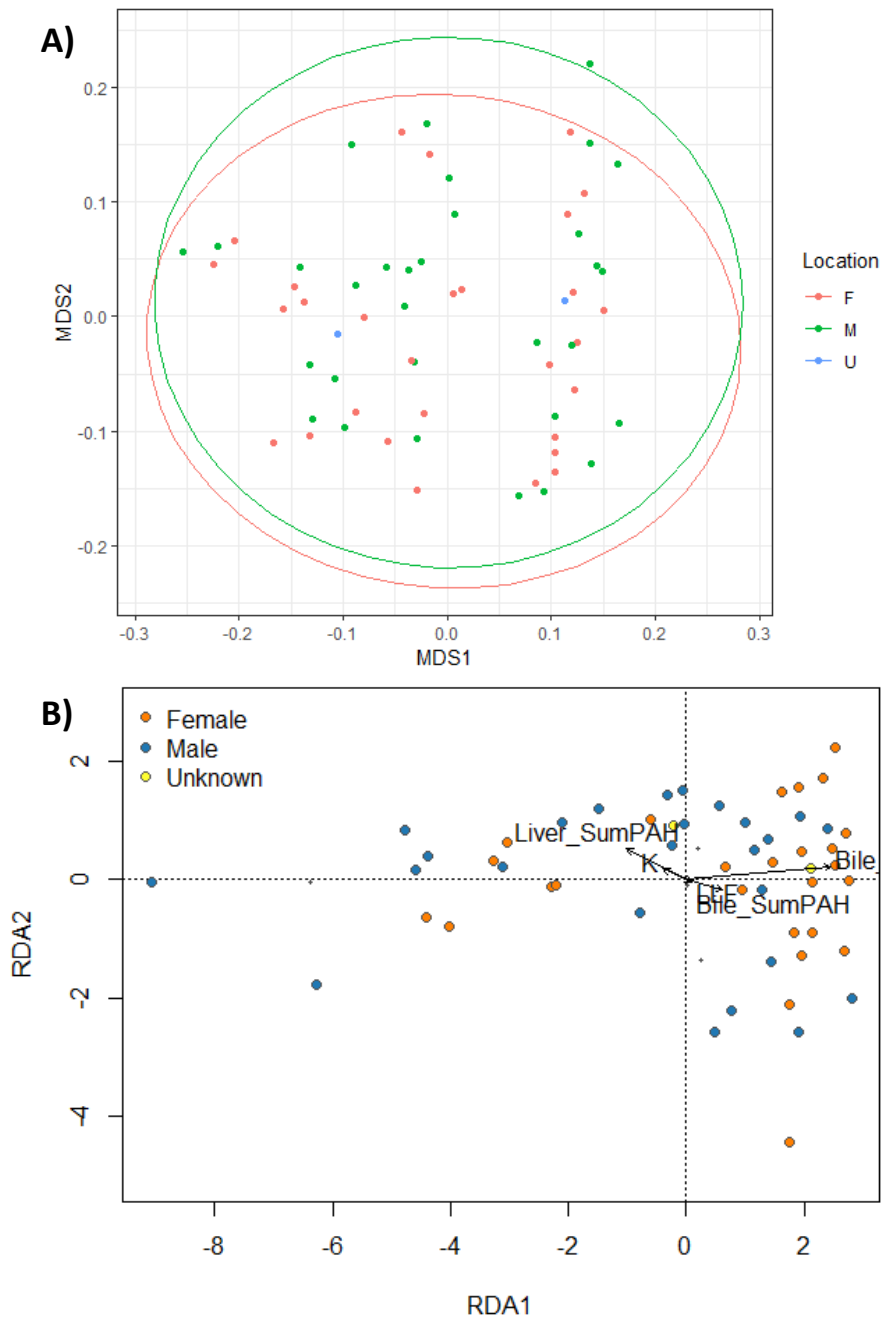


Figure 4.4: A) NMDS and B) RDA for explanatory variables and oxidative stress biomarkers in NC2015, NC2017, and NW specimens, grouped by sex.

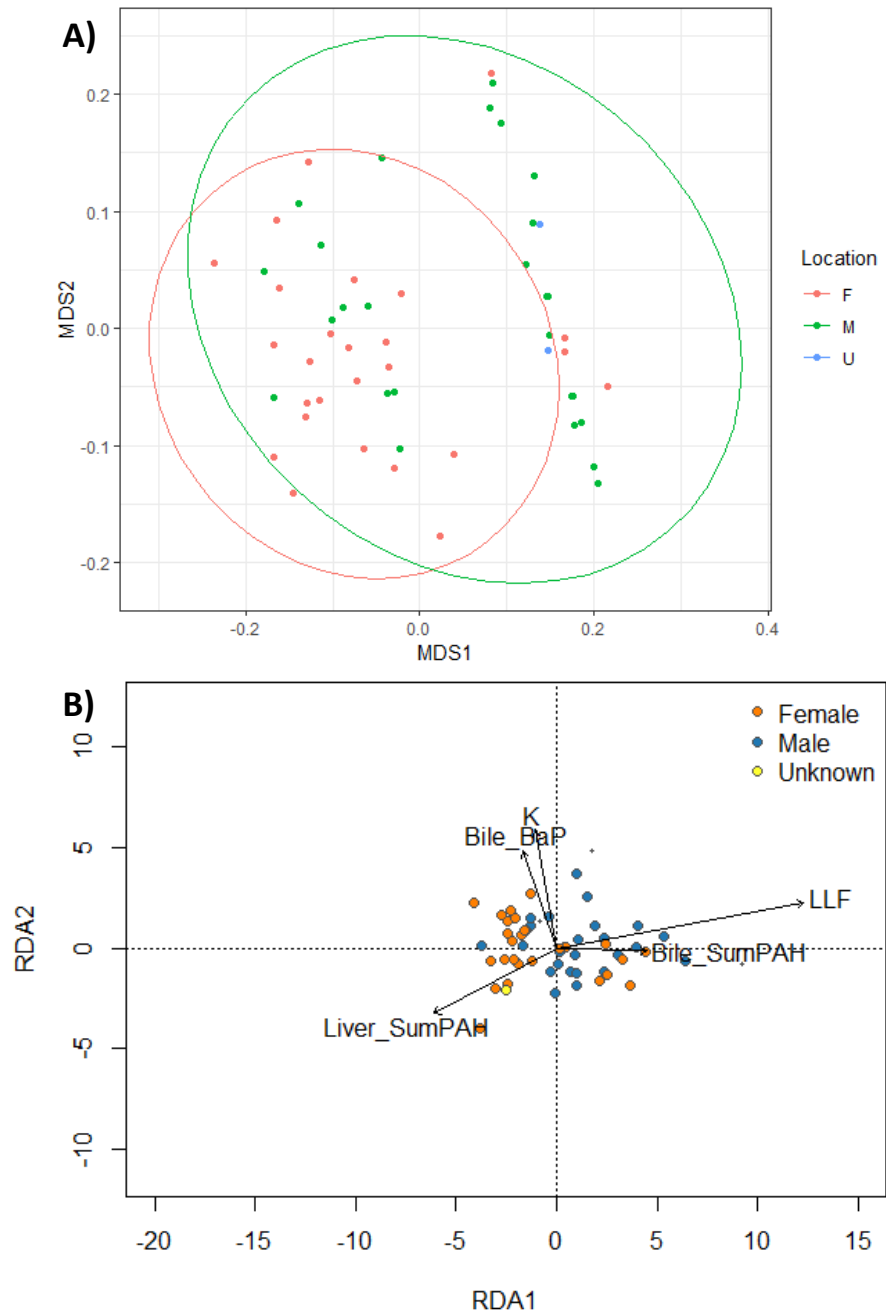


Figure 4.5: A) NMDS and B) RDA for explanatory variables and immune system biomarkers in NC2015, NC2017, and NW specimens, grouped by sex.

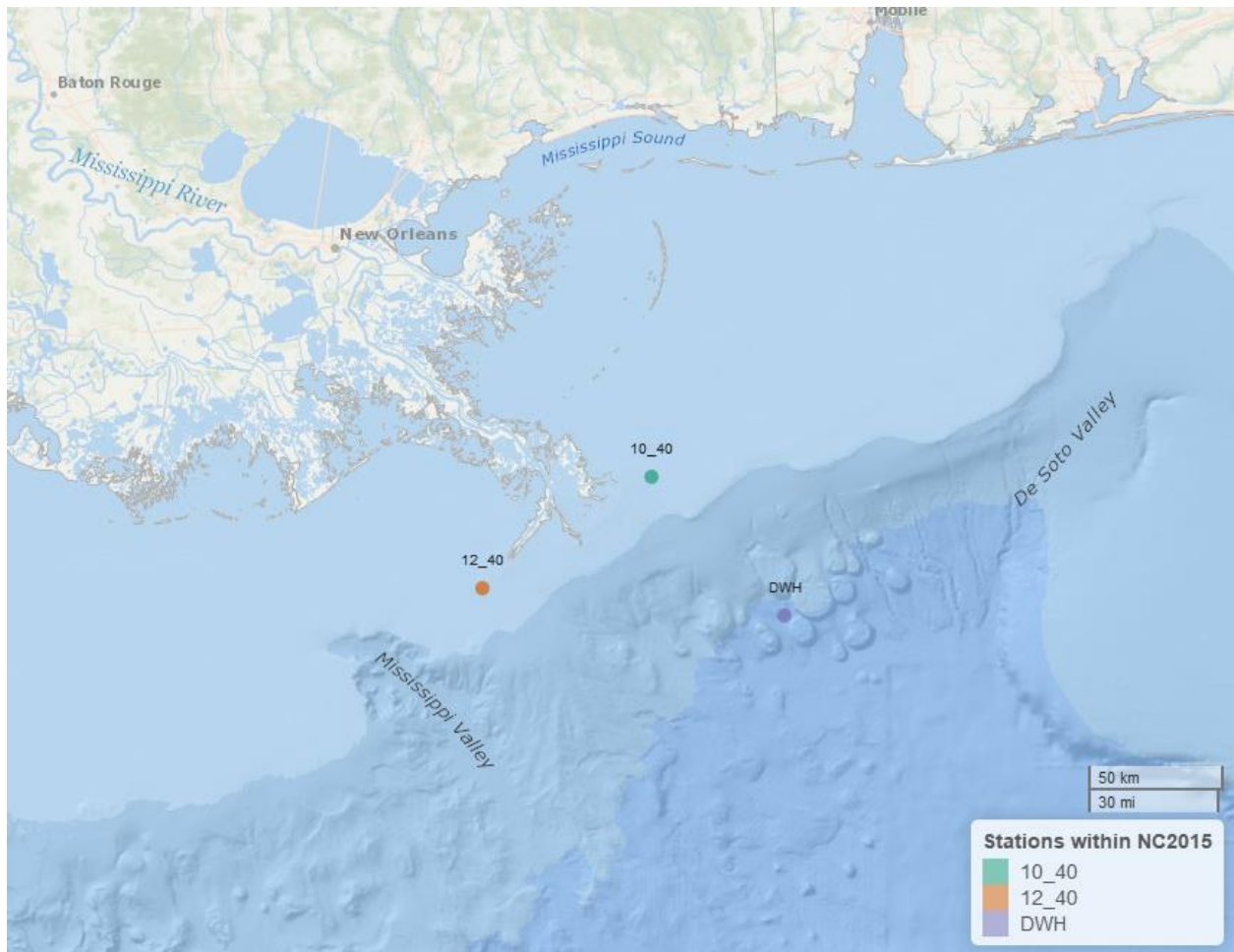


Figure 4.6: Station locations within the NC2015 sampling group.

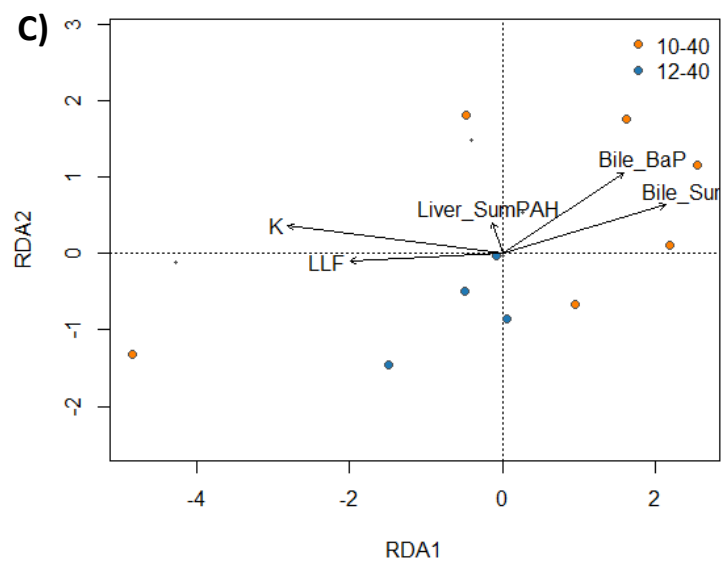
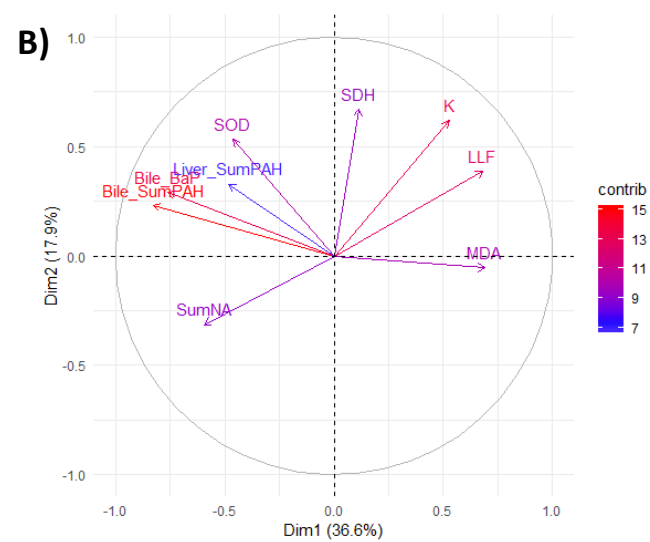
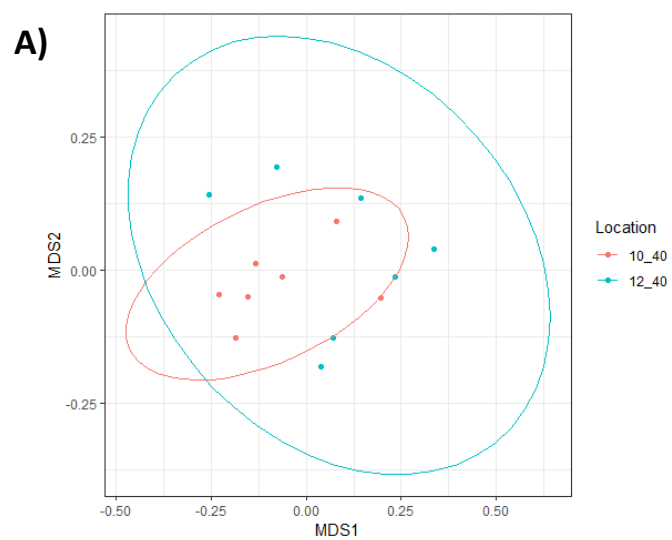


Figure 4.7: A) NMDS, B) PCA, and C) RDA for explanatory variables and oxidative stress biomarkers in the NC2015 sampling group.

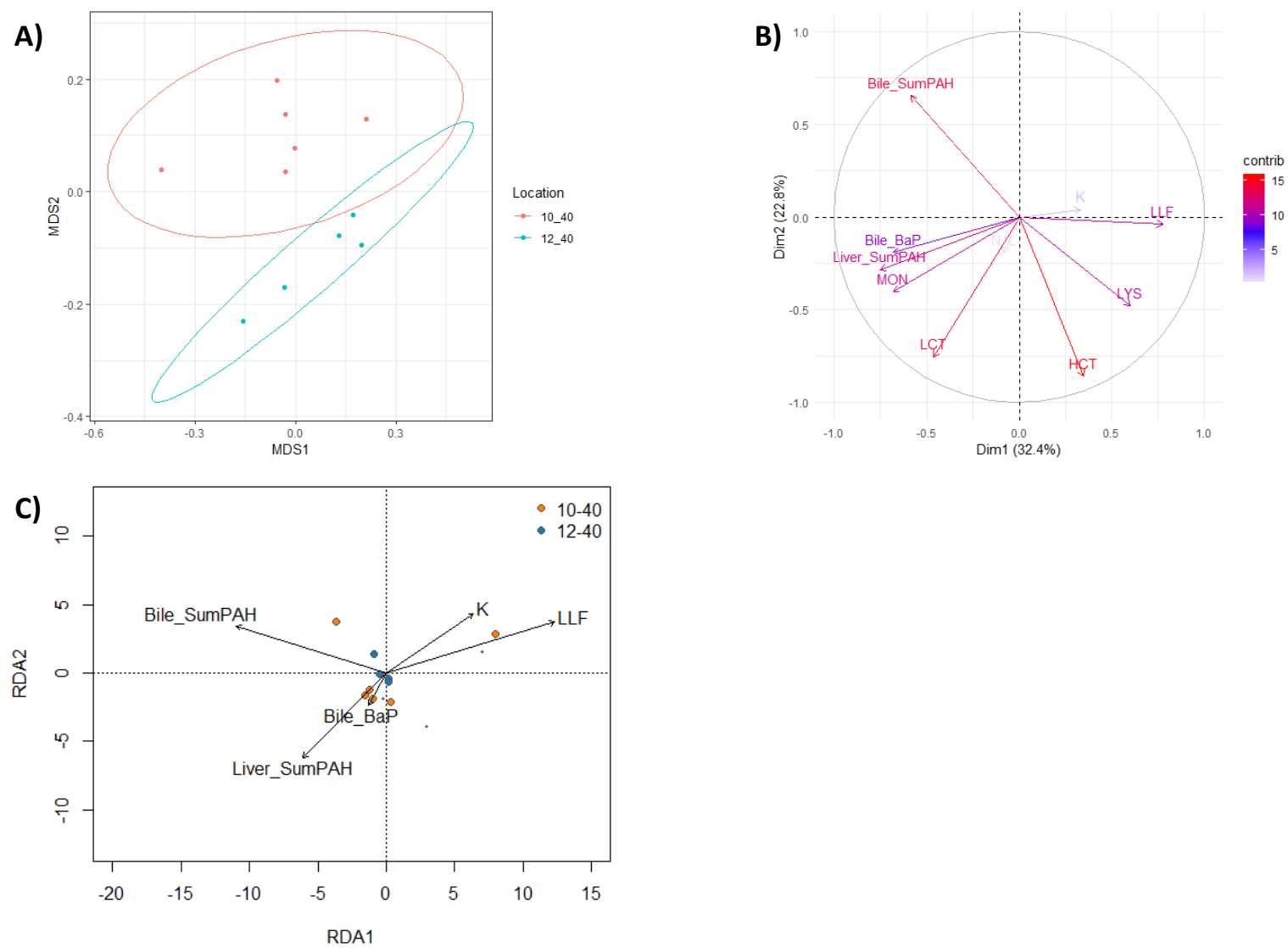


Figure 4.8: A) NMDS, B) PCA, and C) RDA for explanatory variables and immune system biomarkers in the NC2015 sampling group.

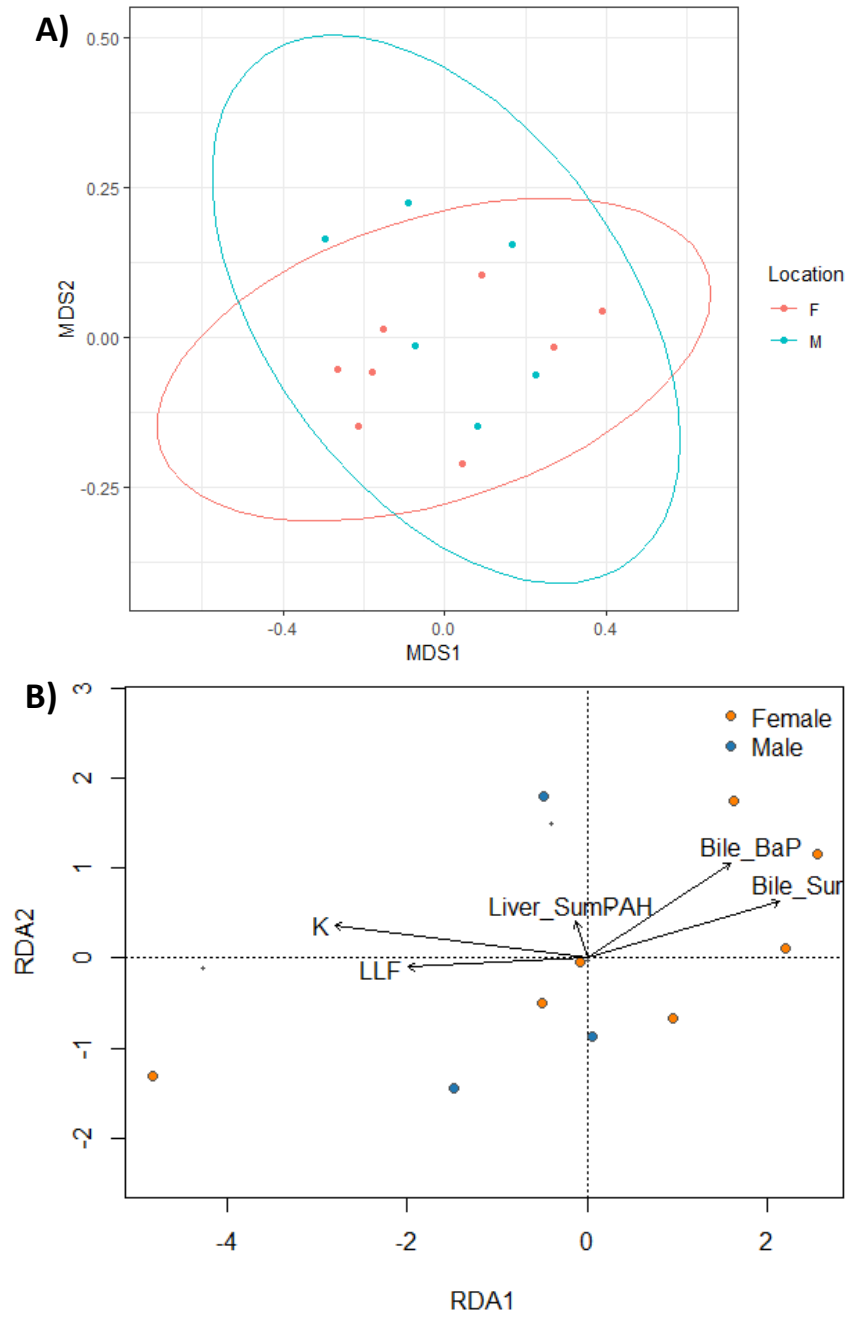


Figure 4.9: A) NMDS and B) RDA for explanatory variables and oxidative stress biomarkers in the NC2015 sampling group, by sex.

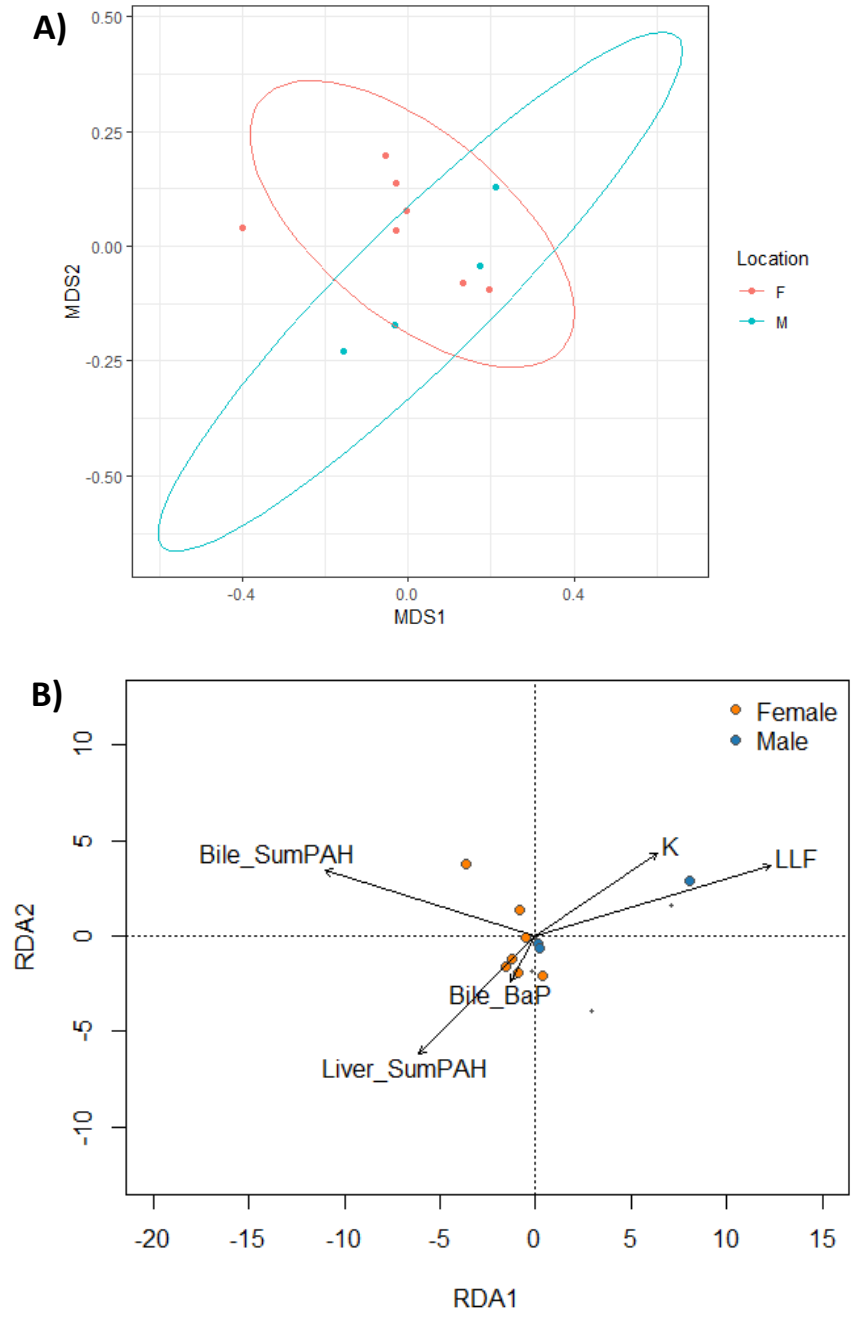


Figure 4.10: A) NMDS and B) RDA for explanatory variables and immune system biomarkers in the NC2015 sampling group, by sex.

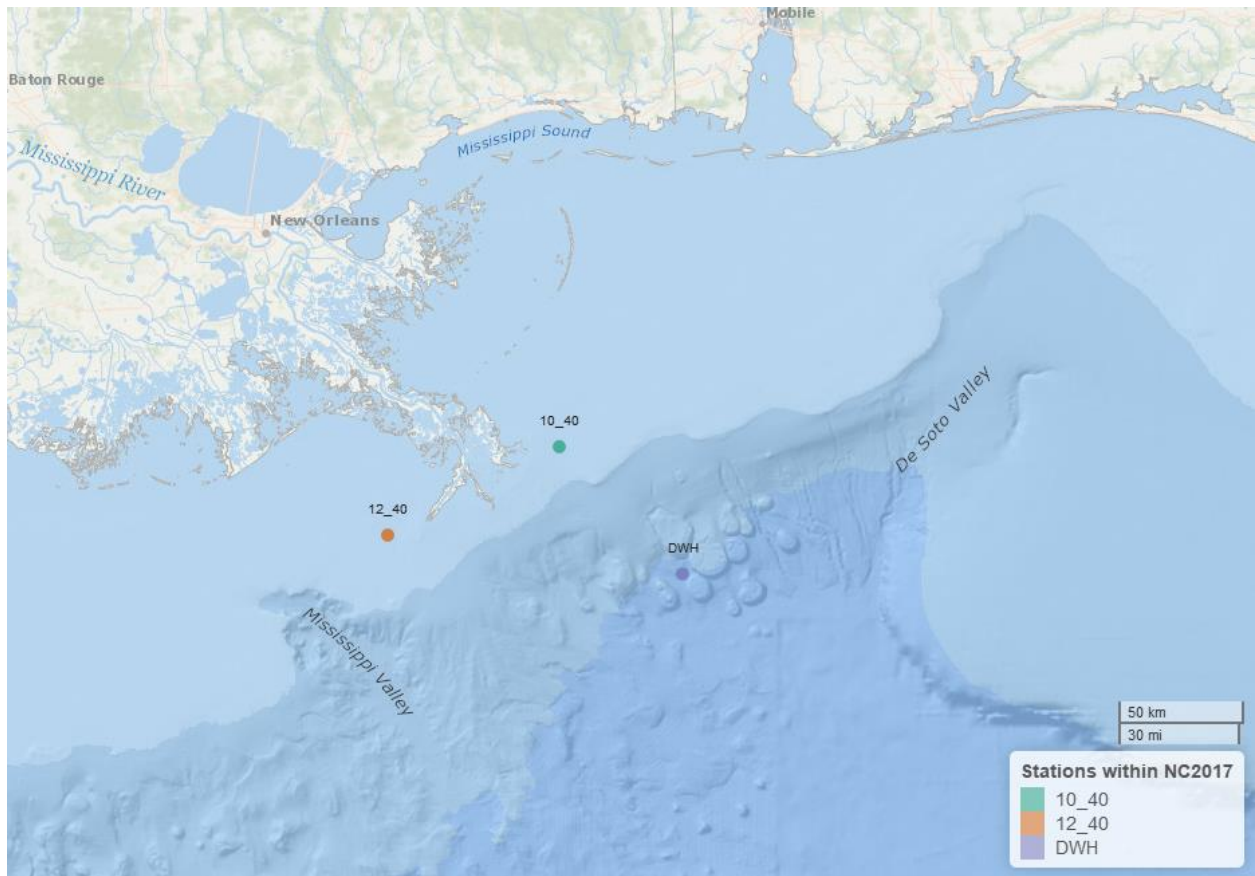


Figure 4.11: Map of station locations within sampling group NC2017.

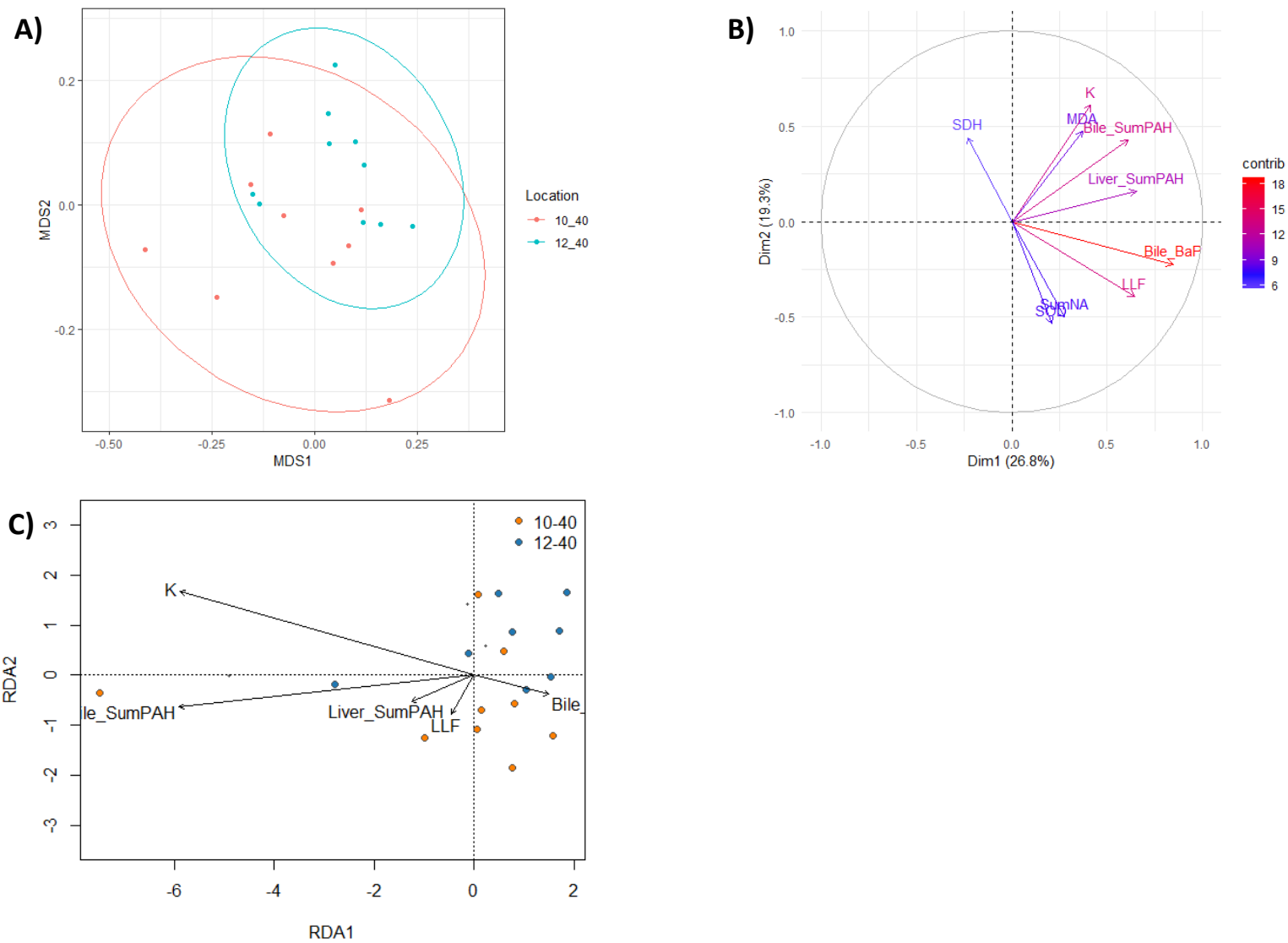


Figure 4.12: A) NMDS, B) PCA, and C) RDA for explanatory variables and oxidative stress biomarkers in NC2017 specimens.

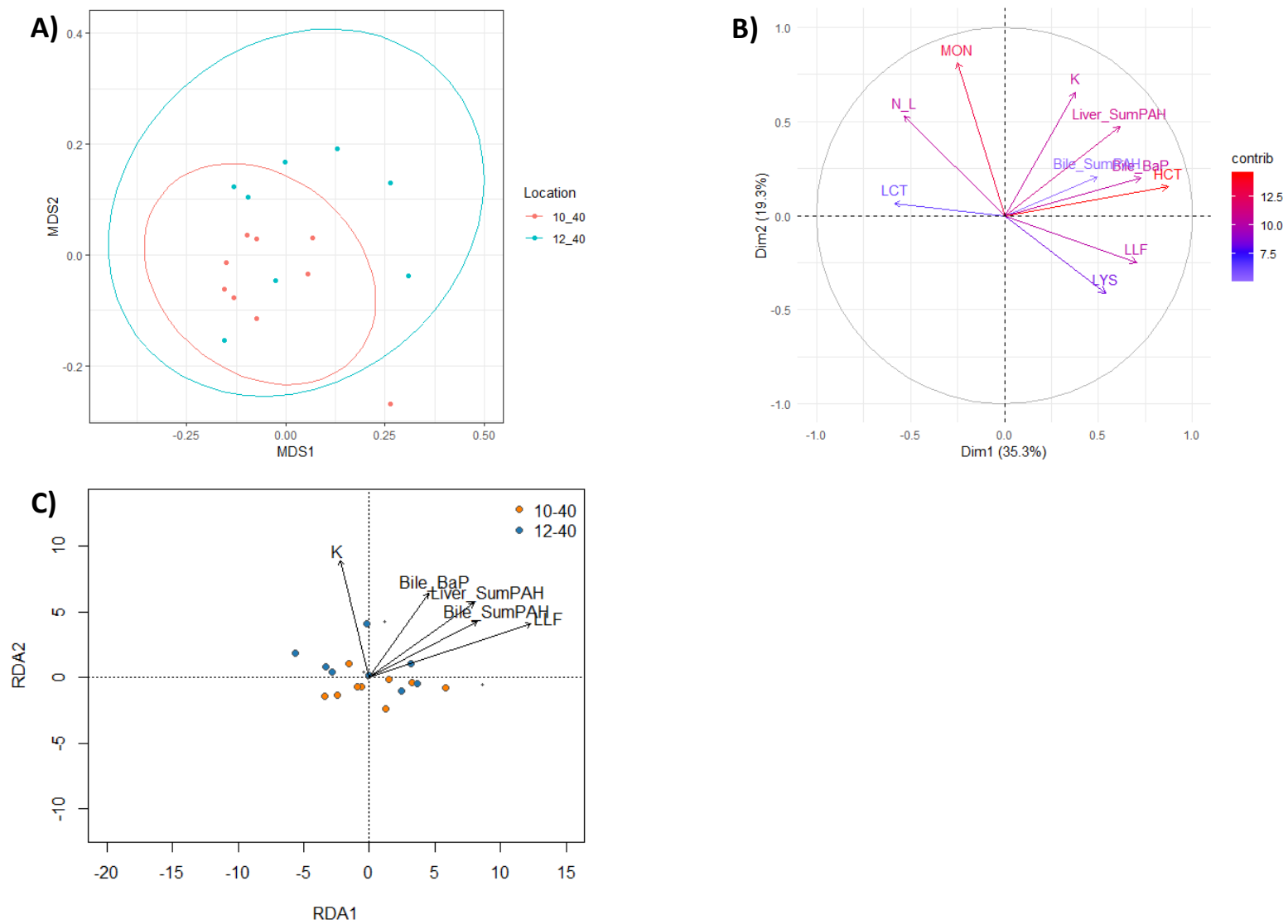


Figure 4.13: A) NMDS, B) PCA, and C) RDA for explanatory variables and immune system biomarkers in NC2017 specimens.

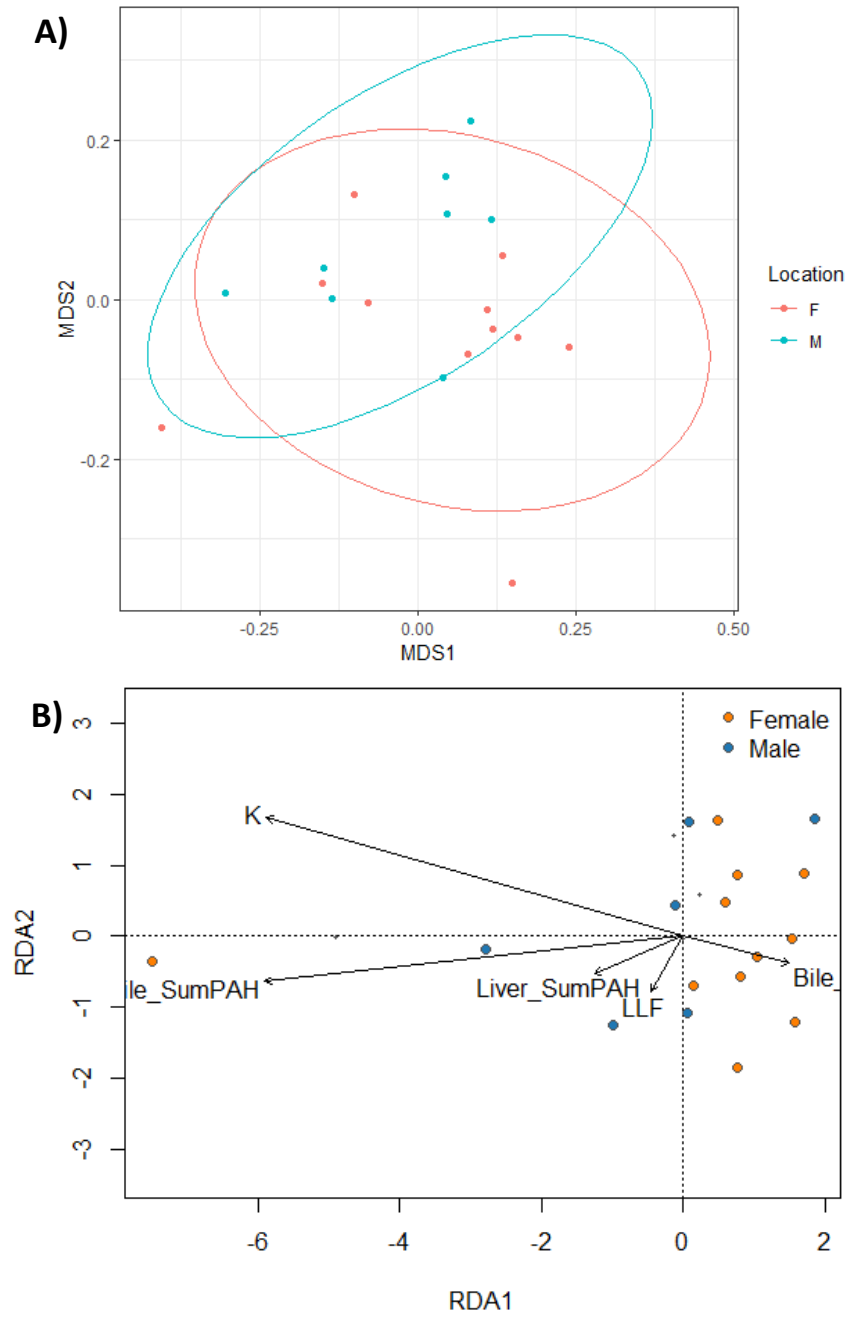


Figure 4.14: A) NMDS and B) RDA for explanatory variables and oxidative stress biomarkers in the NC2017 sampling group, by sex.

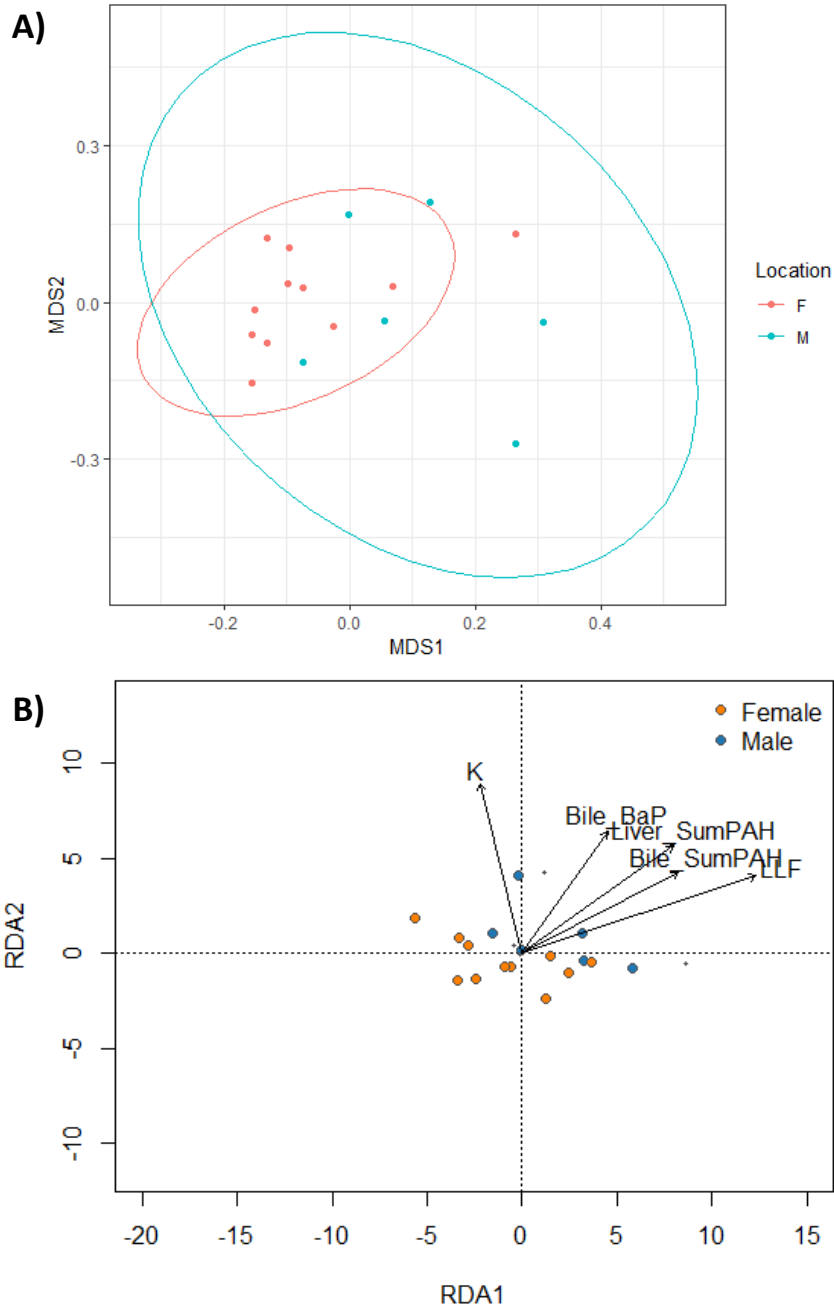


Figure 4.15: A) NMDS and B) RDA for explanatory variables and immune system biomarkers in the NC2017 sampling group, by sex.

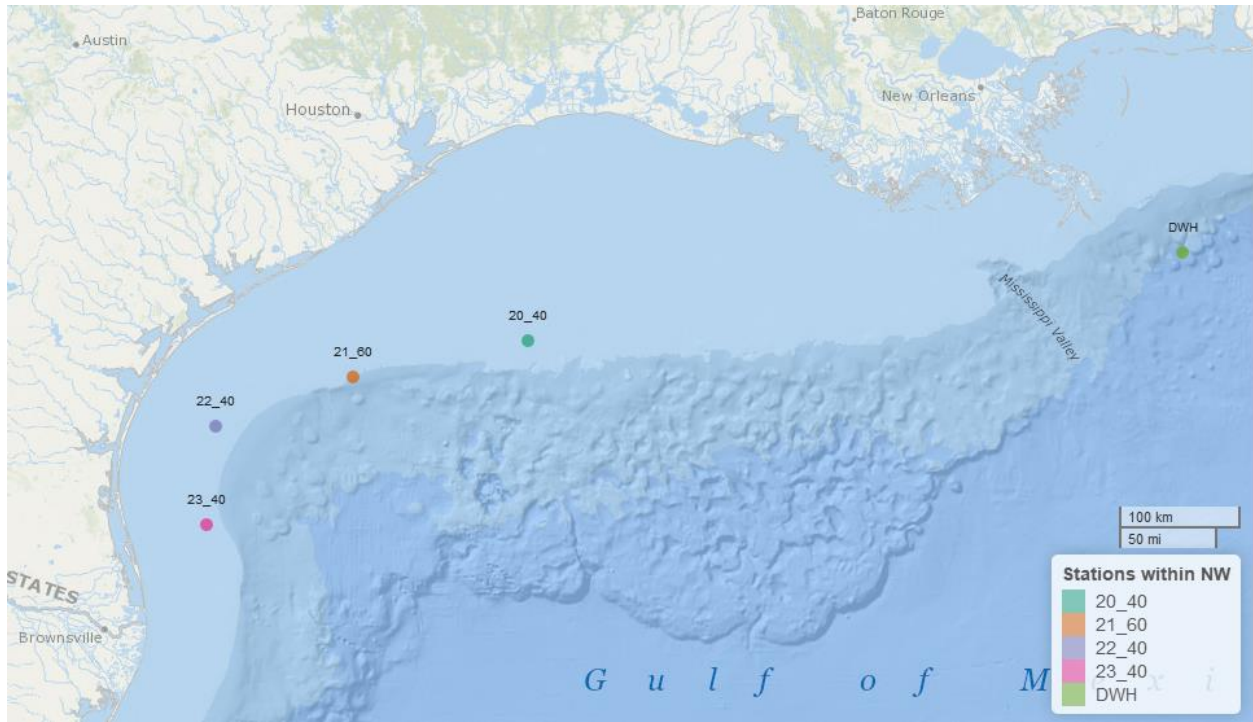


Figure 4.16: Station locations within the NW sampling group.

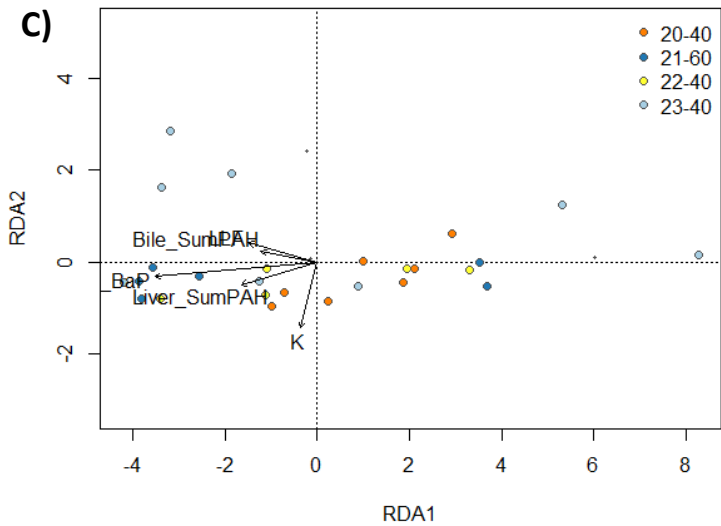
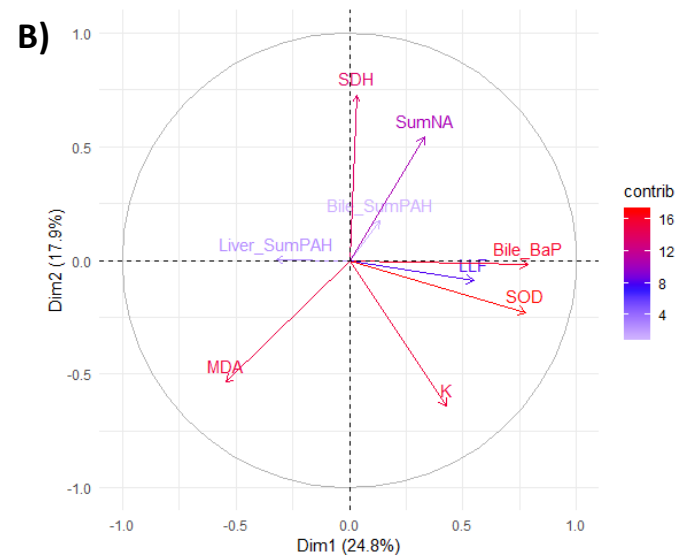
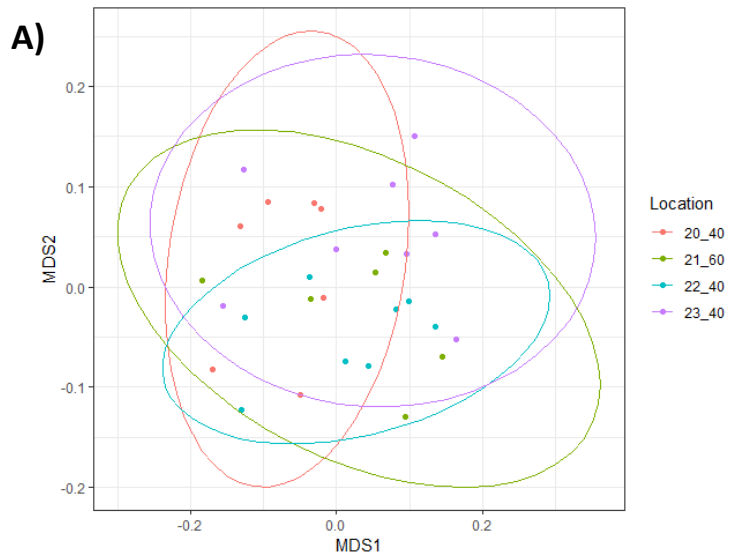


Figure 4.17: A) NMDS, B) PCA, and C) RDA for explanatory variables and oxidative stress biomarkers in NW specimens.

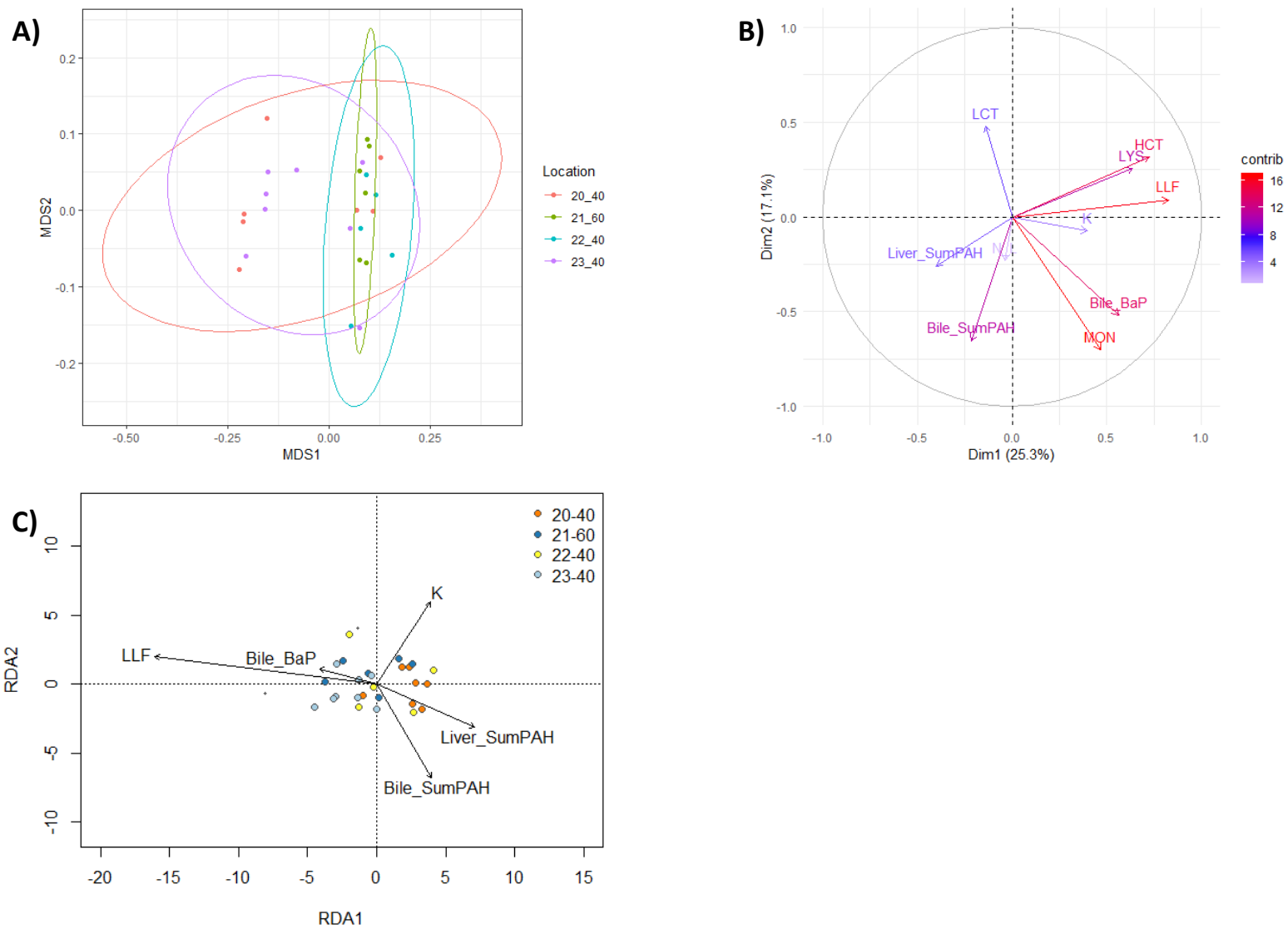


Figure 4.18: A) NMDS, B) PCA, and C) RDA for explanatory variables and immune system biomarkers in NW specimens.

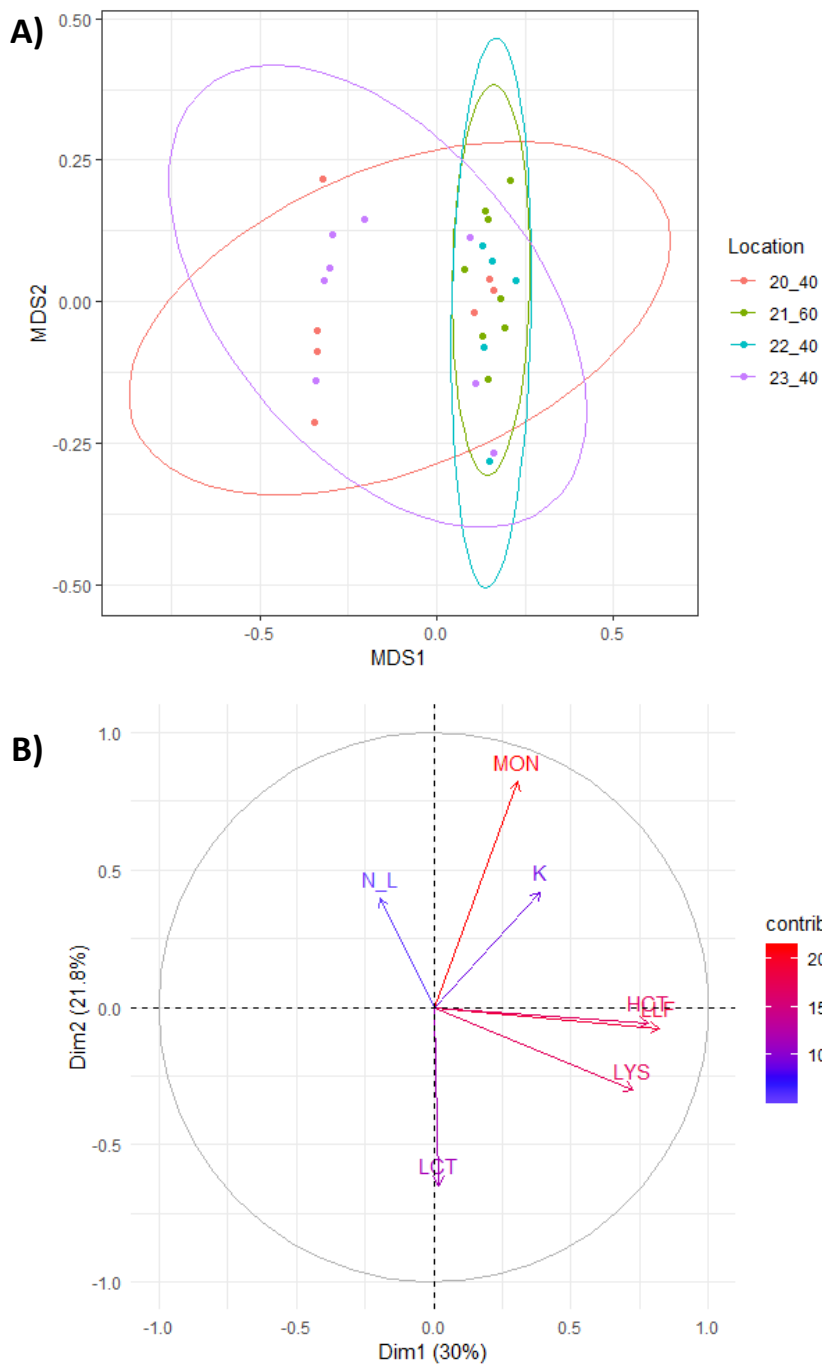


Figure 4.19: A) NMDS and B) PCA for explanatory variables and immune system biomarkers in NW specimens upon removal of PAH data.

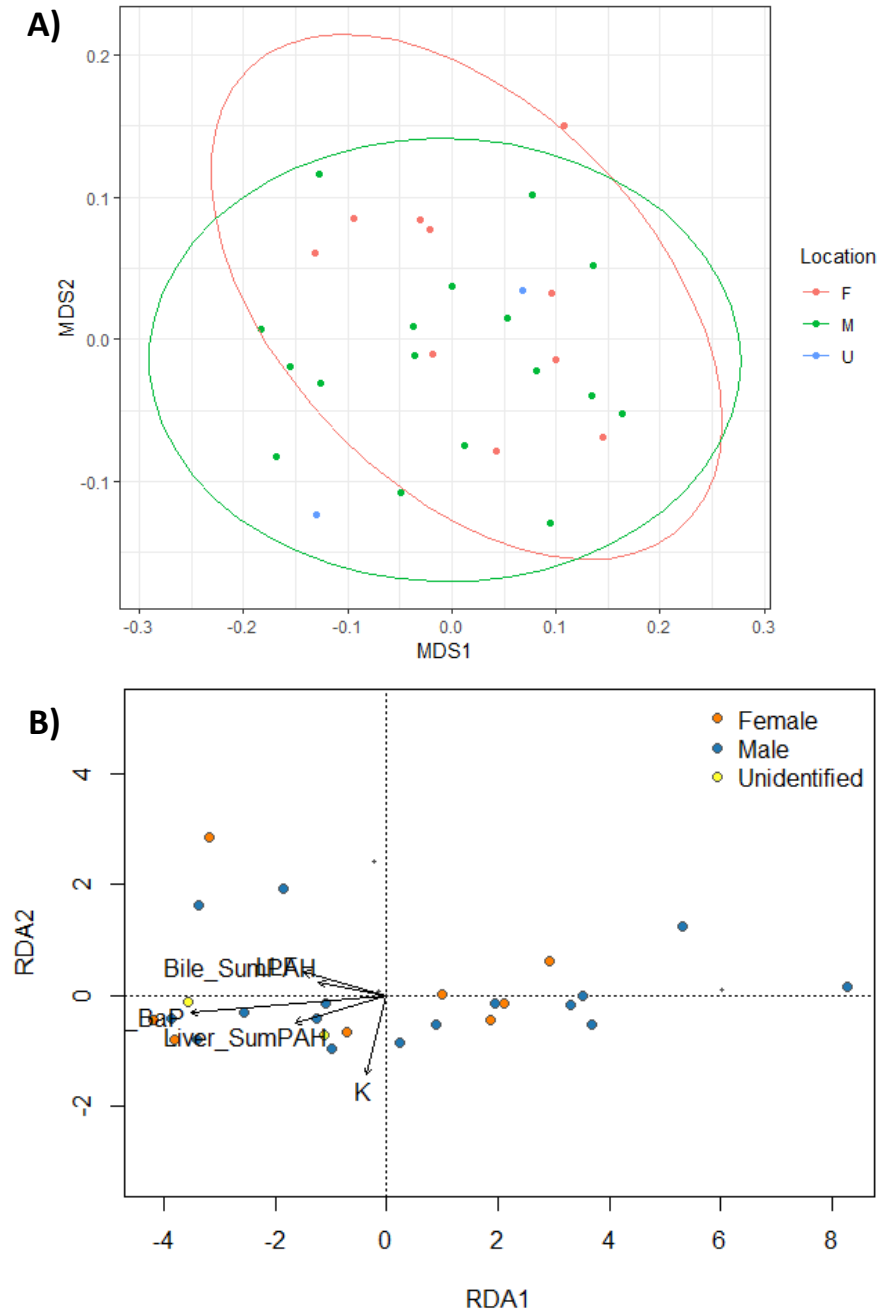


Figure 4.20: A) NMDS and B) RDA for oxidative stress and explanatory variables in NW specimens, by sex.

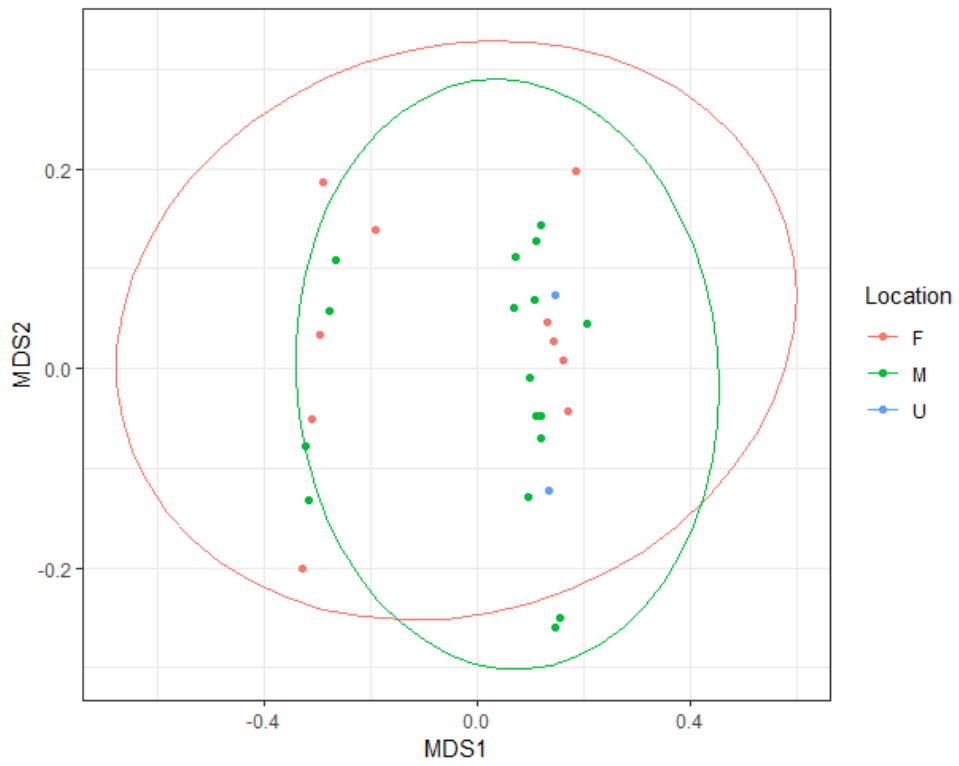


Figure 4.21: NMDS of immune system biomarkers and explanatory variables upon removal of PAH data.

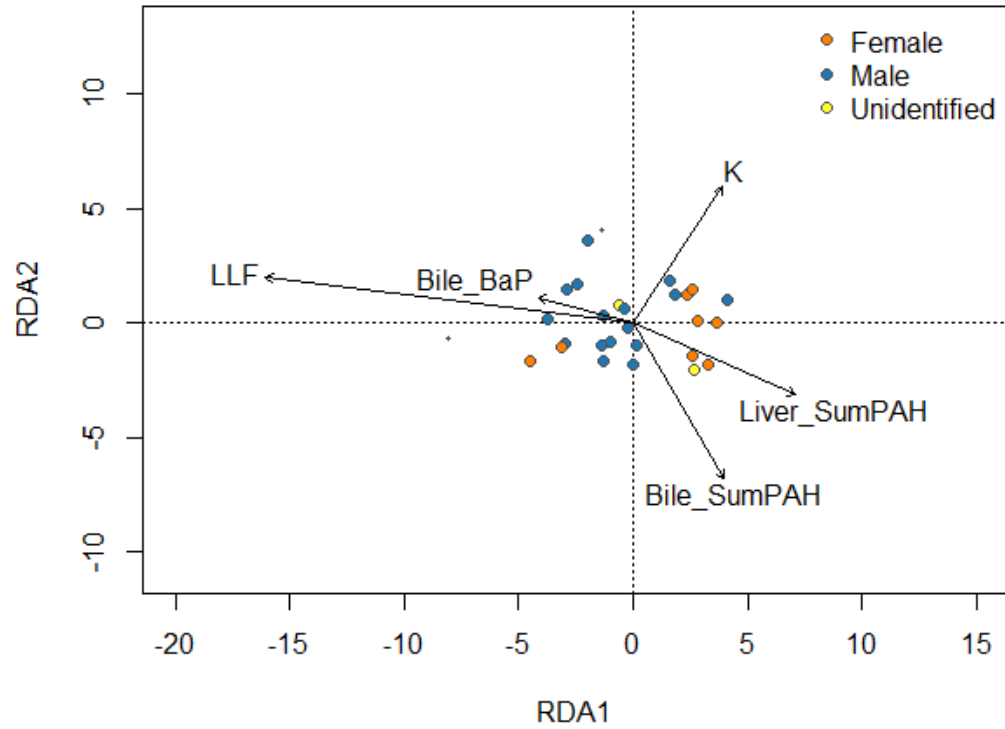


Figure 4.22: RDA of immune system biomarkers and explanatory variables for NW specimens, by sex.

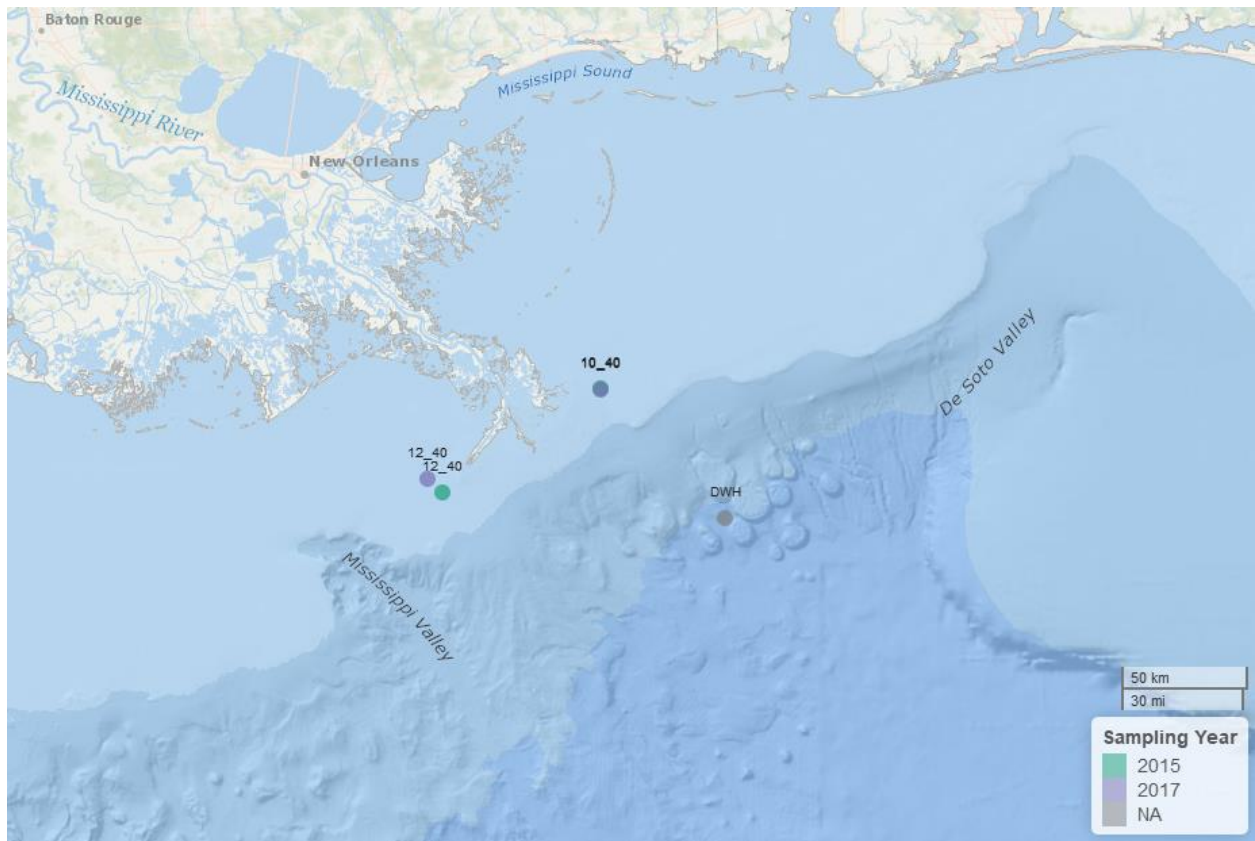


Figure 4.23: Map of NC stations sampled in 2015 and 2017.

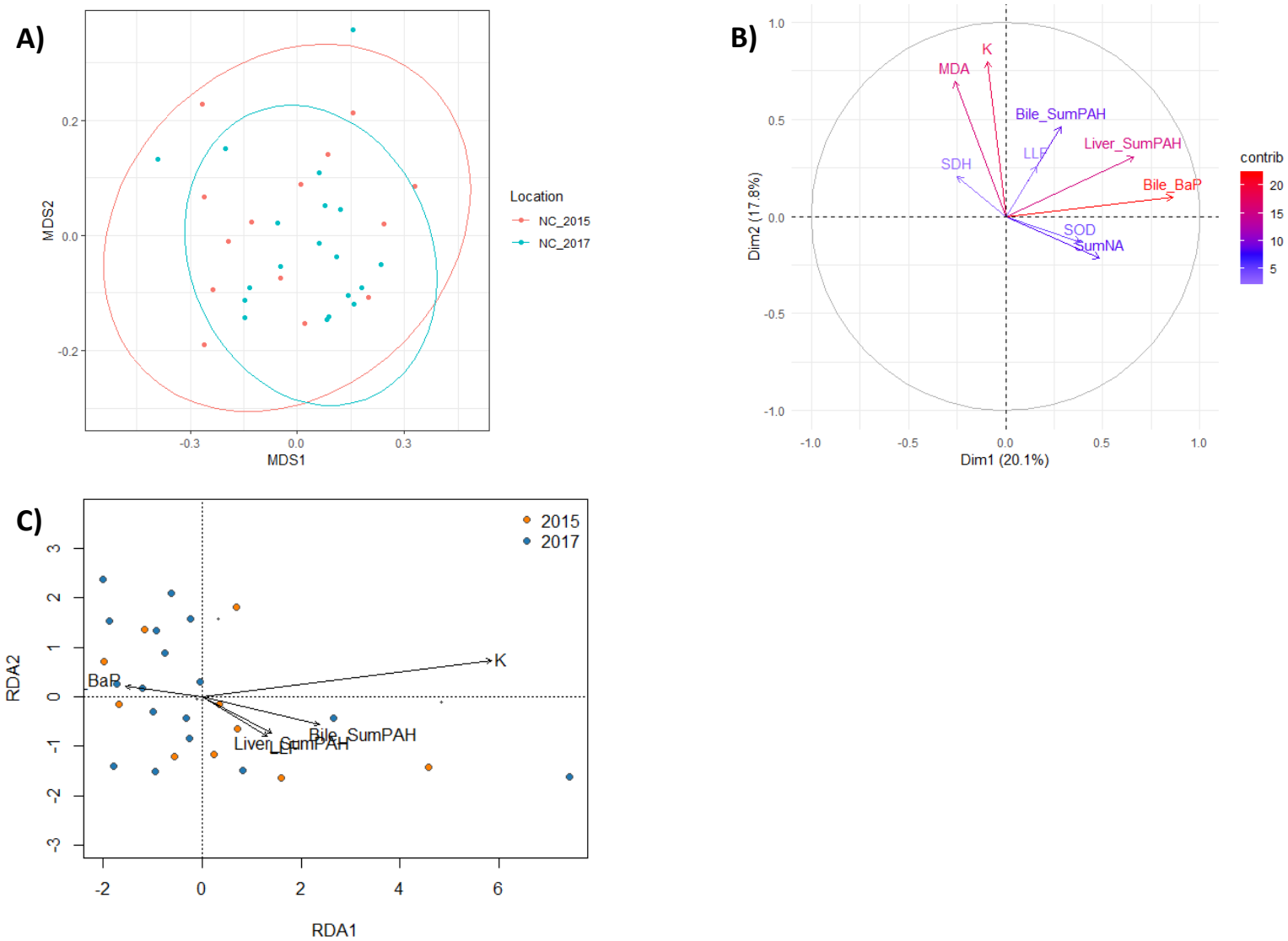


Figure 4.24: A) NMDS, B) PCA, and C) RDA of oxidative stress biomarkers and explanatory variables for specimens from NC, by sampling year.

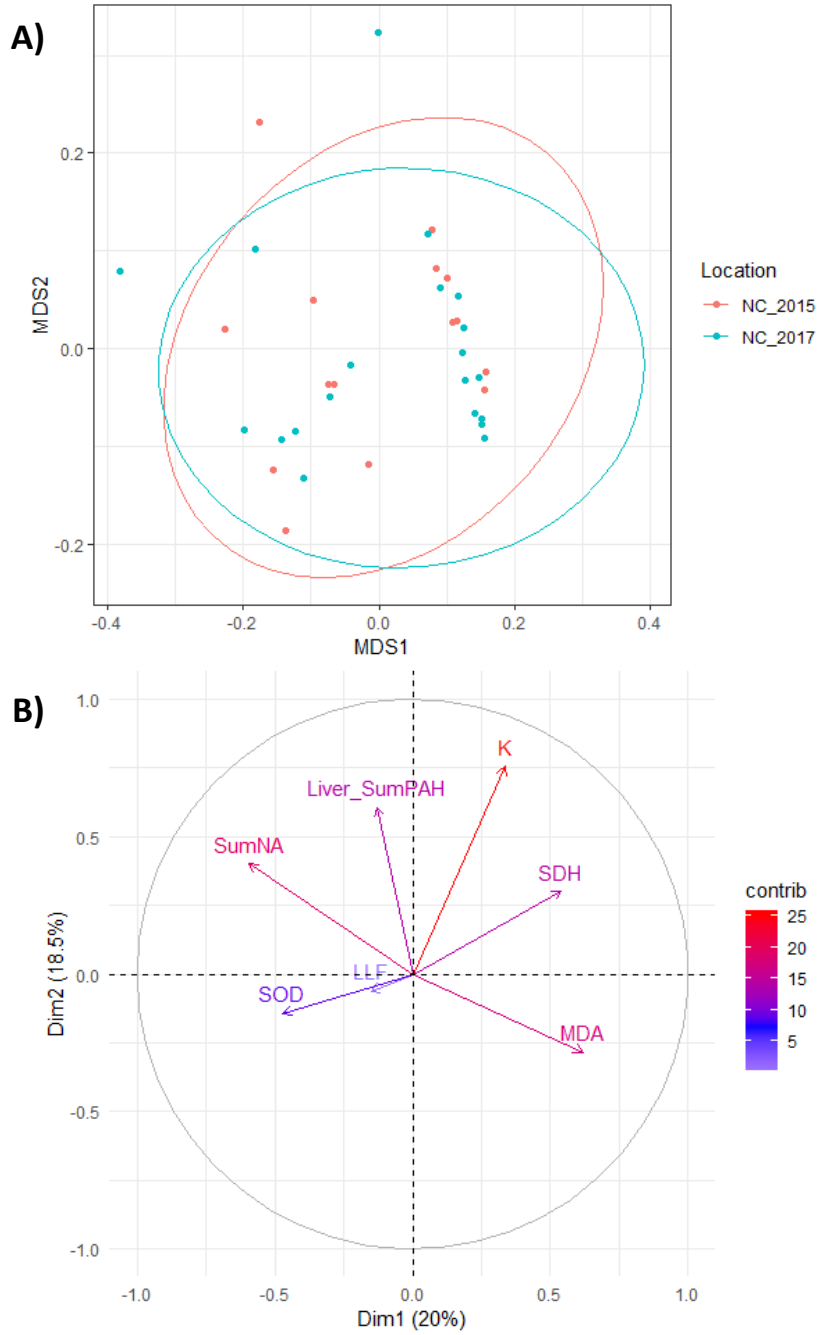


Figure 4.25: A) NMDS and B) PCA of oxidative stress biomarkers and explanatory variables for specimens from NC, by sampling year, upon removal of biliary PAH data.

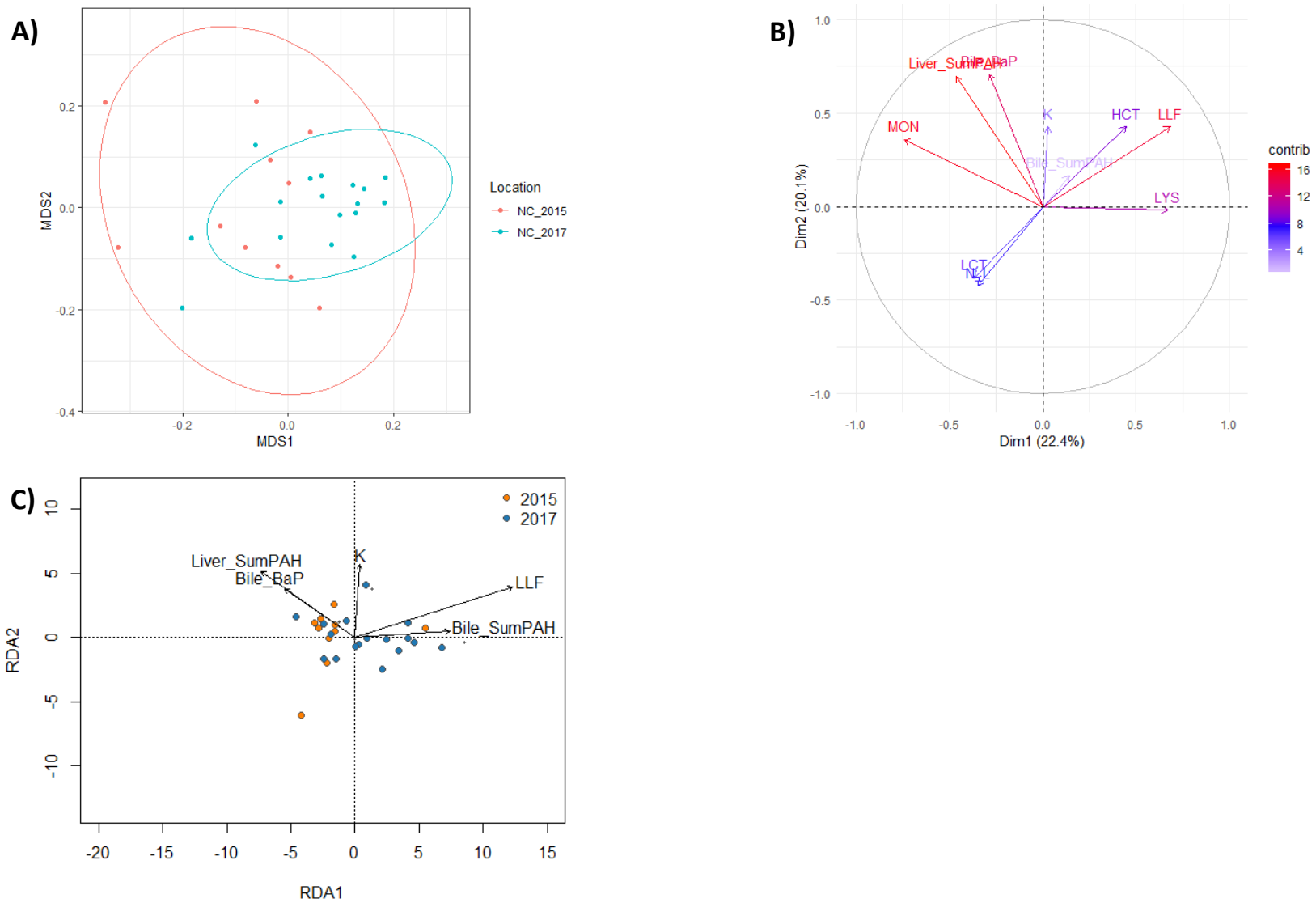


Figure 4.26: A) NMDS, B) PCA, and C) RDA of immune response biomarkers and explanatory variables for specimens from NC, by sampling year.

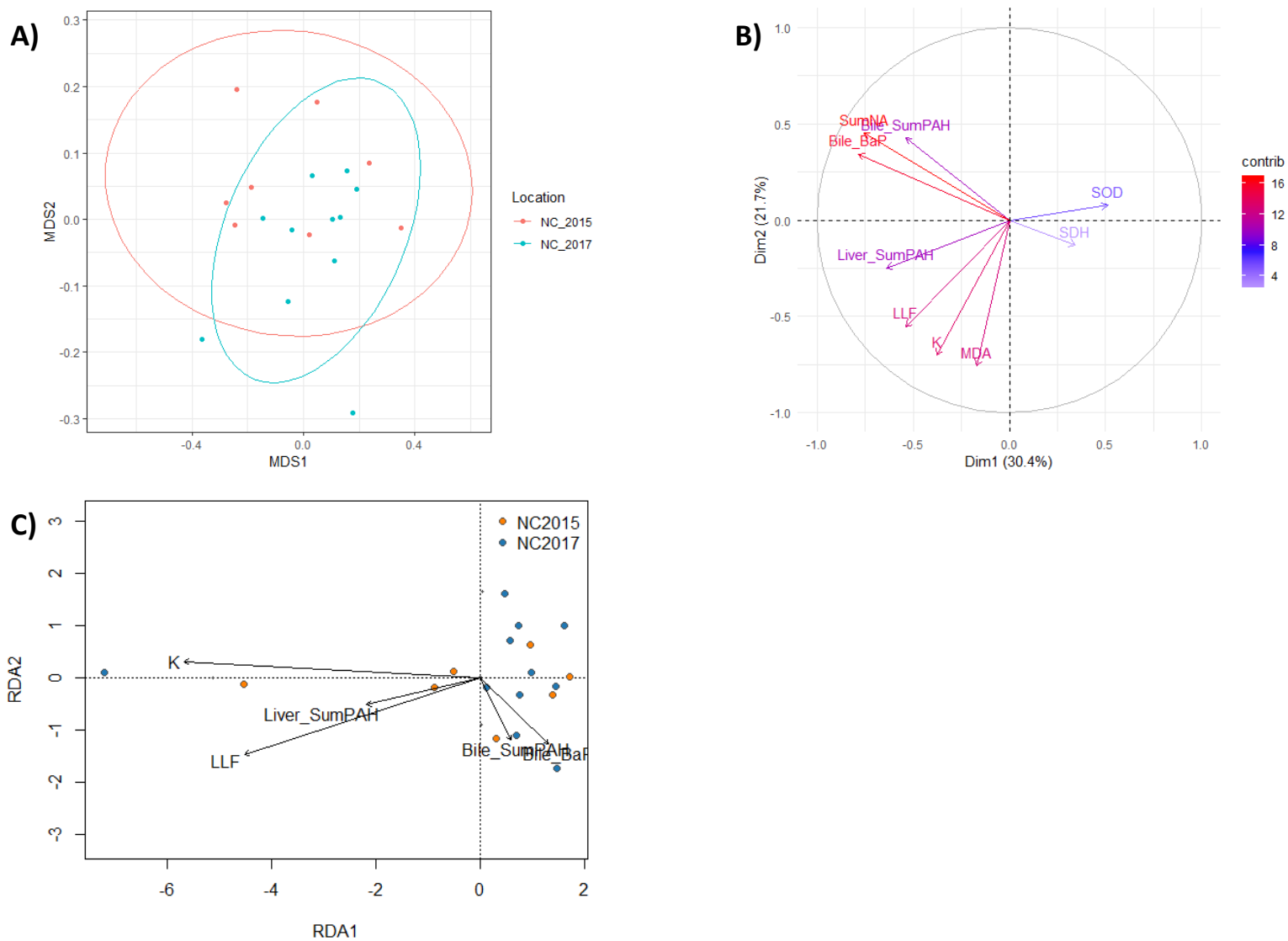


Figure 4.27: A) NMDS, B) PCA, and C) RDA for oxidative stress biomarkers and explanatory variables for females from NC stations sampled in 2015 and 2017.

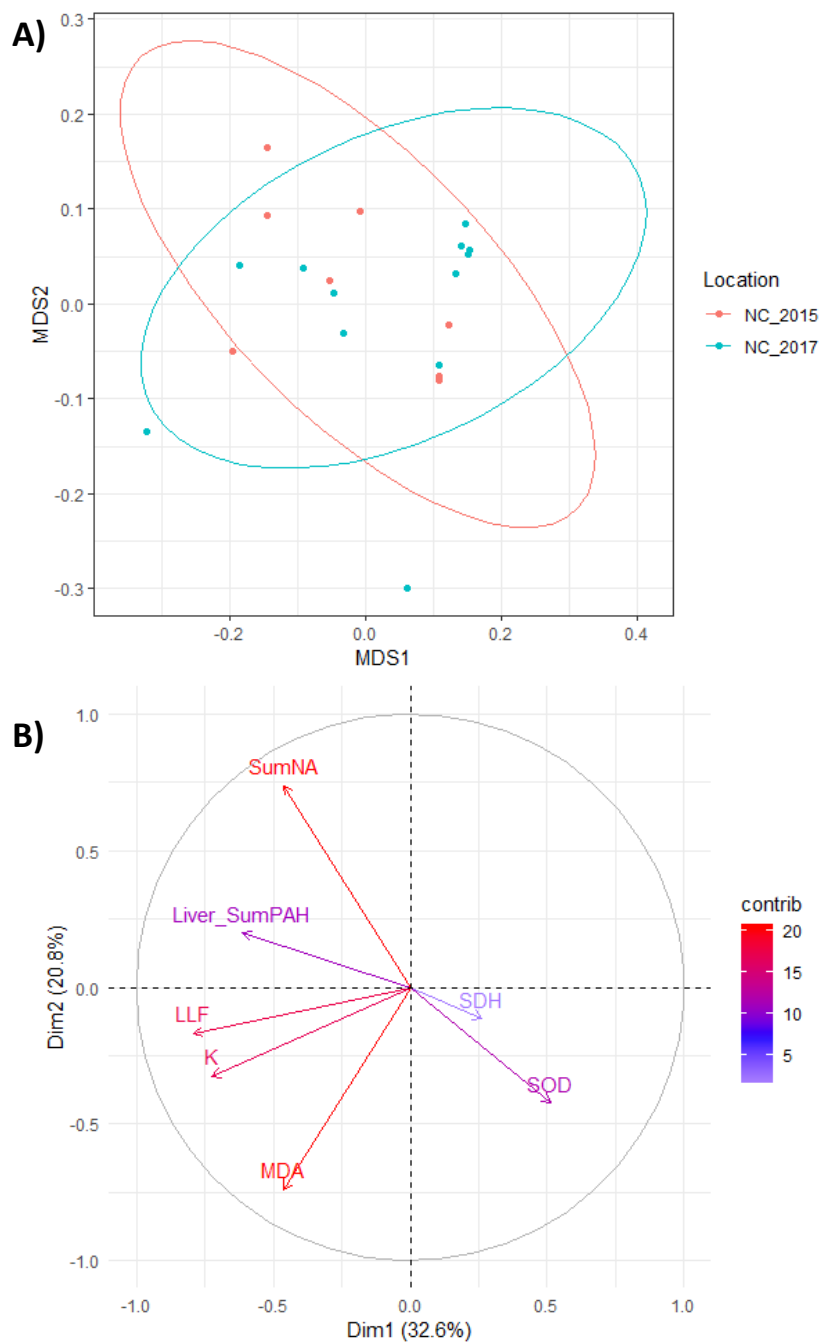


Figure 4.28: A) NMDS and B) PCA for oxidative stress biomarkers and explanatory variables for females from NC stations sampled in 2015 and 2017, upon removal of biliary PAH data.

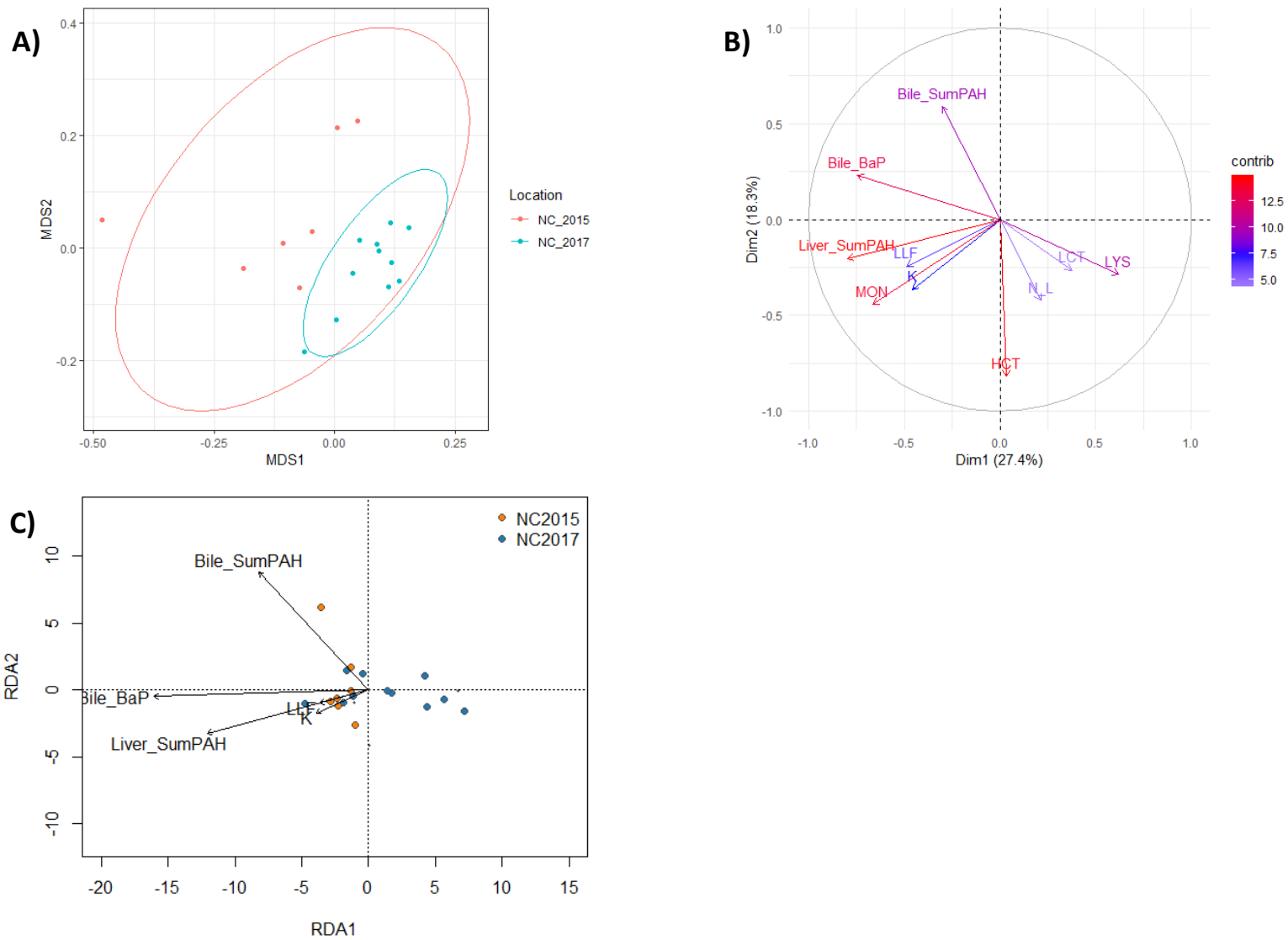


Figure 4.29: A) NMDS, B) PCA, and C) RDA for immune system biomarkers and explanatory variables for females from NC stations sampled in 2015 and 2017.

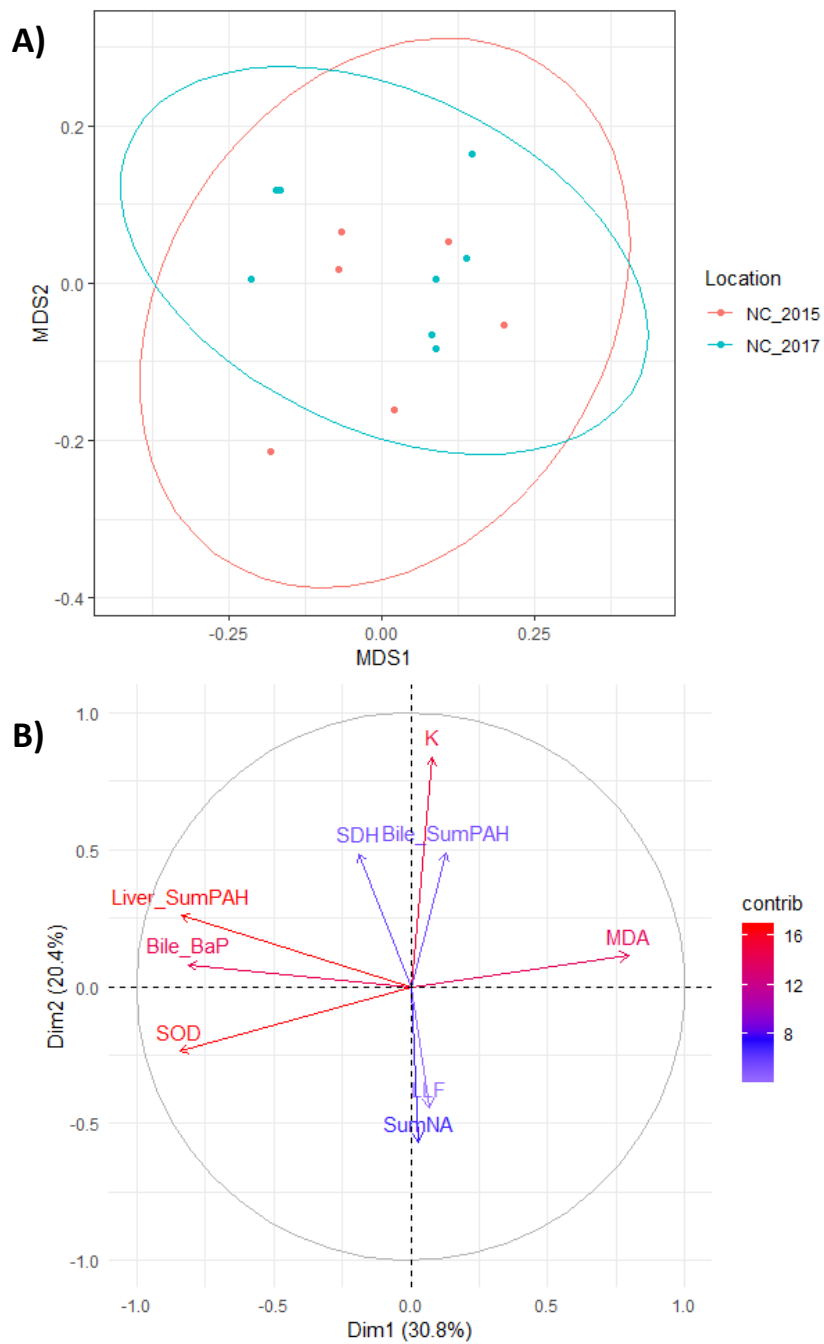


Figure 4.30: A) NMDS and B) PCA for oxidative stress biomarkers and explanatory variables in males caught within NC in 2015 and 2017.

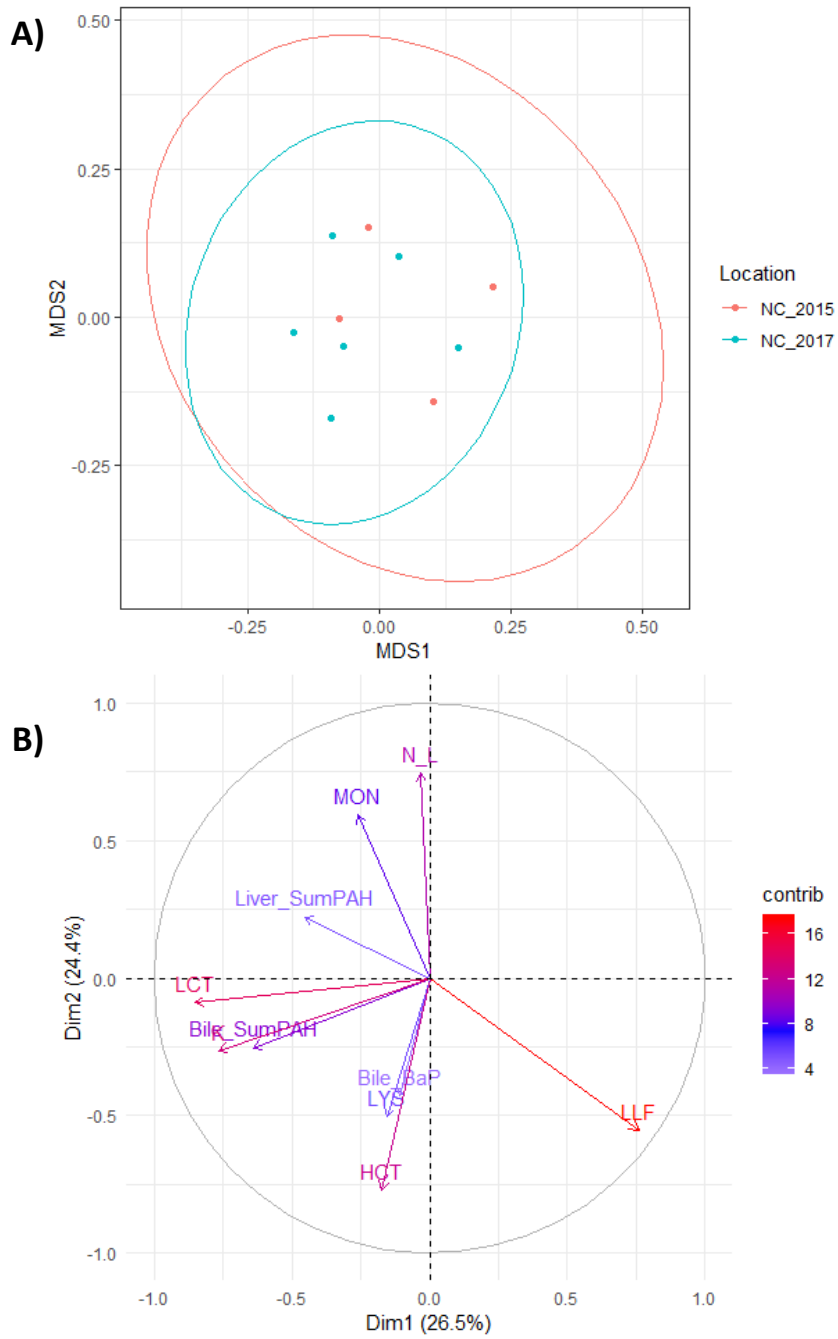


Figure 4.31: A) NMDS and B) PCA for immune system biomarkers and explanatory variables in males caught within NC in 2015 and 2017.

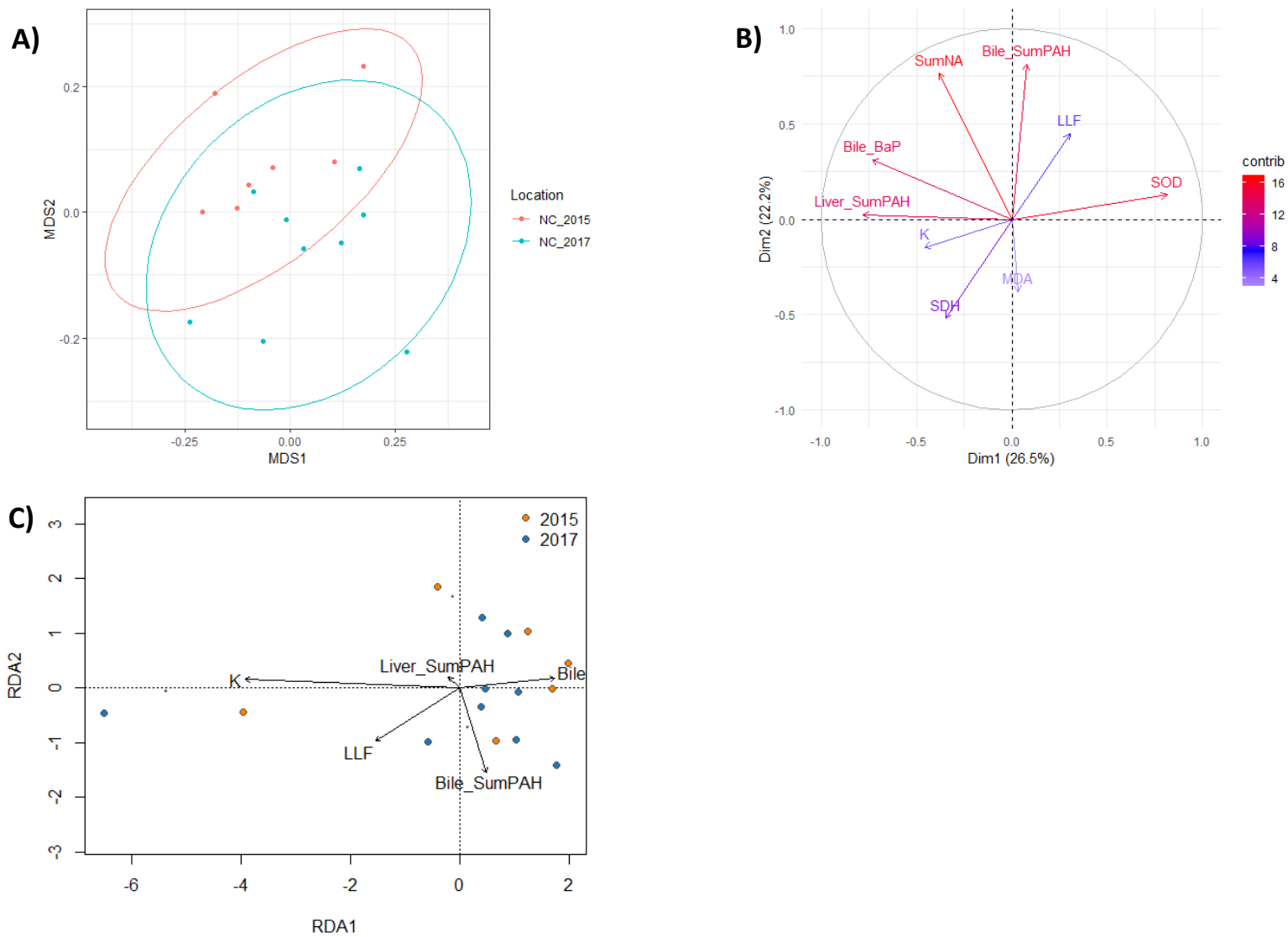


Figure 4.32: A) NMDS, B) PCA, and C) RDA for oxidative stress biomarkers and explanatory variables from specimens caught at stations 10-40, compared by sampling year.

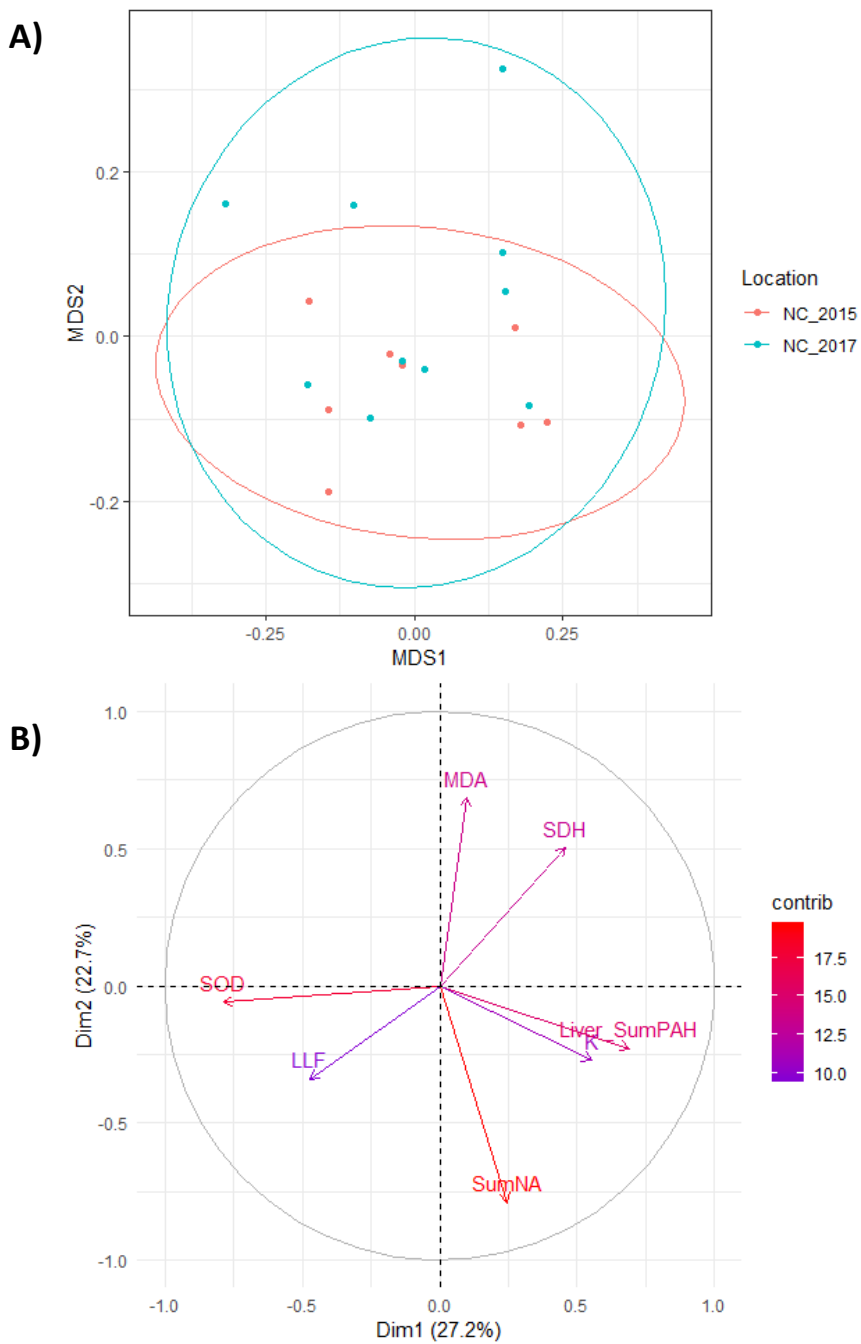


Figure 4.33: A) NMDS and B) PCA for oxidative stress biomarkers and explanatory variables from specimens caught at stations 10-40, compared by sampling year, upon removal of biliary PAH data.

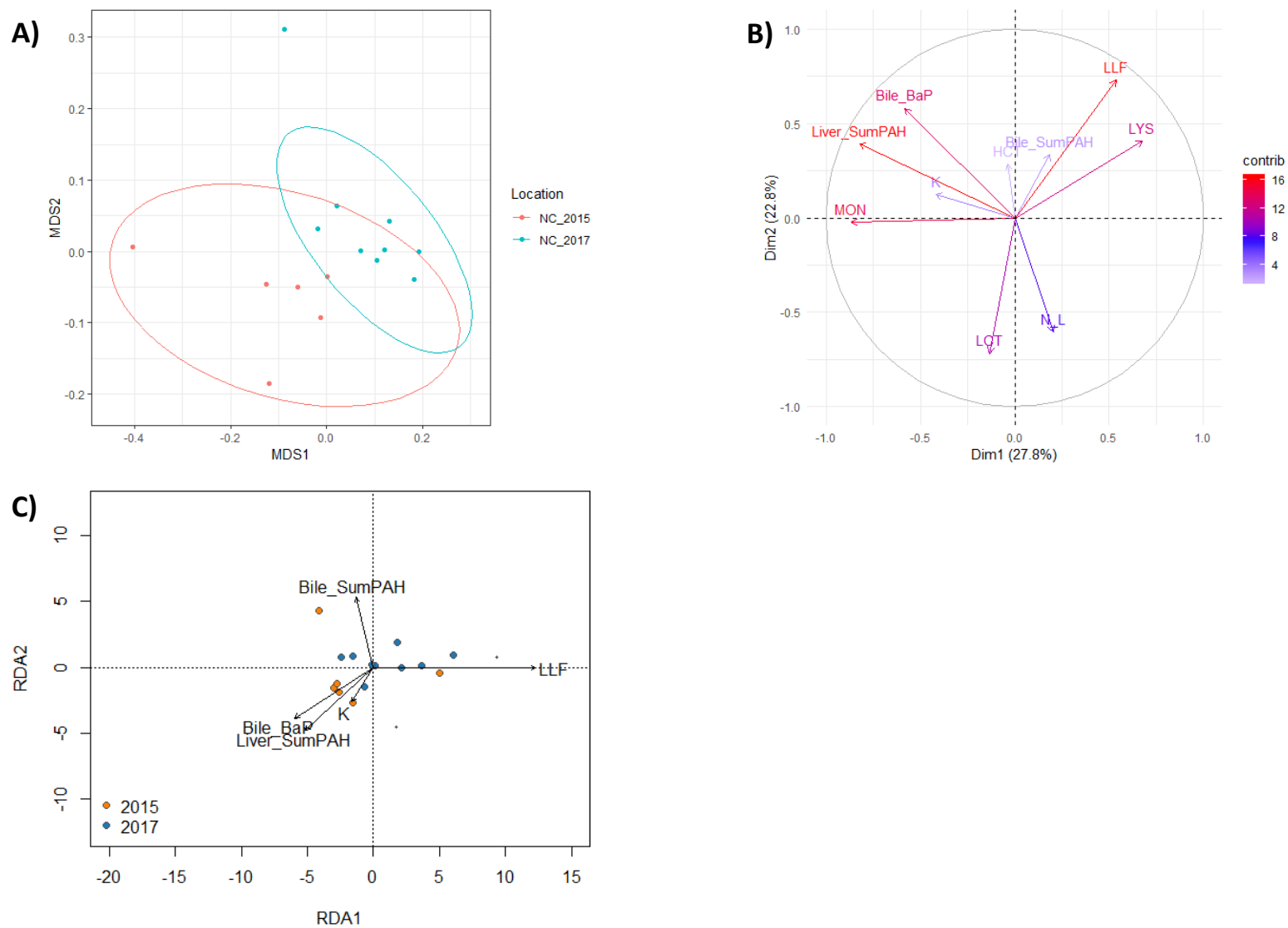


Figure 4.34: A) NMDS, B) PCA, and C) RDA for immune system biomarkers and explanatory variables from specimens caught at stations 10-40, compared by sampling year.

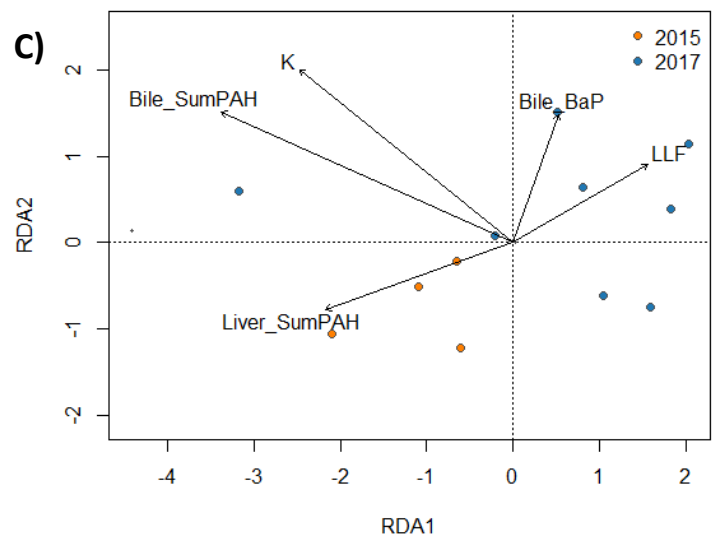
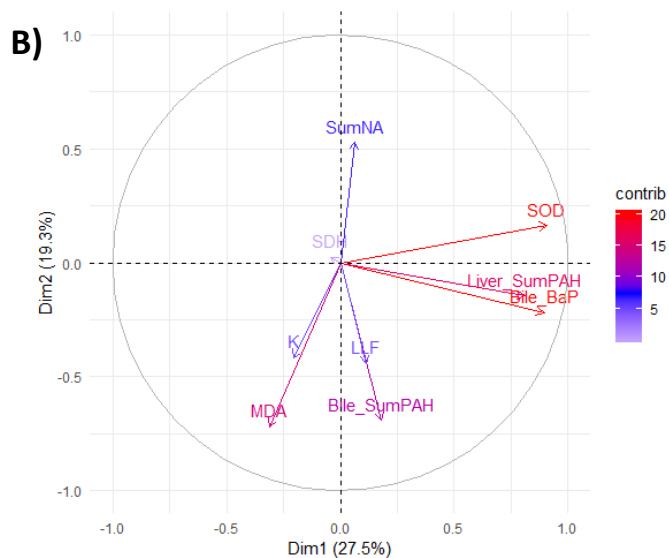
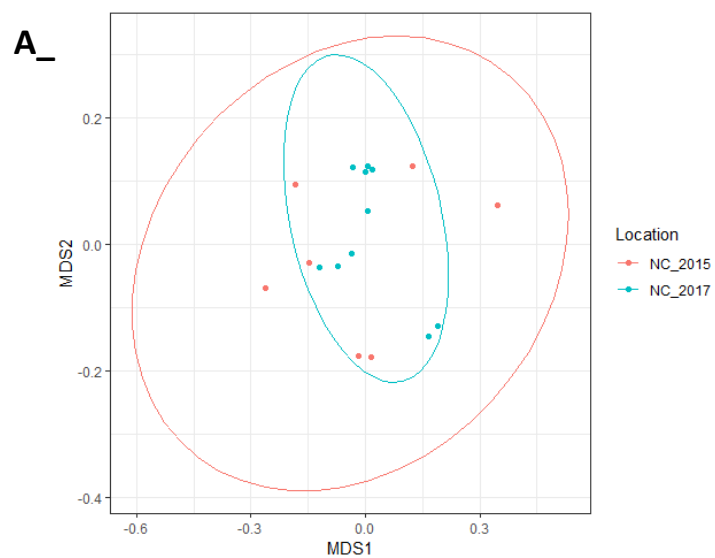


Figure 4.35: A) NMDS, B) PCA, and C) RDA for oxidative stress biomarkers and explanatory variables from specimens caught at stations 12-40, compared by sampling year.

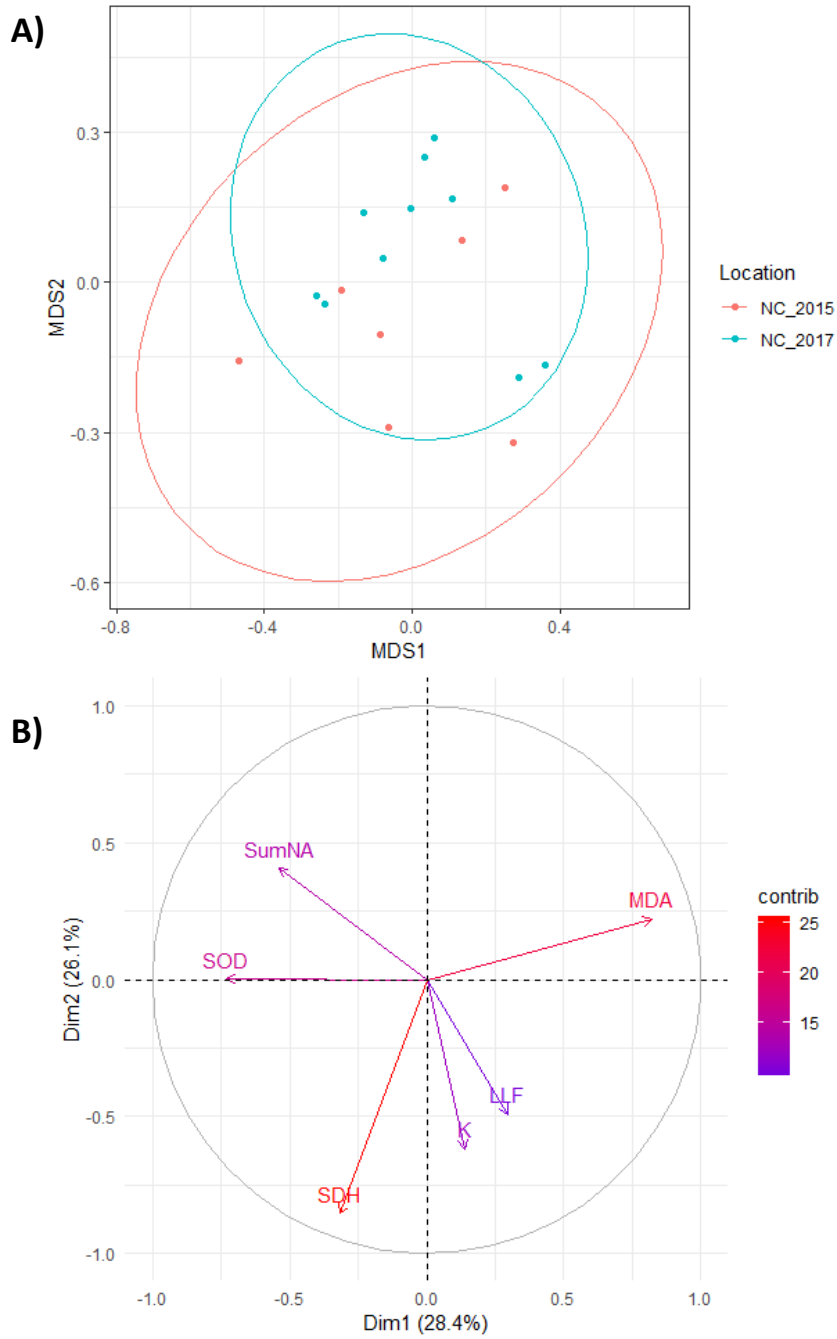


Figure 4.36: A) NMDS and B) PCA for oxidative stress biomarkers and explanatory variables from specimens caught at stations 12-40, compared by sampling year, upon removal of PAH data.

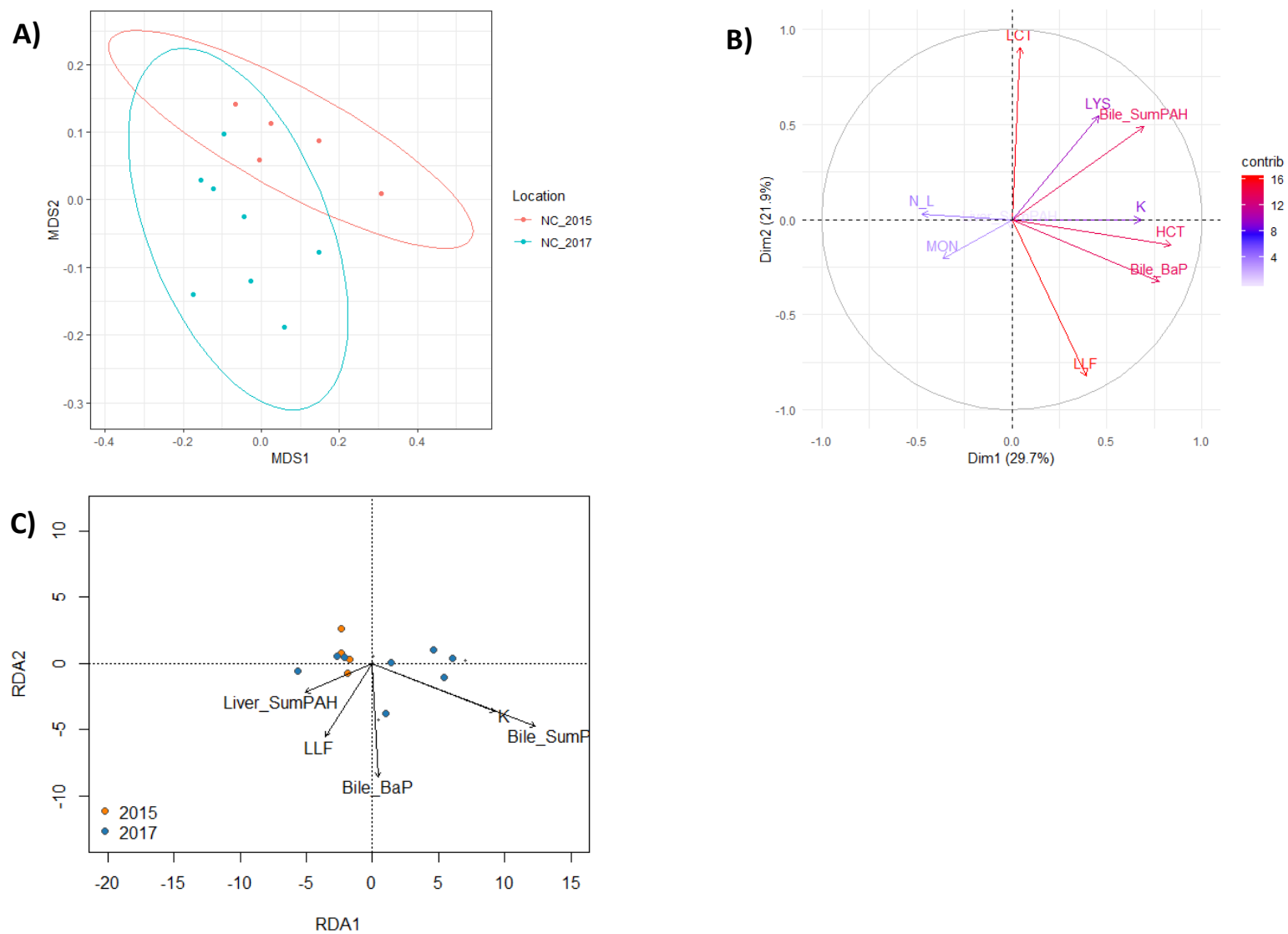


Figure 4.37: A) NMDS, B) PCA, and C) RDA for immune system biomarkers and explanatory variables from specimens caught at stations 12-40, compared by sampling year.

CHAPTER FIVE:
***DE NOVO* GOLDEN TILEFISH (*LOPHOLATILUS CHAMAELEONTICEPS*)**
TRANSCRIPTOME ASSEMBLY AND DIFFERENTIAL GENE EXPRESSION IN FISH
CAUGHT FROM THE DE SOTO CANYON, CAMPECHE BAY, AND YUCATAN
PENINSULA, IN THE GULF OF MEXICO

5.1 Abstract

Wild-caught fish are exposed to complex mixtures of chemical contaminants over their lifetime, significantly complicating ecological risk assessments following major pollution events. Laboratory-based dose-response studies typically examine the effects of exposures to a single chemical or simple mixtures over limited timeframes, reducing their applicability to real-world scenarios. Transcriptomics may assist in the interpretation of complex physiological responses in field-based studies by cataloging global, unbiased gene expression in an organism. This may allow for the discovery of novel pathways or candidate genes for further targeted research. In this paper, the relationship between polycyclic aromatic hydrocarbon (PAH) exposure and differential gene expression in Golden Tilefish (*Lopholatilus chamaeleonticeps*) was explored at three locations in the Gulf of Mexico (GoM): the northern De Soto Canyon offshore the United States of America; within the Campeche Bay, Mexico; and offshore the Yucatan Peninsula, Mexico. Despite relatively high levels of PAH contamination in all sampled fish, distinct and differential gene expression patterns were observed across stations, after pooling individuals to

minimize the influence of inter-individual variation. In particular, fish from the northern De Soto Canyon, likely exposed to contamination from the DWH spill, displayed altered metabolic response, activation of genes associated with clearance of cellular debris, and down-regulation of reproductive genes. Fish captured within the Campeche Bay oil fields demonstrated evidence of possible immunosuppression and reduced engagement of protective pathways, despite elevated biomarkers of oxidative stress-related damage. Fish from the Yucatan Shelf had more similar patterns of differential gene expression to fish from the northern De Soto Canyon than those from Campeche Bay. This underscores the discrepancies in gene expression observed in Campeche Bay specimens.

5.2 Introduction

Predicting deleterious effects of anthropogenic contamination on wild-caught marine species is far more complicated than extrapolations from the impacts from laboratory-based dose-response studies (Baillon et al., 2016; Hamilton et al., 2016; Williams et al., 2014). Rather than being exposed to single compounds, over controlled time intervals, wild specimens receive life-long doses of chemical mixtures and are affected by countless other environmental signals. While exposure levels to individual toxicants may be lower than those experienced in the laboratory, interactions among various contaminants can have additive or multiplicative effects, complicating the interpretation of subsequent physiological change (Crain et al., 2008; Hamilton et al., 2016; Kortenkamp, 2007). Furthermore, the extent to which an animal's prey items or external environmental matrices (like sediments) are contaminated by pollutants may consistently increase their chronic exposure and resulting body burdens over time (Kane Driscoll et al., 2010; Koenig et al., 2013; Santana et al., 2018). Such chronic exposure to toxicants may impact the subsequent uptake and metabolism of additional or novel contaminants, compared to

observations made on previously unpolluted laboratory animals (Marchand et al., 2004; Santana et al., 2018; Whitehead et al., 2017; Wirgin et al., 2011). Oceanic ecosystems themselves are dynamic, with seasonal variation in current flow, atmospheric deposition of contaminants, levels of sediment and pollutant flux due to runoff from land, and changes in food webs, with impacts on fish spawning, development, and nutrient availability (Cerón et al., 2007; Díaz-Asencio et al., 2019; R. Harris, Pollman, Landing, et al., 2012; Madeira et al., 2019; Smith & Jacobs, 2005). Synergistic interactions between natural stressors and bioavailable contaminants can result in greater and more unpredictable deleterious effects than either group would have had on its own (Gandar et al., 2017; Holmstrup et al., 2010).

Given such complexities, advocacy for a multi-biomarker approach analyzed using multivariate statistical analysis has grown in the ecological risk assessment community (Baudou et al., 2019; Broeg et al., 2005; Gagnon & Rawson, 2016; Iturburu et al., 2018). Biomarker selection, however, can be complicated and expensive, particularly when studying non-model species exposed to unknown stressors and undocumented lifetime chemical exposures through uncertain pathways of expression (Hook et al., 2014; Madeira et al., 2019). The advent of RNA sequencing (RNA-seq) technology and recent declines of sequencing and computational costs has increased applications of transcriptomics in environmental studies (Qian et al., 2014; Wang et al., 2009; Ye et al., 2018). The ability to assemble a transcriptome *de novo*, without a reference genome, allows researchers to examine non-model species, and to further distinguish the full complement of differentially expressed genes as reflective of environmental exposure (Conesa et al., 2016; Oshlack et al., 2010). The resulting data from these studies may reveal important and/or novel response pathways or individual target genes for further research.

In this study, RNA-seq was utilized to determine whether geographically separated groups of Golden Tilefish (*Lopholatilus chamaeleonticeps*) from the Gulf of Mexico (GoM) had differential gene expression signatures, and if such differences may be attributable to environmental exposure to polycyclic aromatic hydrocarbons (PAHs). Organisms were also analyzed for individual biomarkers of oxidative stress and non-specific immune response, as described in Chapters II and III. Golden Tilefish are an attractive study species for contaminant analysis, given their close affiliation with sediments, consumption of benthic prey, relatively long lives, and high site fidelity (Able et al., 1982; Lombardi-Carlson & Andrews, 2015). The three sampling locations chosen for this study were: the northern De Soto Canyon (station 8-100) off the United States of America, likely impacted by the 2010 *Deepwater Horizon* (DWH) oil spill; Campeche Bay (station 31-150), within Mexican oil fields and proximity to the 1979 *Ixtoc I* oil spill; and one offshore the Yucatan Peninsula (station 36-150) in Mexico, with no known proximity to oil extraction activities (Fig. 5.1).

5.3 Methods

5.3.1 Sampling

Specimens were collected from three locations (Fig. 5.1) via demersal longline sampling aboard the *R/V Weatherbird II* in accordance with state, federal, and international permits, as previously described (Murawski et al., 2018). Location, depth, and temperature information were recorded by data loggers (Star:Oddi CDST Centi-TD), attached to the 544-kg-test monofilament at both ends of each 5 mile long set, each of which contained approximately 500 Atlantic Mackerel (*Scomber scombus*) or squid (primarily *Doidicus gigas*) baited size 13/0 circle hooks. Station information may be found in Table 5.1, with additional data available in Appendix A.

Within 15 minutes of landing on deck, specimens were processed as described in Chapters II-IV. Unique to this chapter, duplicate portions of liver (approximately 50 mg) were excised using ethanol rinsed tools, placed in 1000 μ L RNAlater (Sigma-Aldrich, St. Louis, MO) and stored at 4°C for 24 hours, prior to short-term (<20 days) storage at -20°C, while offshore. As soon as possible, samples were transferred to long-term storage at -80°C.

5.3.2 RNA sequencing

Liver samples (approximately 50 mg) frozen in RNAlater at -80°C were submitted to GENEWIZ (South Plainfield, NJ) for RNA extraction, strand-specific library preparation with rRNA depletion, and sequencing by Illumina HiSeq. Quality of the RNA was assessed by both Nanodrop and Qubit assay. In sum, liver samples from fifteen Golden Tilefish were submitted for RNA-seq, five from each of the three sampling locations.

5.3.3 *De novo* Golden Tilefish transcriptome assembly

Raw FASTQ-formatted files were screened using the FastQC tool in Galaxy (<http://usegalaxy.org>). Sequences were examined for length, % guanine-cytosine (GC) content, overall quality, per base sequence quality, per sequence quality, per base sequence content, per base GC content, per base N content, sequence length distribution, sequence duplication levels, overrepresented sequences, and residual adaptor content from the sequencing method. Paired end reads were trimmed using the Trimmomatic tool in Galaxy to remove low quality bases and artifacts, using a series of sliding window methods. After each trim, sequences were again analyzed by the FASTQC tool in order to confirm sequence quality.

Trimmed files were compiled into a master assembly using the Trinity (github.com/trinityrnaseq/trinityrnaseq/wiki) in Linux. Trinity allows for *de novo* assembly of

RNA-seq data by the creation of several de Bruijn graphs, representative of transcriptional complexity at a given locus, and by extracting full-length isoforms from these plots. The alignment of each individual to the master assembly was assessed using the fast gapped-read aligner Bowtie2 (bowtie-bio.sourceforge.net/bowtie2/index.shtml) in Linux. Bowtie2 utilizes both an initial, ungapped stage and a gapped extension stage through aid of single-instruction multiple data parallel processing. Trinity alignment statistics were obtained using the TrinityStats.pl code in Linux (v 2.4; github.com/trinityrnaseq/trinityrnaseq/releases).

Although individual variability was anticipated in wild-caught organisms, general observations concerning differential gene expression between sampling locations were achieved by pooling specimens by station. Abundance estimation was performed using the RSEM package (which does not require the use of a reference genome) and differential gene expression of individual fish by station was determined using Bioconductor package edgeR, both of which were run as dependencies within the Trinity package, in Linux (Li & Dewey, 2011). The edgeR package determines differential expression for transcript count data using an over-dispersed Poisson model, requiring minimal levels of replication (Robinson et al., 2010). Heat maps were generated and cluster analysis was performed after running trimmed mean of M values (TMM) normalization in Trinity, with a significance of $p < 0.001$, to identify potential outliers among individuals within the data for each station. This method estimates total RNA production by using a weighted mean of the log-fold-change expression ratios (Robinson & Oshlack, 2010).

5.3.4 Annotation and gene ontology

Differentially expressed transcripts with a false discovery rate (FDR) < 0.05 were annotated using the BLASTn and BLASTx basic local alignment search tools for nucleotide and protein data from the National Center for Biotechnology Information (<http://ncbi.nlm.nih.gov>).

Gene ontologies were obtained using the InterPro protein classification database from the European Bioinformatics Institute (<http://ebi.ac.uk/interpro>). Additional functional information was obtained about select genes from review of the relevant literature.

5.3.5 Biomarkers and liver lipid fraction

Biomarkers for oxidative stress (superoxide dismutase (SOD), malondialdehyde (MDA), sorbitol dehydrogenase (SDH), and sum erythrocyte nuclear abnormalities (NA)), non-specific immune response (hematocrit (HCT), leukocrit (LCT), plasma lysozyme (LYS), and differential white blood cell counts (DWBC)) and liver lipid fraction (LLF) were measured in these specimens, as part of work previously described in Chapters II and III.

5.3.6 Polycyclic aromatic hydrocarbon metabolites

Biliary PAH and liver PAH metabolites were measured as previously described in Chapter III (Snyder et al., 2019).

5.3.7 Biometrics, biomarker, liver lipid fraction and polycyclic aromatic hydrocarbon metabolite data analysis

Statistical analysis was performed on biometric, biomarker, liver lipid fraction and PAH data using the R Project for Statistical Computing version 3.4.1 with the *vegan*, *pastecs*, and *ggplot2* packages and their dependencies. All significant differences between station responses were calculated by either ANOVA or Kruskal-Wallis tests, followed by *post hoc* pairwise comparisons by Tukey HSD, after screening for normality by Shapiro-Wilk criterion. Condition factor (K) was calculated as: $K = 100 * W/L^3$, where W was total weight (kg), and L was fork length (cm; Froese 2006). All data are publicly available at <https://data.gulfresearchinitiative.org/pelagos-symfony/data/R6.x805.000:0083> and <https://data.gulfresearchinitiative.org/pelagos-symfony/data/R6.x805.000:0078>.

5.4 Results

5.4.1 *De novo* assembly of the Golden Tilefish transcriptome

In sum, 886,912,622 raw sequences with average lengths of 151 base pairs (bp) and average GC content of 53.3% were returned by GENEWIZ in FASTQ files (Table 5.2). Sequences were trimmed to remove low quality bases and artifacts with Trimmomatic, yielding 460,877,078 sequences with lengths ranging from 36 to 151 bp and an average GC content of 52.9% (Table 5.3). The master "reference" assembly, generated from the combination of all sequenced individuals, consisted of 220,988,747 sequences with a %GC of 44.43 and an average alignment rate for individual samples of 96.58% by Bowtie2 (Table 5.4).

5.4.2 Differential gene expression

Based upon visual inspection of heat maps and cluster analysis of differentially expressed genes by station, one putative outlier individual was removed from each station (specimen identification numbers: 8-100-051, 31-150-006, 36-150-025). Upon later inspection of finalized QA/QC'd biometrics data (available after initial specimen selection was performed) one of these outliers was classified as a male (specimen 31-150-006), further substantiating the need for removal of this individual and subsequent removal of one individual from the remaining stations to balance the numbers of specimens compared. All remaining results in this paper refer to the data with outliers removed. An additional heat map was generated (Fig. 5.2) and cluster analysis was performed (Fig. 5.3) to visually inspect differential expression ($p < 0.001$) between stations. Volcano plots were created in Trinity to explore statistical difference (false discovery rate < 0.05) versus magnitude of change (fold change) in differential gene expression between stations (Fig. 5.4).

5.4.3 Annotation and gene ontology

In total, 1,475 differentially expressed genes between stations were annotated (Table 5.5). Of these genes, an average of 56.30% had associated biological function gene ontology (GO) terms (Tables 5.5, 5.6), 71.96% had associated molecular function GO terms (Tables 5.5, 5.7), and 33.83% had associated cellular component GO terms (Tables 5.5, 5.8). Based upon these GO terms and review of the relevant literature, selected genes were classified into functional groups to better compare relative differential gene expression between stations. These groups included: xenobiotic metabolism (Tables 5.9), lipid metabolism (Table 5.10), glucose metabolism and release (Table 5.11), cholesterol biosynthesis (Table 5.12), reproduction (Table 5.13), immune response (Table 5.14), oxidative stress and debris clearance (Table 5.15), circadian rhythm (Table 5.16), and transcription factors and solute carriers (Table 5.17). Genes with multiple documented functions may appear in several tables.

5.4.4 Biomarker response and liver lipid fraction

Statistically significant differences in biomarker response were noted for LYS and HCT. Individuals from station 31-150 had significantly elevated plasma LYS compared to station 8-100 ($p = 0.026$) and individuals from station 36-150 ($p = 0.011$; Fig. 5.5). Individuals from station 31-150 had significantly elevated HCT compared to individuals from station 36-150 ($p = 0.006$).

5.4.5 Polycyclic aromatic hydrocarbon metabolites

Statistically significant differences in PAH metabolite concentrations were observed for both sum biliary PAH and biliary benzo(*a*)pyrene (B(*a*)P). Individuals from station 8-100 had significantly elevated values of sum biliary PAH compared to individuals from station 31-150 (p

= 0.018) and 36-150 ($p = 0.032$; Fig. 5.6). Individuals from station 31-150 had significantly elevated biliary B(a)P values compared to the remaining stations ($p = 0.012$; Fig. 5.6)

5.5 Discussion

No significant difference was observed in temperature or depth by station, nor in mean fish total weight, fork length, or condition factor. The most common biological function terms explaining differentially expressed genes between fish from station 8-100 and the remaining stations included: oxidation-reduction processes, regulation of transcription, metabolic processes, steroid hormone mediated signaling pathways, and proteolysis, however, none of these accounted for more than 7.05% of the annotated genes with associated GO terms (Table 5.6). All of these pathways were within the top ten most frequent terms for differentially expressed genes between 31-150 and 36-150 as well, apart from metabolic processes, suggesting a slightly greater significance for genes of this latter function at station 8-100.

The majority of the most common molecular function GO terms were similar when differential gene expression was compared between stations, with protein binding being the most frequently observed among all groups, accounting for an average of 16.06% of GO-associated differentially expressed genes (Table 5.7). Oxidoreductase activity was cited only when comparing fish from station 8-100 to the remaining stations, suggesting greater importance of this function at this station. Cellular component GO functions were similar among all groups, as may be expected from analysis of gene expression from identical tissue types (Table 5.8).

Hundreds of differentially expressed genes were annotated between stations, using BLASTn and BLASTx. Notably, individuals within stations had more similar patterns of differential gene expression to one another than to individuals from different sampling regions (Fig. 5.2). While this was hypothesized to occur, given the different contaminant exposure

regimes at each station, the inherently high amount of variability in gene expression among wild-caught individuals could have obscured these data. Overall patterns of gene expression appeared to be more similar between stations 8-100 and 36-150, with station 31-150 clustering separately (Fig. 5.3). While 598 annotated genes were identified as differentially expressed (FDR < 0.05) between stations 8-100 and 31-150, only 272 were differentially expressed between 8-100 and 36-150. Station 31-150 and 36-150 had 605 differentially expressed genes between them (Table 5.5).

Relatively large numbers of differentially expressed genes between stations 8-100 and 31-150 were unexpected, considering both stations were located proximal to oil extraction activity and in sediments likely contaminated from past oil spills (the *DWH* for 8-100 and *Ixtoc I* for 31-150). It was hypothesized that this exposure to PAHs would result in a similar signature of gene expression patterns among these stations, as compared to overall expression at 36-150, where any PAH exposure was most likely associated with deposition from shipping channels, atmospheric outfall, and natural seeps. However, discrepancies may be driven by incident-driven PAH elevation at station 8-100 as compared to general chronic contamination at station 31-150. In addition, while station 31-150 was located within dense Mexican oil platform aggregations, station 8-100 was located to the northeast of United States oil fields. When PAH data were evaluated for the included specimens, those from 8-100 had significantly elevated sum biliary PAH compared to the remaining stations, indicating recent exposure and metabolism of the contaminant (Fig. 5.6). Despite lower levels of sum biliary PAH compared to fish collected from 8-100 and 36-150, individuals from station 31-150 had significantly elevated levels of the particularly toxic and carcinogenic PAH metabolite B(a)P in their bile compared to the remaining stations (Fig. 5.6). This may be a result of different crude oil types found in the

various locations studied or of persistent rig flaming and atmospheric deposition at station 31-150.

Perhaps most curious is the elevation of average sum liver PAH in individuals from station 36-150 compared to those from other locations. While not statistically significant, the pattern indicates the potential for relatively rapid clearance of PAHs at station 8-100, with greater deposition of PAHs into tissues at station 36-150. Fish are capable of rapidly metabolizing and clearing PAHs upon intake, with tissue accumulation primarily occurring when their metabolic capacity is overwhelmed (Collier et al., 2013; Meador et al., 1995; Santana et al., 2018; Vuontisjärvi et al., 2004). The ubiquitous PAH exposure observed among these fish may explain the lack of differential expression among genes commonly associated with PAHs, including aryl hydrocarbon receptor 2 (AHR2) and cytochrome P450 subfamily 1A (CYP1A; Hook et al., 2014; Oziolor et al., 2014). Field studies, however, indicate the reduced expression of CYP1A can be due to developing resiliency or due to cross-talk with genes simultaneously triggered by other environmental factors (Koenig et al., 2013; Trisciani et al., 2011).

Unfortunately, neither hypothesis can be supported or refuted by the data provided in this study. Patterns among genes involved with Phase I-III xenobiotic metabolism were also inconclusive (Table 5.9). While UDP-glucuronosyltransferases (UGTs) were generally elevated at station 8-100 compared to other stations, suggesting an engaged Phase II xenobiotic metabolism, the response among this class of genes can vary widely among fish species and can be impacted by other factors, including nutrition and seasonality (Solé et al., 2010; Trisciani et al., 2011).

More widespread patterns of differential expression were observed between stations for genes associated with lipid metabolism. Approximately 82.6% of genes associated with lipid metabolism were down-regulated at station 8-100 compared to 36-150 and 84.2% down-

regulated compared to 31-150 (Table 5.10). The perturbation of lipid metabolism by PAHs has been linked to aberrant health outcomes in both mammalian and teleost literature (Balk et al., 2011; Martins et al., 2015; Sørhus et al., 2017). However, when undergoing a stress response, lipid stores may be actively metabolized as a compensatory energy source for the repair of damaged cellular components (Petitjean et al., 2019). The marked down-regulation of these genes at station 8-100, a location with a documented history of PAH contamination since the DWH spill (Snyder et al., 2015, 2019) is connected with depletion of lipid stores in chronically stressed organisms as reflected in the corresponding liver lipid fraction data from the larger cohort of fish from these stations (Snyder 2020). A compensatory response was not conclusively indicated in genes associated with glycolysis, although glucose-6-phosphatase (G6PASE), associated with glucose release, was comparatively up-regulated at 8-100 compared to the remaining stations (Table 5.11; Tintos et al., 2008).

It is possible that differences in metabolic gene expression are simply related to varying prey availability or quality among geographic stations. Benthic community change in the De Soto Canyon after the DWH spill has been hypothesized, following oil-associated marine snow sedimentation (Daly et al., 2016; Schwing et al., 2015). Unfortunately, most fish collected in this study had inverted their stomachs upon being rapidly pulled from depth, precluding the ability to perform meaningful dietary analysis by gut content. Fewer genes associated with lipid metabolism were differentially expressed between fish from stations 31-150 and 36-150, however, 75% of those found were comparatively up-regulated at 31-150 (Table 5.10), while the majority of glucose-related genes were down-regulated at 31-150 (Table 5.11).

Laboratory transcriptomic studies in a variety of fish species have recently indicated enrichment of the cholesterol biosynthetic pathway upon PAH exposure (Loughery et al., 2018;

McGruer et al., 2019; Sørhus et al., 2017; Xu, Khursigara, et al., 2017). Fish from station 8-100 had comparatively up-regulated solute carrier 13 family member 5 (SLC13A5), a gene associated with transport of citrate, which is in turn a precursor of cholesterol biosynthesis (Klotz et al., 2016), compared to other stations (Table 5.12). Four cholesterol related genes were comparatively down-regulated in fish from station 8-100 compared to those from 31-150 (24-dehydrocholesterol reductase (DHCR24), cholesterol 7 alpha-hydroxylase (CYP7A1), apolipoprotein B100 (APOB100), methylsterol monooxygenase 1 (MSMO1) and two genes (DHCR24, MSMO1) were down-regulated compared to 36-150 (Table 5.12). Based upon differentially expressed genes between stations, it is unlikely that PAH exposure is causing enrichment to the cholesterol biosynthetic pathway in these wild-caught fish.

A number of genes associated with reproduction were down-regulated in fish from station 8-100 compared to those from both 31-150 and 36-150 (Table 5.13). This includes estrogen receptor- α (ER α), vitellogenin Aa (VTGAA), vitellogenin Ab (VTGAB), vitellogenin B (VTGB), vitellogenin C (VTGC), zona pellucida protein 4 (ZP4R), and zona pellucida protein Bb (ZPBB). All of these genes are sensitive to estrogenic compounds and can be suppressed in female fish upon exposure to PAHs (Fertuck et al., 2001; Holth et al., 2008; Marty et al., 2018; Zhang et al., 2018). Fish in this study were caught between August and September, after the typical spawning cycle of Golden Tilefish in the northern GoM (Lombardi-Carlson, 2012), making a decline in pre-spawning levels of vitellogenin likely (Bon et al., 1997; Hara et al., 2016). However, as all individuals were caught within the same timeframe relative to their spawning cycle, it is surprising that differential expression of these genes was observed between stations. It should be noted that little is known regarding the spawning cycle of Golden Tilefish in the southern GoM, and temporal shifts in the spawning cycle are possible between the

presumably distinct populations. This study, however, cannot eliminate possible effects of recent biliary PAH exposure or chronic contamination on the down-regulation of these genes.

Fish from station 8-100 had comparatively increased expression of immune response-related genes, including complement genes, antigen receptors, cytokines, chemokines, and other genes associated with inflammation and antibacterial or antiviral properties (Table 5.14). Compared to station 31-150, 86.4% of immune response-related genes were up-regulated at 8-100, with 57.14% up-regulated relative to station 36-150. Approximately 82% of immune response-related genes were down-regulated at 31-150 compared to 36-150, suggesting possible immunosuppression at this station. Alteration of the immune response has been frequently linked to PAH exposure, although the interpretation of the response can be difficult (Reynaud & Deschaux, 2006; Stevens et al., 2009). Several sources cite the ability of PAHs to induce immunosuppression, subsequently increasing pathogen susceptibility in fish (Kennedy & Farrell, 2008; Reynaud & Deschaux, 2006; Santana et al., 2018). Elevated levels of non-specific immune biomarkers were observed in individuals from 31-150, including LCT and LYS (Fig. 5.7), indicating a possible pathogen response at this station.

Several genes associated with the response to oxidative stress, apoptosis, ubiquitination, and cell differentiation and survival were up-regulated in fish from station 8-100 compared to those from both 36-150 and 31-150 (particularly the latter; Table 5.15). Glucose-6-phosphate dehydrogenase (G6PDH), a gene engaged in xenobiotic biotransformation through production of nicotinamide adenine dinucleotide phosphate (NADPH), with subsequent roles in antioxidant defense, was up-regulated in 8-100 compared to the remaining stations (Winzer et al., 2001). Previous studies have demonstrated G6PDH inactivation upon chronic exposure to contaminants

in flounder species, a trend that does not appear to be occurring at station 8-100 (Van Noorden et al., 1997; Winzer et al., 2001).

Several genes associated with protein ubiquitination were up-regulated at station 8-100 compared to station 31-150, including the E3 ubiquitin-protein ligases MSL2, NEURL1, and TRIM8, transcription factor BACH1, cytokine inducible SH2 containing protein (CISH), and suppressor of cytokine signaling 3 (SOCS3; Table 5.15). Induction of protein ubiquitination and protein degradation pathways has been documented after exposure to PAHs in fish, presumably in order to clear cells affected by the oxidative damage incurred from production of reactive metabolites (Song et al., 2019). As these genes are also generally down-regulated at station 31-150 compared to station 36-150, and no differences are observed between stations 8-100 and 36-150, a relative down-regulation of protein degradation may be occurring at station 31-150. Biomarker data, however, suggest relatively higher levels of lipid peroxidation (MDA), liver damage (SDH) and genotoxicity (SumNA) at station 31-150 compared to station 8-100, suggesting fish at this station may be experiencing oxidative damage.

Recent transcriptomics research has demonstrated alterations in expression of genes associated with circadian rhythm in animals exposed to contaminants (Labaronne et al., 2017; Rhee et al., 2014). This may be due to the role of AHR in both circadian regulation for homeostatic balance and xenobiotic metabolism (Anderson et al., 2013; Esser et al., 2009). In this study, circadian rhythm-related genes circadian-associated transcriptional repressor (CIART), fatty acid desaturase (FAD6), and period circadian protein homolog (PER1) were comparatively up-regulated at station 8-100 compared to station 36-150 and both FAD6 and nuclear factor interleukin 3 regulated protein (NFIL3) were up-regulated at 8-100 compared to 31-150 (Table 5.16). Both CIART and PER1 were also up-regulated at 31-150 compared to 36-

150. It is possible the up-regulated genes are related to xenobiotic metabolism at stations 8-100 and 31-150, although further research would be needed into the functional significance of these pathways in demersal fish.

Several transcription factors and solute carriers were comparatively up-regulated in fish from 8-100 compared to those from 31-150 and 36-150 (Table 5.17). Xenobiotic-related transcription factor genes up-regulated at 8-100 include JunB, JunD, and Kruppel-like transcription factor 9 (KLF9). Jun transcription factors have been associated with oil exposure and biotransformation, while KLF9 is associated with hepatic repair (Andersen et al., 2015; Meixner et al., 2010). Nearly all annotated transcription factor genes were comparatively down-regulated at station 31-150 compared to 36-150. Solute carriers (SLCs) have importance in xenobiotic transport, particularly in hepatic uptake of materials (Lee et al., 2018; Keith B. Tierney et al., 2013). Several SLC genes were comparatively up-regulated at station 8-100 compared to 31-150, which may be related to enhanced xenobiotic transport (Table 5.17).

5.6 Conclusions

Interpretation of the results of this field-based transcriptomics study were complicated by the lack of a true control, as all fish experienced some exposure to PAHs as documented in their bile and liver tissue. In addition, few conclusive statements may be extrapolated about gene expression at a station overall, as a single time point of expression was observed in a limited number of individuals. However, broad generalizations could be made, which may warrant further study.

Fish collected from station 8-100, a location likely impacted by the *DWH* spill, were observed to have unique patterns of metabolic gene expression, according to both the frequency of the biological function GO term and analysis of annotated genes frequently cited in relevant

literature. While this shift may be due to compensatory change with xenobiotic exposure, differences may also be due to plausible variation in prey item or quality among the geographically diverse stations examined. The down-regulation of reproductive genes at station 8-100 would be better explored by sampling individuals caught within the Golden Tilefish spawning season and paired with histological screening of gonadal tissue for confirmation of the reproductive stage. Increased levels of ubiquitination, transcription factors, and solute carriers at station 8-100 suggests active processing of xenobiotics and clearing of oxidative damage, which may explain the lack of significant accumulation of PAH in the livers of these fish, despite recent PAH exposure indicated by elevated biliary concentrations.

Gene expression patterns at station 31-150 indicated possible immunosuppression. While several genes associated with xenobiotic metabolism and clearance of compromised cells were down-regulated at this station, biomarker data suggested ongoing oxidative stress. Although these fish had significantly higher levels of biliary B(a)P than others in this study, which may contribute to these findings, it is also possible that they are experiencing greater physiological disruption resulting from some other unevaluated stressor.

This study demonstrated that differential gene expression patterns could be observed between field locations by pooling individual fish. When considering these data in relation to PAH exposure, the most prominent gene groups for further research include those associated with lipid metabolism, oxidative stress and clearance of damaged cells, the immune response, and reproduction.

5.7 Tables

Table 5.1 Sampling station data.

Station	Latitude	Longitude	Depth (m)	Temp. (°C)	Date
8-100	29.7491	-87.0919	218.66	12.90	8/24/2015
31-150	19.5656	-92.7211	233.52	14.60	9/23/2015
36-150	23.7853	-87.3905	301.00	14.18	8/7/2016

Table 5.2: Raw sequence data.

Sample	Raw Sequences (#)	Mean Sequence Length (bp)	%GC
8-100-028_R1	39,228,576	151	52
8-100-028_R2	39,228,576	151	52
8-100-031_R1	26,535,515	151	53
8-100-031_R2	26,535,515	151	54
8-100-035_R1	24,948,795	151	53
8-100-035_R2	24,948,795	151	54
8-100-047_R1	25,411,025	151	54
8-100-047_R2	25,411,025	151	54
8-100-051_R1	42,679,987	151	52
8-100-051_R2	42,679,987	151	53
31-150-002_R1	27,934,028	151	53
31-150-002_R2	27,934,028	151	53
31-150-003_R1	28,262,021	151	53
31-150-003_R2	28,262,021	151	53
31-150-004_R1	25,323,526	151	53
31-150-004_R2	25,323,526	151	53
31-150-005_R1	27,864,530	151	54
31-150-005_R2	27,864,530	151	55
31-150-006_R1	30,443,388	151	54
31-150-006_R2	30,443,388	151	54
36-150-008_R1	27,021,873	151	53
36-150-008_R2	27,021,873	151	53
36-150-009_R1	32,101,307	151	53
36-150-009_R2	32,101,307	151	53
36-150-014_R1	28,259,685	151	53
36-150-014_R2	28,259,685	151	53
36-150-025_R1	31,124,906	151	54
36-150-025_R2	31,124,906	151	54
36-150-027_R1	26,317,149	151	53
36-150-027_R2	26,317,149	151	54

Table 5.3: Results of the trimming method used in Trimmomatic that resulted in acceptable FastQC metrics for each sequence.

Sample	Trimmed Sequence (#)	Sequence Length (bp)	%GC	Trim method
8-100-028_R1	21,068,216	36-151	52	Immunoclip: Truseq3, Leading:3, Trailing:3, Slidingwindow:4:15, MinLen:36
8-100-028_R2	21,068,216	36-151	52	Immunoclip: Truseq3, Leading:3, Trailing:3, Slidingwindow:4:15, MinLen:36
8-100-031_R1	14,577,453	150-151	53	Immunoclip:Truseq3: Leading:3, Trailing:3, Minlen:36
8-100-031_R2	14,577,453	133-151	53	Immunoclip:Truseq3: Leading:3, Trailing:3, Minlen:36
8-100-035_R1	11,608,730	36-151	53	Immunoclip: Truseq3, Leading:3, Trailing:3, Slidingwindow:4:15, MinLen:36
8-100-035_R2	11,608,730	36-151	53	Immunoclip: Truseq3, Leading:3, Trailing:3, Slidingwindow:4:15, MinLen:36
8-100-047_R1	14,128,564	150-151	53	Immunoclip:Truseq3: Leading:3, Trailing:3, Minlen:36
8-100-047_R2	14,128,564	133-151	53	Immunoclip:Truseq3: Leading:3, Trailing:3, Minlen:36
8-100-051_R1	20,273,616	40-151	52	Immunoclip:Truseq3, Leading:3, Trailing:20, Slidingwindow:4:20, Minlen:40
8-100-051_R2	20,273,616	40-151	53	Immunoclip:Truseq3, Leading:3, Trailing:20, Slidingwindow:4:20, Minlen:40
31-150-002_R1	15,213,797	150-151	52	Immunoclip:Truseq3: Leading:3, Trailing:3, Minlen:36
31-150-002_R2	15,213,797	133-151	53	Immunoclip:Truseq3: Leading:3, Trailing:3, Minlen:36
31-150-003_R1	15,112,414	36-151	53	Immunoclip: Truseq3, Leading:3, Trailing:3, Slidingwindow:4:15, MinLen:36
31-150-003_R2	15,112,414	36-151	53	Immunoclip: Truseq3, Leading:3, Trailing:3, Slidingwindow:4:15, MinLen:36
31-150-004_R1	14,104,750	150-141	53	Immunoclip:Truseq3: Leading:3, Trailing:3, Minlen:36
31-150-004_R2	14,104,750	133-151	53	Immunoclip:Truseq3: Leading:3, Trailing:3, Minlen:36
31-150-005_R1	13,584,615	36-151	54	Immunoclip: Truseq3, Leading:3, Trailing:3, Slidingwindow:4:15, MinLen:36
31-150-005_R2	13,584,615	36-151	54	Immunoclip: Truseq3, Leading:3, Trailing:3, Slidingwindow:4:15, MinLen:36

Table 5.3 (continued)

31-150-006_R1	15,596,775	150-151	54	Immunoclip:Truseq3: Leading:3, Trailing:3, Minlen:36
31-150-006_R2	15,596,775	133-151	54	Immunoclip:Truseq3: Leading:3, Trailing:3, Minlen:36
36-150-008_R1	13,862,624	36-151	52	Immunoclip:Truseq3, Leading:3, Trailing:15, Slidingwindow:3:15, Minlen:36
36-150-008_R2	13,862,624	36-151	52	Immunoclip:Truseq3, Leading:3, Trailing:15, Slidingwindow:3:15, Minlen:36
36-150-009_R1	17,634,618	150-151	52	Immunoclip:Truseq3: Leading:3, Trailing:3, Minlen:36
36-150-009_R2	17,634,618	133-151	53	Immunoclip:Truseq3: Leading:3, Trailing:3, Minlen:36
36-150-014_R1	15,723,037	150-151	53	Immunoclip:Truseq3: Leading:3, Trailing:3, Minlen:36
36-150-014_R2	15,723,037	133-151	53	Immunoclip:Truseq3: Leading:3, Trailing:3, Minlen:36
36-150-025_R1	14,241,994	36-144	53	Immunoclip:Truseq3:Headcrop:7, Trailing:15:Slidingwindow:4:20, minlen:36
36-150-025_R2	14,241,994	36-144	53	Immunoclip:Truseq3:Headcrop:7, Trailing:15:Slidingwindow:4:20, minlen:36
36-150-027_R1	13,707,336	150-151	53	Immunoclip:Truseq3: Leading:3, Trailing:3, Minlen:36
36-150-027_R2	13,707,336	133-151	53	Immunoclip:Truseq3: Leading:3, Trailing:3, Minlen:36

Table 5.4 Statistics for Trinity assemblies and Bowtie2 alignments.

Sample	Trinity transcripts (#)	Trinity 'genes' (#)	%GC	Contig stats based on only longest isoform per Trinity 'gene'								Bowtie Alignment Rate (%)
				N10	N20	N30	N40	N50	Median	Average	Total assembled bases (#)	
8-100-028	165,402	146,898	45.96	3151	1995	1310	899	633	331	533.04	78,302,504	97.37
8-100-031	86,027	79,581	47.17	2570	1665	1142	819	608	328	510.87	40,655,784	96.56
8-100-035	117,791	107,013	46.46	2244	1364	929	670	509	314	465.27	49,789,758	96.83
8-100-047	118,827	108,607	46.38	2566	1622	1098	781	579	327	502.72	54,599,206	95.99
8-100-051	195,155	172,921	45.84	2945	1774	1142	779	571	327	507.55	87,765,462	97.31
31-150-002	130,822	118,016	46.21	2684	1678	1103	763	560	318	493.25	58,211,359	95.95
31-150-003	97,708	89,538	46.59	2867	1896	1323	940	684	339	547.12	48,988,395	98
31-150-004	102,720	93,469	46.79	2640	1728	1182	842	617	328	516.96	48,319,730	96.38
31-150-005	93,435	86,256	47.39	2200	1347	906	657	501	307	456.72	39,394,478	97.56
31-150-006	153,248	136,842	46.51	2237	1358	898	640	483	303	450.85	61,695,443	94.45
36-150-008	109,145	100,370	46.46	2711	1691	1136	794	586	328	508.66	51,054,613	97.38
36-150-009	158,629	141,408	46.31	2706	1691	1104	771	569	330	506.07	71,562,336	96.16
36-150-014	126,561	115,456	46.53	2803	1790	1205	842	619	334	524.15	60,516,750	95.81
36-150-025	122,824	110,478	46.51	2727	1719	1147	806	593	324	508.45	56,172,035	97.18
36-150-027	91,876	84,991	46.95	2410	1505	1019	723	540	316	480.76	40,860,049	95.74
Master Assembly	491,431	394,502	44.43	3643	2210	1424	968	690	342	560.17	220,988,747	NA

Table 5.5 Annotation statistics for differentially expressed (DE) genes between stations.

Comparison	# DE genes	% with associated gene ontology terms		
		Biological function	Molecular function	Cellular component
8-100 v 31-150	598	58.39	72.48	33.56
8-100 v 36-150	272	56.62	74.63	32.72
31-150 v 36-150	605	53.88	68.76	35.21

Table 5.6 The ten most frequent gene ontology biological function terms associated with annotated differentially expressed (DE) genes (FDR < 0.05), between stations.

Group	GO: Biological Function	% DE Genes
8-100 vs. 36-150	GO:0055114 oxidation-reduction process	6.99
	GO:0006355 regulation of transcription, DNA-templated	5.88
	GO:0008152 metabolic process	4.04
	GO:0043401 steroid hormone mediated signaling pathway	3.68
	GO:0055085 transmembrane transport	3.68
	GO:0006508 proteolysis	3.31
	GO:0006468 protein phosphorylation	2.57
	GO:0007186 G-protein coupled receptor signaling pathway	2.57
	GO:0006629 lipid metabolic process	2.21
	GO:0006813 potassium ion transport	1.84
8-100 vs. 31-150	GO:0006355 regulation of transcription, DNA-templated	7.05
	GO:0055114 oxidation-reduction process	5.54
	GO:0006468 protein phosphorylation	4.19
	GO:0008152 metabolic process	3.36
	GO:0007186 G-protein coupled receptor signaling pathway	2.85
	GO:0055085 transmembrane transport	2.85
	GO:0006508 proteolysis	2.35
	GO:0043401 steroid hormone mediated signaling pathway	2.18
	GO:0007165 signal transduction	1.85
	GO:0006955 immune response	1.68
31-150 vs. 36-150	GO:0006355 regulation of transcription, DNA-templated	8.10
	GO:0055085 transmembrane transport	4.30
	GO:0006468 protein phosphorylation	3.64
	GO:0055114 oxidation-reduction process	3.47
	GO:0006508 proteolysis	3.31
	GO:0007165 signal transduction	2.15
	GO:0007186 G-protein coupled receptor signaling pathway	1.98
	GO:0043401 steroid hormone mediated signaling pathway	1.82
	GO:0006955 immune response	1.65
	GO:0006357 regulation of transcription from RNA polymerase II promoter	1.49

Table 5.7 The ten most frequent gene ontology molecular function terms associated with annotated differentially expressed (DE) genes (FDR < 0.05), between stations.

Group	GO: Molecular Function	% DE Genes
8-100 vs. 36-150	GO:0005515 protein binding	14.71
	GO:0003824 catalytic activity	5.88
	GO:0003677 DNA binding	5.51
	GO:0005524 ATP binding	5.51
	GO:0005509 calcium ion binding	5.15
	GO:0003700 DNA binding transcription factor activity	4.41
	GO:0008270 zinc ion binding	4.41
	GO:0003707 steroid hormone receptor activity	4.04
	GO:0016491 oxidoreductase activity	4.04
	GO:0043565 sequence-specific DNA binding	3.31
8-100 vs. 31-150	GO:0005515 protein binding	17.28
	GO:0003677 DNA binding	6.88
	GO:0005524 ATP binding	6.04
	GO:0003700 DNA binding transcription factor activity	5.87
	GO:0008270 zinc ion binding	5.37
	GO:0003824 catalytic activity	4.53
	GO:0004672 protein kinase activity	4.19
	GO:0005509 calcium ion binding	3.19
	GO:0043565 sequence-specific DNA binding	2.85
	GO:0016491 oxidoreductase activity	2.68
31-150 vs. 36-150	GO:0005515 protein binding	16.20
	GO:0003677 DNA binding	7.27
	GO:0005524 ATP binding	6.78
	GO:0003700 DNA binding transcription factor activity	6.28
	GO:0003676 nucleic acid binding	4.96
	GO:0008270 zinc ion binding	4.63
	GO:0004672 protein kinase activity	3.47
	GO:0005509 calcium ion binding	3.14
	GO:0003824 catalytic activity	2.64
	GO:0004252 serine-type endopeptidase activity	2.48

Table 5.8 The ten most frequent gene ontology cellular component terms associated with annotated differentially expressed (DE) genes (FDR < 0.05), between stations.

Group	GO: Cellular Component	% DE Genes
8-100 vs. 36-150	GO:0016021 integral component of membrane	9.19
	GO:0016020 membrane	7.35
	GO:0005634 nucleus	6.25
	GO:0005576 extracellular region	2.94
	GO:0005615 extracellular space	2.57
	GO:0005737 cytoplasm	2.21
	GO:0005783 endoplasmic reticulum	1.10
	GO:0005856 cytoskeleton	1.10
	GO:0005891 voltage-gated calcium channel complex	0.74
	GO:0000015 phosphopyruvate hydratase complex	0.37
8-100 vs. 31-150	GO:0016021 integral component of membrane	9.40
	GO:0005634 nucleus	6.04
	GO:0016020 membrane	5.37
	GO:0005576 extracellular region	3.86
	GO:0005615 extracellular space	2.52
	GO:0005737 cytoplasm	1.68
	GO:0005622 intracellular	0.84
	GO:0005578 proteinaceous extracellular matrix	0.67
	GO:0005577 fibrinogen complex	0.50
	GO:0005777 peroxisome	0.50
31-150 vs. 36-150	GO:0016021 integral component of membrane	7.60
	GO:0016020 membrane	6.12
	GO:0005634 nucleus	5.62
	GO:0005576 extracellular region	4.63
	GO:0005615 extracellular space	2.98
	GO:0005737 cytoplasm	2.15
	GO:0005622 intracellular	0.99
	GO:0005783 endoplasmic reticulum	0.83
	GO:0008076 voltage-gated potassium channel complex	0.66
	GO:0005578 proteinaceous extracellular matrix	0.50

Table 5.9 Relative up-regulation (red) and down-regulation (green) of differentially expressed genes (FDR < 0.05) associated with xenobiotic metabolism, between stations. Colors display level of gene expression at the first listed station, compared to the second. For example, CYP450 2G1 is up-regulated at 8-100 compared to 36-150.

Subcategory	Gene	8-100 vs 36-150	8-100 vs 31-150	31-150 vs 36-150
Phase I	CYP450 19A2			
	CYP450 2G1			
	CYP450 2J6			
	SLC22A2			
	SLCO1C1			
Phase II	GSTM3			
	GSTZ1			
	UGT2A1			
	UGT2B15			
	UGT2B20			
	UGT2C1			
Phase III	ABC2			
	ABCC10			
	CYP7A1			
	MATE1			
Heavy Metals	HIP			
Other	G6PC			
	G6PDH			
	PPARA			

Table 5.10 Relative up-regulation (red) and down-regulation (green) of differentially expressed genes (FDR < 0.05) associated with lipid metabolism, between stations. Colors display level of gene expression at the first listed station, compared to the second. For example, ACAA is down-regulated at 8-100 compared to 36-150.

Gene	8-100 vs 36-150	8-100 vs 31-150	31-150 vs 36-150
ACAA	Green	Green	Grey
ACLY	Green	Green	Grey
ACOT4	Grey	Green	Red
ACS	Green	Green	Grey
ACSBG2	Green	Green	Green
ACSF2	Green	Grey	Grey
ACSL3	Green	Grey	Grey
ADH3	Grey	Green	Grey
APMAP	Green	Green	Grey
BAL	Grey	Green	Red
DEGS1	Grey	Red	Grey
ELOVL4	Green	Green	Grey
ELOVL6	Green	Green	Grey
FA2H	Red	Grey	Red
FAAH	Green	Green	Grey
GPCD1	Grey	Green	Red
HL	Green	Grey	Green
LIPH	Grey	Red	Green
LPIN1	Green	Grey	Grey
LPL	Grey	Red	Green
MID1P1B	Green	Green	Red
MSMO1	Green	Green	Grey
PLA2	Green	Green	Grey
PLA2G12B	Grey	Green	Red
PLTP	Grey	Red	Green
PNPLA2	Red	Green	Grey
PPARA	Grey	Green	Red
SCD	Green	Green	Grey
SLC13A5	Red	Red	Grey

Table 5.11 Relative up-regulation (red) and down-regulation (green) of differentially expressed genes (FDR < 0.05) associated with glucose metabolism and release, between stations. Colors display level of gene expression at the first listed station, compared to the second. For example, APOAIV is up-regulated at 8-100 compared to 36-150.

Gene	8-100 vs 36-150	8-100 vs 31-150	31-150 vs 36-150
APOAIV	Red	Green	Red
CAP3C	Red	Red	Grey
CHAC1	Grey	Green	Green
CHST11	Grey	Grey	Green
CRYM	Grey	Green	Red
ENO1	Green	Grey	Green
G6PASE	Red	Red	Green
HLF	Red	Green	Red
KLF15	Grey	Red	Green
PFKL	Green	Grey	Green
PGK1	Green	Red	Grey
SLC2A2	Grey	Green	Grey
SULT6B1	Grey	Red	Green
UGGT1	Green	Grey	Grey

Table 5.12 Relative up-regulation (red) and down-regulation (green) of differentially expressed genes (FDR < 0.05) associated with cholesterol biosynthesis, between stations. Colors display level of gene expression at the first listed station, compared to the second. For example, DHCR24 is down-regulated at 8-100 compared to 36-150.

Gene	8-100 vs 36-150	8-100 vs 31-150	31-150 vs 36-150
APOB100	Grey	Green	Grey
APOE	Grey	Grey	Red
CYP7A1	Grey	Green	Red
DHCR24	Green	Green	Grey
MSMO1	Green	Green	Grey
PLTP	Grey	Red	Green
SLC13A5	Red	Red	Grey

Table 5.13 Relative up-regulation (red) and down-regulation (green) of differentially expressed genes (FDR < 0.05) associated with reproduction, between stations. Colors display level of gene expression at the first listed station, compared to the second. For example, ER α is down-regulated at 8-100 compared to 36-150.

Gene	8-100 vs 36-150	8-100 vs 31-150	31-150 vs 36-150
ER α	Green	Green	Green
Er β	Red	Red	Grey
GNRHR	Green	Grey	Green
GNRH3	Grey	Red	Green
INGHH	Grey	Red	Red
THRAA	Red	Grey	Grey
VTGAA	Green	Green	Grey
VTGAB	Green	Green	Grey
VTGB	Green	Green	Grey
VTGC	Green	Green	Grey
ZP4R	Green	Green	Grey
ZPBB	Green	Green	Grey

Table 5.14 Relative up-regulation (red) and down-regulation (green) of differentially expressed genes (FDR < 0.05) associated with immune response, between stations. Colors display level of gene expression at the first listed station, compared to the second. For example, C1S is down-regulated at 8-100 compared to 36-150.

Subcategory	Gene	8-100 vs 36-150	8-100 vs 31-150	31-150 vs 36-150
Complement	C1S	Green	Grey	Green
	C1R	Green	Grey	Green
	C1QC	Red	Grey	Grey
	C1Q4	Grey	Red	Green
	C1Q2	Grey	Red	Green
	C3	Red	Red	Green
	C4	Red	Red	Green
	C7	Grey	Grey	Green
	C8A	Grey	Red	Green
	C8B	Grey	Grey	Green
	C9	Grey	Green	Green
	CFB	Red	Red	Grey
	CFH	Grey	Red	Green
	CFI	Grey	Grey	Green
Antigen receptors	CD209	Grey	Grey	Green
	CD79B	Grey	Grey	Green
	HLAA	Red	Red	Green
	HLADQA1	Grey	Red	Grey
	HLADQB1	Red	Red	Green
	PIGR	Green	Grey	Grey
	RELB	Grey	Grey	Green
	RT1B	Grey	Green	Grey
	TLR2	Grey	Red	Green
	TLR3	Red	Red	Grey
Antibacterial, antiviral	CH25H	Grey	Grey	Red
	GIG1	Grey	Red	Green
	GVINP1	Green	Grey	Green
	HAMP	Green	Grey	Green
	IFN1A	Grey	Red	Green
	IRF3	Grey	Grey	Green
	IRF5	Grey	Grey	Green
	TF	Grey	Red	Green
Inflammation	ATG16L1	Red	Red	Grey
	CRP	Grey	Red	Grey
	FGB	Grey	Red	Grey
	NFKBIZ	Grey	Grey	Red

Table 5.14 (Continued)

Inflammation (Continued)	PPARA			
	SAA			
	SAP			
	VWA1			
	VWA7			
	VWC2			
Cytokines	API			
	CISH			
	ILR1R1			
	IL1RAPL1			
	IL6R			
	IL12RB2			
	IL34			
	IRAK4			
	SOCS3			
Chemokines	ACKR3			
	CCL20			
	CD97			
	CD99			
	CMKLR			
	CXCL10			
	FGA			
	FGG			
	Blood regulation	A2M		
AGT				
ANGPTL4				
ECE1				
ENPP2				
ET1				
ET2				
IFI44L				
IRF2BP2				
KLF3				
NKIRAS1				
PAI1				
THBS1				
URIIR				

Table 5.15 Relative up-regulation (red) and down-regulation (green) of differentially expressed genes (FDR < 0.05) associated with oxidative stress and debris clearance, between stations. Colors display level of gene expression at the first listed station, compared to the second. For example, ATG16L1 is up-regulated at 8-100 compared to 36-150.

Subcategory	Gene	8-100 vs 36-150	8-100 vs 31-150	31-150 vs 36-150
Apoptosis	AIF1			
	AEN			
	AP1			
	ATG16L1			
	BNIP3L			
	CHAC1			
	CHST11			
	SIVA1			
Negative regulation, resistance, clearance	ACKR3			
	CIQ2			
	CIQC			
	GAL1			
	JUND			
	NEDD4			
	NFATC3			
Ubiquitination	BACH1			
	BTF3			
	CBLB			
	CHIP			
	CISH			
	MSL2			
	NEURL1			
	RING1			
	RNF19B			
	SOCS3			
	TRIM8			
	UBB			
	UBC			
	UBL3			
Antioxidant	APOA4			
	COX			
	G6PDH			
	GPX3			
	GPX4			
	GSTM3			

Table 5.15 (Continued)

Antioxidant (Continued)	GSTZ1			
	KLF9			
	SLC25A33			
Stress response, tissue repair	BHMT			
	CRJ1B			
	CRYM			
	FGF1			
	GADD45			
	JUNB			
	JUNDM2			
	KLF15			
	TCM2			
	TXNIP			

Table 5.16 Relative up-regulation (red) and down-regulation (green) of differentially expressed genes (FDR < 0.05) associated with circadian rhythm, between stations. Colors display level of gene expression at the first listed station, compared to the second. For example, CIART is up-regulated at 8-100 compared to 36-150.

Gene	8-100 vs 36-150	8-100 vs 31-150	31-150 vs 36-150
CIART	Red	Grey	Red
CLOCK	Grey	Grey	Green
FAD6	Red	Red	Grey
NFIL3	Grey	Red	Grey
PER1	Red	Green	Red
RELB	Grey	Grey	Green

Table 5.17 Relative up-regulation (red) and down-regulation (green) of differentially expressed genes (FDR < 0.05) associated with transcription factors and solute carriers, between stations. Colors display level of gene expression at the first listed station, compared to the second. For example, BTF3 is up-regulated at 8-100 compared to 36-150.

Subcategory	Gene	8-100 vs 36-150	8-100 vs 31-150	31-150 vs 36-150
Transcription factors	API		Red	Green
	BACH1		Red	Green
	BTF3	Red		Green
	HDAC4			Green
	HDAC10			Green
	KLF9	Red		
	JUNB		Red	Green
	JUND		Red	Green
	MATF		Red	Green
	SOX6			Red
Solute carriers	SLC3A2		Red	
	SLC7A2	Green		
	SLC7A3		Red	Green
	SLC11A2		Red	
	SLC13A2		Green	Red
	SLC13A5	Red	Red	
	SLC17A9	Green		
	SLC23A2	Green	Red	
	SLC22A2		Red	Green
	SLC25A33		Red	Green
	SLC25A39			Red
	SLC25A48		Red	Green
	SLC26A6			Red
	SLCO1C1			Red

5.8 Figures



Figure 5.1: Map of sampling locations, including 8-100 (DWH), 31-150 (Campeche Bay) and 36-150 (Yucatan Peninsula). Yellow dots indicate the presence of active oil and gas extraction platforms.

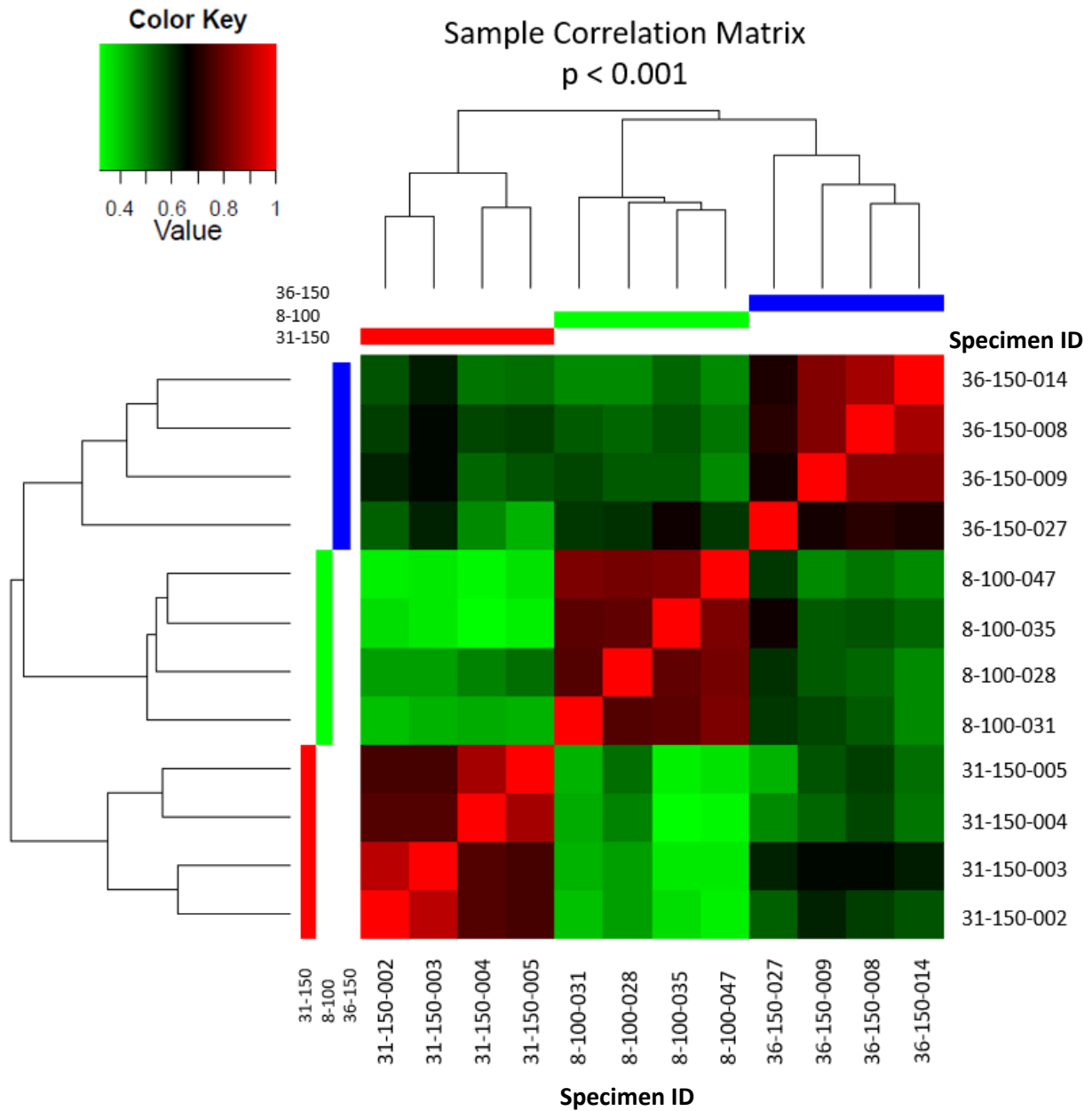


Figure 5.2: Heat map of differentially expressed genes ($p < 0.001$) in individuals from various sampling stations (Fig. 5.1) based upon TMM-normalized transcripts, after outlier removal.

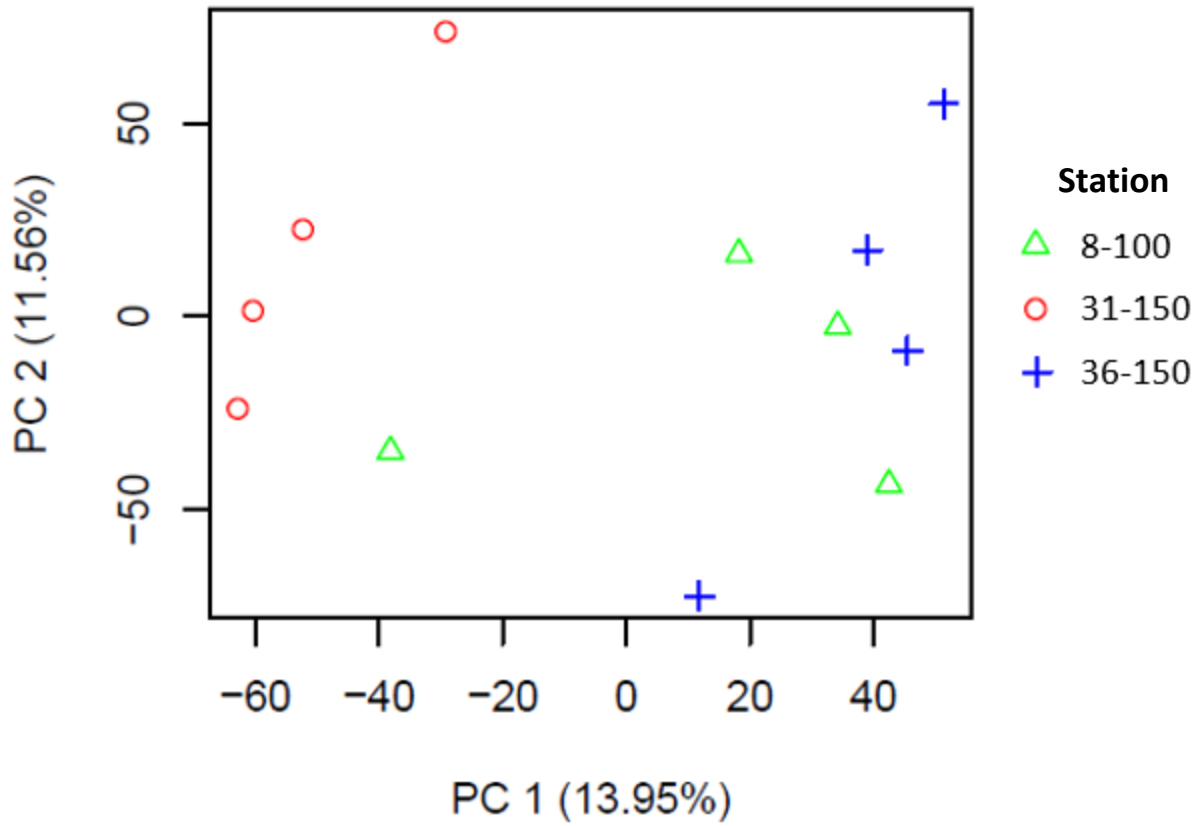


Figure 5.3 Cluster analysis of differentially expressed genes ($p < 0.001$) in individuals from various stations (Fig. 5.1) based upon TMM-normalized transcripts, after outlier removal.

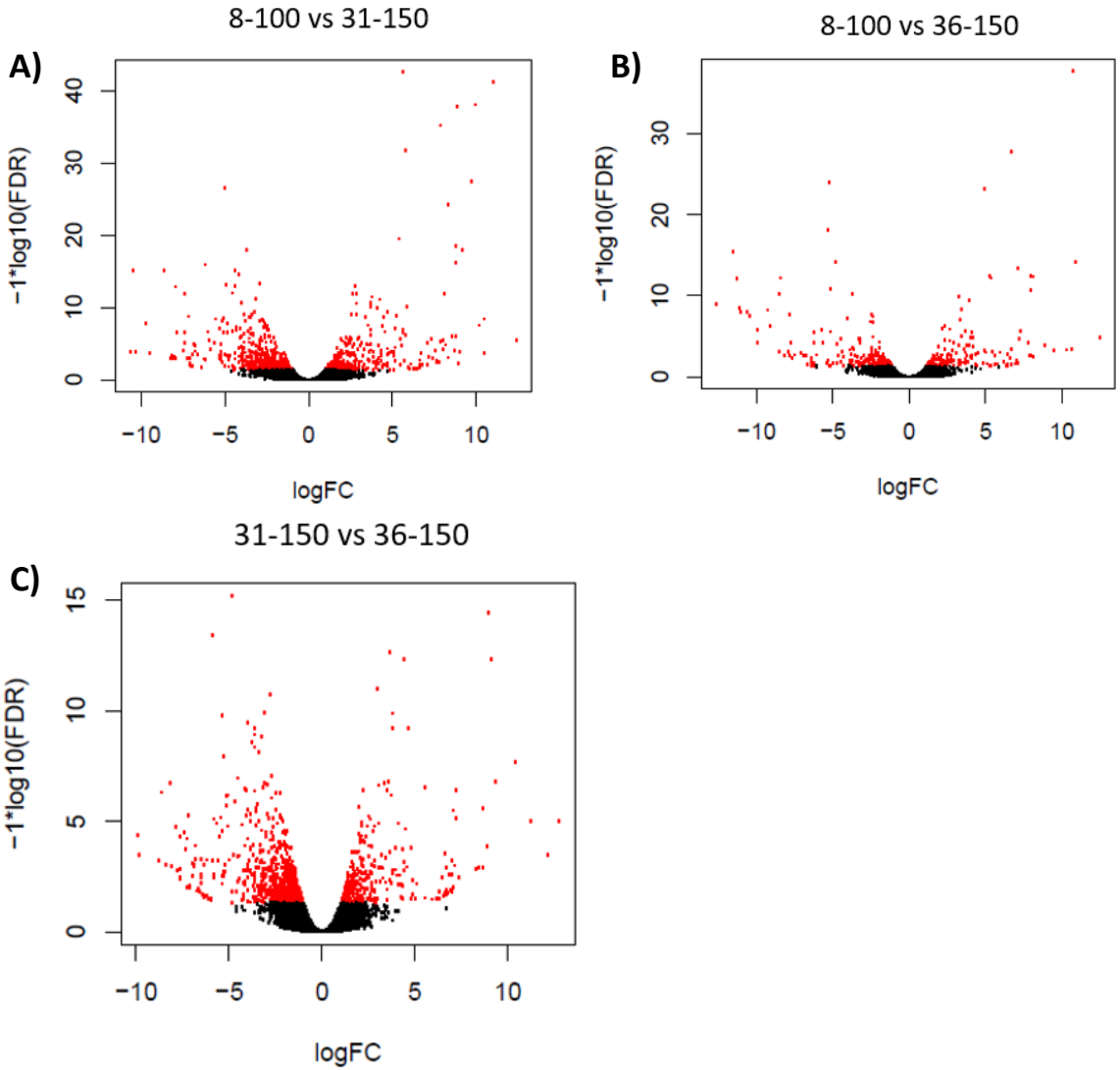


Figure 5.4 Volcano plots displaying the significance (false discover rate; FDR) versus magnitude (fold change; FC) of differential gene expression (FDR < 0.05) between stations: A) 8-100 versus 31-150, B) 8-100 versus 36-150, and C) 31-150 vs 36-150.

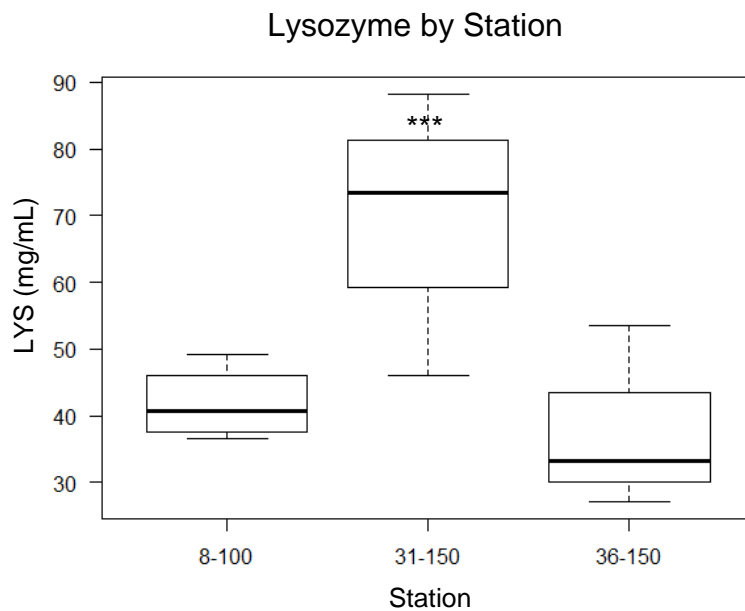
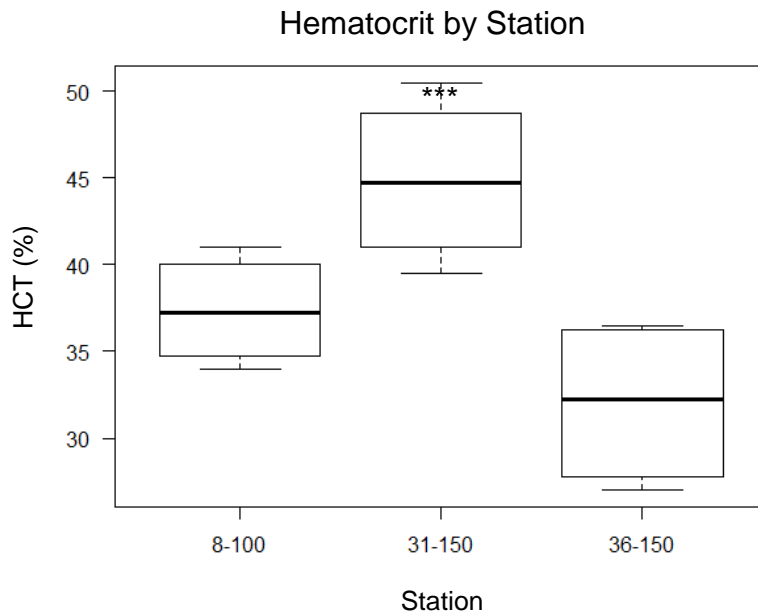


Figure 5.5 Immune system biomarkers that varied significantly between stations, following outlier removal. Station 31-150 had significantly ($p = 0.006$, ***) elevated HCT compared to 36-150 and significantly elevated LYS compared to station 8-100 ($p = 0.026$, **) and 36-150 ($p = 0.011$, **).

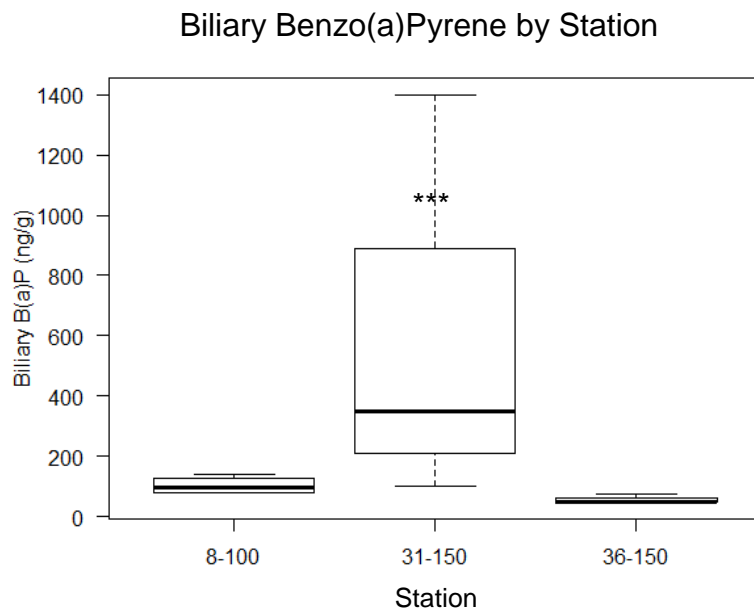
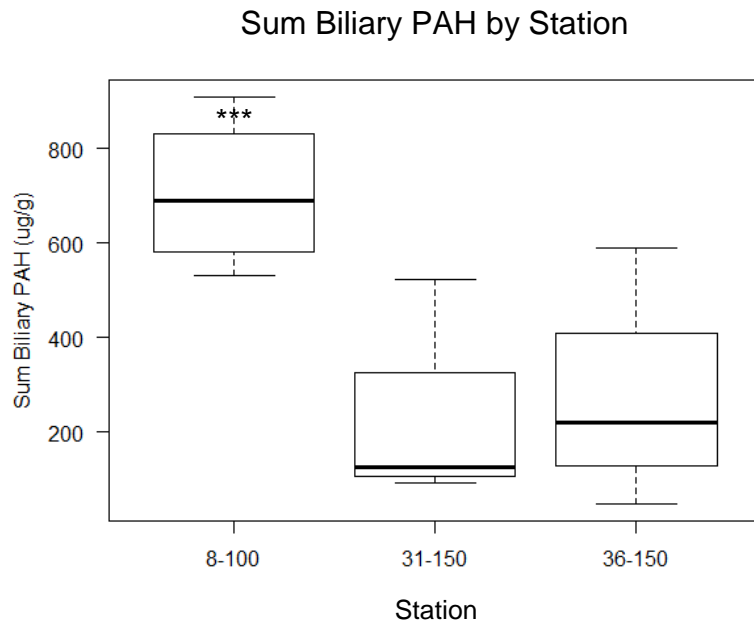


Figure 5.6 Biliary PAH values that varied significantly between stations, following outlier removal. Station 8-100 had significantly elevated sum biliary PAH levels compared to 31-150 ($p = 0.018$, **) and 36-150 ($p = 0.032$, **). Station 31-150 had significantly elevated biliary B(a)P compared to the remaining stations ($p = 0.012$, **).

CHAPTER SIX: CONCLUSIONS

6.1 Summary of dissertation

The objectives of this study were to 1) establish baseline biomarker indices for Golden Tilefish (*Lopholatilus chamaeleonticeps*) and Red Snapper (*Lutjanus campechanus*) in the Gulf of Mexico (GoM); 2) examine GoM-wide variability of biomarker expression in these fishes; 3) determine whether biomarker expression could be correlated with polycyclic aromatic hydrocarbon (PAH) body burdens; 4) evaluate whether fish caught in the vicinity of the *Deepwater Horizon* (DWH) spill exhibited an altered biomarker response in comparison to fish from other parts of the GoM; and 5) to construct a Golden Tilefish transcriptome and determine whether patterns of differential gene expression were observed between different geographic regions, which may be beneficial targets for future health assessments following PAH contamination events.

In Chapter II, the first reference intervals for a number of oxidative stress and immune system biomarkers were successfully created for Golden Tilefish and Red Snapper. Because these intervals were created from geographically diverse specimens, they are broadly applicable to all fish of the same species, reproductive state, and size range throughout the GoM. While additional sampling efforts would improve the specificity of these intervals, they provide a meaningful representation of biomarker expression levels for 95% of a presumably healthy population, acknowledging persistent background contamination sources prevalent throughout

the ecosystem. Statistically significant differences in reference intervals for genotoxicity (sum erythrocyte nuclear abnormalities) and antioxidant response (superoxide dismutase) between species may be explained by known increased contaminant exposure in Golden Tilefish relative to Red Snapper, due to the close association Tilefish have with contaminated sediments. This study added utility to a suite of economical and practical indicators that can be routinely evaluated in field-caught fish when immediate bleeding is possible, and samples may be stored at -20°C prior to returning to shore.

In Chapter III, Golden Tilefish biomarker responses were evaluated spatially, temporally, and in relation to PAH body burdens. Golden Tilefish have historical records of mercury and PAH exposure in the GoM, attributable to their life history of benthic association, consumption of benthic prey, and bioturbation of muddy sediments. Coupled with site fidelity as adults, this species provides an excellent model for the evaluation of physiological effects of chronic contamination and possible health responses to additional pulse pollution events. While Golden Tilefish were expected to have varying levels of different contaminants throughout the GoM, it was anticipated that those fish caught in the vicinity of the DWH spill would have unique health signatures, given documented settling and absorption of contaminants into the sediments. Contrary to literature-documented effects of PAH exposure on oxidative stress biomarkers, weak but statistically significant negative correlations were consistently observed between sum liver PAH and superoxide dismutase, sorbitol dehydrogenase, and sum erythrocyte nuclear abnormalities in the GoM-wide dataset. Despite higher PAH levels in fish from the north central GoM, their oxidative stress biomarkers also failed to respond as anticipated.

Coupled with reduced liver lipid fraction in specimens with elevated contaminant burden, these data suggest a possible compensatory metabolism strategy in some northern GoM Tilefish,

whereby energy is released from lipid stores to aid in cellular repair, limiting oxidative damage to lipids, proteins, and DNA upon chronic contamination. This is especially relevant to fish from the north central stations, where genotoxicity and antioxidant levels were comparatively elevated in 2015 compared to 2017, when the liver lipid fraction was notably reduced. Immune system biomarkers did not appear to be uniformly affected by PAH exposure, GoM-wide. Despite some compelling patterns, correlations between biomarker expression and biliary and liver PAH levels were weak and variable, suggesting multiple influences on biomarkers, as one may expect in natural ecosystems.

Using a similar approach to Chapter III, in Chapter IV Red Snapper biomarker responses and their relationship to PAH exposure was compared between specimens from the north central GoM caught during repeat sampling in 2015 and 2017 and those from the northwestern GoM. For this study, fish caught from the southwestern GoM, Campeche Bay, and the Yucatan Peninsula were excluded, due to low sample numbers. Relatively low levels of PAH contamination were observed in all specimens included in this chapter, however, no significant differences in biomarker response were observed in animals caught within the hypothesized footprint of the DWH spill and those from the northwestern GoM. Immune system biomarker response was more variable than oxidative stress response across sampling stations, years, and geographic zones, however, this did not appear to be statistically related to PAH exposure, rather, it was likely due to external environmental or physiological factors. While sex differences were observed, particularly in specimens from the 2017 north central GoM sampling event, this was likely attributable to specimen collection during the spawning season, with subsequent impacts on female fish physiology, lipid levels, and potential contaminant offloading

to eggs. Overall, Red Snapper did not appear to have lasting effects from possible exposure to the DWH spill or to background contamination in the GoM.

In Chapter V, the first *de novo* assembly of the Golden Tilefish transcriptome was performed, differential gene expression patterns of fish pooled by geographic station was explored, and possible correlations with PAH exposure and biomarker response were evaluated. Hundreds of annotated genes varied in expression between the De Soto Canyon (influenced by DWH, oil extraction activity, and natural seeps), Campeche Bay (influenced by the *Ixtoc I* spill, oil extraction activity, and natural seeps), and the Yucatan Peninsula (possible natural seep exposure, near heavy shipping traffic). Surprisingly, while 598 genes were differentially expressed between fish from the De Soto Canyon and Campeche Bay, only 272 genes were differentially expressed between the De Soto Canyon and the Yucatan Peninsula, a site with no known oil extraction activity or history of oil spills. Gene expression was also highly variable between Campeche Bay and the Yucatan Peninsula, with 605 differentially expressed genes between them. While these stations were sampled one year apart, no significant climatic variation or pollution events occurred to contribute to these observed discrepancies. Similarities between the Yucatan Peninsula and the De Soto Canyon may underscore unique patterns of expression in Campeche Bay.

Fish from the De Soto Canyon displayed indicators of an altered metabolic response, with reduced genes associated with lipid metabolism and enhanced glycolysis when compared to specimens from other stations, however, these data could not be conclusively linked to oil exposure given the lack of information regarding prey quantity and nutritional quality between stations. The relative suppression of reproduction-related genes in fish from the De Soto Canyon may, however, be attributed to oil exposure, given the capture of all specimens at approximately

the same point in the spawning cycle. Genes associated with response to oxidative stress, apoptosis, ubiquitination, and cell survival were also elevated in De Soto Canyon fish, suggesting potential protective responses to ongoing xenobiotic metabolism. Fish from the Campeche Bay station displayed evidence of relative immunosuppression and down-regulation of cellular protective mechanisms, despite PAH exposure and biomarker evidence of oxidative-stress induced damage. Differences in expression between stations may be attributable to varying lifetime exposures of different chemical contaminants and PAH sources. Overall, these data suggest an application for RNA sequencing (RNA-seq) in exploratory data analysis in field-caught fish and provide support for additional examination of pathways involved with lipid and carbohydrate metabolism, oxidative stress and clearance of cellular damage, and reproduction for PAH-related work in wild-caught teleosts.

6.2 Implications for future field studies

This study was the first to attempt a GoM-wide evaluation of baseline health in Golden Tilefish and Red Snapper. As such, valuable methodological insights were gained toward how to better construct studies and analyze future data, in the event of another large oil spill or significant pollution event in the survey region.

The interpretation of biomarkers in wild-caught specimens is inherently complicated, due to unknown life histories of contaminant exposure, the influence of unquantifiable stressors in the natural environment, and physiological fluctuations during the reproductive cycle. Given non-linear correlations between biomarker response and contaminant exposure, a multi-biomarker approach to examine physiological disruption is necessary. In non-model species, such studies can be difficult to achieve in a cost-effective manner, due to the lack of suitable reagents and the time required to develop species-specific reagents or reference intervals for

targets of interest. This study provides data for the utilization of several oxidative stress and immune system biomarkers that can be economically applied to non-model specimens, when immediate bleeding in the field and sample storage at -20°C is possible. It also proved that differential gene expression patterns could be explored by pooling small numbers of specimens from geographically distinct locations, in order to investigate novel targets for further research.

Future studies would benefit from sampling the same locations at multiple time points, to gain confidence in any observed biomarker trends. A minimum of three years of sampling is suggested, ideally with two events each year, both during and after the spawning cycle. While fishing a site does not guarantee adequate specimens will be caught, ideally ten individuals should be examined per site, to account for inter-individual variability and sex-related differences. In addition, while examining both biliary PAH levels as an indicator for recent exposure and liver PAH levels as a record of long-term exposure was useful, additional knowledge about chronic contaminant exposure would have been gained from analysis of other widespread pollutants like heavy metals or polychlorinated biphenyls.

Non-specific immune system biomarkers were of little utility in this study, given the complexity of their interpretation and lack of correlation with PAH levels. That being said, they could be of use in the immediate aftermath of a large contamination event, when immunosuppression is hypothesized given the prevalence of dermal lesions or other gross pathologies observed in available field studies. Oxidative stress biomarkers, however, can provide data suggesting both damage from xenobiotic metabolism and possible mechanisms of resiliency. Finally, as RNA-seq becomes more affordable, the inclusion of transcriptomics in field work is increasingly feasible. While sequencing may be cost prohibitive, the quality control, assembly, annotation, and differential expression analysis in this dissertation were all

performed using freely accessible online tools and downloadable packages. The routine collection of tissue samples in RNAlater is suggested from every fish utilized in a biomarker study. This would allow for future RNA-seq evaluation in subsets of samples upon analysis of their biomarker and contaminant levels and could provide additional information regarding pathways of physiological disruption or resiliency.

CHAPTER SEVEN:

REFERENCES

- Abele, D., Vazquez-Medina, J., & Zenteno-Savin, T. (2012). *Oxidative Stress in Aquatic Environments*. New York: Wiley-Blackwell.
- Able, K. W., Grimes, C. B., Cooper, R. A., & Uzmann, J. R. (1982). Burrow construction and behavior of tilefish, *Lopholatilus chamaeleonticeps*, in Hudson Submarine Canyon. *Environmental Biology of Fishes*, 7(3), 199–205. <https://doi.org/10.1007/BF00002496>
- Aluru, N., Karchner, S. I., Franks, D. G., Nacci, D., Champlin, D., & Hahn, M. E. (2015). Targeted mutagenesis of aryl hydrocarbon receptor 2a and 2b genes in Atlantic killifish (*Fundulus heteroclitus*). *Aquatic Toxicology*, 158, 192–201. <https://doi.org/10.1016/j.aquatox.2014.11.016>
- Aluru, N., Karchner, S. I., & Hahn, M. E. (2011). Role of DNA methylation of AHR1 and AHR2 promoters in differential sensitivity to PCBs in Atlantic Killifish, *Fundulus heteroclitus*. *Aquatic Toxicology*, 101(1), 288–294. <https://doi.org/10.1016/j.aquatox.2010.10.010>
- Álvarez Torres, P., Rabalais, N. N., Piña Gutiérrez, J. M., & Padrón López, R. M. (2017). Research and community of practice of the Gulf of Mexico large marine ecosystem. In *Environmental Development* (Vol. 22, pp. 166–174). Elsevier B.V. <https://doi.org/10.1016/j.envdev.2017.04.004>
- Ameur, W. Ben, El Megdiche, Y., de Lapuente, J., Barhoumi, B., Trabelsi, S., Ennaceur, S., Camps, L., Serret, J., Ramos-López, D., Gonzalez-Linares, J., Touil, S., Driss, M. R., & Borràs, M. (2015). Oxidative stress, genotoxicity and histopathology biomarker responses in *Mugil cephalus* and *Dicentrarchus labrax* gill exposed to persistent pollutants. A field study in the Bizerte Lagoon: Tunisia. *Chemosphere*, 135, 67–74. <https://doi.org/10.1016/j.chemosphere.2015.02.050>
- Andersen, Ø., Frantzen, M., Rosland, M., Timmerhaus, G., Skugor, A., & Krasnov, A. (2015). Effects of crude oil exposure and elevated temperature on the liver transcriptome of polar cod (*Boreogadus saida*). *Aquatic Toxicology*, 165, 9–18. <https://doi.org/10.1016/j.aquatox.2015.04.023>
- Anderson, G., Beischlag, T. V., Vinciguerra, M., & Mazzocchi, G. (2013). The circadian clock circuitry and the AHR signaling pathway in physiology and pathology. In *Biochemical Pharmacology* (Vol. 85, Issue 10, pp. 1405–1416). Elsevier Inc. <https://doi.org/10.1016/j.bcp.2013.02.022>
- Ayllon, F., & Garcia-Vazquez, E. (2000). Induction of micronuclei and other nuclear abnormalities in European minnow *Phoxinus phoxinus* and mollie *Poecilia latipinna*: An assessment of the fish micronucleus test. *Mutation Research - Genetic Toxicology and Environmental Mutagenesis*, 467(2), 177–186. [https://doi.org/10.1016/S1383-5718\(00\)00033-4](https://doi.org/10.1016/S1383-5718(00)00033-4)
- Babcock-Adams, L., Chanton, J. P., Joye, S. B., & Medeiros, P. M. (2017). Hydrocarbon

- composition and concentrations in the Gulf of Mexico sediments in the 3 years following the Macondo well blowout. *Environmental Pollution*, 229, 329–338.
<https://doi.org/10.1016/j.envpol.2017.05.078>
- Bacanskas, L. R., Whitaker, J., & Di Giulio, R. T. (2004). Oxidative stress in two populations of killifish (*Fundulus heteroclitus*) with differing contaminant exposure histories. *Marine Environmental Research*, 58(2–5), 597–601.
<https://doi.org/10.1016/j.marenvres.2004.03.048>
- Bado-Nilles, A., Quentel, C., Thomas-Guyon, H., & Le Floch, S. (2009). Effects of two oils and 16 pure polycyclic aromatic hydrocarbons on plasmatic immune parameters in the European sea bass, *Dicentrarchus labrax* (Linné). *Toxicology in Vitro*, 23(2), 235–241.
<https://doi.org/10.1016/j.tiv.2008.12.001>
- Baillon, L., Pierron, F., Pannetier, P., Normandeau, E., Couture, P., Labadie, P., Budzinski, H., Lambert, P., Bernatchez, L., & Baudrimont, M. (2016). Gene transcription profiling in wild and laboratory-exposed eels: Effect of captivity and in situ chronic exposure to pollution. *Science of the Total Environment*, 571, 92–102.
<https://doi.org/10.1016/j.scitotenv.2016.07.131>
- Balfry, S. K., & Iwama, G. K. (2004). Observations on the inherent variability of measuring lysozyme activity in coho salmon (*Oncorhynchus kisutch*). *Comparative Biochemistry and Physiology - B Biochemistry and Molecular Biology*, 138(3), 207–211.
<https://doi.org/10.1016/j.cbpc.2003.12.010>
- Balk, L., Hylland, K., Hansson, T., Berntssen, M. H. G., Beyer, J., Jonsson, G., Melbye, A., Grung, M., Torstensen, B. E., Børseth, J. F., Skarphedinsdottir, H., & Klungsøyr, J. (2011). Biomarkers in natural fish populations indicate adverse biological effects of offshore oil production. *PLoS ONE*, 6(5). <https://doi.org/10.1371/journal.pone.0019735>
- Bantz, A., Camon, J., Froger, J. A., Goven, D., & Raymond, V. (2018). Exposure to sublethal doses of insecticide and their effects on insects at cellular and physiological levels. *Current Opinion in Insect Science*, 30, 73–78. <https://doi.org/10.1016/j.cois.2018.09.008>
- Bard, S. (2000). Multixenobiotic resistance as a cellular defense mechanism in aquatic organisms. *Aquatic Toxicology*, 48(4), 357–389. [https://doi.org/10.1016/S0166-445X\(00\)00088-6](https://doi.org/10.1016/S0166-445X(00)00088-6)
- Baršienė, J., Dedonyte, V., Rybakovas, A., Andreikenaite, L., & Andersen, O. K. (2006a). Investigation of micronuclei and other nuclear abnormalities in peripheral blood and kidney of marine fish treated with crude oil. *Aquatic Toxicology*, 78(SUPPL.), 99–104.
<https://doi.org/10.1016/j.aquatox.2006.02.022>
- Baršienė, J., Dedonyte, V., Rybakovas, A., Andreikenaite, L., & Andersen, O. K. (2006b). Investigation of micronuclei and other nuclear abnormalities in peripheral blood and kidney of marine fish treated with crude oil. *Aquatic Toxicology*, 78(SUPPL.).
<https://doi.org/10.1016/j.aquatox.2006.02.022>
- Baudou, F. G., Ossana, N. A., Castañé, P. M., Mastrángelo, M. M., González Núñez, A. A., Palacio, M. J., & Ferrari, L. (2019). Use of integrated biomarker indexes for assessing the impact of receiving waters on a native neotropical teleost fish. *Science of the Total Environment*, 650, 1779–1786. <https://doi.org/10.1016/j.scitotenv.2018.09.342>
- Bayha, K. M., Ortell, N., Ryan, C. N., Griffitt, K. J., Krasnec, M., Sena, J., Ramaraj, T., Takeshita, R., Mayer, G. D., Schilkey, F., & Griffitt, R. J. (2017). Crude oil impairs immune function and increases susceptibility to pathogenic bacteria in southern flounder. *PLOS ONE*, 12(5), e0176559. <https://doi.org/10.1371/journal.pone.0176559>

- Beg, M. U., Al-Jandal, N., Al-Subiai, S., Karam, Q., Husain, S., Butt, S. A., Ali, A., Al-Hasan, E., Al-Dufaileej, S., & Al-Husaini, M. (2015). Metallothionein, oxidative stress and trace metals in gills and liver of demersal and pelagic fish species from Kuwait's marine area. *Marine Pollution Bulletin*, *100*(2), 662–672. <https://doi.org/10.1016/j.marpolbul.2015.07.058>
- Bélangier-Deschênes, S., Couture, P., Campbell, P. G. C., & Bernatchez, L. (2013). Evolutionary change driven by metal exposure as revealed by coding SNP genome scan in wild yellow perch (*Perca flavescens*). *Ecotoxicology*, *22*(5), 938–957. <https://doi.org/10.1007/s10646-013-1083-8>
- Ben, Y., Fu, C., Hu, M., Liu, L., Wong, M. H., & Zheng, C. (2019). Human health risk assessment of antibiotic resistance associated with antibiotic residues in the environment: A review. In *Environmental Research* (Vol. 169, pp. 483–493). Academic Press Inc. <https://doi.org/10.1016/j.envres.2018.11.040>
- Benedetti, M., Giuliani, M. E., & Regoli, F. (2015). Oxidative metabolism of chemical pollutants in marine organisms: Molecular and biochemical biomarkers in environmental toxicology. *Annals of the New York Academy of Sciences*, *1340*(1), 8–19. <https://doi.org/10.1111/nyas.12698>
- Beyer, J., Trannum, H. C., Bakke, T., Hodson, P. V., & Collier, T. K. (2016). Environmental effects of the Deepwater Horizon oil spill: A review. In *Marine Pollution Bulletin* (Vol. 110, Issue 1, pp. 28–51). Elsevier Inc. <https://doi.org/10.1016/j.marpolbul.2016.06.027>
- Bolognesi, C., Perrone, E., Roggieri, P., Pampanin, D. M., & Sciutto, A. (2006). Assessment of micronuclei induction in peripheral erythrocytes of fish exposed to xenobiotics under controlled conditions. *Aquatic Toxicology*, *78*(SUPPL.), 93–98. <https://doi.org/10.1016/j.aquatox.2006.02.015>
- Bon, E., Barbe, U., Nuñez Rodriguez, J., Cuisset, B., Pelissero, C., Sumpter, J. P., & Le Menn, F. (1997). Plasma vitellogenin levels during the annual reproductive cycle of the female rainbow trout (*Oncorhynchus mykiss*): establishment and validation of an ELISA. *Comparative Biochemistry and Physiology. Part B, Biochemistry & Molecular Biology*, *117*(1), 75–84. [https://doi.org/10.1016/s0305-0491\(96\)00252-0](https://doi.org/10.1016/s0305-0491(96)00252-0)
- Botello, A. V., Soto, L. A., Ponce-Vélez, G., & Susana Villanueva, F. (2015). Baseline for PAHs and metals in NW Gulf of Mexico related to the Deepwater Horizon oil spill. *Estuarine, Coastal and Shelf Science*, *156*(1), 124–133. <https://doi.org/10.1016/j.ecss.2014.11.010>
- Broeg, K., Westernhagen, H. V., Zander, S., Körting, W., & Koehler, A. (2005). The “bioeffect assessment index” (BAI): A concept for the quantification of effects of marine pollution by an integrated biomarker approach. *Marine Pollution Bulletin*, *50*(5), 495–503. <https://doi.org/10.1016/j.marpolbul.2005.02.042>
- Brown-Peterson, N. J., Peterson, C. R., & Fitzhugh, G. R. (2018). Multidecadal meta-analysis of reproductive parameters of female red snapper (*Lutjanus campechanus*) in the northern gulf of Mexico. *Fishery Bulletin*, *117*(1), 37–49. <https://doi.org/10.7755/FB.117.1.5>
- Brulé, T., Colás-Marrufo, T., Pérez-Díaz, E., & Sámano-Zapata, J. C. (2010). Red Snapper reproductive biology in the southern Gulf of Mexico. *Transactions of the American Fisheries Society*, *139*(4), 957–968. <https://doi.org/10.1577/t09-125.1>
- Burkina, V., Rasmussen, M. K., Pilipenko, N., & Zamaratskaia, G. (2017). Comparison of xenobiotic-metabolising human, porcine, rodent, and piscine cytochrome P450. In *Toxicology* (Vol. 375, pp. 10–27). Elsevier Ireland Ltd. <https://doi.org/10.1016/j.tox.2016.11.014>

- Çakal Arslan, Ö., Boyacıoğlu, M., Parlak, H., Katalay, S., & Karaaslan, M. A. (2015). Assessment of micronuclei induction in peripheral blood and gill cells of some fish species from Aliğa Bay Turkey. *Marine Pollution Bulletin*, 94(1–2), 48–54. <https://doi.org/10.1016/j.marpolbul.2015.03.018>
- Cappello, T., Brandão, F., Guilherme, S., Santos, M. A., Maisano, M., Mauceri, A., Canário, J., Pacheco, M., & Pereira, P. (2016). Insights into the mechanisms underlying mercury-induced oxidative stress in gills of wild fish (*Liza aurata*) combining 1H NMR metabolomics and conventional biochemical assays. *Science of the Total Environment*, 548–549, 13–24. <https://doi.org/10.1016/j.scitotenv.2016.01.008>
- Carrasco, K. R., Tilbury, K. L., & Myers, M. S. (1990). Assessment of the piscine micronucleus test as an in situ biological indicator of chemical contaminant effects. *Canadian Journal of Fisheries and Aquatic Sciences*, 47(11), 2123–2136. <https://doi.org/10.1139/f90-237>
- Cavas, T., Garanko, N. N., & Arkhipchuk, V. V. (2005). Induction of micronuclei and binuclei in blood, gill and liver cells of fishes subchronically exposed to cadmium chloride and copper sulphate. *Food and Chemical Toxicology*, 43(4), 569–574. <https://doi.org/10.1016/j.fct.2004.12.014>
- Celis-Hernandez, O., Rosales-Hoz, L., Cundy, A. B., & Carranza-Edwards, A. (2017). Sedimentary heavy metal(loid) contamination in the Veracruz shelf, Gulf of Mexico: A baseline survey from a rapidly developing tropical coast. *Marine Pollution Bulletin*, 119(2), 204–213. <https://doi.org/10.1016/j.marpolbul.2017.03.039>
- Ceriotti, F., Hinzmann, R., & Panteghini, M. (2009). Reference intervals: The way forward. In *Annals of Clinical Biochemistry* (Vol. 46, Issue 1, pp. 8–17). <https://doi.org/10.1258/acb.2008.008170>
- Cerón, R. M., Cerón, J. G., & Muriel, M. (2007). Diurnal and seasonal trends in carbonyl levels in a semi-urban coastal site in the Gulf of Campeche, Mexico. *Atmospheric Environment*, 41(1), 63–71. <https://doi.org/10.1016/j.atmosenv.2006.08.008>
- Clark, B. W., & Di Giulio, R. T. (2012). *Fundulus heteroclitus* adapted to PAHs are cross-resistant to multiple insecticides. *Ecotoxicology*, 21(2), 465–474. <https://doi.org/10.1007/s10646-011-0807-x>
- Claus, S. P., Guillou, H., & Ellero-Simatos, S. (2016). The gut microbiota: A major player in the toxicity of environmental pollutants? In *NPJ Biofilms and Microbiomes* (Vol. 2). Nature Publishing Group. <https://doi.org/10.1038/npjbiofilms.2016.3>
- Coleman, J., Baker, C., Cooper, C., Fingas, M., Hunt, G., Kvenvolden, K., ... Spies, R. (2003). Oil in the sea III: Inputs, fates, and effects. Committee on Oil in the Sea: Inputs and Effects, Ocean Studies Board and Marine Board, Divisions of Earth and Life Studies and Transportation Research Board, National Research Council. National Academies Press, Washington, DC. USA.
- Collier, T. K., Anulacion, B. F., Arkoosh, M. R., Dietrich, J. P., Incardona, J. P., Johnson, L. L., Ylitalo, G. M., & Myers, M. S. (2013). Effects on fish of polycyclic aromatic hydrocarbons (PAHS) and naphthenic acid exposures. In *Fish Physiology* (First Edit, Vol. 33). Elsevier Inc. <https://doi.org/10.1016/B978-0-12-398254-4.00004-2>
- Conesa, A., Madrigal, P., Tarazona, S., Gomez-Cabrero, D., Cervera, A., McPherson, A., Szcześniak, M. W., Gaffney, D. J., Elo, L. L., Zhang, X., & Mortazavi, A. (2016). A survey of best practices for RNA-seq data analysis. *Genome Biology*, 17(1), 1–19. <https://doi.org/10.1186/s13059-016-0881-8>
- Cowan, J. H., Grimes, C. B., Patterson, W. F., Walters, C. J., Jones, A. C., Lindberg, W. J.,

- Sheehy, D. J., Pine, W. E., Powers, J. E., Campbell, M. D., Lindeman, K. C., Diamond, S. L., Hilborn, R., Gibson, H. T., & Rose, K. A. (2011). Red snapper management in the Gulf of Mexico: Science- or faith-based? In *Reviews in Fish Biology and Fisheries* (Vol. 21, Issue 2, pp. 187–204). <https://doi.org/10.1007/s11160-010-9165-7>
- Crain, C. M., Kroeker, K., & Halpern, B. S. (2008). Interactive and cumulative effects of multiple human stressors in marine systems. *Ecology Letters*, *11*(12), 1304–1315. <https://doi.org/10.1111/j.1461-0248.2008.01253.x>
- Crowe, K. M., Newton, J. C., Kaltenboeck, B., & Johnson, C. (2014). Oxidative stress responses of gulf killifish exposed to hydrocarbons from the Deepwater Horizon oil spill: Potential implications for aquatic food resources. *Environmental Toxicology and Chemistry*, *33*(2), 370–374. <https://doi.org/10.1002/etc.2427>
- Daly, K. L., Passow, U., Chanton, J., & Hollander, D. (2016). Assessing the impacts of oil-associated marine snow formation and sedimentation during and after the Deepwater Horizon oil spill. In *Anthropocene* (Vol. 13, pp. 18–33). Elsevier Ltd. <https://doi.org/10.1016/j.ancene.2016.01.006>
- Dance, M. A., & Rooker, J. R. (2019). Cross-shelf habitat shifts by red snapper (*Lutjanus campechanus*) in the Gulf of Mexico. *PLOS ONE*, *14*(3), e0213506. <https://doi.org/10.1371/journal.pone.0213506>
- Daneshgar A., S., Amos, J., Woods, P., Garcia-Pineda, O., & MacDonald, I. R. (2016). Chronic, Anthropogenic Hydrocarbon Discharges in the Gulf of Mexico. *Deep-Sea Research Part II: Topical Studies in Oceanography*, *129*, 187–195. <https://doi.org/10.1016/j.dsr2.2014.12.006>
- de Mitcheson, Y. S., & Liu, M. (2008). Functional hermaphroditism in teleosts. *Fish and Fisheries*, *9*(1), 1–43. <https://doi.org/10.1111/j.1467-2979.2007.00266.x>
- Di Giulio, R. T., & Clark, B. W. (2015). The Elizabeth River Story: A Case Study in Evolutionary Toxicology. In *Journal of Toxicology and Environmental Health - Part B: Critical Reviews* (Vol. 18, Issue 6, pp. 259–298). Taylor and Francis Inc. <https://doi.org/10.1080/15320383.2015.1074841>
- Díaz-Asencio, M., Bartrina, V. F., & Herguera, J. C. (2019). Sediment accumulation patterns on the slopes and abyssal plain of the southern Gulf of Mexico. *Deep-Sea Research Part I: Oceanographic Research Papers*, *146*, 11–23. <https://doi.org/10.1016/j.dsr.2019.01.003>
- Dixon, D. G., Hodson, P. V., & Kaiser, K. L. E. (1987). Serum sorbitol dehydrogenase activity as an indicator of chemically induced liver damage in rainbow trout. *Environmental Toxicology and Chemistry*, *6*(9), 685–696. <https://doi.org/10.1002/etc.5620060906>
- Doerpinghaus, J., Hentrich, K., Troup, M., Stavrinaky, A., & Anderson, S. (2014). An assessment of sector separation on the Gulf of Mexico recreational red snapper fishery. *Marine Policy*, *50*(PA), 309–317. <https://doi.org/10.1016/j.marpol.2014.06.007>
- Duteil, O., Damien, P., Sheinbaum, J., & Spinner, M. (2019). Ocean currents and coastal exposure to offshore releases of passively transported material in the Gulf of Mexico. *Environmental Research Communications*, *1*(8), 081006. <https://doi.org/10.1088/2515-7620/ab3aad>
- Ellis, A. E. (1977). The leucocytes of fish: A review. *Journal of Fish Biology*, *11*(5), 453–491. <https://doi.org/10.1111/j.1095-8649.1977.tb04140.x>
- Ellis, A. E. (1999). Immunity to bacteria in fish. *Fish and Shellfish Immunology*, *9*(4), 291–308. <https://doi.org/10.1006/fsim.1998.0192>
- Esser, C., Rannug, A., & Stockinger, B. (2009). The aryl hydrocarbon receptor in immunity. *Trends in Immunology*, *30*(9), 447–454. <https://doi.org/10.1016/j.it.2009.06.005>

- Faria, S. S., Fernandes, P. C., Silva, M. J. B., Lima, V. C., Fontes, W., Freitas, R., Eterovic, A. K., & Forget, P. (2016). The neutrophil-to-lymphocyte ratio: A narrative review. In *ecancermedicalscience* (Vol. 10). Cancer Intelligence. <https://doi.org/10.3332/ecancer.2016.702>
- Farmer, N. A., Malinowski, R. P., McGovern, M. F., & Rubec, P. J. (2016). Stock complexes for fisheries management in the Gulf of Mexico. *Marine and Coastal Fisheries*, 8(1), 177–201. <https://doi.org/10.1080/19425120.2015.1024359>
- Felder, D. L., Thoma, B. P., Schmidt, W. E., Sauvage, T., Self-Krayesky, S. L., Chistoserdov, A., Bracken-Grissom, H. D., & Fredericq, S. (2014). Seaweeds and decapod crustaceans on gulf deep banks after the macondo oil spill. *BioScience*, 64(9), 808–819. <https://doi.org/10.1093/biosci/biu119>
- Fenech, M. (2000). The in vitro micronucleus technique. *Mutation Research - Fundamental and Molecular Mechanisms of Mutagenesis*, 455(1–2), 81–95. [https://doi.org/10.1016/S0027-5107\(00\)00065-8](https://doi.org/10.1016/S0027-5107(00)00065-8)
- Fertuck, K. C., Kumar, S., Sikka, H. C., Matthews, J. B., & Zacharewski, T. R. (2001). Interaction of PAH-related compounds with the α and β isoforms of the estrogen receptor. *Toxicology Letters*, 121(3), 167–177. [https://doi.org/10.1016/S0378-4274\(01\)00344-7](https://doi.org/10.1016/S0378-4274(01)00344-7)
- Fletcher, T. C., White, A., & Baldo, B. A. (1977). C-reactive protein-like precipitin and lysozyme in the lumpsucker *Cyclopterus lumpus* L. during the breeding season. *Comparative Biochemistry and Physiology -- Part B: Biochemistry And*, 57(4), 353–357. [https://doi.org/10.1016/0305-0491\(77\)90066-9](https://doi.org/10.1016/0305-0491(77)90066-9)
- Fonseca, V. F., França, S., Vasconcelos, R. P., Serafim, A., Company, R., Lopes, B., Bebianno, M. J., & Cabral, H. N. (2011). Short-term variability of multiple biomarker response in fish from estuaries: Influence of environmental dynamics. *Marine Environmental Research*, 72(4), 172–178. <https://doi.org/10.1016/j.marenvres.2011.08.001>
- Franco, M. E., & Lavado, R. (2019). Applicability of in vitro methods in evaluating the biotransformation of polycyclic aromatic hydrocarbons (PAHs) in fish: Advances and challenges. In *Science of the Total Environment* (Vol. 671, pp. 685–695). Elsevier B.V. <https://doi.org/10.1016/j.scitotenv.2019.03.394>
- Friedrichs, K. R., Harr, K. E., Freeman, K. P., Szlodovits, B., Walton, R. M., Barnhart, K. F., & Blanco-Chavez, J. (2012). ASVCP reference interval guidelines: Determination of de novo reference intervals in veterinary species and other related topics. *Veterinary Clinical Pathology*, 41(4), 441–453. <https://doi.org/10.1111/vcp.12006>
- Furnus, G., Caffetti, J., García, E., Benítez, M., Pastori, M., & Fenocchio, A. (2014). Baseline micronuclei and nuclear abnormalities frequencies in native fishes from the Paraná River (Argentina). *Brazilian Journal of Biology*, 74(1), 217–221. <https://doi.org/10.1590/1519-6984.13712>
- Gagnon, M. M., & Rawson, C. A. (2016). Integrating multiple biomarkers of fish health: A case study of fish health in ports. *Archives of Environmental Contamination and Toxicology*, 70(2), 192–203. <https://doi.org/10.1007/s00244-015-0258-0>
- Gallaway, B. J., Szedlmayer, S. T., & Gazey, W. J. (2009). A life history review for red snapper in the Gulf of Mexico with an evaluation of the importance of offshore petroleum platforms and other artificial reefs. In *Reviews in Fisheries Science* (Vol. 17, Issue 1, pp. 48–67). <https://doi.org/10.1080/10641260802160717>
- Gandar, A., Laffaille, P., Canlet, C., Tremblay-Franco, M., Gautier, R., Perrault, A., Gress, L., Mormède, P., Tapie, N., Budzinski, H., & Jean, S. (2017). Adaptive response under

- multiple stress exposure in fish: From the molecular to individual level. *Chemosphere*, 188, 60–72. <https://doi.org/10.1016/j.chemosphere.2017.08.089>
- García-Cruz, N. U., Sánchez-Avila, J. I., Valdés-Lozano, D., Gold-Bouchot, G., & Aguirre-Macedo, L. (2018). Biodegradation of hexadecane using sediments from rivers and lagoons of the Southern Gulf of Mexico. *Marine Pollution Bulletin*, 128, 202–207. <https://doi.org/10.1016/j.marpolbul.2018.01.026>
- Geffré, A., Friedrichs, K., Harr, K., Concordet, D., Trumel, C., & Braun, J.-P. (2009). Reference values: a review. *Veterinary Clinical Pathology*, 38(3), 288–298. <https://doi.org/10.1111/j.1939-165X.2009.00179.x>
- Gekara, N. O. (2017). DNA damage-induced immune response: Micronuclei provide key platform. In *Journal of Cell Biology* (Vol. 216, Issue 10, pp. 2999–3001). Rockefeller University Press. <https://doi.org/10.1083/jcb.201708069>
- Ghafoori, Z., Heidari, B., Farzadfar, F., & Aghamaali, M. (2014). Variations of serum and mucus lysozyme activity and total protein content in the male and female *Caspian kutum* (*Rutilus frisii kutum*, Kamensky 1901) during reproductive period. *Fish and Shellfish Immunology*, 37(1), 139–146. <https://doi.org/10.1016/j.fsi.2014.01.016>
- Glenn, H. D., Cowan, J. H., & Powers, J. E. (2017). A comparison of Red Snapper reproductive potential in the northwestern Gulf of Mexico: Natural versus Artificial Habitats. *Marine and Coastal Fisheries*, 9(1), 139–148. <https://doi.org/10.1080/19425120.2017.1282896>
- González-Doncel, M., Sastre, S., Carbonell, G., Beltrán, E. M., González Anaya, C., García-Mauriño, J. E., & Fernández Torija, C. (2017). Bioaccumulation, maternal transfer and effects of dietary 2,2",4,4"-tetrabromodiphenyl ether (BDE-47) exposure on medaka fish (*Oryzias latipes*) offspring. *Aquatic Toxicology*, 192, 241–250. <https://doi.org/10.1016/j.aquatox.2017.09.024>
- Granneman, J. E., Jones, D. L., & Peebles, E. B. (2017). Associations between metal exposure and lesion formation in offshore Gulf of Mexico fishes collected after the Deepwater Horizon oil spill. *Marine Pollution Bulletin*, 117(1–2), 462–477. <https://doi.org/10.1016/j.marpolbul.2017.01.066>
- Grimes, C.B., Idelberger, C.F., Able, K.W., & Tuner, S.C. (1988). The reproductive biology of tilefish, *Lopholatilus chamaeleonticeps* Goode and Bean, from the United States Mid-Atlantic Bight, and the effects of fishing on the breeding system. *Fisheries Bulletin*. 86:745-762.
- Grinde, B., Lie, Ø., Poppe, T., & Salte, R. (1988). Species and individual variation in lysozyme activity in fish of interest in aquaculture. *Aquaculture*, 68(4), 299–304. [https://doi.org/10.1016/0044-8486\(88\)90243-8](https://doi.org/10.1016/0044-8486(88)90243-8)
- Hall, R.A., Zook, E.G., & Meaburn, G.M. (1978). National Marine Fisheries Service survey of trace elements in the fishery resource. NOAA Technical Report NMFS SSRF-721 Washington, D.C., 313 p.
- Hamilton, P. B., Cowx, I. G., Oleksiak, M. F., Griffiths, A. M., Grahn, M., Stevens, J. R., Carvalho, G. R., Nicol, E., & Tyler, C. R. (2016). Population-level consequences for wild fish exposed to sublethal concentrations of chemicals - a critical review. *Fish and Fisheries*, 17(3), 545–566. <https://doi.org/10.1111/faf.12125>
- Hao, N., & Whitelaw, M. L. (2013). The emerging roles of AhR in physiology and immunity. *Biochemical Pharmacology*, 86(5), 561–570. <https://doi.org/10.1016/j.bcp.2013.07.004>
- Hara, A., Hiramatsu, N., & Fujita, T. (2016). Vitellogenesis and choriogenesis in fishes. In *Fisheries Science* (Vol. 82, Issue 2, pp. 187–202). Springer Tokyo. <https://doi.org/10.1007/s12562-015-0957-5>

- Harr, K. E., Deak, K., Murawski, S. A., Reavill, D. R., & Takeshita, R. A. (2018). Generation of red drum (*Sciaenops ocellatus*) hematology Reference Intervals with a focus on identified outliers. *Veterinary Clinical Pathology*, 47(1), 22–28. <https://doi.org/10.1111/vcp.12569>
- Harris, E. K., & Boyd, J. C. (1990). On dividing reference data into subgroups to produce separate reference ranges. *Clinical Chemistry*, 36(2), 265–270. <https://doi.org/10.1093/clinchem/36.2.265>
- Harris, R., Pollman, C., Hutchinson, D., Landing, W., Axelrad, D., Morey, S. L., Dukhovskoy, D., & Vijayaraghavan, K. (2012). A screening model analysis of mercury sources, fate and bioaccumulation in the Gulf of Mexico. *Environmental Research*, 119, 53–63. <https://doi.org/10.1016/j.envres.2012.08.013>
- Harris, R., Pollman, C., Landing, W., Evans, D., Axelrad, D., Hutchinson, D., Morey, S. L., Rumbold, D., Dukhovskoy, D., Adams, D. H., Vijayaraghavan, K., Holmes, C., Atkinson, R. D., Myers, T., & Sunderland, E. (2012). Mercury in the Gulf of Mexico: Sources to receptors. *Environmental Research*, 119, 42–52. <https://doi.org/10.1016/j.envres.2012.08.001>
- Hayward, A., & Gillooly, J. F. (2011). The cost of sex: quantifying energetic investment in gamete production by males and females. *PLoS ONE*, 6(1), e16557. <https://doi.org/10.1371/journal.pone.0016557>
- Heap, I. (2014). Global perspective of herbicide-resistant weeds. In *Pest Management Science* (Vol. 70, Issue 9, pp. 1306–1315). John Wiley and Sons Ltd. <https://doi.org/10.1002/ps.3696>
- Helm Mueller, G. (2019). Population demographics of Golden Tilefish (*Lopholatilus chamaeleonticeps*) in the Gulf of Mexico. University of South Florida. Thesis.
- Herdter, E. S., Chambers, D. P., Stallings, C. D., & Murawski, S. A. (2017). Did the Deepwater Horizon oil spill affect growth of Red Snapper in the Gulf of Mexico? *Fisheries Research*, 191, 60–68. <https://doi.org/10.1016/j.fishres.2017.03.005>
- Hogan, N. S., Lee, K. S., Köllner, B., & van den Heuvel, M. R. (2010). The effects of the alkyl polycyclic aromatic hydrocarbon retene on rainbow trout (*Oncorhynchus mykiss*) immune response. *Aquatic Toxicology*, 100(3), 246–254. <https://doi.org/10.1016/j.aquatox.2010.07.020>
- Holmstrup, M., Bindesbøl, A. M., Oostingh, G. J., Duschl, A., Scheil, V., Köhler, H. R., Loureiro, S., Soares, A. M. V. M., Ferreira, A. L. G., Kienle, C., Gerhardt, A., Laskowski, R., Kramarz, P. E., Bayley, M., Svendsen, C., & Spurgeon, D. J. (2010). Interactions between effects of environmental chemicals and natural stressors: A review. In *Science of the Total Environment* (Vol. 408, Issue 18, pp. 3746–3762). <https://doi.org/10.1016/j.scitotenv.2009.10.067>
- Holth, T. F., Nourizadeh-Lillabadi, R., Blaesbjerg, M., Grung, M., Holbech, H., Petersen, G. I., Aleström, P., & Hylland, K. (2008). Differential gene expression and biomarkers in zebrafish (*Danio rerio*) following exposure to produced water components. *Aquatic Toxicology*, 90(4), 277–291. <https://doi.org/10.1016/j.aquatox.2008.08.020>
- Hook, S. E., Gallagher, E. P., & Batley, G. E. (2014). The role of biomarkers in the assessment of aquatic ecosystem health. In *Integrated Environmental Assessment and Management* (Vol. 10, Issue 3, pp. 327–341). Wiley-Blackwell. <https://doi.org/10.1002/ieam.1530>
- Horta-Puga, G., & Carriquiry, J. D. (2014). The last two centuries of lead pollution in the southern Gulf of Mexico recorded in the annual bands of the scleractinian coral *Orbicella faveolata*. *Bulletin of Environmental Contamination and Toxicology*, 92(5), 567–573.

- <https://doi.org/10.1007/s00128-014-1222-9>
- Hussain, B., Sultana, T., Sultana, S., Masoud, M. S., Ahmed, Z., & Mahboob, S. (2018). Fish eco-genotoxicology: Comet and micronucleus assay in fish erythrocytes as in situ biomarker of freshwater pollution. *Saudi Journal of Biological Sciences*, 25(2), 393–398. <https://doi.org/10.1016/j.sjbs.2017.11.048>
- Incardona, J. P., Swarts, T. L., Edmunds, R. C., Linbo, T. L., Aquilina-Beck, A., Sloan, C. A., Gardner, L. D., Block, B. A., & Scholz, N. L. (2013). Exxon Valdez to Deepwater Horizon: Comparable toxicity of both crude oils to fish early life stages. *Aquatic Toxicology*, 142–143, 303–316. <https://doi.org/10.1016/j.aquatox.2013.08.011>
- Iturburu, F. G., Bertrand, L., Mendieta, J. R., Amé, M. V., & Menone, M. L. (2018). An integrated biomarker response study explains more than the sum of the parts: Oxidative stress in the fish *Australoheros facetus* exposed to imidacloprid. *Ecological Indicators*, 93, 351–357. <https://doi.org/10.1016/j.ecolind.2018.05.019>
- Javed, M., Ahmad, M. I., Usmani, N., & Ahmad, M. (2017). Multiple biomarker responses (serum biochemistry, oxidative stress, genotoxicity and histopathology) in *Channa punctatus* exposed to heavy metal loaded waste water /704/172/4081 /631/601 article. *Scientific Reports*, 7(1). <https://doi.org/10.1038/s41598-017-01749-6>
- Joye, S. B., Teske, A. P., & Kostka, J. E. (2014). Microbial dynamics following the Macondo oil well blowout across Gulf of Mexico environments. *BioScience*, 64(9), 766–777. <https://doi.org/10.1093/biosci/biu121>
- Kane Driscoll, S. B., McArdle, M. E., Menzie, C. A., Reiss, M., & Steevens, J. A. (2010). A framework for using dose as a metric to assess toxicity of fish to PAHs. *Ecotoxicology and Environmental Safety*, 73(4), 486–490. <https://doi.org/10.1016/j.ecoenv.2009.11.004>
- Karadag, H., Firat, Ö., & Firat, Ö. (2014). Use of oxidative stress biomarkers in *Cyprinus carpio* L. for the evaluation of water pollution in ataturk dam lake (Adiyaman, Turkey). *Bulletin of Environmental Contamination and Toxicology*, 92(3), 289–293. <https://doi.org/10.1007/s00128-013-1187-0>
- Karlmark, K. R., Tacke, F., & Dunay, I. R. (2012). Monocytes in health and disease - Minireview. *European Journal of Microbiology & Immunology*, 2(2), 97–102. <https://doi.org/10.1556/EuJMI.2.2012.2.1>
- Kennedy, C. J., & Farrell, A. P. (2008). Immunological alterations in juvenile Pacific herring, *Clupea pallasii*, exposed to aqueous hydrocarbons derived from crude oil. *Environmental Pollution*, 153(3), 638–648. <https://doi.org/10.1016/j.envpol.2007.09.003>
- Kennicutt, M. C. (2017). Oil and gas seeps in the Gulf of Mexico. In *Habitats and Biota of the Gulf of Mexico: Before the Deepwater Horizon Oil Spill* (Vol. 1, pp. 275–358). Springer New York. https://doi.org/10.1007/978-1-4939-3447-8_5
- Khan, M. F., & Wang, G. (2018). Environmental agents, oxidative stress and autoimmunity. In *Current Opinion in Toxicology* (Vol. 7, pp. 22–27). Elsevier B.V. <https://doi.org/10.1016/j.cotox.2017.10.012>
- Klotz, J., Porter, B. E., Colas, C., Schlessinger, A., & Pajor, A. M. (2016). Mutations in the Na⁺/citrate cotransporter NaCT (SLC13A5) in pediatric patients with epilepsy and developmental delay. *Molecular Medicine*, 22, 310–321. <https://doi.org/10.2119/molmed.2016.00077>
- Koenig, S., Porte, C., Solé, M., & Sturve, J. (2013). Biliary PAH and alkylphenol metabolites, biomarker enzyme activities, and gene expression levels in the deep-sea fish *Alepocephalus rostratus*. *Environmental Science and Technology*, 47(6), 2854–2861.

- <https://doi.org/10.1021/es304345s>
- Kortenkamp, A. (2007). Ten years of mixing cocktails: A review of combination effects of endocrine-disrupting chemicals. In *Environmental Health Perspectives* (Vol. 115, Issue SUPPL1, pp. 98–105). <https://doi.org/10.1289/ehp.9357>
- Krahn, M. M., Myers, M. S., Burrows, D. G., & Malins, D. C. (1984). Determination of metabolites of xenobiotics in the bile of fish from polluted waterways. *Xenobiotica*, *14*(8), 633–646. <https://doi.org/10.3109/00498258409151461>
- Kulaw, D. H., Cowan, J. H., & Jackson, M. W. (2017). Temporal and spatial comparisons of the reproductive biology of northern Gulf of Mexico (USA) red snapper (*Lutjanus campechanus*) collected a decade apart. *PLOS ONE*, *12*(3), e0172360. <https://doi.org/10.1371/journal.pone.0172360>
- Labaronne, E., Pinteur, C., Vega, N., Pesenti, S., Julien, B., Meugnier-Fouilloux, E., Vidal, H., Naville, D., & Le Magueresse-Battistoni, B. (2017). Low-dose pollutant mixture triggers metabolic disturbances in female mice leading to common and specific features as compared to a high-fat diet. *Journal of Nutritional Biochemistry*, *45*, 83–93. <https://doi.org/10.1016/j.jnutbio.2017.04.001>
- Lahti, A., Hyltoft Petersen, P., Boyd, J. C., Fraser, C. G., & Jørgensen, N. (2002). Objective criteria for partitioning Gaussian-distributed reference values into subgroups. *Clinical Chemistry*, *48*(2), 338–352. <http://www.ncbi.nlm.nih.gov/pubmed/11805016>
- Lahti, A., Hyltoft Petersen, P., Boyd, J. C., Rustad, P., Laake, P., & Solberg, H. E. (2004). Partitioning of nongaussian-distributed biochemical reference data into subgroups. *Clinical Chemistry*, *50*(5), 891–900. <https://doi.org/10.1373/clinchem.2003.027953>
- Laurent, A., Fennel, K., Ko, D. S., & Lehrter, J. (2018). Climate change projected to exacerbate impacts of coastal eutrophication in the northern Gulf of Mexico. *Journal of Geophysical Research: Oceans*, *123*(5), 3408–3426. <https://doi.org/10.1002/2017JC013583>
- Lauretta, R., Sansone, A., Sansone, M., Romanelli, F., & Appetecchia, M. (2019). Endocrine disrupting chemicals: effects on endocrine glands. *Frontiers in Endocrinology*, *10*. <https://doi.org/10.3389/fendo.2019.00178>
- Lee, B. Y., Lee, M. C., Jeong, C. B., Kim, H. J., Hagiwara, A., Souissi, S., Han, J., & Lee, J. S. (2018). RNA-Seq-based transcriptome profiling and expression of 16 cytochrome P450 genes in the benzo[α]pyrene-exposed estuarine copepod *Eurytemora affinis*. *Comparative Biochemistry and Physiology - Part D: Genomics and Proteomics*, *28*, 142–150. <https://doi.org/10.1016/j.cbd.2018.08.002>
- Levenson, C. W., & Axelrad, D. M. (2006). Too much of a good thing? Update on fish consumption and mercury exposure. *Nutrition Reviews*, *64*(3), 139–145. <https://doi.org/10.1111/j.1753-4887.2006.tb00197.x>
- Li, B. & Dewey, C.N. (2011). RSEM: accurate transcript quantification from RNA-Seq data with or without a reference genome. *BMC Bioinformatics*, *12*(323). <https://doi.org/10.1186/1471-2105-12-323>.
- Liguori, I., Russo, G., Curcio, F., Bulli, G., Aran, L., Della-Morte, D., Gargiulo, G., Testa, G., Cacciatore, F., Bonaduce, D., & Abete, P. (2018). Oxidative stress, aging, and diseases. In *Clinical Interventions in Aging* (Vol. 13, pp. 757–772). Dove Medical Press Ltd. <https://doi.org/10.2147/CIA.S158513>
- Livingstone, D. R. (2007). Biotechnology and pollution monitoring: Use of molecular biomarkers in the aquatic environment. *Journal of Chemical Technology & Biotechnology*, *57*(3), 195–211. <https://doi.org/10.1002/jctb.280570302>

- Lohitnavy, M., Lu, Y., Lohitnavy, O., Chubb, L. S., Hirono, S., & Yang, R. S. H. (2008). A possible role of multidrug resistance - Associated protein 2 (Mrp2) in hepatic excretion of PCB126, an environmental contaminant: PBPK/PD modeling. *Toxicological Sciences*, *104*(1), 27–39. <https://doi.org/10.1093/toxsci/kfn026>
- Lombardi, L., Fitzhugh, G., & Lyon, H. (2010). Golden Tilefish (*Lopholatilus chamaeleonticeps*) age, growth, and reproduction from the northeastern Gulf of Mexico:1985, 1997-2009. SEDAR22-DW-01. SEDAR, Panama City, FL.
- Lombardi-Carlson, L. (2012). Life history, population dynamics, and fishery management of the Golden Tilefish, *Lopholatilus chamaeleonticeps*, from the southeast Atlantic and Gulf of Mexico. University of Florida, PhD Dissertation.
- Lombardi-Carlson, L. A., & Andrews, A. H. (2015). Age estimation and lead-radium dating of golden tilefish, *Lopholatilus chamaeleonticeps*. *Environmental Biology of Fishes*, *98*(7), 1787–1801. <https://doi.org/10.1007/s10641-015-0398-0>
- López-López, E., Sedeño-Díaz, J. E., Soto, C., & Favari, L. (2011). Responses of antioxidant enzymes, lipid peroxidation, and Na⁺/K⁺-ATPase in liver of the fish *Goodea atripinnis* exposed to Lake Yuriria water. *Fish Physiology and Biochemistry*, *37*(3), 511–522. <https://doi.org/10.1007/s10695-010-9453-0>
- Loughery, J. R., Kidd, K. A., Mercer, A., & Martyniuk, C. J. (2018). Part A: Temporal and dose-dependent transcriptional responses in the liver of fathead minnows following short term exposure to the polycyclic aromatic hydrocarbon phenanthrene. *Aquatic Toxicology*, *199*, 90–102. <https://doi.org/10.1016/j.aquatox.2018.03.027>
- Lubchenco, J., McNutt, M. K., Dreyfus, G., Murawski, S. A., Kennedy, D. M., Anastas, P. T., Chu, S., & Hunter, T. (2012). Science in support of the Deepwater Horizon response. In *Proceedings of the National Academy of Sciences of the United States of America* (Vol. 109, Issue 50, pp. 20212–20221). <https://doi.org/10.1073/pnas.1204729109>
- Lucas, D. & Zhao, L. (2015). PAH analysis in salmon with enhanced matrix removal. Agilent Technologies Application Note, publication number 5991-6088EN.
- Lushchak, V. I. (2011). Environmentally induced oxidative stress in aquatic animals. *Aquatic Toxicology*, *101*(1), 13–30. <https://doi.org/10.1016/j.aquatox.2010.10.006>
- Lyon, H. (2010). Evidence of hermaphroditism in Golden Tilefish (*Lopholatilus chamaeleonticeps*) in the Gulf of Mexico. NMFS, SEFSC, Panama City Laboratory, 3500 Delwood Beach Road, Panama City, Florida 32408. Panama City Laboratory Contribution 10-07. p. 4
- Macdonald, I. R. (1993). Natural oil slicks in the Gulf of Mexico visible from space. *Journal of Geophysical Research*, *98*(C9). <https://doi.org/10.1029/93jc01289>
- MacKenzie, K. J., Carroll, P., Martin, C. A., Murina, O., Fluteau, A., Simpson, D. J., Olova, N., Sutcliffe, H., Rainger, J. K., Leitch, A., Osborn, R. T., Wheeler, A. P., Nowotny, M., Gilbert, N., Chandra, T., Reijns, M. A. M., & Jackson, A. P. (2017). CGAS surveillance of micronuclei links genome instability to innate immunity. *Nature*, *548*(7668), 461–465. <https://doi.org/10.1038/nature23449>
- Madeira, D., Mendonça, V., Madeira, C., Gaiteiro, C., Vinagre, C., & Diniz, M. S. (2019). Molecular assessment of wild populations in the marine realm: Importance of taxonomic, seasonal and habitat patterns in environmental monitoring. *Science of the Total Environment*, *654*, 250–263. <https://doi.org/10.1016/j.scitotenv.2018.11.064>
- Marchand, J., Quiniou, L., Riso, R., Thebaut, M. T., & Laroche, J. (2004). Physiological cost of tolerance to toxicants in the European flounder *Platichthys flesus*, along the French Atlantic

- Coast. *Aquatic Toxicology*, 70(4), 327–343. <https://doi.org/10.1016/j.aquatox.2004.10.001>
- Marentette, J. R., Tong, S., & Balshine, S. (2013). The cortisol stress response in male round goby (*Neogobius melanostomus*): Effects of living in polluted environments? *Environmental Biology of Fishes*, 96(6), 723–733. <https://doi.org/10.1007/s10641-012-0064-8>
- Martínez-Gómez, C., & Vethaak, A. D. (2019). Understanding the impact of chemicals on marine fish populations: the need for an integrative approach involving population and disease ecology. In *Current Opinion in Environmental Science and Health* (Vol. 11, pp. 71–77). Elsevier B.V. <https://doi.org/10.1016/j.coesh.2019.08.001>
- Martins, M., Santos, J. M., Diniz, M. S., Ferreira, A. M., Costa, M. H., & Costa, P. M. (2015). Effects of carcinogenic versus non-carcinogenic AHR-active PAHs and their mixtures: Lessons from ecological relevance. *Environmental Research*, 138, 101–111. <https://doi.org/10.1016/j.envres.2015.02.010>
- Marty, M. S., Borgert, C., Coady, K., Green, R., Levine, S. L., Mihaich, E., Ortego, L., Wheeler, J. R., Yi, K. D., & Zorrilla, L. M. (2018). Distinguishing between endocrine disruption and non-specific effects on endocrine systems. In *Regulatory Toxicology and Pharmacology* (Vol. 99, pp. 142–158). Academic Press Inc. <https://doi.org/10.1016/j.yrtph.2018.09.002>
- Matsche, M. A., Arnold, J., Jenkins, E., Townsend, H., & Rosemary, K. (2014). Determination of hematology and plasma chemistry reference intervals for 3 populations of captive Atlantic sturgeon (*Acipenser oxyrinchus oxyrinchus*). *Veterinary Clinical Pathology*, 43(3), 387–396. <https://doi.org/10.1111/vcp.12174>
- Matyash, V., Liebisch, G., Kurzchalia, T. V., Shevchenko, A., & Schwudke, D. (2008). Lipid extraction by methyl-terf-butyl ether for high-throughput lipidomics. *Journal of Lipid Research*, 49(5), 1137–1146. <https://doi.org/10.1194/jlr.D700041-JLR200>
- McBride, R. S., Vidal, T. E., & Cadrin, S. X. (2013). Changes in size and age at maturity of the northern stock of Tilefish (*Lopholatilus chamaeleonticeps*) after a period of overfishing. *Fishery Bulletin*, 111(2), 161–174. <https://doi.org/10.7755/FB.111.2.4>
- McClain, C. R., Nunnally, C., & Benfield, M. C. (2019). Persistent and substantial impacts of the Deepwater Horizon oil spill on deep-sea megafauna. *Royal Society Open Science*, 6(8). <https://doi.org/10.1098/rsos.191164>
- McGruer, V., Pasparakis, C., Grosell, M., Stieglitz, J. D., Benetti, D. D., Greer, J. B., & Schlenk, D. (2019). Deepwater Horizon crude oil exposure alters cholesterol biosynthesis with implications for developmental cardiotoxicity in larval mahi-mahi (*Coryphaena hippurus*). *Comparative Biochemistry and Physiology Part - C: Toxicology and Pharmacology*, 220, 31–35. <https://doi.org/10.1016/j.cbpc.2019.03.001>
- McLeay, D. J., & Gordon, M. R. (1977). Leucocrit: A simple hematological technique for measuring acute stress in Salmonid fish, including stressful concentrations of pulpmill effluent. *Journal of the Fisheries Research Board of Canada*, 34(11), 2156–2163. <https://doi.org/10.1139/f77-284>
- McNutt, M. K., Camilli, R., Crone, T. J., Guthrie, G. D., Hsieh, P. A., Ryerson, T. B., Savas, O., & Shaffer, F. (2012). Review of flow rate estimates of the Deepwater Horizon oil spill. In *Proceedings of the National Academy of Sciences of the United States of America* (Vol. 109, Issue 50, pp. 20260–20267). <https://doi.org/10.1073/pnas.1112139108>
- Meador, J. P., Stein, J. E., Reichert, W. L., & Varanasi, U. (1995). Bioaccumulation of polycyclic aromatic hydrocarbons by marine organisms. In *Reviews of environmental contamination and toxicology* (Vol. 143, Issue February). <https://doi.org/10.1007/978-1->

- Meixner, A., Karreth, F., Kenner, L., Penninger, J. M., & Wagner, E. F. (2010). Jun and JunD-dependent functions in cell proliferation and stress response. *Cell Death and Differentiation*, *17*(9), 1409–1419. <https://doi.org/10.1038/cdd.2010.22>
- Miller, J., Esselman, P. C., Alameddine, I., Blackhart, K., & Obenour, D. R. (2018). Hierarchical modeling assessment of the influence of watershed stressors on fish and invertebrate species in Gulf of Mexico estuaries. *Ecological Indicators*, *90*, 142–153. <https://doi.org/10.1016/j.ecolind.2018.02.040>
- Montagna, P. A., Baguley, J. G., Cooksey, C., Hartwell, I., Hyde, L. J., Hyland, J. L., Kalke, R. D., Kracker, L. M., Reuscher, M., & Rhodes, A. C. E. (2013). Deep-Sea Benthic Footprint of the Deepwater Horizon Blowout. *PLoS ONE*, *8*(8), e70540. <https://doi.org/10.1371/journal.pone.0070540>
- Munns, W. R., Black, D. E., Gleason, T. R., Salomon, K., Bengtson, D., & Gutjahr-Gobell, R. (1997). Evaluation of the effects of dioxin and PCBs on *Fundulus heteroclitus* populations using a modeling approach. *Environmental Toxicology and Chemistry*, *16*(5), 1074–1081. <https://doi.org/10.1002/etc.5620160530>
- Murawski, S. A., Hogarth, W. T., Peebles, E. B., & Barbeiri, L. (2014). Prevalence of external skin lesions and polycyclic aromatic hydrocarbon concentrations in Gulf of Mexico fishes, post-Deepwater Horizon. *Transactions of the American Fisheries Society*, *143*(4), 1084–1097. <https://doi.org/10.1080/00028487.2014.911205>
- Murawski, S. A., Peebles, E. B., Gracia, A., Tunnell, J. W., & Armenteros, M. (2018). Comparative abundance, species composition, and demographics of continental shelf fish assemblages throughout the Gulf of Mexico. *Marine and Coastal Fisheries*, *10*(3), 325–346. <https://doi.org/10.1002/mcf2.10033>
- Nacci, D., Proestou, D., Champlin, D., Martinson, J., & Waits, E. R. (2016). Genetic basis for rapidly evolved tolerance in the wild: adaptation to toxic pollutants by an estuarine fish species. *Molecular Ecology*, *25*(21), 5467–5482. <https://doi.org/10.1111/mec.13848>
- Nahrgang, J., Camus, L., Gonzalez, P., Goksøyr, A., Christiansen, J. S., & Hop, H. (2009). PAH biomarker responses in polar cod (*Boreogadus saida*) exposed to benzo(a)pyrene. *Aquatic Toxicology*, *94*(4), 309–319. <https://doi.org/10.1016/j.aquatox.2009.07.017>
- Noga, E. J. (n.d.). Skin ulcers in fish: Pfiesteria and other etiologies. *Toxicologic Pathology*, *28*(6), 807–823. <https://doi.org/10.1177/019262330002800607>
- Nowling, L. (2011). Successful discrimination using otolith microchemistry among samples of Red Snapper *Lutjanus campechanus* from artificial reefs and samples of *L. campechanus* taken from nearby oil and gas platforms. *The Open Fish Science Journal*, *4*(1), 1–9. <https://doi.org/10.2174/1874401x01104010001>
- Oliver, S. V., & Brooke, B. D. (2018). The effect of commercial herbicide exposure on the life history and insecticide resistance phenotypes of the major malaria vector *Anopheles arabiensis* (Diptera: culicidae). *Acta Tropica*, *188*, 152–160. <https://doi.org/10.1016/j.actatropica.2018.08.030>
- Omicinski, C. J., Vanden Heuvel, J. P., Perdew, G. H., & Peters, J. M. (2011). Xenobiotic metabolism, disposition, and regulation by receptors: From biochemical phenomenon to predictors of major toxicities. In *Toxicological Sciences* (Vol. 120, Issue SUPPL.1). <https://doi.org/10.1093/toxsci/kfq338>
- Oshlack, A., Robinson, M. D., & Young, M. D. (2010). From RNA-seq reads to differential expression results. *Genome Biology*, *11*(12), 1–10. <https://doi.org/10.1186/gb-2010-11-12->

- Osterberg, J. S., Cammen, K. M., Schultz, T. F., Clark, B. W., & Di Giulio, R. T. (2018). Genome-wide scan reveals signatures of selection related to pollution adaptation in non-model estuarine Atlantic killifish (*Fundulus heteroclitus*). *Aquatic Toxicology*, *200*, 73–82. <https://doi.org/10.1016/j.aquatox.2018.04.017>
- Oziolor, E. M., Bigorgne, E., Aguilar, L., Usenko, S., & Matson, C. W. (2014). Evolved resistance to PCB- and PAH-induced cardiac teratogenesis, and reduced CYP1A activity in Gulf killifish (*Fundulus grandis*) populations from the Houston Ship Channel, Texas. *Aquatic Toxicology*, *150*, 210–219. <https://doi.org/10.1016/j.aquatox.2014.03.012>
- Ozmen, I., Bayir, A., Cengiz, M., Sirkecioglu, A. N., & Atamanalp, M. (2004). Effects of water reuse system on antioxidant enzymes of rainbow trout (*Oncorhynchus mykiss* W., 1792). *Veterinarni Medicina*, *49*(10), 373–378. <https://doi.org/10.17221/5726-VETMED>
- Padgett, D. A., & Glaser, R. (2003). How stress influences the immune response. In *Trends in Immunology* (Vol. 24, Issue 8, pp. 444–448). Elsevier Ltd. [https://doi.org/10.1016/S1471-4906\(03\)00173-X](https://doi.org/10.1016/S1471-4906(03)00173-X)
- Palmer, S.M., Harris, P.J., & Powers, P.T. (2004). Age, growth and reproduction of tilefish, *Lopholatilus chamaeleonticeps*, along the southeast coast of the United States, 1980–1987 and 1996–1998. SEDAR04-DW-18. SEDAR/SAFMC, Charleston, SC.
- Pandelides, Z., Guchardi, J., & Holdway, D. (2014). Dehydroabietic acid (DHAA) alters metabolic enzyme activity and the effects of 17 β -estradiol in rainbow trout (*Oncorhynchus mykiss*). *Ecotoxicology and Environmental Safety*, *101*(1), 168–176. <https://doi.org/10.1016/j.ecoenv.2013.11.027>
- Parry, R. M., Chandan, R. C., & Shahani, K. M. (1965). A Rapid and Sensitive Assay of Muramidase. *Experimental Biology and Medicine*, *119*(2), 384–386. <https://doi.org/10.3181/00379727-119-30188>
- Pastore, A. S., Santacroce, M. P., Narracci, M., Cavallo, R. A., Acquaviva, M. I., Casalino, E., Colamonaco, M., & Crescenzo, G. (2014). Genotoxic damage of benzo[a]pyrene in cultured sea bream (*Sparus aurata* L.) hepatocytes: Harmful effects of chronic exposure. *Marine Environmental Research*, *100*, 74–85. <https://doi.org/10.1016/j.marenvres.2014.04.003>
- Perrault, J. R., Stacy, N. I., Lehner, A. F., Poor, S. K., Buchweitz, J. P., & Walsh, C. J. (2017). Toxic elements and associations with hematology, plasma biochemistry, and protein electrophoresis in nesting loggerhead sea turtles (*Caretta caretta*) from Casey Key, Florida. *Environmental Pollution*, *231*, 1398–1411. <https://doi.org/10.1016/j.envpol.2017.09.001>
- Perrot, V., Landing, W. M., Grubbs, R. D., & Salters, V. J. M. (2019). Mercury bioaccumulation in tilefish from the northeastern Gulf of Mexico 2 years after the Deepwater Horizon oil spill: Insights from Hg, C, N and S stable isotopes. *Science of the Total Environment*, *666*, 828–838. <https://doi.org/10.1016/j.scitotenv.2019.02.295>
- Perry, H., Ispording, W., Trigg, C., & Riedel, R. (2015). Heavy metals in red crabs, *Chaceon quinque-dens*, from the Gulf of Mexico. *Marine Pollution Bulletin*, *101*(2), 845–851. <https://doi.org/10.1016/j.marpolbul.2015.11.020>
- Petitjean, Q., Jean, S., Gandar, A., Côte, J., Laffaille, P., & Jacquin, L. (2019). Stress responses in fish: From molecular to evolutionary processes. In *Science of the Total Environment* (Vol. 684, pp. 371–380). Elsevier B.V. <https://doi.org/10.1016/j.scitotenv.2019.05.357>
- Ponce-Vélez, G., Botello, A. V., & Díaz-González, G. (2006). Organic and inorganic pollutants in marine sediments from northern and southern continental shelf of the Gulf of Mexico. *International Journal of Environment and Pollution*, *26*(1–3), 295–311.

<https://doi.org/10.1504/IJEP.2006.009113>

- Porch, C. E., Fitzhugh, G. R., Lang, E. T., Lyon, H. M., & Linton, B. C. (2015). Estimating the dependence of spawning frequency on size and age in Gulf of Mexico Red Snapper. *Marine and Coastal Fisheries*, 7(1), 233–245. <https://doi.org/10.1080/19425120.2015.1040567>
- Pulster, E. L., Fogelson, S., Carr, B. E., Mrowicki, J., & Murawski, S. (2020). Hepatobiliary PAHs and prevalence of pathological changes in Red Snapper from the Gulf of Mexico. *Aquatic Toxicology; In Review*.
- Pulster, E. L., Gracia, A., Armenteros, M., Toro-Farmer, G., Snyder, S.M., Carr, B. E., Schwaab, M. R., Nicholson, T. J., Mrowicki, J., & Murawski, S. A. (2020). A first comprehensive baseline of hydrocarbon pollution in Gulf of Mexico fishes. *Scientific Reports*. 10(6347). <https://doi.org/10.1038/s41598-020-62944-6>.
- Pulster, E. L., Gracia, A., Armenteros, M., Carr, B. E., Mrowicki, J., & Murawski, S. A. (2020). Chronic PAH exposures and associated declines in fish health indices observed for ten grouper species in the Gulf of Mexico. *Science of the Total Environment*, 703. <https://doi.org/10.1016/j.scitotenv.2019.135551>
- Qian, X., Ba, Y., Zhuang, Q., & Zhong, G. (2014). RNA-seq technology and its application in fish transcriptomics. *OMICS A Journal of Integrative Biology*, 18(2), 98–110. <https://doi.org/10.1089/omi.2013.0110>
- Rahal, A., Kumar, A., Singh, V., Yadav, B., Tiwari, R., Chakraborty, S., & Dhama, K. (2014). Oxidative stress, prooxidants, and antioxidants: The interplay. *BioMed Research International*, 2014. <https://doi.org/10.1155/2014/761264>
- Rebich, R. A., Houston, N. A., Mize, S. V., Pearson, D. K., Ging, P. B., & Evan Hornig, C. (2011). Sources and delivery of nutrients to the northwestern Gulf of Mexico from streams in the south-central United States. *Journal of the American Water Resources Association*, 47(5), 1061–1086. <https://doi.org/10.1111/j.1752-1688.2011.00583.x>
- Rehberger, K., Werner, I., Hitzfeld, B., Segner, H., & Baumann, L. (2017). 20 Years of fish immunotoxicology—what we know and where we are. In *Critical Reviews in Toxicology* (Vol. 47, Issue 6, pp. 509–535). Taylor and Francis Ltd. <https://doi.org/10.1080/10408444.2017.1288024>
- Reynaud, S., & Deschaux, P. (2006). The effects of polycyclic aromatic hydrocarbons on the immune system of fish: A review. *Aquatic Toxicology*, 77(2), 229–238. <https://doi.org/10.1016/j.aquatox.2005.10.018>
- Rhee, J. S., Kim, B. M., Lee, B. Y., Hwang, U. K., Lee, Y. S., & Lee, J. S. (2014). Cloning of circadian rhythmic pathway genes and perturbation of oscillation patterns in endocrine disrupting chemicals (EDCs)-exposed mangrove killifish *Kryptolebias marmoratus*. *Comparative Biochemistry and Physiology Part - C: Toxicology and Pharmacology*, 164, 11–20. <https://doi.org/10.1016/j.cbpc.2014.04.001>
- Robinson, M. D., McCarthy, D. J., & Smyth, G. K. (2010). edgeR: a Bioconductor package for differential expression analysis of digital gene expression data. *Bioinformatics*, 26(1): 139–140.
- Robinson, M. D. & Oshlack, A. (2010) A scaling normalization method for differential expression analysis of RNA-seq data. *Genome Biology*, 11(R25). <https://doi.org/10.1186/gb-2010-11-3-r25>.
- Rodgers, M. L., Takeshita, R., & Griffitt, R. J. (2018). Deepwater Horizon oil alone and in conjunction with *Vibrio anguillarum* exposure modulates immune response and growth in red snapper (*Lutjanus campechanus*). *Aquatic Toxicology*, 204, 91–99.

- <https://doi.org/10.1016/j.aquatox.2018.09.002>
- Romero, I. C., Schwing, P. T., Brooks, G. R., Larson, R. A., Hastings, D. W., Ellis, G., Goddard, E. A., & Hollander, D. J. (2015). Hydrocarbons in deep-sea sediments following the 2010 Deepwater Horizon blowout in the northeast Gulf of Mexico. *PLOS ONE*, *10*(5), e0128371. <https://doi.org/10.1371/journal.pone.0128371>
- Romero, I. C., Toro-Farmer, G., Diercks, A. R., Schwing, P., Muller-Karger, F., Murawski, S., & Hollander, D. J. (2017). Large-scale deposition of weathered oil in the Gulf of Mexico following a deep-water oil spill. *Environmental Pollution*, *228*, 179–189. <https://doi.org/10.1016/j.envpol.2017.05.019>
- Rooker, J. R., Kitchens, L. L., Dance, M. A., Wells, R. J. D., Falterman, B., & Cornic, M. (2013). Spatial, temporal, and habitat-related variation in abundance of pelagic fishes in the Gulf of Mexico: potential implications of the *Deepwater Horizon* oil spill. *PLoS ONE*, *8*(10), e76080. <https://doi.org/10.1371/journal.pone.0076080>
- Ruiz-Fernández, A. C., Betancourt Portela, J. M., Sericano, J. L., Sanchez-Cabeza, J. A., Espinosa, L. F., Cardoso-Mohedano, J. G., Pérez-Bernal, L. H., & Garay Tinoco, J. A. (2016). Coexisting sea-based and land-based sources of contamination by PAHs in the continental shelf sediments of Coatzacoalcos River discharge area (Gulf of Mexico). *Chemosphere*, *144*, 591–598. <https://doi.org/10.1016/j.chemosphere.2015.08.081>
- Sammarco, P. W., Kolian, S. R., Warby, R. A. F., Bouldin, J. L., Subra, W. A., & Porter, S. A. (2013). Distribution and concentrations of petroleum hydrocarbons associated with the BP/Deepwater Horizon Oil Spill, Gulf of Mexico. *Marine Pollution Bulletin*, *73*(1), 129–143. <https://doi.org/10.1016/j.marpolbul.2013.05.029>
- Santana, M. S., Sandrini-Neto, L., Filipak Neto, F., Oliveira Ribeiro, C. A., Di Domenico, M., & Prodocimo, M. M. (2018). Biomarker responses in fish exposed to polycyclic aromatic hydrocarbons (PAHs): Systematic review and meta-analysis. *Environmental Pollution*, *242*, 449–461. <https://doi.org/10.1016/j.envpol.2018.07.004>
- Schieber, M., & Chandel, N. S. (2014a). ROS function in redox signaling and oxidative stress. *Current Biology*, *24*(10), R453–R462. <https://doi.org/10.1016/j.cub.2014.03.034>
- Scholz-Böttcher, B. M., Ahlf, S., Vazquez-Gutierrez, F., & Rullkötter, J. (2008). Sources of hydrocarbon pollution in surface sediments of the Campeche Sound, Gulf of Mexico, revealed by biomarker analysis. *Organic Geochemistry*, *39*(8), 1104–1108. <https://doi.org/10.1016/j.orggeochem.2008.01.004>
- Schwing, P. T., O'Malley, B. J., & Hollander, D. J. (2018). Resilience of benthic foraminifera in the Northern Gulf of Mexico following the Deepwater Horizon event (2011–2015). *Ecological Indicators*, *84*, 753–764. <https://doi.org/10.1016/j.ecolind.2017.09.044>
- Schwing, P. T., Romero, I. C., Brooks, G. R., Hastings, D. W., Larson, R. A., & Hollander, D. J. (2015). A decline in benthic foraminifera following the *Deepwater Horizon* event in the northeastern Gulf of Mexico. *PLOS ONE*, *10*(3), e0120565. <https://doi.org/10.1371/journal.pone.0120565>
- Section, J., Judge, C., Barbier, M., & Judge, S. S. (2010). *IN THE UNITED STATES DISTRICT COURT FOR THE EASTERN DISTRICT OF LOUISIANA In re: Oil Spill by the Oil Rig "Deepwater Horizon" in the Gulf of Mexico.*
- SEDAR 52. 2018. Stock assessment report Gulf of Mexico red snapper, North Charleston, SC, 435 p.
- Serra-Sogas, N., O'Hara, P. D., Canessa, R., Keller, P., & Pelot, R. (2008). Visualization of spatial patterns and temporal trends for aerial surveillance of illegal oil discharges in

- western Canadian marine waters. *Marine Pollution Bulletin*, 56(5), 825–833.
<https://doi.org/10.1016/j.marpolbul.2008.02.005>
- Shailaja, M. S., & D’Silva, C. (2003). Evaluation of impact of PAH on a tropical fish, *Oreochromis mossambicus* using multiple biomarkers. *Chemosphere*, 53(8), 835–841.
[https://doi.org/10.1016/S0045-6535\(03\)00667-2](https://doi.org/10.1016/S0045-6535(03)00667-2)
- Shinde, R., & McGaha, T. L. (2018). The Aryl Hydrocarbon Receptor: Connecting immunity to the microenvironment. In *Trends in Immunology* (Vol. 39, Issue 12, pp. 1005–1020). Elsevier Ltd. <https://doi.org/10.1016/j.it.2018.10.010>
- Sinkus, W., Shervette, V., Ballenger, J., Reed, L. A., Plante, C., & White, B. (2017). Mercury bioaccumulation in offshore reef fishes from waters of the Southeastern USA. *Environmental Pollution*, 228, 222–233. <https://doi.org/10.1016/j.envpol.2017.04.057>
- Smeltz, M., Rowland-Faux, L., Ghiran, C., Patterson, W. F., Garner, S. B., Beers, A., Mièvre, Q., Kane, A. S., & James, M. O. (2017). A multi-year study of hepatic biomarkers in coastal fishes from the Gulf of Mexico after the Deepwater Horizon Oil Spill. *Marine Environmental Research*, 129, 57–67. <https://doi.org/10.1016/j.marenvres.2017.04.015>
- Smith, S. R., & Jacobs, G. A. (2005). Seasonal circulation fields in the northern Gulf of Mexico calculated by assimilating current meter, shipboard ADCP, and drifter data simultaneously with the shallow water equations. *Continental Shelf Research*, 25(2), 157–183.
<https://doi.org/10.1016/j.csr.2004.09.010>
- Snyder, S. M. (2010). Polycyclic aromatic hydrocarbon exposure, hepatic accumulation, and associated health impacts in Gulf of Mexico Golden Tilefish (*Lopholatilus chamaeleonticeps*). University of Sotuh Florida, p. 191.
- Snyder, S. M., Olin, J. A., Pulster, E. L., & Murawski, S. A. (2020). Spatial contrasts in hepatic and biliary PAHs in Tilefish (*Lopholatilus chamaeleonticeps*) throughout the Gulf of Mexico, with comparison to the Northwest Atlantic. *Environmental Pollution*, 258.
<https://doi.org/10.1016/j.envpol.2019.113775>
- Snyder, S. M., Pulster, E. L., & Murawski, S. A. (2019). Associations between chronic exposure to polycyclic aromatic hydrocarbons and health indices in Gulf of Mexico Tilefish (*Lopholatilus chamaeleonticeps*) post *Deepwater Horizon*. *Environmental Toxicology and Chemistry*, 38(12), 2659–2671. <https://doi.org/10.1002/etc.4583>
- Snyder, S. M., Pulster, E. L., Wetzel, D. L., & Murawski, S. A. (2015). PAH exposure in Gulf of Mexico demersal fishes, Post- *Deepwater Horizon*. *Environmental Science & Technology*, 49(14), 8786–8795. <https://doi.org/10.1021/acs.est.5b01870>
- Sokolova, I. (2018). Mitochondrial adaptations to variable environments and their role in animals’ stress tolerance. *Integrative and Comparative Biology*, 58(3), 519–531.
<https://doi.org/10.1093/icb/icy017>
- Solé, M., Antó, M., Baena, M., Carrasson, M., Cartes, J. E., & Maynou, F. (2010). Hepatic biomarkers of xenobiotic metabolism in eighteen marine fish from NW Mediterranean shelf and slope waters in relation to some of their biological and ecological variables. *Marine Environmental Research*, 70(2), 181–188. <https://doi.org/10.1016/j.marenvres.2010.04.008>
- Song, Y., Nahrgang, J., & Tollefsen, K. E. (2019). Transcriptomic analysis reveals dose-dependent modes of action of benzo(a)pyrene in polar cod (*Boreogadus saida*). *Science of the Total Environment*, 653, 176–189. <https://doi.org/10.1016/j.scitotenv.2018.10.261>
- Sørhus, E., Incardona, J. P., Furmanek, T., Goetz, G. W., Scholz, N. L., Meier, S., Edvardsen, R. B., & Jentoft, S. (2017). Novel adverse outcome pathways revealed by chemical genetics in a developing marine fish. *ELife*, 6. <https://doi.org/10.7554/eLife.20707>

- Steimle, F. W., Zdanowicz, V. S., & Gadbois, D. F. (1990). Metals and organic contaminants in northwest Atlantic deep-sea tilefish tissues. *Marine Pollution Bulletin*, 21(11), 530–535. [https://doi.org/10.1016/0025-326X\(90\)90301-N](https://doi.org/10.1016/0025-326X(90)90301-N)
- Steimle, F.W., Zetlin, C.A., Berrien, P.L., Johnson, D.L., & Chang, S. (1999). Essential Fish Habitat source document: tilefish *Lopholatilus chamaeleonticeps*, life history and habitat characteristics. NOAA Technical Memorandum. NMFS-NE-152.
- Stevens, E. A., Mezrich, J. D., & Bradfield, C. A. (2009). The aryl hydrocarbon receptor: A perspective on potential roles in the immune system. *Immunology*, 127(3), 299–311. <https://doi.org/10.1111/j.1365-2567.2009.03054.x>
- Struch, R. E., Pulster, E. L., Schreier, A. D., & Murawski, S. A. (2019). Hepatobiliary analyses suggest chronic PAH exposure in Hakes (*Urophycis* spp.) following the *Deepwater Horizon* oil spill. *Environmental Toxicology and Chemistry*, 38(12), 2740–2749. <https://doi.org/10.1002/etc.4596>
- Subbotkina, T. A., & Subbotkin, M. F. (2003). Lysozyme content in organs and blood serum in various species in the Volga River. *Journal of Evolutionary Biochemistry and Physiology*, 39(5), 537–546. <https://doi.org/10.1023/B:JOEY.0000015961.99374.62>
- Szedlmayer, S. T., & Mudrak, P. A. (2014). Influence of age-1 conspecifics, sediment type, dissolved oxygen, and the *Deepwater Horizon* oil spill on recruitment of age-0 Red Snapper in the northeast Gulf of Mexico during 2010 and 2011. *North American Journal of Fisheries Management*, 34(2), 443–452. <https://doi.org/10.1080/02755947.2014.882457>
- Tarnecki, J. H., & Patterson, W. F. (2015). Changes in Red Snapper diet and trophic ecology following the *Deepwater Horizon* oil spill. *Marine and Coastal Fisheries*, 7(1), 135–147. <https://doi.org/10.1080/19425120.2015.1020402>
- Tavares-Dias, M., & Moraes, F. R. (2007). Haematological and biochemical reference intervals for farmed channel catfish. *Journal of Fish Biology*, 71(2), 383–388. <https://doi.org/10.1111/j.1095-8649.2007.01494.x>
- Tierney, K. B., Farrell, A. P., & Kennedy, C. J. (2004). The differential leucocyte landscape of four teleosts: Juvenile *Oncorhynchus kisutch*, *Clupea pallasii*, *Culaea inconstans* and *Pimephales promelas*. *Journal of Fish Biology*, 65(4), 906–919. <https://doi.org/10.1111/j.0022-1112.2004.00491.x>
- Tierney, Keith B., Kennedy, C. J., Gobas, F., Gledhill, M., & Sekela, M. (2013). Organic Contaminants and Fish. In *Fish Physiology* (Vol. 33, pp. 1–52). Elsevier Inc. <https://doi.org/10.1016/B978-0-12-398254-4.00001-7>
- Tintos, A., Gesto, M., Míguez, J. M., & Soengas, J. L. (2008). β -Naphthoflavone and benzo(a)pyrene treatment affect liver intermediary metabolism and plasma cortisol levels in rainbow trout *Oncorhynchus mykiss*. *Ecotoxicology and Environmental Safety*, 69(2), 180–186. <https://doi.org/10.1016/j.ecoenv.2007.03.009>
- Tort, L. (2011). Stress and immune modulation in fish. *Developmental and Comparative Immunology*, 35(12), 1366–1375. <https://doi.org/10.1016/j.dci.2011.07.002>
- Trisciani, A., Corsi, I., Torre, C. Della, Perra, G., & Focardi, S. (2011). Hepatic biotransformation genes and enzymes and PAH metabolites in bile of common sole (*Solea solea*, Linnaeus, 1758) from an oil-contaminated site in the Mediterranean Sea: A field study. *Marine Pollution Bulletin*, 62(4), 806–814. <https://doi.org/10.1016/j.marpolbul.2011.01.001>
- U.S. Bureau of Ocean Energy Management. 2012. Ocean Energy and Minerals Management. U.S. Department of Interior, Bureau of Ocean Energy Management (BOEM).

- <http://www.boemre.gov/offshore/>
U.S. District Court Findings of Facts and Conclusions of Law - Phase 2 Trial. Case 2: 10-md-02179-cjb-ss, pp 1e44. Document 14021 Filed Jan. 15, 2015.
<http://www.laed.uscourts.gov/sites/default/files/OilSpill/Orders/1152015FindingsPhaseTwo.pdf>
- Valentine, D. L., Mezić, I., Maćešić, S., Črnjarić-Žic, N., Ivić, S., Hogan, P. J., Fonoberov, V. A., & Loire, S. (2012). Dynamic autoinoculation and the microbial ecology of a deep water hydrocarbon irruption. *Proceedings of the National Academy of Sciences of the United States of America*, *109*(50), 20286–20291. <https://doi.org/10.1073/pnas.1108820109>
- Van der Oost, R., Beyer, J., & Vermeulen, N. P. E. (2003). Fish bioaccumulation and biomarkers in environmental risk assessment: A review. *Environmental Toxicology and Pharmacology*, *13*(2), 57–149. [https://doi.org/10.1016/S1382-6689\(02\)00126-6](https://doi.org/10.1016/S1382-6689(02)00126-6)
- Van Noorden, C. J., Bahns, S., & Köhler, A. (1997). Adaptational changes in kinetic parameters of G6PDH but not of PGDH during contamination-induced carcinogenesis in livers of North Sea flatfish. *Biochimica et Biophysica Acta*, *1342*(2), 141–148. [https://doi.org/10.1016/s0167-4838\(97\)00061-7](https://doi.org/10.1016/s0167-4838(97)00061-7)
- Vega-López, A., Galar-Martínez, M., Jiménez-Orozco, F. A., García-Latorre, E., & Domínguez-López, M. L. (2007). Gender related differences in the oxidative stress response to PCB exposure in an endangered goodeid fish (*Girardinichthys viviparus*). *Comparative Biochemistry and Physiology - A Molecular and Integrative Physiology*, *146*(4), 672–678. <https://doi.org/10.1016/j.cbpa.2006.04.022>
- Vethaak, A. D., Jol, J. G., & Martínez-Gómez, C. (2011). Effects of cumulative stress on fish health near freshwater outlet sluices into the sea: A case study (1988-2005) with evidence for a contributing role of chemical contaminants. *Integrated Environmental Assessment and Management*, *7*(3), 445–458. <https://doi.org/10.1002/ieam.163>
- Vogelbein, W. K., Shields, J. D., Haas, L. W., Reece, K. S., & Zwerner, D. E. (2001). Skin ulcers in estuarine fishes: a comparative pathological evaluation of wild and laboratory-exposed fish. *Environmental Health Perspectives*, *109*(suppl 5), 687–693. <https://doi.org/10.1289/ehp.01109s5687>
- Vuontisjärvi, H., Keinänen, M., Vuorinen, P. J., & Peltonen, K. (2004). A comparison of HPLC with fluorescence detection and fixed wavelength fluorescence methods for the determination of polycyclic aromatic hydrocarbon metabolites in fish bile. *Polycyclic Aromatic Compounds*, *24*(4–5), 333–342. <https://doi.org/10.1080/10406630490468478>
- Walton, R. M. (2001). Establishing reference intervals: Health as a relative concept. *Seminars in Avian and Exotic Pet Medicine*, *10*(2), 66–71. [https://doi.org/10.1053/s1055-937x\(01\)80026-8](https://doi.org/10.1053/s1055-937x(01)80026-8)
- Wang, Z., Gerstein, M., & Snyder, M. (2009). RNA-Seq: A revolutionary tool for transcriptomics. *Nature Reviews Genetics*, *10*(1), 57–63. <https://doi.org/10.1038/nrg2484>
- Webb, D., & Gagnon, M. M. (2007). Serum sorbitol dehydrogenase activity as an indicator of chemically induced liver damage in black bream (*Acanthopagrus butcheri*). *Environmental Bioindicators*, *2*(3), 172–182. <https://doi.org/10.1080/15555270701591006>
- Wedemeyer, G. A., Gould, R. W., & Yasutake, W. T. (1983). Some potentials and limits of the leucocrit test as a fish health assessment method. *Journal of Fish Biology*, *23*(6), 711–716. <https://doi.org/10.1111/j.1095-8649.1983.tb02948.x>
- Weldetinsae, A., Dawit, M., Getahun, A., Patil, H. S., Alemayehu, E., Gizaw, M., Abate, M., & Abera, D. (2017). Aneugenicity and clastogenicity in freshwater fish *Oreochromis niloticus*

- exposed to incipient safe concentration of tannery effluent. *Ecotoxicology and Environmental Safety*, 138, 98–104. <https://doi.org/10.1016/j.ecoenv.2016.10.026>
- White, H. K., Hsing, P. Y., Cho, W., Shank, T. M., Cordes, E. E., Quattrini, A. M., Nelson, R. K., Camilli, R., Demopoulos, A. W. J., German, C. R., Brooks, J. M., Roberts, H. H., Shedd, W., Reddy, C. M., & Fisher, C. R. (2012). Impact of the Deepwater Horizon oil spill on a deep-water coral community in the Gulf of Mexico. In *Proceedings of the National Academy of Sciences of the United States of America* (Vol. 109, Issue 50, pp. 20303–20308). <https://doi.org/10.1073/pnas.1118029109>
- Whitehead, A., Clark, B. W., Reid, N. M., Hahn, M. E., & Nacci, D. (2017). When evolution is the solution to pollution: Key principles, and lessons from rapid repeated adaptation of killifish (*Fundulus heteroclitus*) populations. *Evolutionary Applications*, 10(8), 762–783. <https://doi.org/10.1111/eva.12470>
- Whitehead, A., Pilcher, W., Champlin, D., & Nacci, D. (2012). Common mechanism underlies repeated evolution of extreme pollution tolerance. *Proceedings of the Royal Society B: Biological Sciences*, 279(1728), 427–433. <https://doi.org/10.1098/rspb.2011.0847>
- Williams-Grove, L. J., & Szedlmayer, S. T. (2017). Depth preferences and three-dimensional movements of red snapper, *Lutjanus campechanus*, on an artificial reef in the northern Gulf of Mexico. *Fisheries Research*, 190, 61–70. <https://doi.org/10.1016/j.fishres.2017.01.003>
- Williams, T. D., Davies, I. M., Wu, H., Diab, A. M., Webster, L., Viant, M. R., Chipman, J. K., Leaver, M. J., George, S. G., Moffat, C. F., & Robinson, C. D. (2014). Molecular responses of European flounder (*Platichthys flesus*) chronically exposed to contaminated estuarine sediments. *Chemosphere*, 108, 152–158. <https://doi.org/10.1016/j.chemosphere.2014.01.028>
- Wilson, J., & Nieland, D. (2001). Age and growth of Red Snapper *Lutjanus campechanus*, from the northern Gulf of Mexico off Louisiana. *Fish Bulletin*. 99:653-664.
- Winzer, K., Winston, G. W., Becker, W., Van Noorden, C. J., & Köehler, A. (2001). Sex-related responses to oxidative stress in primary cultured hepatocytes of European flounder (*Platichthys flesus* L.). *Aquatic Toxicology (Amsterdam, Netherlands)*, 52(2), 143–155. [https://doi.org/10.1016/s0166-445x\(00\)00137-5](https://doi.org/10.1016/s0166-445x(00)00137-5)
- Wirgin, I., Roy, N. K., Loftus, M., Chambers, R. C., Franks, D. G., & Hahn, M. E. (2011). Mechanistic basis of resistance to PCBs in Atlantic tomcod from the Hudson River. *Science*, 331(6022), 1322–1325. <https://doi.org/10.1126/science.1197296>
- Wise, J. P., Wise, J. T. F., Wise, C. F., Wise, S. S., Gianios, C., Xie, H., Thompson, W. D., Perkins, C., & Falank, C. (2014). Concentrations of the genotoxic metals, chromium and nickel, in whales, tar balls, oil slicks, and released oil from the Gulf of Mexico in the immediate aftermath of the deepwater horizon oil crisis: Is genotoxic metal exposure part of the deepwater horizon legacy? *Environmental Science and Technology*, 48(5), 2997–3006. <https://doi.org/10.1021/es405079b>
- World Health Organization., International Agency for Research on Cancer., & IARC Working Group on the Evaluation of Carcinogenic Risks to Humans. (2012). *A review of human carcinogens. Part F, Chemical agents and related occupations*. International Agency for Research on Cancer.
- Wunderlich, A. C., Silva, R. J., Zica, É. O. P., Rebelo, M. F., Parente, T. E. M., & Vidal-Martínez, V. M. (2015). The influence of seasonality, fish size and reproductive status on EROD activity in *Plagioscion squamosissimus*: Implications for biomonitoring of tropical/subtropical reservoirs. *Ecological Indicators*, 58, 267–276. <https://doi.org/10.1016/j.ecolind.2015.05.063>

- Xu, E. G., Khursigara, A. J., Magnuson, J., Hazard, E. S., Hardiman, G., Esbaugh, A. J., Roberts, A. P., & Schlenk, D. (2017). Larval Red Drum (*Sciaenops ocellatus*) Sublethal exposure to weathered *Deepwater Horizon* crude oil: developmental and transcriptomic consequences. *Environmental Science and Technology*, 51(17), 10162–10172. <https://doi.org/10.1021/acs.est.7b02037>
- Xu, E. G., Mager, E. M., Grosell, M., Hazard, E. S., Hardiman, G., & Schlenk, D. (2017). Novel transcriptome assembly and comparative toxicity pathway analysis in mahi-mahi (*Coryphaena hippurus*) embryos and larvae exposed to Deepwater Horizon oil. *Scientific Reports*, 7. <https://doi.org/10.1038/srep44546>
- Yan, B., Passow, U., Chanton, J. P., Nöthig, E. M., Asper, V., Sweet, J., Pitiranggon, M., Diercks, A., & Pak, D. (2016). Sustained deposition of contaminants from the Deepwater Horizon spill. *Proceedings of the National Academy of Sciences of the United States of America*, 113(24), E3332–E3340. <https://doi.org/10.1073/pnas.1513156113>
- Ye, H., Lin, Q., & Luo, H. (2018). Applications of transcriptomics and proteomics in understanding fish immunity. In *Fish and Shellfish Immunology* (Vol. 77, pp. 319–327). Academic Press. <https://doi.org/10.1016/j.fsi.2018.03.046>
- Zaldívar-Jiménez, A., Ladrón de Guevara-Porras, P., Pérez-Ceballos, R., Díaz-Mondragón, S., & Rosado-Solórzano, R. (2017). US-Mexico joint gulf of Mexico large marine ecosystem based assessment and management: Experience in community involvement and mangrove wetland restoration in Términos lagoon, Mexico. In *Environmental Development* (Vol. 22, pp. 206–213). Elsevier B.V. <https://doi.org/10.1016/j.envdev.2017.02.007>
- Zhang, M., Miao, Y., Chen, Q., Cai, M., Dong, W., Dai, X., Lu, Y., Zhou, C., Cui, Z., & Xiong, B. (2018). BaP exposure causes oocyte meiotic arrest and fertilization failure to weaken female fertility. *FASEB Journal*, 32(1), 342–352. <https://doi.org/10.1096/fj.201700514R>

**APPENDIX A:
STATION AND CATCH DATA**

Table A1 Station locations, coordinates, depth, temperature, year sampled, primary fish species caught, and number of individuals of that species sampled.

Station	Latitude	Longitude	Species	# Sampled	Average Depth (m)	Average Temperature (°C)	Year
11_150	28.989217	-88.681800	Golden Tilefish	4	305.13	11.07	2015
14_100	29.329467	-87.527300	Golden Tilefish	2	315.20	10.63	2015
14_60	29.506900	-87.377400	Golden Tilefish	7	184.13	14.50	2015
30_100	18.700033	-94.418983	Golden Tilefish	2	182.30	16.48	2015
30_150	18.749900	-94.414333	Golden Tilefish	7	287.19	12.85	2015
31_150	19.565633	-92.721133	Golden Tilefish	10	233.52	14.63	2015
33_100	22.313967	-91.650283	Golden Tilefish	2	195.78	15.00	2015
33_150	22.326517	-91.688900	Golden Tilefish	10	370.62	11.44	2015
34_100	22.820800	-90.173450	Golden Tilefish	3	344.49	11.77	2015
34_150	22.809200	-90.236250	Golden Tilefish	1	267.35	13.17	2015
7_150	29.481417	-86.675400	Golden Tilefish	12	337.97	10.41	2015
8_100	29.749133	-87.091900	Golden Tilefish	10	218.66	12.90	2015
9_150	29.244633	-87.959900	Golden Tilefish	6	356.61	10.19	2015
9_80	29.291050	-87.979600	Golden Tilefish	1	186.65	13.41	2015
DSH_07	29.260533	-87.732400	Golden Tilefish	9	391.27	9.11	2015
MC04	29.324533	-86.603700	Golden Tilefish	3	388.23	9.99	2015
GP03	28.672367	-89.222900	Golden Tilefish	2	211.85	12.02	2015
20_100	27.778750	-93.360617	Golden Tilefish	5	185.00	15.52	2016
20_150	27.604417	-93.303483	Golden Tilefish	10	291.00	12.73	2016
21_100	27.774533	-95.309333	Golden Tilefish	10	223.00	15.21	2016
22_150	27.302450	-96.155467	Golden Tilefish	9	300.00	12.34	2016
23_150	26.716283	-96.383150	Golden Tilefish	10	292.54	12.50	2016
24_100	25.504617	-96.377300	Golden Tilefish	10	250.15	14.06	2016
24_150	25.490050	-96.340250	Golden Tilefish	10	308.98	11.86	2016
25_150	24.022267	-97.115967	Golden Tilefish	7	290.61	13.17	2016
26_100	22.359433	-97.387817	Golden Tilefish	1	171.07	17.72	2016
26_150	22.365183	-97.365450	Golden Tilefish	5	272.59	14.35	2016
27_100	19.918200	-96.235600	Golden Tilefish	3	202.47	15.80	2016

Table A1 (Continued)

27_150	19.937917	-96.233600	Golden Tilefish	10	282.94	13.72	2016
28_100	19.153933	-95.664500	Golden Tilefish	3	183.16	16.62	2016
28_150	19.181050	-95.717500	Golden Tilefish	5	383.50	12.20	2016
36_100	23.605033	-87.359800	Golden Tilefish	5	208.51	17.44	2016
36_150	23.785300	-87.390500	Golden Tilefish	10	301.00	14.18	2016
1-150	24.925100	-84.146600	Golden Tilefish	1	301.15	9.84	2017
11_150	29.034700	-88.678900	Golden Tilefish	10	282.70	13.18	2017
14_100	29.394000	-87.494500	Golden Tilefish	8	354.20	12.62	2017
14_60	29.461800	-87.435000	Golden Tilefish	10	229.15	12.53	2017
7_150	29.441400	-86.733800	Golden Tilefish	10	324.05	10.47	2017
8_100	29.734000	-87.170500	Golden Tilefish	10	217.85	13.08	2017
9_150	29.242400	-87.966000	Golden Tilefish	6	341.40	13.21	2017
9_80	29.289500	-87.970400	Golden Tilefish	4	187.00	13.71	2017
MC04	29.290000	-86.662800	Golden Tilefish	8	370.95	10.45	2017
10_40	29.200000	-88.871300	Red Snapper	10	65.10	22.42	2015
12_40	28.830733	-89.514900	Red Snapper	10	59.85	22.81	2015
32_40	20.831267	-92.400200	Red Snapper	9	81.23	19.36	2015
33_60	22.158417	-91.502183	Red Snapper	1	114.30	18.74	2015
34_60	22.662017	-90.113017	Red Snapper	2	114.22	18.83	2015
4_40	28.074350	-84.440800	Red Snapper	4	66.05	20.70	2015
8_40	29.890333	-87.215600	Red Snapper	8	75.51	20.89	2015
EZ02	19.387033	-92.330933	Red Snapper	2	63.09	21.34	2015
HE_265	28.372183	-90.512200	Red Snapper	10	50.84	22.21	2015
20_40	28.079567	-93.906083	Red Snapper	7	67.82	21.96	2016
21_60	27.805883	-95.389650	Red Snapper	8	131.00	20.79	2016
22_40	27.441950	-96.554733	Red Snapper	10	76.50	22.65	2016
23_20	26.629600	-96.947833	Red Snapper	8	36.99	24.76	2016
23_40	26.700783	-96.638317	Red Snapper	8	86.84	21.86	2016
25_40	24.022900	-97.313333	Red Snapper	3	90.54	21.14	2016
27_40	19.956717	-96.400367	Red Snapper	1	90.32	20.40	2016
28_40	19.169100	-95.754900	Red Snapper	1	121.04	19.20	2016
10_40	29.194900	-88.872800	Red Snapper	10	59.84	19.59	2017
12_40	28.879700	-89.576100	Red Snapper	10	62.46	19.10	2017

APPENDIX B

BIOMETRICS DATA FOR FISH UTILIZED IN THE CREATION OF REFERENCE INTERVALS

Table B1 Biometrics information (total weight (TW) and standard length (SL)) for Golden Tilefish utilized for the creation of reference intervals.

	Variable statistics after outlier removal											
	All	MDA	SOD	SDH	ΣNA	HCT	LCT	Lymph	Thromb	Mon	Neut	LYS
All fish (n)	255	210	210	195	211	224	221	211	211	212	212	209
TW Mean (kg)	3.477	3.494	3.496	3.576	3.514	3.533	3.563	3.513	3.513	3.503	3.505	3.504
TW STDEV (kg)	2.517	2.632	2.63	2.617	2.614	2.579	2.586	2.632	2.632	2.63	2.628	2.634
TW Median (kg)	2.668	2.617	2.617	2.696	2.634	2.668	2.668	2.634	2.634	2.617	2.617	2.634
TW Min (kg)	0.038	0.344	0.344	0.344	0.344	0.344	0.344	0.344	0.344	0.344	0.344	0.344
TW Max (kg)	14.8	14.8	14.8	14.8	14.8	14.8	14.8	14.8	14.8	14.8	14.8	14.8
SL Mean (cm)	56.04	55.414	55.429	55.923	55.682	55.853	56.005	55.678	55.678	55.656	55.646	55.431
SL STDEV (cm)	12.16	12.316	12.314	12.296	12.475	12.194	12.194	12.479	12.479	12.453	12.458	12.343
SL Median (cm)	54	53	53	54	53	53	53	53	53	53	53	53
SL Min (cm)	33	33	33	33	33	33	33	33	33	33	33	33
SL Max (cm)	93	93	93	93	93	93	93	93	93	93	93	93
Female (n)	157	132	132	121	132	139	137	132	132	132	132	131
TW Mean (kg)	2.98	2.912	2.924	3.052	2.921	3.012	3.047	2.92	2.92	2.92	2.92	2.924
TW STDEV (kg)	2.08	2.1339	2.143	2.18	2.134	2.136	2.141	2.135	2.135	2.135	2.135	2.143
TW Median (kg)	2.29	2.165	2.166	2.29	2.165	2.244	2.29	2.165	2.165	2.165	2.165	2.166
TW Min (kg)	0.038	0.854	0.854	0.854	0.854	0.885	0.885	0.854	0.854	0.854	0.854	0.854
TW Max (kg)	13.4	13.4	13.4	13.4	13.4	13.4	13.4	13.4	13.4	13.4	13.4	13.4
SL Mean (cm)	53.452	52.545	52.55	53.355	52.727	53.353	53.562	52.72	52.72	52.72	52.72	52.55
SL STDEV (cm)	10.858	11.039	11.081	11.19	11.061	10.984	10.968	11.066	11.066	11.066	11.066	11.081
SL Median (cm)	52	51	51	52	51	52	52	51	51	51	51	51
SL Min (cm)	36	36	36	36	36	36	36	36	36	36	36	36

Table B1 (Continued)

SL Max (cm)	89	89	89	89	89	89	89	89	89	89	89	89
Male (n)	55	46	46	43	47	50	49	47	47	47	47	46
TW Mean (kg)	5.862	6.051	6.051	6.025	6.064	5.902	5.964	6.064	6.064	6.064	6.064	6.051
TW STDEV (kg)	2.812	2.867	2.867	2.803	2.837	2.834	2.828	2.837	2.837	2.837	2.837	2.867
TW Median (kg)	5.268	5.46	5.46	5.615	5.615	5.286	5.304	5.615	5.615	5.615	5.615	5.46
TW Min (kg)	1.528	1.68	1.68	1.68	1.68	1.68	1.68	1.68	1.68	1.68	1.68	1.68
TW Max (kg)	14.8	14.8	14.8	14.8	14.8	14.8	14.8	14.8	14.8	14.8	14.8	14.8
SL Mean (cm)	67.4	67.304	67.304	67.209	67.745	66.84	67.061	67.745	67.745	67.745	67.745	67.304
SL STDEV (cm)	10.73	9.73	9.729	9.831	10.85	10.471	10.461	10.085	10.085	10.085	10.085	9.729
SL Median (cm)	67	67.5	67.5	68	68	67	67	68	68	68	68	67.5
SL Min (cm)	46	46	46	46	46	46	46	46	46	46	46	46
SL Max (cm)	93	93	93	93	93	93	93	93	93	93	93	93
Unknown (n)	43	32	32	31	32	35	35	32	32	33	33	32
TW Mean (kg)	2.222	2.214	2.203	2.228	2.214	2.218	2.128	2.214	2.214	2.187	2.2	2.214
TW STDEV (kg)	1.432	1.614	1.59	1.639	1.614	1.544	1.544	1.614	1.614	1.597	1.591	1.614
TW Median (kg)	1.836	1.748	1.79	1.705	1.748	1.826	1.826	1.748	1.748	1.705	1.738	1.748
TW Min (kg)	0.344	0.344	0.344	0.344	0.344	0.344	0.344	0.344	0.344	0.344	0.344	0.344
TW Max (kg)	7.12	7.12	7.12	7.12	7.12	7.12	7.12	7.12	7.12	7.12	7.12	7.12
SL Mean (cm)	51	50.156	50.303	50.29	50.156	50.086	50.086	50.156	50.156	50.182	50.121	50.156
SL STDEV (cm)	9.388	9.848	9.729	9.981	9.848	9.497	9.497	9.848	9.848	9.694	9.695	9.848
SL Median (cm)	50	49	49	49	49	49	49	49	49	49	49	49
SL Min (cm)	33	33	33	33	33	33	33	33	33	33	33	33
SL Max (cm)	73	73	73	73	73	73	73	73	73	73	73	73

Table B2 Biometrics information (total weight (TW) and standard length (SL)) for Red Snapper utilized for the creation of reference intervals.

	Variable statistics after outliers were removed											
	All	MDA	SOD	SDH	Σ(NA)	HCT	LCT	Lymph	Thromb	Mon	Neut	LYS
All fish (n)	125	105	104	105	113	123	123	110	110	110	110	114
TW Mean (kg)	4.529	4.11	4.42	4.42	4.427	4.545	4.545	4.47	4.47	4.47	4.47	4.434
TW St dev. (kg)	2.037	1.816	1.823	1.823	1.799	2.048	2.048	1.8	1.8	1.8	1.8	1.792
TW Median (kg)	4.47	4.398	4.415	4.415	4.432	4.762	4.762	4.557	4.557	4.557	4.557	4.451
TW Min (kg)	0.674	1.296	1.296	1.296	1.296	0.674	0.674	1.296	1.296	1.296	1.296	1.296
TW Max (kg)	13.2	13.2	13.2	13.2	13.2	13.2	13.2	13.2	13.2	13.2	13.2	13.2
SL Mean (cm)	54.01	53.86	53.89	53.89	53.97	54.07	54.07	54.17	54.17	54.17	54.17	54.02
SL St dev. (cm)	9.526	8.215	8.25	8.25	8.243	9.588	9.588	8.244	8.244	8.244	8.244	8.22
SL Median (cm)	54	54	54	54	54	55	55	54	54	54	54	54
SL Min (cm)	28	34	34	34	34	28	28	34	34	34	34	34
SL Max (cm)	76	76	76	76	76	76	76	76	76	76	76	76
Female (n)	65	55	55	55	58	65	65	56	56	56	56	58
TW Mean (kg)	4.942	4.69	4.69	4.69	4.687	4.942	4.942	4.757	4.757	4.757	4.757	4.687
TW St dev. (kg)	2.146	2.036	2.036	2.036	2.016	2.146	2.146	2.005	2.005	2.005	2.005	2.016
TW Median (kg)	4.962	4.85	4.85	4.85	4.9	4.962	4.962	4.9	4.9	4.9	4.9	4.9
TW Min (kg)	1.266	1.37	1.37	1.37	1.37	1.266	1.266	1.37	1.37	1.37	1.37	1.37
TW Max (kg)	13.2	13.2	13.2	13.2	13.2	13.2	13.2	13.2	13.2	13.2	13.2	13.2
SL Mean (cm)	55.754	54.909	54.909	54.909	55.034	55.754	55.754	55.357	55.357	55.357	55.357	55.034
SL St dev. (cm)	9.148	8.553	8.553	8.553	8.627	9.148	9.148	8.529	8.529	8.529	8.529	8.627
SL Median (cm)	55	55	55	55	55	55	55	55	55	55	55	55
SL Min (cm)	35	36	36	36	36	35	35	36	36	36	36	36
SL Max (cm)	76	76	76	76	76	76	76	76	76	76	76	76
Male (n)	58	48	47	48	53	56	56	52	52	52	52	54
TW Mean (kg)	4.08	4.102	4.115	4.115	4.154	4.1	4.1	4.173	4.173	4.173	4.173	4.171
TW St dev. (kg)	1.857	1.529	1.543	1.543	1.536	1.884	1.884	1.549	1.549	1.549	1.549	1.5
TW Median (kg)	3.977	3.8	3.848	3.848	3.977	3.976	3.976	4.058	4.058	4.058	4.058	4.058
TW Min (kg)	0.674	1.296	1.296	1.296	1.296	0.674	0.674	1.296	1.296	1.296	1.296	1.296

Table B2 (Continued)

TW Max (kg)	9.778	7.08	7.08	7.08	7.08	9.778	9.778	7.08	7.08	7.08	7.08	7.08
SL Mean (cm)	52.035	52.625	52.66	52.66	52.792	52.089	52.089	52.885	52.885	52.885	52.885	52.964
SL St dev. (cm)	9.798	7.9	7.982	7.982	7.88	9.959	9.959	7.972	7.972	7.972	7.972	7.713
SL Median (cm)	53	52.5	53	53	53	53	53	53	53	53	53	53
SL Min (cm)	28	34	34	34	34	28	28	34	34	34	34	34
SL Max (cm)	70	70	70	70	70	70	70	70	70	70	70	70
Unknown (n)	2	2	2	2	2	2	2	2	2	2	2	2
TW Mean (kg)	4.134	4.134	4.134	4.134	4.134	4.134	4.134	4.134	4.134	4.134	4.134	4.134
TW St dev. (kg)	0.421	0.421	0.421	0.421	0.421	0.421	0.421	0.421	0.421	0.421	0.421	0.421
TW Median (kg)	4.134	4.134	4.134	4.134	4.134	4.134	4.134	4.134	4.134	4.134	4.134	4.134
TW Min (kg)	3.836	3.836	3.836	3.836	3.836	3.836	3.836	3.836	3.836	3.836	3.836	3.836
TW Max (kg)	4.432	4.432	4.432	4.432	4.432	4.432	4.432	4.432	4.432	4.432	4.432	4.432
SL Mean (cm)	54.5	54.5	54.5	54.5	54.5	54.5	54.5	54.5	54.5	54.5	54.5	54.5
SL St dev. (cm)	0.707	0.707	0.707	0.707	0.707	0.707	0.707	0.707	0.707	0.707	0.707	0.707
SL Median (cm)	54.5	54.5	54.5	54.5	54.5	54.5	54.5	54.5	54.5	54.5	54.5	54.5
SL Min (cm)	54	54	54	54	54	54	54	54	54	54	54	54
SL Max (cm)	55	55	55	55	55	55	55	55	55	55	55	55